Titre: Title:	P-Delta effects on the inelastic seismic response of reinforced concrete shear wall buildings
Auteur: Author:	Jianhua Tu
Date:	2000
Type:	Mémoire ou thèse / Dissertation or Thesis
Référence: Citation:	Tu, J. (2000). P-Delta effects on the inelastic seismic response of reinforced concrete shear wall buildings [Mémoire de maîtrise, École Polytechnique de Montréal]. PolyPublie. https://publications.polymtl.ca/8888/

UNIVERSITÉ DE MONTRÉAL

P-DELTA EFFECTS ON THE INELASTIC SEISMIC RESPONSE OF REINFORCED CONCRETE SHEAR WALL BUILDINGS

JIANHUA TU
DÉPARTEMENT DES GÉNIES CIVIL, GÉOLOGIQUE ET DES MINES
ÉCOLE POLYTECHNIQUE DE MONTRÉAL

MÉMOIRE PRÉSENTÉ EN VUE DE L'OBTENTION
DU DIPLÔME DE MAÎTRISE ÈS SCIENCES APPLIQUÉES
(GÉNIE CIVIL)
AVRIL 2000

UNIVERSITÉ DE MONTRÉAL

ÉCOLE POLYTECHNIQUE DE MONTRÉAL

Ce mémoire intitulé:

P-DELTA EFFECTS ON THE INELASTIC SEISMIC RESPONSE OF REINFORCED CONCRETE SHEAR WALL BUILDINGS

présenté par : TU Jianhua

en vue de l'obtention de diplôme de : Maîtrise ès sciences appliquées

a été dûment accepté par le jury d'examen constitué de :

M. TINAWI Réné, Ph.D..ing., président

M. LÉGER Pierre, Ph.D., ing., directeur de recherche

M. TREMBLAY Robert, Ph.D., ing., codirecteur de recherche

M. MASSICOTTE Bruno, Ph.D.,ing., membre

ACKNOWLEDGEMENTS

The author would like to sincerely thank his research supervisors, Professor Pierre Léger and Professor Robert Tremblay, for their assistance, all their suggestions and comments throughout this Masters thesis. This project has been made possible through funding support provided by the FCAR and NSERC.

Finally, the author would also like to thank his friends, family and especially his wife for their continual support and their encouragement.

RÉSUMÉ

En général, de grands déplacements et des efforts internes importants sont produits quand des bâtiments sont soumis à de forts tremblements de terre. L'augmentation des efforts internes et des déplacements dus aux effets du deuxième ordre des chargements verticaux agissant sur une structure transversalement déplacée est désigné généralement sous le nom des effets P-Δ. Les effets P-Δ peuvent réduire la résistance séismique des bâtiments. Par conséquent, la capacité de déformation et des capacités supplémentaires de résistance devraient être fournies pour empêcher l'effondrement sous les tremblements de terre de conception. Une approche de facteur de stabilité a été ainsi présentée par le CNBC 1995 pour considérer les effets P-Δ. Cette approche augmente la résistance des ossatures de bâtiments, réduisant de ce fait l'incidence des effets P-Δ. L'utilisation de facteurs de stabilité s'est avérée conservatrice pour les cadres résistant aux moments démontrant un mode de déformation de cisaillement lors des séismes. Toutefois l'utilisation de facteurs de stabilité pour contrecarrer les effets P-Δ dans les murs démontrant un mode de déformation en flexion, n'a pas été correctement abordée dans la littérature. Quelques études précédentes sur des structures simplifiées de murs indiquent que ceux-ci sont relativement peu sensibles aux effets P-Δ. Par conséquent, la nécessité d'augmenter la résistance, et le coût associé, des structures contreventées à l'aide de murs peut être sérieusement remise en cause.

Il devient de ce fait important d'étudier les effets P-Δ sur une structure réaliste contreventée par des murs de cisaillement conçus selon le CNBC 1995. Le but de cette thèse est ainsi d'étudier l'influence des effets P-Δ sur un mur de cisaillement faisant partie d'un bâtiment typique en béton armé de 12 étages. Trois aspects principaux de recherche sont présentés: (a) le modèle dynamique d'une structure typique de mur de cisaillement, (b) des analyses dynamiques non linéaires sous divers types de secousses séismiques pour évaluer les effets P-Δ sur la réponse séismique du bâtiment, et (c) les effets de variations des paramètres de modélisation sur la réponse séismique.

D'abord, l'état actuel des recherches associées aux effets P-Δ, est présenté. Le bâtiment contreventé par des murs de cisaillement considéré dans cette étude est adapté du manuel de conception des structures en béton de l'association canadienne de ciment de Portland (CPCA 1985). Le bâtiment répond également aux exigences du code (CSA) A23.3-M94 pour la conception des structures en béton. Les chargements axiaux du mur, induits par les charges mortes et les charges vives, sont considérés lors des calculs des relations non linéaires entre les moments du mur et les courbures.

Des analyses dynamiques inélastiques du mur de cisaillement, considérant une règle bilinéaire d'hystérésis pour représenter les capacités moments-rotations des rotules plastiques se formant dans le mur, sont alors effectuées pour examiner les effets P-Δ sur la réponse séismique. Puisque des analyses dynamiques inélastiques rigoureuses sont effectuées, la résistance du mur a été choisie pour répondre aux exigences du CNBC 1995 sans augmentation de résistance pour réduire les effets P-Δ. Pour évaluer le comportement séismique du mur, le déplacement au toit, les forces de cisaillement et les moments de flexion à la base du mur, la ductilité le long de la hauteur, et divers indices d'endommagement sont considérés comme indicateurs de réponse. Des analyses statiques non linéaires de poussées latérales monotones sont aussi effectuées pour évaluer l'importance des effets P-Δ.

Les effets de variations des paramètres de modélisation du bâtiment sont étudiés pour le séisme du Saguenay (1988) à haut contenu de fréquences typique de l'est de l'Amérique du Nord et pour des séismes à bas contenu de fréquences typiques de l'ouest de l'Amérique du Nord. Ces enregistrements de tremblements de terre sont ajustés pour une accélération de pointe au sol de 0.18g correspondant à la condition du CNBC 1995 pour Montréal. Quelques paramètres de modélisation, telles que la force axiale dans la structure, la règle d'hystérésis, et la constante d'amortissement visqueuse, sont choisis pour évaluer leur influence sur la réponse séismique du mur.

Les résultats de ce travail de recherche indiquent que les effets P-Δ ne sont pas importants lors des analyses du mur de cisaillement initialement conçu sans considérer les effets P-Δ. Par conséquent, l'approche des facteurs de stabilité présentée dans le CNBC 1995 semble être trop conservatrice. Les résultats des analyses dynamiques inélastiques ont indiquées une influence minimale des effets P-Δ sur les déplacements, le cisaillement à la base, la demande de ductilité en déplacement, la demande de ductilité en courbure, et les valeurs maximales des indices d'endommagement. Les analyses ont également indiquées que si la force axiale dans le poteau de gravité est augmentée de P à 2P, il n'y a pas d'augmentation significative des effets P-Δ pour le mur de cisaillement. Donc une incertitude raisonnable pour le chargement axial n'est pas susceptible d'augmenter substantiellement l'importance des effets P-Δ pour les structures contreventées à l'aide de murs.

Les résultats de cette étude indiquent donc que l'approche des facteurs de stabilité du CNBC 1995 pour les bâtiments contreventés par des murs de cisaillement devrait être mise à jour pour éviter l'augmentation inutile de résistance de ce type de structure pour contrer les effets P-Δ.

ABSTRACT

In general, large displacements and strains are produced when building structures are subjected to major earthquakes. The increase in internal forces and displacements due to second order effects of vertical loads acting upon a laterally displaced structure are commonly referred to as P-Δ effects. It is generally recognized that P-Δ effects can contribute to reduce the seismic performance of buildings. Therefore, additional deformation and strength capacities should be provided to prevent collapse under selected design earthquakes. A stability factor approach was thus introduced in NBCC (1995) to consider P-Δ effects for frame and wall structures to increase strength of buildings thus reducing the incidence of P-Δ effects. This concept has been shown to be conservative for moment resisting frame structure, exhibiting shear type of seismic displacements. However its applicability to counteract P-Δ effects in shear wall structures, exhibiting bending type of seismic displacements, has not been properly addressed in the literature. Some previous studies on simplified shear wall structures indicate that walls are relatively insensitive to P-Δ effects. Therefore, the necessity to increase the strength, and associated cost, of shear wall structures can be seriously questioned.

It is thus becoming important to study P-Δ effects in an actual and detailed shear wall structure designed according to NBCC 1995. The purpose of this thesis is thus to investigate the influence of P-Δ effects on a typical 12-storey reinforced concrete (r/c) shear wall building. Three major research aspects are presented: (a) the dynamic model of a typical shear wall structure, (b) nonlinear dynamic analyses under earthquake ground motions to assess P-Δ effects on the seismic response of the 12-storey building, and (c) the effects of variations in modeling parameters on the seismic response.

First, the current state of research work related to P-Δ effects, and a review of previously published work in this field, are introduced. The shear wall building considered in this study is then adapted from Canadian Portland Cement Association (CPCA), 1985 Concrete Design Handbook. The building meets also the requirements of Canadian Standard Association (CSA) A23.3-M94 for design of concrete structures. The wall axial loads caused by the dead and live loads are considered to compute the nonlinear relations between the wall moments and curvatures.

Inelastic dynamic analyses of the shear wall considering a bilinear hysteresis rule to model the rotational hysteretic hinging capabilities of the wall are then performed to examine P-Δ effects on its seismic response. Since rigorous inelastic dynamic analyses are performed, the wall strength was selected to meet NBCC 1995 requirement without any strength increase to reduce P-Δ effects. To assess the seismic behaviour of the wall, roof displacement, shear forces and bending moments at the base of the wall, ductility along the height, and various damage indices are considered as response indicators. Nonlinear static push-over analyses under incremental lateral loading are also performed to assess the importance of P-Δ effects.

The effects of variations in modelling parameters of the shear wall building on the seismic response are investigated when subjected to Eastern, high frequency, and Western North America, low frequency, types of earthquake ground motions. These earthquake records are scaled to a peak ground acceleration of 0.18g corresponding to NBCC 1995 requirement for Montreal. Some modelling parameters, such as the axial force in the structure, hysteresis rule, and viscous damping ratio, are selected to assess their influence on the seismic response of the wall.

The results of the research work in this thesis show that P-Δ effects were insignificant in the response analyses of the shear wall structure initially designed without considering P-Δ effects. Therefore, the stability factor approach introduced in NBCC 1995 appears

to be overly conservative. The results of detailed inelastic dynamic analyses indicated that the influence of P-Δ effects on the maximum lateral displacements, base shear, displacement ductility demand, curvature ductility demand, and damage indices is minimal. The analyses also showed that the axial force in the gravity column did not significantly increase P-Δ effects for shear wall structure if the axial force is increased from P to 2P. Therefore uncertainties in the axial load are not likely to increase significantly the importance of P-Δ effects for wall structures.

The results of this study thus indicate that the NBCC 1995 stability factor approach for shear wall structures should be seriously revised to avoid unnecessary strength increase of this type of structure.

CONDENSÉ EN FRANÇAIS

Introduction

Les ouvrages en béton armé peuvent subir des déplacements horizontaux quand le chargement séismique latéral agit sur ces structures. L'action des chargements de gravité sur une telle structure déformée peut mener à une augmentation significative du déplacement latéral et des efforts internes. L'effet du deuxième ordre des chargements verticaux agissant sur une structure déformée est nommé effet P-Δ. Il est très important d'étudier en détail ces effets du second ordre lors de la conception des bâtiments. Si les effets P-Δ sur l'ossature peuvent être négligés, le coût du bâtiment peut être grandement diminué.

Le but de ce projet est d'étudier l'influence des effets P-Δ sur un mur de cisaillement typique en béton armé de 12 étages. Les secousses séismiques intenses produisent généralement une réponse structurale dynamique des bâtiments avec des déformations inélastiques. Par conséquent, des analyses dynamiques non linéaires sont effectuées avec et sans effets P-Δ sur un mur typique de 12 étages. D'abord, le modèle du bâtiment pour les analyses dynamiques est présenté. Puis, le logiciel RESPONSE (Collins and Mitchell,1987) est utilisé pour déterminer les relations moments-courbures nonlinéaires du mur pour différentes valeurs de charges axiales. Ensuite, le modèle d'hystérésis bilinéaire est présenté pour modéliser le comportement inélastique du mur. En outre, les résultats d analyses dynamiques inélastiques du mur de cisaillement, avec et sans effets P-Δ, sous différents enregistrements de tremblement de terre sont présentés au chapitre 4. Trois enregistrements de tremblement de terre sont choisis pour représenter différents types de chargements séismiques et calibrés pour être représentatifs des spectres élastiques de calcul du Code National du Bâtiment du Canada (CNBC 1995)

pour Montréal. Différents paramètres de réponses, telles que le déplacement latéral supérieur du mur, le cisaillement à la base, la réponse moment-courbure à la base du mur, et la demande en ductilité sont examinées pour comparer le comportement du mur de cisaillement avec et sans effets P-Δ.

L'étude démontre que les effets P-Δ ont peu d'influence sur les déplacements latéraux maximum, les incréments de cisaillement à la base et les dommages sous les tremblements de terre de El Centro (1940) et de Taft (1959), ainsi les effets P-Δ peuvent être négligés. Pour le tremblement de terre de Parkfield (1966), le cisaillement à la base et le déplacement latéral au sommet sont légèrement augmentés à causes des effets P-Δ. Les résultats obtenus de cette étude démontrent également que les effets P-Δ sur les demandes en ductilité de déplacement et en ductilité de courbure du mur sont minimaux sous le chargement séismique. Les effets P-Δ peuvent donc être négligés pour le bâtiment considéré.

Les effets de la variation des paramètres de modélisation du mur sur la réponse séismique sont étudiés pour des séismes de haut contenu fréqentiel, typiques de l'Est de l'Amérique du Nord, et des séismes de bas contenu fréqentiel, typiques de l'Ouest de l'Amérique que du Nord. Les paramètres principaux, tels que la force axiale dans les poteaux de gravité, les règles d'hystérésis, l écrouissage de l'acier, le coefficient d'amortissement visqueux, sont choisis pour examiner leur influence sur la réponse séismique du mur. Les résultats des analyses démontrent que la force axiale dans les poteaux de gravité n'a pas un effet important sur les déplacements horizontaux du mur pour l ensemble des séismes considérés si la force axiale est augmentée de P à 2P. L'écrouissage de l'acier produit une augmentation de la courbure et du déplacement maximum du mur avec le coefficient d'amortissement 2%, pour le séisme du Saguenay 1988 (typique de l'Est de l'Amérique du Nord). Si la règle d'hystérésis trilinéaire avec dégradation de la rigidité est considérée pour les analyses inélastiques, les effets sur la

courbure et le déplacement maximum du mur sont importants par rapport aux résultats obtenus tout en utilisant l'hystérésis bilinéaire avec ou sans l'écrouissage.

Revue de la littérature sur les effets P-Δ affectant les bâtiments avec murs de cisaillement lors des séismes

L'état actuel des recherches effectuées sur les effets P-Δ telles que rapportées dans la littérature est présenté au chapitre 2. Trois aspects principaux sont présentés: (a) le concept des effets P-Δ sur les bâtiments, (b) les effets P-Δ dans les dispositions séismiques du CNBC, et ensuite (c) les travaux de recherches précédents sur les effets P-Δ dans les bâtiments. Les effets P-Δ sur un système à un degré-de-liberté sont présentés à la Fig.2-1. Le moment P-Δ à la base de la structure est augmenté quand le déplacement horizontal augmente. Il peut de manière significative influencer la réponse d'une structure. Par conséquent, il est important d'évaluer si les effets de second ordre sont significatifs dans la conception des bâtiments. Dans le code national de bâtiment du Canada (CNBC, 1990), il n'y avait aucune condition définie pour la considération des effets P-Δ. Dans le CNBC 1995 les effets P-Δ sont considérés à l'aide d un facteur de stabilité. Le code exige que le cisaillement de conception d'étage à tout niveau soit augmenté pour contrer les effets P-Δ. Après, les recherches sur les effets P-Δ sous le chargement séismique sont présentés (Montgomery, 1980; Neuss et Maison, 1983; Thomson et al. 1991; Fenwick et al. 1992; Côté, 1997). Montgomery a présenté l'approche du coefficient de stabilité pour estimer l'influence des effets de P-Δ. Une formulation de la matrice de rigidité géométrique a été développée pour expliquer les effets P-Δ pour l analyse séismique de bâtiments de plusieurs étages par Neuss et Maison (1983).Thomson et al. 1991 ont étudié les effets P-Δ sur les cadres en béton armé sous des excitations séismiques importantes. La conclusion suivante a été obtenue: les effets P-Δ peuvent causer une augmentation significative de la déformation des cadres conçus pour se déformer de façon importante

lorsque soumis à des secousses d'intensités fortes. Trois types de coefficients d'amplification de force ont été étudiés par Côté (1997) pour considérer les effets P-Δ lors de la conception séismique des murs de cisaillement.

Modèle du bâtiment analysé

Un mur de cisaillement typique en béton armé de 12 étages a été choisi pour cette étude. Ce mur est adapté du manuel de CPCA, 1985 de conception des ouvrages en béton. Le bâtiment est situé à Montréal, Québec. La vitesse maximale horizontale au sol est $v = 0.1$ m/s. Deux systèmes structuraux différents sont disponibles pour résister aux chargements latéraux. Dans la direction E-O, les murs de cisaillement sont conçus pour résister à l'action horizontale entière du tremblement de terre, tandis que les poteaux et les poutres sont seulement conçus pour supporter des chargements de gravité. Dans la direction N-S, la résistance latérale est assurée par les cadres. Les chargements axiaux sur le mur sont principalement produits par des chargements de gravité. Les chargements axiaux dans le mur sont calculés selon le code CNBC, 1995.

Le bâtiment initial a été conçu selon la norme CSA A23.3-M84 pour les bâtiments en béton. Par conséquent, le bâtiment doit être vérifié selon la norme A23.3-M94 présentement en application. Le moment résistant pondéré à la base obtenu à partir du logiciel RESPONSE excède le moment pondéré exigé, ainsi le bâtiment répond à l'exigence de CNBC, 1995. Le calcul des facteurs de stabilité du CNBC 1995 indique qu'une augmentation de résistance latérale des étages du mur de l'ordre de 39% devrait être utilisée pour contrer les effets P-Δ. Cependant, on n'a pas majoré la résistance du mur dans cette étude puisque des analyses dynamiques nonlinéaires rigoureuses ont été effectuées. Ces analyses, avec et sans effets P-Δ, permettent d'évaluer la nécessité de majorer la résistance du mur. Le modèle du mur de 12 étages comprend le mur et les poteaux de gravité. Le mur est représenté par 12 élément de poteaux avec 3 degrés-de-liberté par nœud correspondant aux déplacements horizontaux, verticaux, et

de rotation, respectivement. Les chargements de gravité agissant à une élévation sont regroupés. Les poteaux de gravité jouent un rôle significatif dans la stabilité du bâtiment. Les poteaux de gravité sont considérées rotulés à leur base et à chaque plancher.

Le logiciel RESPONSE est employé pour obtenir les réponses non linéaires de moments-courbures des sections de béton armé. Trois couches de béton et dix couches d'acier sont employées pour décrire une section dans le logiciel. Le rapport entre le moment et la courbure du mur pour chaque étage est obtenu. Selon les résultats, un modèle inélastique bilinéaire est employé pour modéliser la rotule plastique de rotation aux extrémités de chaque élément représentant le mur.

Analyses de réponse aux séismes du bâtiment de 12 étages

Des analyses dynamiques non linéaires sont effectuées sur le bâtiment avec mur de cisaillement de 12 étages pour évaluer les effets P-Δ. Le déplacement du toit, les incréments de ductilité et l'endommagement sont considérés comme paramètres de réponse et indicateurs d'endommagement pour évaluer la réponse séismique des bâtiments. Le déplacement horizontal maximal du toit est un paramètre important pour l'étude des effets P-Δ pendant un tremblement de terre. La ductilité est définie comme la déformation maximum divisée par la déformation initiant la plasticité. La ductilité de déplacement, basée sur le déplacement du toit, est calculée comme le ratio du déplacement horizontal maximal du toit, sur le déplacement du toit qui correspond à la formation de la première rotule plastique dans la structure. La ductilité de courbure est le rapport de la courbure maximale sur la courbure initiant la plasticité.

Pour mesurer le niveau d'endommagement séismique de la structure, plusieurs valeurs d'indices d'endommagement sont calculées lors des analyses dynamiques non

linéaires. Le paramètre $D\mu_{\Delta}$ est le ratio du déplacement maximal calculé sur le déplacement ultime. La valeur maximale du déplacement calculé pour chaque étage peut être obtenue à partir des résultats du logiciel RUAUMOKO (Carr 1996). Les déplacements ultimes sont déterminés à partir des résultats des analyses de poussées latérales. Le paramètre de dommage, $D\mu_{\Phi}$, est défini comme la courbure maximale divisée par la courbure ultime. Les courbures maximales sont obtenues à partir des résultats du logiciel RUAUMOKO, alors que les courbures ultimes sont obtenues à partir des résultats du logiciel RESPONSE. L'indice d'endommagement de Park et Ang (1985) est défini comme la combinaison linéaire du déplacement maximum et du déplacement ultime plus l'énergie de plastification dissipée divisée par l'énergie absorbée à l'initiation de la plastification.

Les analyses de vibration libres sont effectuées avec le programme d'analyse structural SAP90. Différents modes de vibration sont étudiés pour en comparer les résultats. Différentes méthodes sont considérées pour le calcul de l'inertie du mur: sections non fissurées (I_g), sections fissurées, et sections effectives, sont considérées pour ces modèles. Les trois premières périodes de vibration sont obtenues pour chaque modèle. Les périodes de la vibration augmentent lorsque la section est fissurée. Les trois premières périodes de vibration sont 3.389 s, 0.555 s, 0.217s (avec P-Δ) et 3.225 s, 0.551 s, 0.216 s (sans P-Δ), si l'inertie effective 0.7 I_g, recommandée par le manuel de conception des structures de béton du CPCA (1995) est utilisée dans le calcul des périodes de vibration.

Des analyses statiques non linéaires de poussées latérales monotones sont effectuées pour examiner le comportement structural et pour évaluer l'importance des effets P-Δ. La configuration du chargement choisi représente les forces statiques équivalentes résultant du premier mode de vibration de la structure. La règle bilinéaire modifiée d'hystérésis de Takeda est employée pour modéliser la réponse moment-courbure du mur de cisaillement. La réponse du modèle de bâtiment

démontre que le mur se plastifie pour un cisaillement à la base de 0.98 fois la valeur du code, V, en incluant l'effet P-Δ, avec un déplacement relatif du toit de 0.261 % de la hauteur du bâtiment. La réponse sans considérer les effets P-Δ pour le modèle de bâtiment indique que le mur subit un cisaillement à la base de 1.04V, avec un déplacement latéral de 0.253 % de la hauteur du bâtiment.

L'analyse spectrale est la plus utilisée dans la conception parasismique. Les spectres élastiques de conception normalisés pour Montréal (CNBC,1995) sont utilisés pour l'analyse spectrale. Ils sont basés sur 5 pour cent d'amortissement critique. Le logiciel SAP90 est employé pour effectuer l'analyse spectrale. Les résultats indiquent que le déplacement pseudo-dynamique latéral relatif au sommet (déplacement élastique) est de 45.4 millimètres lorsque l'effet P-Δ est considéré, et 43.0 millimètres lorsque'il n'est pas considéré. Ainsi, le déplacement latéral du toit n'est pas augmenté de façon significative si les effets P-Δ sont considérés quand le mur est analysé par la méthode du spectre de réponse élastique linéaire.

Les enregistrements des séismes de El Centro 1940, Taft 1959 et Parkfield 1966 sont choisis pour représenter différents types de chargements séismiques. Les 20 premières secondes de tous les enregistrements sont considérées. Ces trois enregistrements sont ajustés pour obtenir une accélération de pointe au sol de 0.18g correspondant à la valeur recommandée par le CNBC, 1995 pour Montréal. Les réponses de la structure soumise à trois excitations au sol sont obtenues à partir du logiciel RUAUMOKO. Différentes quantités structurales sont examinées pour comparer le comportement du mur avec et sans les effets P-Δ. Les déplacements latéraux au toit, les forces de cisaillement et les moments de flexion à la base du mur, et la demande de ductilité sont obtenus pour chaque séisme. Des indices d'endommagement sont également calculés pour le mur.

Les résultats des analyses dynamiques non linéaires ont démontré que l'inclusion des effets P-Δ dans l'analyse des bâtiments subissant un tremblement de terre a peu d'effet

sur le déplacement latéral maximum, le cisaillement à la base et les indices d'endommagement. L'influence des effets P-Δ peut donc être négligés. Pour les secousses au sol contenant de grandes impulsions d'accélérations, les effets P-Δ peuvent augmenter de manière significative les déplacements (non élastiques) résiduels par rapport à la situation où les effets P-Δ sont négligés.

Effets des variations des paramètres de modélisation du bâtiment analysé

Quelques paramètres de modélisation sont étudiés au chapitre 5 pour évaluer la sensibilité de la réponse séismique du mur. Les objectifs de cette étude sont: (1) d'évaluer l'influence du chargement axial sur le déplacement horizontal du mur; (2) d'évaluer les variations de la réponse non linéaire pour un bâtiment typique avec mur de cisaillement en fonction du contenu en fréquences et de la durée des secousses séismiques et (3) d'étudier l'influence de la règle de dégradation de la rigidité trilinéaire d'hystérésis, de l'écrouissage de l'acier et du coefficient d'amortissement visqueux sur la réponse séismique du mur. Les principaux paramètres étudiés sont: (1) la force axiale dans le poteau de gravité; (2) les types de tremblements de terre de l'est et de l'ouest de l'Amérique du Nord; (3) les règles d'hystérésis et l'écrouissage de l'acier; et (4) le coefficient d'amortissement visqueux.

Le chargement axial dans le poteau de gravité est augmenté de P, 2P à 5P. Le logiciel RUAUMOKO est employé pour effectuer les analyses dynamiques inélastiques. Les effets de la variation de la force axiale à divers pas de temps peuvent être obtenus. Les résultats indiquent que les premières périodes de vibration du mur sont rallongées de 3.380 s à 3.556 s si la force axiale est augmentée de P à 2P. Pour une plus longue période de vibration, le déplacement latéral du mur peut être diminué. En même temps, la rigidité effective réduite pour un chargement donné, peut augmenter le déplacement latéral.

Les résultats des analyses dynamiques inélastiques du mur utilisant la règle bilinéaire d'hystérésis sont présentés au chapitre 4. Pour évaluer la variation de la réponse inélastique moment-courbure, la règle d'endommagement trilinéaire d'hystérésis est aussi considérée. La règle d'endommagement trilinéaire d'hystérésis MUTO (Carr 1996) est alors utilisée comme modèle de moment-courbure dans les analyses du mur. Les enveloppes du premier cycle sont obtenues à partir des résultats des analyses de moments-courbures du logiciel RESPONSE. Les historiques des déplacements au toit et de la courbure du mur avec et sans effets P-Δ sont obtenus pour les tremblements de terre d'El Centro (1940) et du Saguenay (1988). La courbure maximum du mur pour le tremblement de terre de El Centro est diminuée de 70% si la règle d'endommagement tri-linéaire est considérée dans l'analyse. Les études précédentes indiquent que la règle bilinéaire est préférable pour modéliser la réponse inélastique des murs de cisaillement (CAMUS 1998).

Pour évaluer l'influence de l'écrouissage de l'acier sur la réponse du mur, le comportement tri-linéaire de la relation contrainte-déformation de l'acier est considéré dans le logiciel RESPONSE pour obtenir la relation de moment-courbure. Les effets de l'écrouissage de l'acier sur le déplacement latéral au toit et sur la courbure maximale pour les types de tremblements de terre de l'est et de l'ouest de l'Amérique du Nord ne sont pas significatifs en comparant les résultats avec et sans effets P-Δ.

Pour examiner les effets de la variation du coefficient d'amortissement visqueux sur le déplacement et la courbure maximale du mur, les coefficients d'amortissement de 2%, 5% ,7% sont utilisés dans les analyses. Les résultats indiquent que le coefficient d'amortissement de 2% a un effet important sur le déplacement au toit et la courbure maximale du mur pour le tremblement de terre de l'est de l'Amérique du Nord (Saguenay 1988), le déplacement maximum est augmenté de 65 % (avec P-Δ) par rapport à la valeur obtenue pour 5% d'amortissement. Si le coefficient d'amortissement visqueux de 7% est utilisée, la courbure maximale du mur pour le tremblement du terre

du Saguenay est très près de celle atteinte en considérant 5% d'amortissement. La plupart des structures avec murs de cisaillement éprouvant une fissuration importante pendant un tremblement de terre auront un coefficient d'amortissement visqueux supérieur à 5%. Le coefficient d'amortissement visqueux ne semble pas être un paramètre critique affectant les effets P-Δ.

Conclusions

Des résultats du travail de recherche rapportés dans ce mémoire de maîtrise, plusieurs conclusions peuvent être tirées:

- L'approche du facteur de stabilité présentée dans le CNBC 1995 pour considérer les effets P-Δ lors de la conception et de l'analyse des murs de cisaillement semble être très conservatrice. Les résultats des analyses dynamiques inélastiques détaillées sans aucune augmentation de résistance pour contrecarrer les effets P-Δ indiquent que l'augmentation de résistance n'est pas nécessaire puisque les effets P-Δ ont été non significatifs dans toutes les analyses effectuées.

- Les déplacements inélastiques résiduels pourraient être augmentés par les effets P-Δ dans le cas où les secousses séismiques contiennent de longues impulsions d'accélérations. Ceci pourrait influencer la capacité portante post-séismique des poteaux d'un bâtiment et mérite d'être approfondi.

- En incluant les effets P-Δ dans l'analyse d'un bâtiment typique avec mur de cisaillement on a démontré que le chargement de tremblement de terre a peu d'effet sur les déplacements, le cisaillement à la base, la demande en ductilité de déplacement, la demande de ductilité de courbure, et les indices d'endommagement.

- Une incertitude raisonnable pour le chargement axial agissant sur la structure au moment du tremblement de terre (P à 2P) n'augmentera pas de manière significative les effets P-Δ pour des structures avec murs de cisaillement.

- Les effets de l'écrouissage de l'acier et de l'hystérésis trilinéaire sur le déplacement au toit et sur la courbure maximale sous les types de tremblements de terre de l'est et de l'ouest de l'Amérique du Nord ne sont pas importants en comparant les résultats avec et sans les effets P-Δ.

- L'étude indique que le déplacement au toit sous le tremblement de terre du Saguenay de 1988 est augmenté de 65 % (avec P-Δ) si le coefficient d'amortissement de 2% est utilisé par rapport aux résultats avec 5% d'amortissement.

- Les variations de réponses structurales calculées avec le coefficient d'amortissement de 7% peuvent être négligées par rapport aux résultats utilisant le coefficient d'amortissement de 5%. La plupart des structures avec murs de cisaillement éprouvant une fissuration importante pendant un tremblement de terre auront un amortissement visqueux supérieure à 5%. Le coefficient d'amortissement visqueux ne semble pas être un paramètre critique affectant les effets P-Δ.

TABLE OF CONTENTS

LIST OF TABLES

LIST OF FIGURES

LIST OF APPENDICES

CHAPTER 1

INTRODUCTION

1.1 Research problem

To resist severe seismic ground motions, it is uneconomical to design all reinforced concrete shear wall structures to remain in the elastic range. In general, seismic loads produce a dynamic structural response of shear walls with some degree of inelastic deformations. In the conventional analysis and design of structures, it is usually assumed that displacements and strains are small. The seismic loads tend to laterally displace the structure but the gravity loads are assumed to act on the undisplaced structure. However, it is generally recognized that large displacements and strains will occur when structures are subjected to major earthquakes. The second order effect of vertical loads acting upon a laterally displaced structure is termed the P-Δ effect. With the current trend in earthquake resistant design being towards buildings using taller and lighter shear wall structures that dissipate earthquake energy by ductile behaviour, thus producing large lateral displacements, it is becoming more important to thoroughly study P-Δ effects.

Some previous research work has been presented on P-Δ effects in reinforced concrete structural wall. Fenwick (1992) studied P-Δ effects in a series of frames and walls. P-Δ effect amplification factors were proposed to account for P-Δ effect in the seismic design. To obtain amplification factors, corresponding single-degree-of-freedom (SDOF) systems were used considering the respective wall and frames properties. It was concluded that the method of assessing the strength increase required to counter the additional effect of P-Δ in SDOF structures can be successfully applied to multi-storey structures. The results showed that the walls are relatively insensitive to P-Δ effects. The P-Δ amplification factors for the walls were only 7.1 percent for a 24 storey building. To further study P-Δ effects on multi-storey reinforced concrete wall structures

of different heights, Côté (1997) introduced several methods to define strength amplification factors for mitigating P-Δ effects. Inelastic dynamic analyses with and without P-Δ effects were performed with the RUAUMOKO computer program (Carr, 1996) on very simplified shear wall structures. The displacement ductility demand was examined. The main conclusions were that: (a) P-Δ effects have little influence on the displacement ductility demand for the walls analysed; (b) due to P-Δ effects, the increase in the ductility demand under high frequency Eastern North America type of earthquakes is less than that for low frequency Western North America type of earthquakes. In the National Building Code of Canada 1995 (NRCC,1995), a stability factor, θ_x , was introduced to consider P-Δ effects for frame and wall structures. The code requires that the design storey shear at any level be multiplied by an amplification factor $(1+\theta_x)$. However, previous studies on simplified systems indicate that P-Δ effects for shear wall structures are not significant as compared to P-Δ effects in moment resisting frames (Fenwick 1992, Côte 1997). Additional research is still needed to confirm these findings with more realistic shear wall structures.

1.2 Objectives

The goal of this thesis is to investigate the influence of P-Δ effects on a typical 12-storey reinforced concrete structural wall being part of a building designed according to the NBCC 1995 and the CSA Standard A23.3-M94 Design of Concrete Structures (CSA,1994). It is recognized that it is important to study the P-Δ effects and inelastic behaviour in actual shear wall design. The objectives of this thesis are to:

1. Present a thorough investigation of the P-Δ effects under earthquake loading in terms of lateral displacement at the top of the wall, base shear, moment-curvature response at the base of the wall, lateral displacement envelopes, ductility demand

and damage indices related to the 12-storey reinforced concrete shear wall building analyzed.

2. Study the influence of the modelling parameters of the shear wall structure on (a) the lateral displacements of the wall, (b) the wall's failure mechanisms, and (c) the top displacements of the wall and its maximum curvatures. The main parameters investigated are:

   - The amount of gravity loads in the structure;
   - The frequency content of the earthquake ground motions;
   - The hysteresis rules (bi-linear or tri-linear with degrading stiffness), and the strain hardening of the reinforcing steel;
   - The viscous damping ratio.

1.3 Methodology

To achieve the above objectives, the methodology used in this study is as follows:

1. To assess the current state of research work done on the P-Δ effects in building structures and review previously published work.
2. To design the wall as part of a 12-storey building located in Montreal using the provisions of NBCC 1995 and the CSA Standard A23.3-M94. The building is adapted from Example 11.5 of the CPCA 1985 Concrete Design Handbook.
3. To present the relationship between moment and curvature of the wall for each storey by using the RESPONSE computer program (Collins and Mitchell,1987) and define the basic properties of the hysteresis rules used in the inelastic model.
4. To perform free-vibration analyses to compute the structural periods of vibration and mode shapes of walls with various assumptions for the cracked inertia by using the SAP90 computer program (Wilson and Habibullah,1992).

5. To perform push over analysis to assess the P-Δ effects on the lateral load-displacement response of the wall.
6. To select three earthquake accelerograms to represent seismic ground motions with different frequency contents. These accelerograms are scaled to 0.18 g, which corresponds to the peak ground acceleration of NBCC 1995 for Montreal.
7. To examine P-Δ effects on the dynamic inelastic response of the shear wall by using the RUAUMOKO computer program (Carr,1996).
8. To perform parametric analyses to assess the effects of variation in the wall modeling parameters on the seismic response.
9. To provide the summary, conclusions, and recommendations for future work.

1.4 Organization of the thesis

This research project is reported in four major sections. First, the review of P-Δ effects on the seismic response of buildings is presented in Chapter 2. In this Chapter, the concept of P-Δ effects on buildings is first introduced. Then, P-Δ effects in NBCC seismic provisions are reviewed. Finally, past research on P-Δ effects in earthquake resistant design of building structures are discussed.

In Chapter 3, the model of a typical 12-storey reinforced concrete shear wall building for carrying out dynamic analyses is presented. The building is located in Montreal, Quebec. The design seismic load is calculated according to NBCC 1995. The wall axial loads are used to compute the relation between the wall moment and curvature using the RESPONSE computer program. A bilinear inelastic hysteresis rule is introduced to model the inelastic behaviour of the wall. The 12-storey wall structure is designed according to the CSA Standard A23.3-M94.

Chapter 4 introduces the earthquake response analyses of the 12-storey shear wall building. The response parameters and damage indices are presented to assess the seismic response of the building. The free vibration analyses are carried out to compute the structural periods of vibration. Three earthquake records are selected as input ground motions. Pushover analyses are performed to assess P-Δ effects on the lateral load-displacement response of the wall. The results of the inelastic dynamic analyses, with and without P-Δ effects, are obtained by using the RUAUMOKO computer program.

Chapter 5 presents the effects of varying the modelling parameters of the wall on its seismic response. Finally, in Chapter 6, a summary of the thesis, conclusions, and recommendations for future work are presented.

CHAPTER 2

REVIEW OF P-Δ EFFECTS ON THE SEISMIC RESPONSE OF SHEAR WALL BUILDINGS

2.1 Introduction

The review of P-Δ effects on the seismic response of shear wall buildings is presented in this chapter. The first section describes the concept of P-Δ effects on buildings. Because the methodology of dynamic analyses that account for both P-Δ effects and inelastic behaviour of buildings are expensive, it is very important to study when such analyses are required in actual building design. The second section reviews P-Δ effects in NBCC seismic provisions. NBCC 1990 (NRCC,1990) required that P-Δ effects in buildings be taken into account under seismic loading, but no practical methodology was proposed. A method was thus proposed in the NBCC user's guide (NRCC,1996). A stability factor was defined to consider P-Δ effects. The code requires that design storey shear at any level be increased to consider P-Δ effects. In the next section, past research on P-Δ effects under seismic loading are presented (Montgomery, 1980; Neuss and Maison, 1983; Thomson et al. 1991; Fenwick et al.1992; Linde et al.1998; Côté, 1997). Several analytical methods are introduced to study P-Δ effects for different types of buildings. Finally, a summary of the key findings from this review are presented.

2.2 P-Δ effects on buildings

When the seismic lateral loading acts on a building, causing it to deflect, the gravity loading on such laterally deformed structure may cause the lateral displacements to increase. The second order effect of vertical loads acting upon a laterally displaced

structure is termed the P-Δ effect, where P is the total vertical load, and Δ is the lateral displacement relative to the ground.

Figure 2-1 shows the P-Δ effect on a SDOF system. The P-Δ effect refers to the mass of the structure with a weight, P, moving through a displacement, Δ, causing a moment at the base of the structure equal to PΔ. The total moment at the base of a structure, M, is given by:

$$M = HL + P\Delta \tag{2.1}$$

where: H = the equivalent lateral force at the top of the structure,

L = the height to the centre of mass,

P = the gravity load,

Δ = the lateral relative displacement.

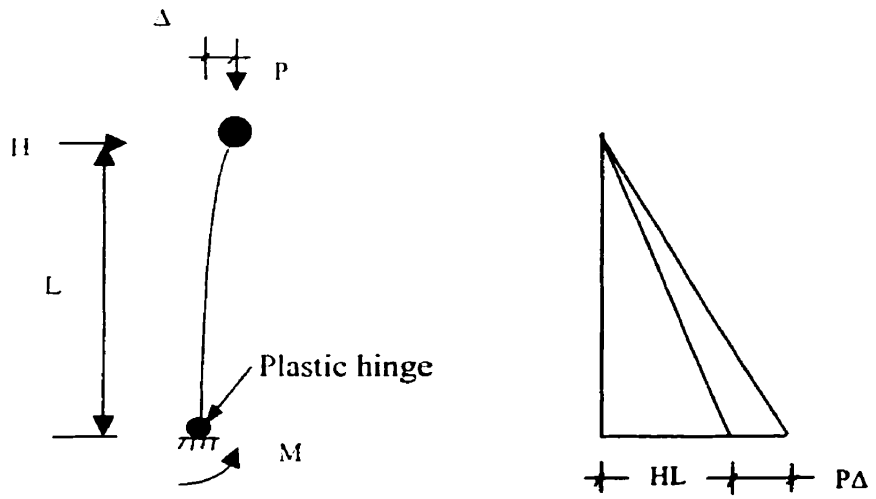

(a) SDOF **(b) Moment**

Figure 2-1 The P- Δ effect on a SDOF system.

As the displacements increase, the P-Δ moment at the base of the structure increases. This P-Δ moment may significantly influence the response of a structure, sometimes causing an increase in the maximum displacement. In low-rise structures, P-Δ effects are often small enough to be neglected. However, in taller buildings, the P-Δ effects become more significant because the buildings tend to be slender and the lateral deflections may be much larger. In an extreme case of a very flexible structure with large gravity loading, the gravity loading acts on such a large deformed structure so that P-Δ effects under seismic excitations are severe enough to initiate collapse. Thus, it is important to assess whether or not the second-order effects are significant and should be taken into account in design.

2.3 P-Δ Effects in NBCC Seismic Provisions

The 1990 National Building Code of Canada demanded that P-Δ effects in buildings be considered under seismic loading, but there was no specific requirements for the inclusion of P-Δ effects in the provisions.

In the National Building Code of Canada 1995, the minimum design lateral seismic force at the base of the structure is given by the following formula:

$$V = \left(\frac{V_e}{R}\right) \cdot U \tag{2.2}$$

where: V = minimum design lateral seismic force,

V_e = equivalent lateral seismic force representing the elastic response,

U = calibration factor ($U = 0.6$),

R = force modification factor, reflecting the capability of a structure to dissipate energy through inelastic behaviour ($1.0 \leq R \leq 4.0$).

The equivalent lateral seismic force, V_e, is given by:

$$V_e = v\,S\,I\,F\,W \tag{2.3}$$

where: v = zonal velocity ratio (peak ground horizontal velocity),

S = seismic response factor,

I = seismic importance factor, (*1.5* for post disaster buildings, *1.3* for schools, *1.0* for other types of buildings),

F = foundation factor ($1.0 \leq F \leq 2.0$),

W = seismic weight, which includes dead load plus 25% of the design snow load, 60% of storage loads, 100% load of tanks.

The base shear, V, is the sum of the inertia forces produced by the masses of the structure as a result of a horizontal movement at the base. It is assumed to mainly be induced by the response of the building in its first mode of vibration. So, the lateral inertial force, F_x , acting at any level x, is given by:

$$F_x = \left(\frac{W_x h_x}{\sum_{i=1}^{N} W_i h_i} \right) (V - F_t) \tag{2.4}$$

where: W_x = the seismic weight at the level under consideration,

h_x = height at level x from the base,

N = number of floors,

F_t = lateral force to be applied at the top of the structure to account for the influence of high vibration modes:

$$F_t = 0.07TV \leq 0.25V \quad , T \geq 0.7s \tag{2.5}$$

$$F_t = 0 \quad , T < 0.7s$$

T = fundamental period of the structure.

A practical methodology is proposed in Appendix J of NBCC 1995 User's Guide to account for P-Δ effects under seismic loading. A stability factor is introduced to account for P-Δ effects. The stability factor at any level x , θ_x, is equal to:

$$\theta_x = \frac{\sum_{i=x}^{N} P_i \cdot \Delta_{max}}{\sum_{i=x}^{N} F_i \cdot h_s} \tag{2.6}$$

where:

$\sum_{i=x}^{N} F_i$ = seismic shear force at the level under consideration, which is equal to the sum of the design lateral forces acting at, and above, the storey under consideration.

$\sum_{i=x}^{N} P_i$ = the total gravity load acting at, and above, the level under consideration,

Δ_{max} = the maximum inelastic interstorey deflection ($\Delta_{max} = R^* \Delta_e$),

h_s = the interstorey height.

The code requires that the design storey shear at any level be increased to account for P-Δ effects according to:

$$\sum_{i=x}^{N} F_i' = \sum_{i=x}^{N} F_i + \sum_{i=x}^{N} P_i \frac{\Delta_{max}}{h_s} = \sum_{i=x}^{N} F_i (1 + \theta_x) \tag{2.7}$$

If θ_x is less than 0.10, P-Δ effects can be ignored. The structure should be redesigned when the stability factor, θ_x, is larger than 0.40.

2.4 Research work on the P- Δ effects in building structures

2.4.1 Influence of P-Δ effects on seismic design (Montgomery, 1980)

Montgomery (1980) presented a study of the influence of P-Δ effects on the response of buildings that are subjected to earthquake base motions using time-history analysis. The influence of P-Δ effects on the responses of 1, 5, and 10-storey shear buildings was studied. The analyses were performed using the Newmark-Beta method with $\beta=1/6$. Five earthquake ground motions were used, which covered a wide variety of intensities, site conditions, and durations of strong motions. The results of the study clearly indicated that P-Δ effects have only a small influence on the response for buildings responding elastically or in a slightly inelastic manner to seismic ground motions. However, P-Δ effects should be taken into account for systems responding in a highly inelastic manner. This study indicated that P-Δ effects are often significant for buildings where the ratio between the weight and base shear, W/V, is greater than or equal to 10, or the ratio of maximum relative storey drift to yield relative storey drift is greater than 2.

The stability factor approach for estimating the influence of P-Δ effects, as later adopted by NBCC 1995, is described by Montgomery (1980). When the response is elastic or slightly inelastic, the method gives reasonable results. However, Montgomery indicated that the method should not be used for systems responding in a strongly inelastic manner. When inelastic behaviour becomes significant, the transient displacement response is quite different from that of simplified NBCC pseudo-static provisions leading to different values for stability factors.

2.4.2 Analysis for P-Δ effects in seismic response of buildings (Neuss and Maison, 1983)

To account for P-Δ effects in computer seismic analysis of multi-storey buildings, Neuss and Maison presented a matrix formulation based on the concept of geometric stiffness. The method is based on a linear solution approach requiring no iteration, and can be used for performing static or dynamic elastic analyses. It has been suggested that a deflection amplification factor, C_d, predicts the magnified deflections and overturning moments caused by P-Δ effects in static or dynamic analysis for elastic displacement levels. In order to compare the influence of different C_d values on analytical response quantities, P-Δ effects were incorporated into the analyses using C_d factors equal to 0 (P-Δ effect ignored), 1 (P-Δ forces based on elastic limit deflection levels), and 5.5 (P-Δ forces based on extreme inelastic deflection levels). Amplified P-Δ effects resulting from inelastic displacement levels that may occur during a major earthquake can therefore be accounted for in an approximate manner.

The method was implemented in a modified version of the ETABS computer program and applied in seismic analyses of a 31-storey steel construction model. The analyses showed that the story drift, shear and overturning moment responses at all levels of a building for any value of C_d are increased if including the P-Δ effects in static analyses. However, the story drift, shear and overturning moment responses at a given story of the building may be increased or decreased in elastic dynamic analyses. So, including the P-Δ effects in elastic dynamic analyses may not necessarily lead to a more conservative design throughout the building than if P-Δ effects are ignored. P-Δ effects magnification corresponding to elastic displacement levels (C_d=1.0) may be viewed as unconservative for design purposes considering the larger inelastic displacement levels that occurs during a major earthquake.

2.4.3 P-Δ effects in the seismic response of ductile reinforced concrete frames (Thomson et al. 1991)

Thomson et al. 1991 analyzed a series of five different frames of six, twelve, eighteen and twenty-four stories to study P-Δ effects in ductile reinforced concrete structures under strong seismic excitations. All structures were subjected to three digitized ground motion records. In all analyses, the duration of the excitation was taken as 15 s. A time step of 0.01 s is used for the majority of analyses. The analyses are carried out using the computer program RUAUMOKO (Carr,1996). which performs inelastic time-history analyses of two-dimensional structures. Plastic hinges are assumed to form at the ends of the members. The columns allow for an interaction between the axial force and yield moments. Rigid end-blocks are allowed for in both the columns and the beams, and the inelastic action used a Giberson one component hysteresis model (Sharpe,1974). Figure 2-2 shows the Giberson one component hysteresis model which has a possible plastic hinge at one or both ends of the elastic central length of the member.

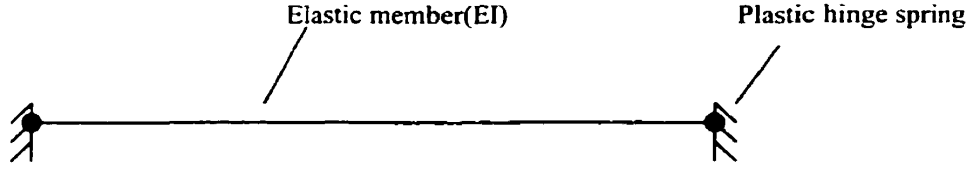

Figure 2-2 Giberson one component hysteresis model.

The evaluation of P-Δ effects included the calculation of the amplification of both the maximum beam curvature ductility demand, as well as the average curvature ductility amplification over the height of the building. The following conclusions have been obtained: P-Δ effects can cause a significant increase in plastic deformations of frames designed to perform in a ductile manner when subjected to strong ground motions. If P-Δ effects are estimated to be excessive, it is considered more practical and effective to strengthen a structure than to stiffen it.

2.4.4 P-Δ actions in seismic resistant structures (Fenwick et al. 1992)

Fenwick et al.1992 reviewed the results of inelastic time history analyses done on SDOF structures to assess P-Δ effects induced in earthquakes. The conclusions from the analyses with different earthquake ground motions are: (1) P-Δ effects increase with the duration of intense ground shaking; (2) P-Δ effects are negligible in elastically responding structures; (3) reducing the equivalent viscous damping increases the P-Δ effects. Analyses showed that changing the hysteretic response to allow for stiffness degradation and changing the strain hardening ratio have only a small influence on the P-Δ response of ductile SDOF structures.

Based on the analyses of SDOF structures under earthquake ground motions with duration of severe shaking in the 15 to 25 second range, a method was proposed to assess the strength increase necessary to prevent the ductility demand to increase when P-Δ effects are included. The required strength increase was determined in terms of the P-Δ amplification factor, β, and a factor K_t, which allows for the influence of the fundamental period and the soil type.

A series of multi-storey walls and frames were analysed to obtain P-Δ amplification factors. The corresponding equivalent SDOF values were also calculated using the respective wall and frames properties. From these analyses it was concluded that the method of assessing the strength increase required to counter the additional effect of P-Δ in SDOF structures can be successfully applied to multi-storey structures. A set of design steps for calculating the strength increase necessary to counter P-Δ effects in structures was outlined. The distribution of strength increase within the structure is determined by a pin jointed truss model with a deflected profile derived from either the equivalent static approach or from the response spectrum method. This strength distribution is then scaled by the appropriate SDOF β factor, modified by the factor K_t.

It was shown that shear wall structures are relatively insensitive to P-Δ effects. The P-Δ amplification factors for walls was only 7.1% for a 24 storey building.

2.4.5 Evaluation of R/C structural walls designed according to EC8 (Linde and Moehle, 1998)

To evaluate the nonlinear dynamic behaviour of walls designed according to the new European seismic code EC8 (1998), two buildings comprising four-storey and eight-storey of three by five bays were studied by Linde and Moehle,1998. Structural walls were designed to resist seismic action, while only the columns and T-beams carried gravity loads. Due to symmetry, half of the lateral storey masses were considered in the static equivalent force calculation. In the EC8 code, ductility classes range from DCL over DCM to DCH, indicating low, medium, and high ductility. According to EC8, the static equivalent force is distributed linearly over the height of the building in a triangular pattern without a concentrated force at the top. Torsion effects may be neglected in a symmetric plan case. The flexural resistance is calculated assuming a strain at the compressive edge of 0.0035, a rectangular concrete stress-block, and an ideal elastic-plastic behaviour of the reinforcing bars. An amplification factor for shear, ε, is introduced in EC8: for DCL, $\varepsilon = 1.3$, for DCH, $\varepsilon = 2.65$.

Linde and Moehle used a numerical model developed particularly for the global analysis of reinforced concrete walls to study a 4 and 8-storey building. The model consisted of nonlinear springs connected by rigid beams. The corresponding designs are referred to as ECL8 and ECH8 for the 8-storey building. Using the EC8 code formula, the resulting periods agreed well with numerical results for the 8-storey wall but were somewhat longer for the 4-storey wall. Two ground acceleration time histories were used to carry out nonlinear dynamic time history analyses. Three response quantities as a function of time were analysed: roof displacements, shear forces at the base of the wall, and bending

moment at this location. The distribution over the wall height of the shear force and bending moment demand were also obtained from the analyses. The maximum curvature ductility demand and maximum inter-storey drift values were also obtained for each design and for each ground motion.

The results of nonlinear dynamic response analyses on the wall lead to the following conclusions: (1) the introduction of a magnification factor for shear in EC8 represents an improvement compared to SIA (Swiss National Standard), (2) the linear design envelope for flexural resistance in EC8 is more conservative than the envelope of SIA, and (3) the EC8 formula for the fundamental frequency proved to agree well with numerical results for the 8-storey wall.

2.4.6 An evaluation of strength amplification factors for mitigating P-Δ effects in multi-storey buildings (Côté, 1997)

Côté (1997) studied the use of strength amplification factors to mitigate the P-Δ effects in multi-story reinforced concrete wall structures (1-,3-,5-,10-,15-,25-storey). These wall models included one node per floor, and each node had three degrees-of-freedom corresponding to the horizontal, vertical and rotational displacements, respectively. The mass was assumed to be lumped at the floor levels, and the gravity loads acting at a given floor were lumped at the corresponding node. The bi-linear degrading stiffness hysteresis rule was considered for the inelastic analysis

Several methods were applied to determine the strength amplification factors for mitigating the P-Δ effects. With the RUAUMOKO computer program, inelastic dynamic analyses with and without P-Δ effects were performed, and the displacement ductility demand was examined. The following results have been obtained: (1) the ductility demand was slightly higher for the bi-linear behaviour with stiffness degradation

compared to the bi-linear behaviour without stiffness degradation. (2) P-Δ effects had little influence on the displacement ductility demand for the different walls. (3) Due to P-Δ effects, the increase in the ductility demand under high frequency Eastern North America type of earthquakes is less than that of low frequency Western North America type of earthquakes. (4) The value of the ductility demand obtained without P-Δ effects decreases with the number of storey because the ductility concept used in the thesis is based on the displacement at the top of the structure.

However, Côté (1997) used a simple dynamic model of the walls that were not designed and detailed as part of a complete building system. The inelastic behaviour was only modeled at the base of the walls. To further study P-Δ effects in multi-storey reinforced concrete wall structures, a more realistic wall model, being part of a complete building system, is studied in this thesis. Inelastic hysteresis rules are used to model each storey of the wall. The effects of variation in wall modeling parameters are studied further.

2.5 Summary

In this chapter, a review of P-Δ effects on the seismic response of shear wall buildings was presented. Key findings are summarised below:

(1) P-Δ effects may be neglected in design for low-rise structures.

(2) Montgomery (1980) presented the stability factor approach for estimating the influence of P-Δ effects when the response is elastic or slightly inelastic. However, Montgomery indicated that the method should not be used for systems responding in a strongly inelastic manner.

(3) A geometric stiffness matrix formulation to account for P-Δ effects in computer seismic analysis of multi-storey buildings was presented by Neuss and Maison (1983). The method can be used for static or dynamic elastic analyses. Amplified P-Δ effects resulting from inelastic displacement levels that may occur during an earthquake can be considered in an approximate manner.

(4) P-Δ effects can in some cases cause a significant increase in plastic deformations of frames designed to perform in a ductile manner.

(5) Fenwick et al. showed that P-Δ effects on concrete structures responding in the inelastic range to earthquakes were less important for walls than for frames.

(6) Evaluation of R/C structural walls designed according to EC8 was presented by Linde and Moehle (1998). The introduction of an amplification factor for shear in EC8 represents an improvement to evaluate the nonlinear dynamic behaviour of walls.

(7) Three types of strength amplification factors have been reviewed by Côté (1997) to account for P-Δ effects in the seismic design of wall buildings. It was found that P-Δ effects induced by seismic excitations on internal forces and displacement ductility demand are very limited. However, the dynamic model of the wall used in Côté's work was very simple.

CHAPTER 3

BUILDING MODEL ANALYZED

3.1 Introduction

A typical 12-storey R/C buildings is used to study further P-Δ effects on the inelastic dynamic seismic response of concrete shear walls. The building is first introduced in this chapter. Then, the modelling of gravity loads as well as the use of a fictitious gravity column to account for P-Δ effects in the seismic analysis are described. Next, the model of the building used for carrying out the dynamic analyses is presented. Furthermore, the wall axial loads caused by the dead and live loads are calculated to derive the relation between the wall moment and curvature using the RESPONSE computer program (Collins and Mitchell, 1987). Finally, a stiffness degrading hysteresis rule is selected to represent the inelastic behaviour of the wall.

3.2 Description of the 12-storey building analyzed

The typical 12-storey reinforced concrete wall-frame building selected for this study is adapted from Example 11.5 of the CPCA 1985 Concrete Design Handbook (CPCA,1985). Figure 3-1 shows the floor plan view of the building. It is located in Montreal, Quebec, and is built on a rock site. The seismic zones for Montreal are Z_a=4 and Z_v=2. The design peak ground horizontal velocity, v=0.1m/s, is obtained by the seismic zoning maps of the 1995 NBCC. In the N-S direction, the structure has seven 6m bays. In the E-W direction, it has two 9 m office bays with 1.5 m cantilever overhangs, and a central 6 m-corridor bay. The storey height is 3.65 m, except for the first storey, which is 4.85 m high. The building is symmetrical in both directions.

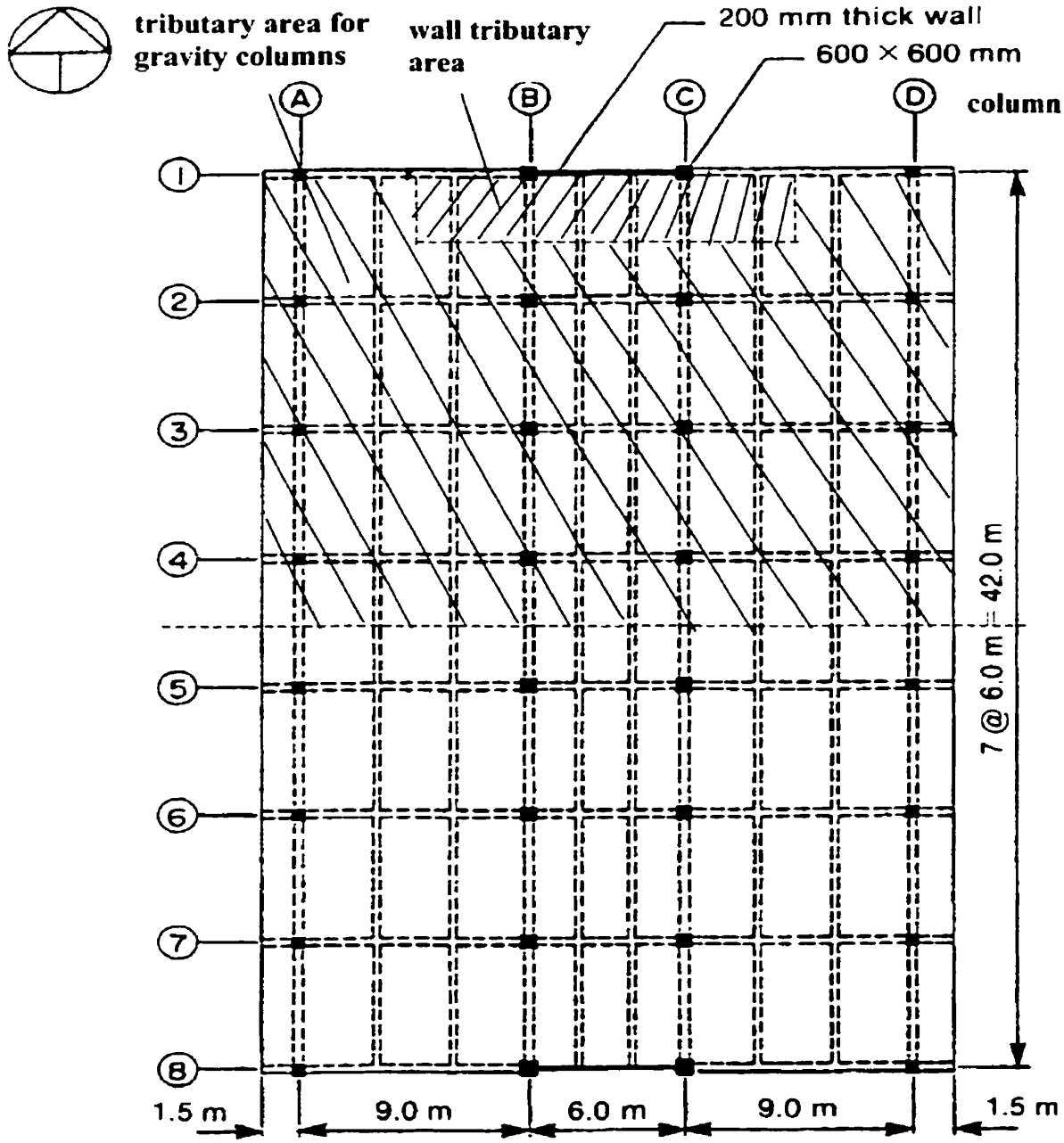

Figure 3-1 The plane of the 12-storey wall frame building.

The response of the building in the E-W direction is examined in this study. In this direction, two identical shear walls are located along column lines 1 and 8. In-plane torsion is neglected in this study and all lateral loads are assumed to be entirely resisted

by the shear wall. Therefore, each wall is assumed to resist half the seismic load. A yield strength of 400 MPa is assumed for the steel reinforcement and a compressive strength of 30 MPa is considered for the normal density concrete. The shear walls are assumed to be fixed at their bases. The dimensions and properties of wall, beam, and column sections are given in Table 3-1.

3.3 Modelling of gravity loads

In the 12-storey wall-frame structure, the design floor live load is 2.4 kN/m^2 for the office floor area and 4.8 kN/m^2 for the 6 m wide corridor bay. The design roof live load includes 2.2 kN/m^2 for full snow load and an additional 1.6 kN/m^2 for mechanical service loading on the 6 m wide strip over the corridor bay. Design dead load includes 1.0 kN/m^2 for partition loading and 0.5 kN/m^2 for mechanical services loading at all levels, and 0.5 kN/m^2 at the roof level for the insulation.

In the E-W direction, the load bearing shear walls are designed to resist the entire horizontal earthquake action, whereas the columns and beams are only designed to carry gravity loads and do not resist any earthquake action. So, the lateral loads mainly induce bending moments and shear forces in the walls. However, wall axial loads are induced by the wall tributary dead and live loads. The lateral loads do not cause any axial loads on the symmetrically placed walls. In the N-S direction, lateral resistance is assumed to be entirely ensured by the frames, Therefore, wall axial loads are only produced by gravity loads.

The axial loads in the wall, P, have been calculated according to NBCC 1995. The detailed calculations are presented in APPENDIX A. As prescribed in the NBCC, the load combination including 100% dead load plus 50% live loads (D+0.5L) was considered in this study. In addition, live load reduction for floor occupancy live load

was applied as permitted in the NBCC. The wall tributary area for calculating N is shown in Figure 3-1. A summary of the results is presented in Table 3-2.

The 12-storey shear wall analytical model used in this study (section 3.6) included the wall as well as a gravity column. The gravity column is fictitious column, which carry only the gravity loads of the real columns stabilised by the wall. The gravity column is coupled to the wall at each floor level. It plays a significant role in the stability of the building as their stability in the E-W direction is provided by the wall. The gravity column is considered pin-connected at its base and at each floor. For each floor, the horizontal degree of freedom of the gravity column is constrained to be the same as that of the wall. The axial loads acting in the gravity column are due to gravity loads applied on the tributary area shown in Figure 3-1. They have been computed for the load combination D+0.5L and the results are given in Table 3-3.

Table 3-1 Dimensions and properties of members sections.

	B * H (mm)	Area (mm^2)
Interior Columns		
1 – 6 storey	600*600	360000
7 –12 storey	550*550	302500
External Columns		
Boundary of walls	600*600	360000
Others	500*500	250000
Secondary Beams	300*350	105000
Beams of Frames		
1 - 3 storey	400*600	240000
4 – 12 storey	400*550	220000
Wall	200	1800000

Table 3-2 Axial load, P, acting on one shear wall.

	Dead, D	Live, L	Combination
Storey	P_D (kN)	P_L (kN)	$P_D + 0.5P_L$ (kN)
12	-406	-128	-470
11	-834	-227	-948
10	-1262	-298	-1411
9	-1690	-366	-1873
8	-2118	-430	-2333
7	-2546	-492	-2792
6	-2974	-553	-3251
5	-3402	-612	-3708
4	-3830	-670	-4165
3	-4266	-727	-4630
2	-4701	-785	-5094
1	-5188	-840	-5608

Table 3-3 Axial load in the gravity column stabilised by one wall.

	Dead, D	Live, L	Combination
Storey	P_D (kN)	P_L (kN)	$P_D + 0.5P_L$ (kN)
12	-3154	-1321	-3815
11	-6569	-1737	-7438
10	-9984	-2228	-11098
9	-13399	-2708	-14753
8	-16814	-3184	-18406
7	-20229	-3658	-22058
6	-23674	-4129	-25739
5	-27119	-4599	-29419
4	-30564	-5067	-33098
3	-34091	-5536	-36859
2	-37618	-6003	-40620
1	-41265	-6471	-44501

3.4 Moment - curvature response of the wall

The cross-section of the wall is uniform over the entire height of the building. The amount of reinforced steel varies along the height. Figure 3-2 (a) shows the cross-section and the reinforcing steel at levels 1 and 2. The reinforcing steel at other floors is given in Figure 3-3.

The **RESPONSE** program (Collins and Mitchell, 1987) was used to produce the complete non-linear moment-curvature response of all wall element cross sections. The relation between stress and strain of concrete is defined in Figure 3-4(a) with $\varepsilon'_c = 2f'_c/E_c$, $f'_c = 30$ MPa, and $E_c = 4500f_c'^{1/2} = 24648$ MPa. The following equation was used: $f_c = (2\varepsilon_c/\varepsilon'_c - (\varepsilon_c/\varepsilon'_c)^2)\, f'_c$. As shown in Figure 3-2 (b) to (e), three concrete layers are used to describe a cross section in the RESPONSE program. The program uses only one type of steel, which is described by a bilinear stress-strain relationship with $E_s = 200.000$ MPa, $f_y = 400$ MPa. The maximum strain of steel used in the program is: $\varepsilon_{su} = 0.2$.

The longitudinal reinforcing steel was lumped into the 10 layers in the RESPONSE program. The steel layers are illustrated in Figures 3-2 (b) to (e).

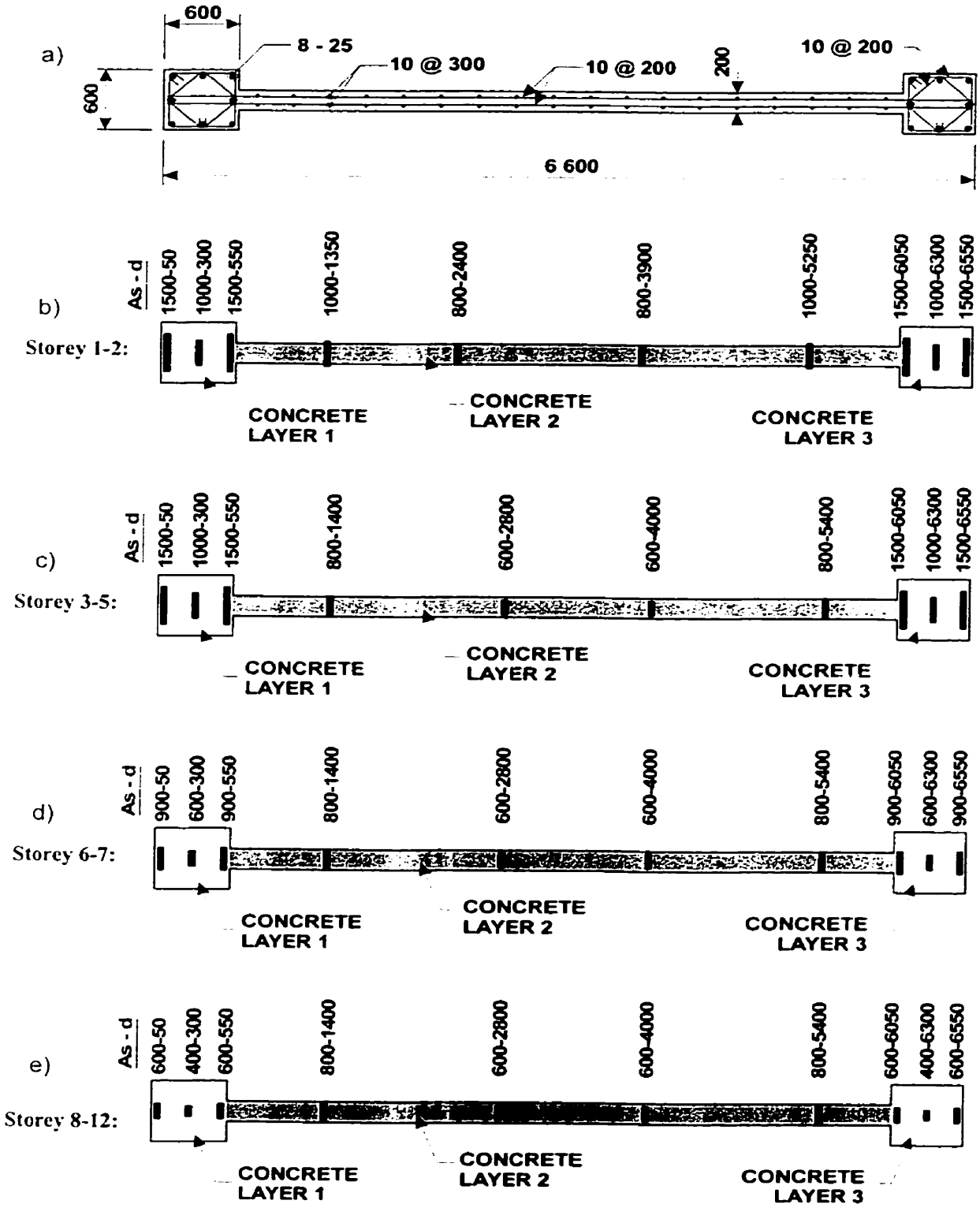

Figure 3-2 Cross-section of the wall.

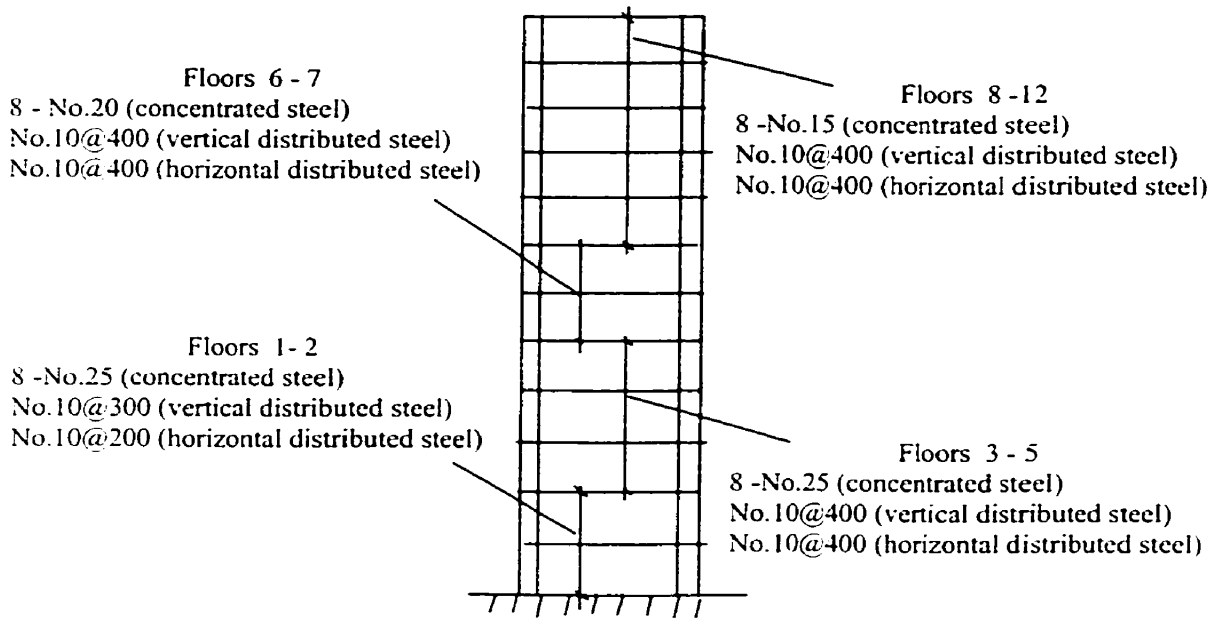

Figure 3-3 Distribution of steel along the height of the wall.

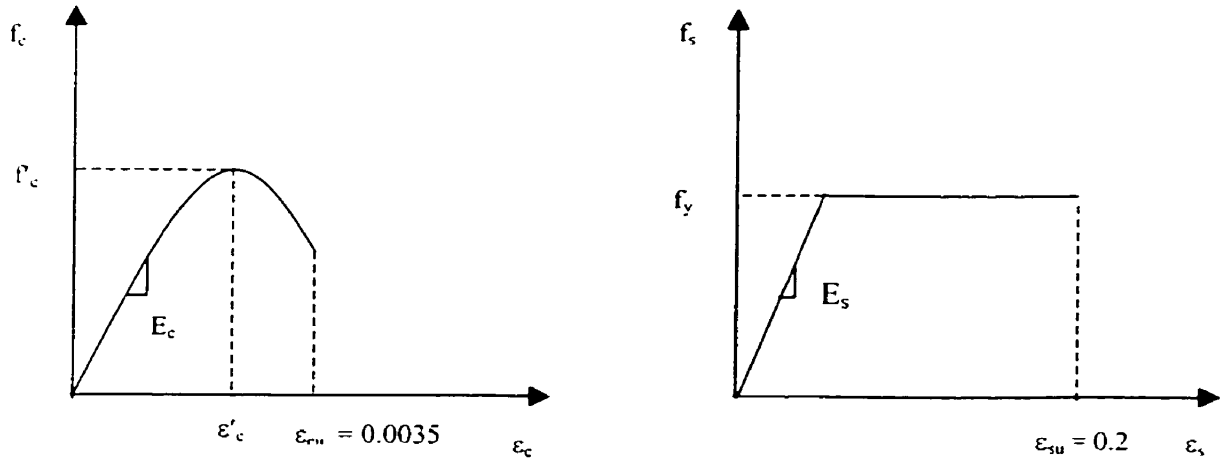

(a) Concrete stress-strain model; (b) Steel stress-strain model.

Figure 3-4 Material models used in Computer Program RESPONSE.

The results are given in Figures 3-5 to 3-16 and the main properties are summarised in Tables 3-4 and 3-5 with P corresponding to axial loads acting in the wall (Table 3-2). The calculations were performed with and without axial load to assess the importance of this parameter. The parameters r, M_y and Φ_y will be explained in the section 3.6.

Table 3-4 Summary of the moment-curvature property ($P \neq 0$).

Storey	$0.7I_g$ (10^6 N.m^2)	r (10^{-3})	M_{cr} (kN-m)	M_y (kN-m)	Φ_y (rad/km)	Φ_u (rad/km)	P (kN)
12	6.388	0.640	9975	8740	0.045	6.30	-470
11	6.388	0.484	10692	10154	0.063	6.30	-948
10	6.388	0.324	11384	11700	0.070	6.30	-1411
9	6.388	0.351	12072	13100	0.079	6.42	-1873
8	6.388	0.368	12756	14500	0.104	6.42	-2333
7	6.388	0.622	13551	17600	0.118	6.42	-2792
6	6.388	0.327	14233	19286	0.129	6.42	-3251
5	6.388	0.35	15162	24546	0.159	6.55	-3708
4	6.388	0.592	15844	25636	0.154	6.42	-4165
3	6.388	0.434	16536	27158	0.186	6.55	-4630
2	6.388	0.762	17219	29263	0.171	6.55	-5094
1	6.388	0.480	17993	31059	0.207	6.67	-5608

Table 3-5 Summary of the moment-curvature properties ($P = 0$).

Storey	$0.7I_g$ (10^6 N.m^2)	r (10^{-3})	M_{cr} (kN-m)	M_y (kN-m)	Φ_y (rad/km)	Φ_u (rad/km)
12	6.388	0.222	9269	7400	0.052	6.30
11	6.388	0.222	9269	7400	0.052	6.30
10	6.388	0.222	9269	7400	0.052	6.30
9	6.388	0.222	9269	7400	0.052	6.30
8	6.388	0.222	9269	7400	0.052	6.30
7	6.388	0.261	9364	9385	0.078	6.30
6	6.388	0.261	9364	9385	0.078	6.30
5	6.388	0.397	9558	13263	0.078	6.30
4	6.388	0.397	9558	13263	0.098	6.30
3	6.388	0.397	9558	13263	0.098	6.30
2	6.388	0.34	9569	14421	0.089	6.30
1	6.388	0.34	9569	14421	0.089	6.30

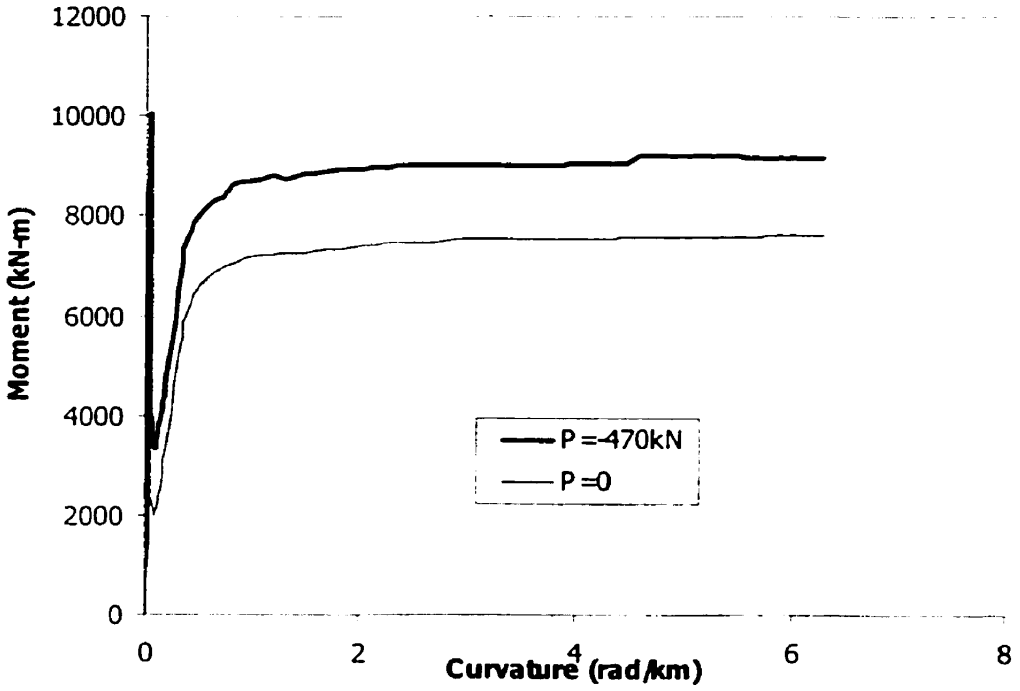

Figure 3-5 Moment-curvature response of the wall (storey 12).

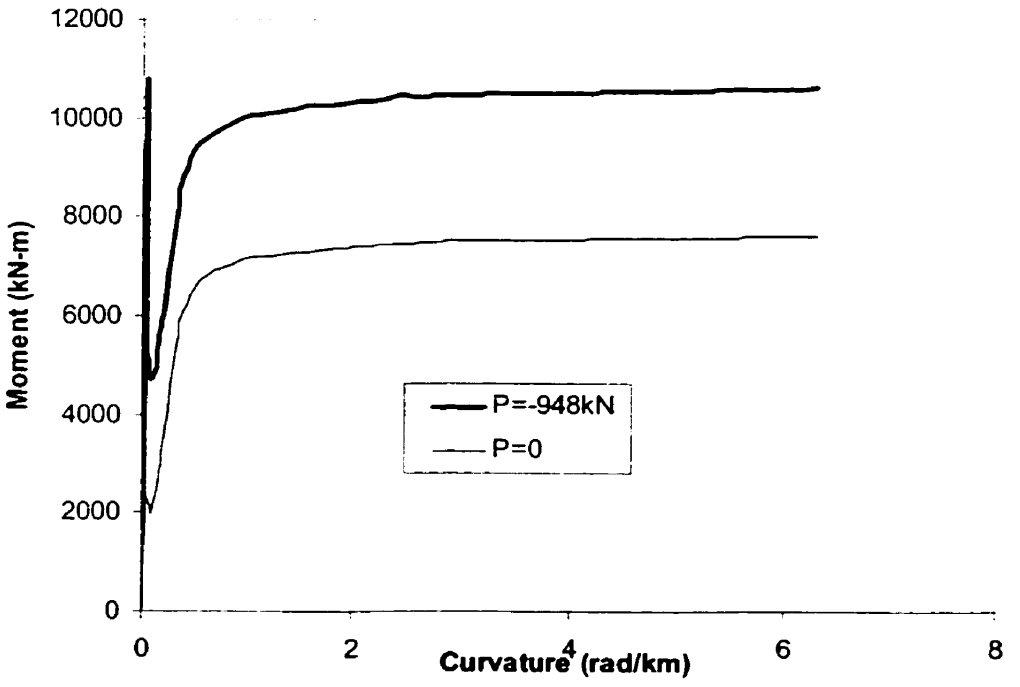

Figure 3-6 Moment-curvature response of the wall (storey 11).

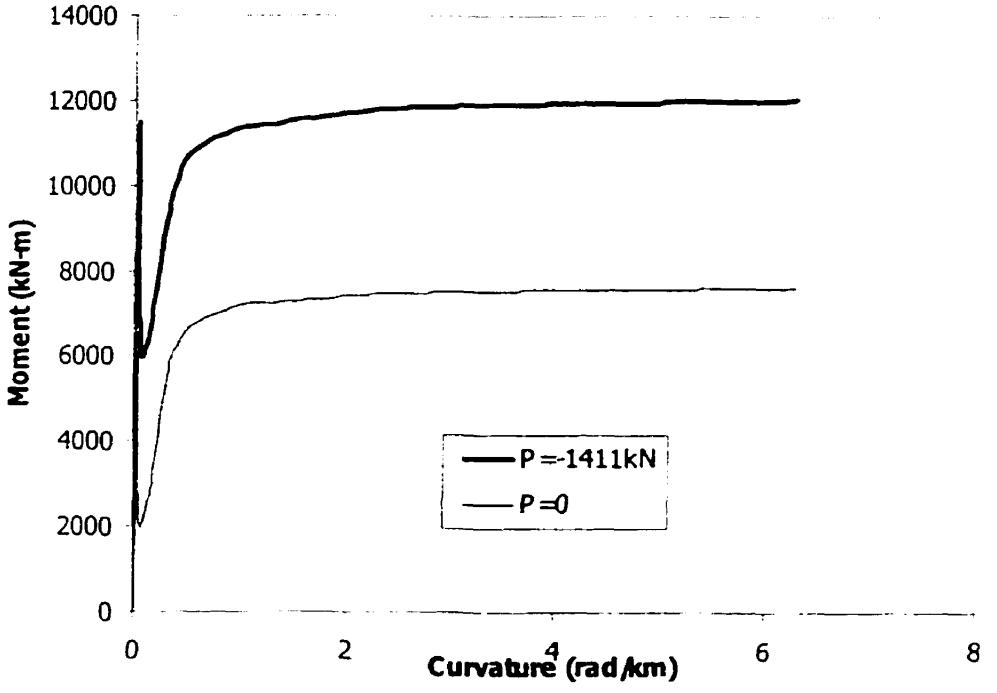

Figure 3-7 Moment-curvature response of the wall (storey 10).

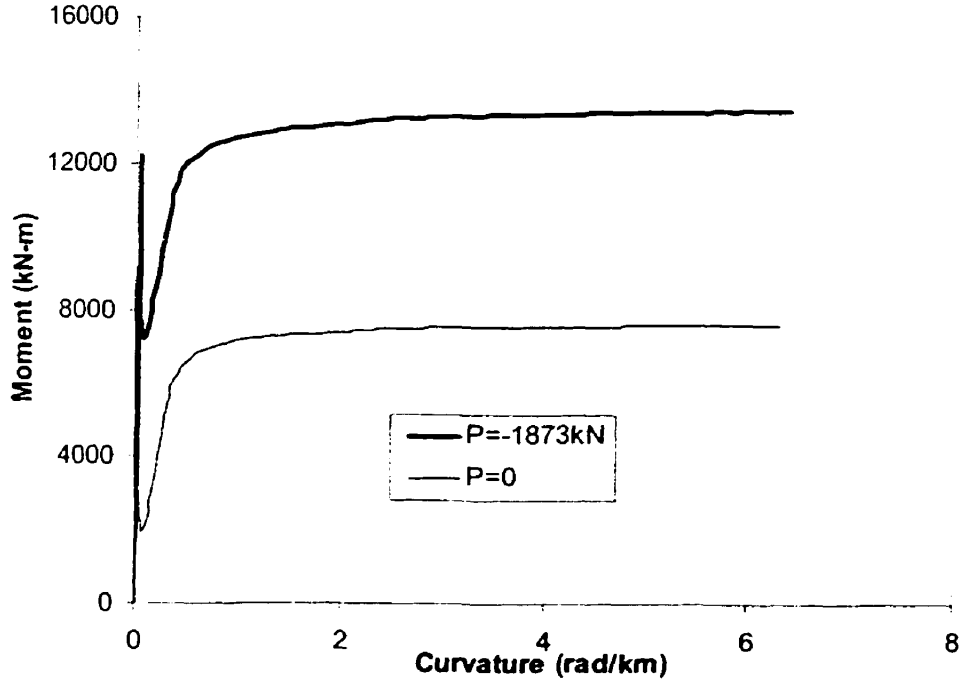

Figure 3-8 Moment-curvature response of the wall (storey 9).

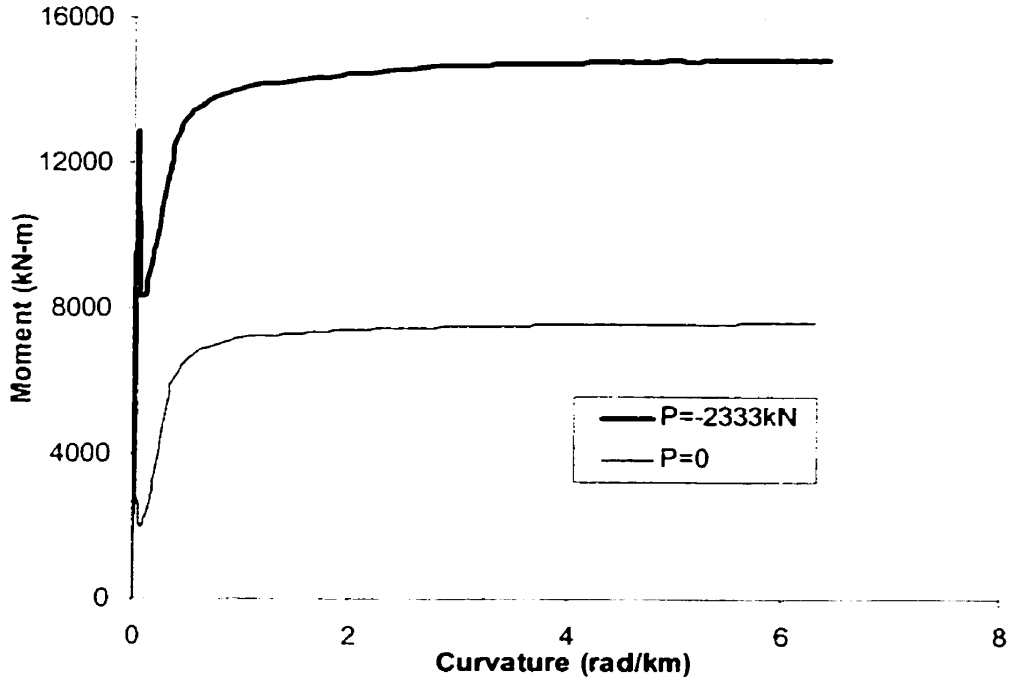

Figure 3-9 Moment-curvature response of the wall (storey 8).

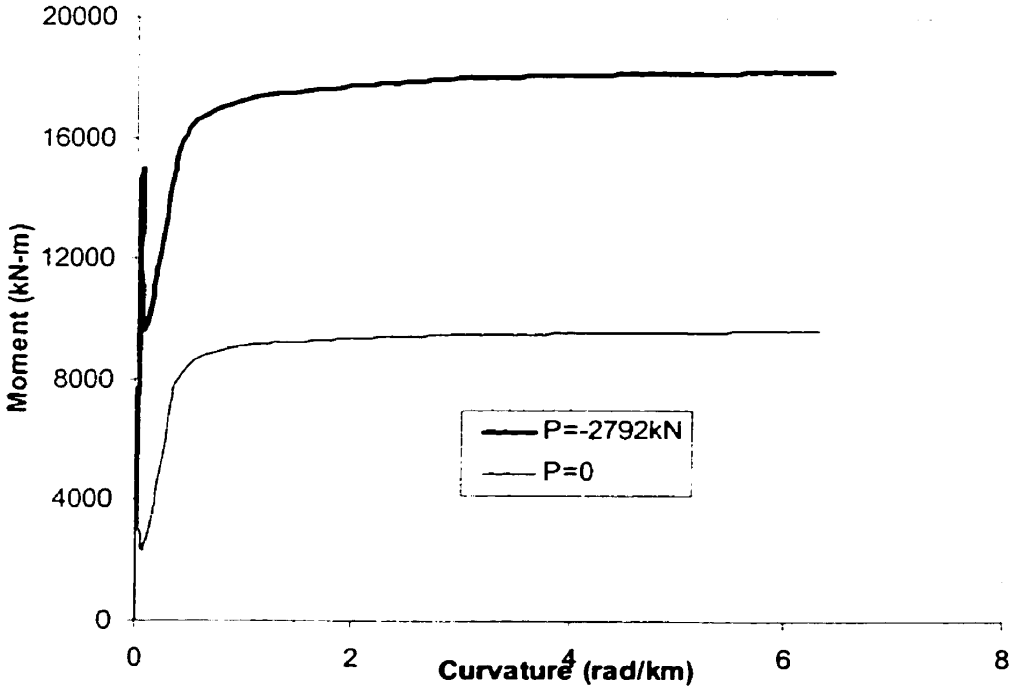

Figure 3-10 Moment-curvature response of the wall (storey 7).

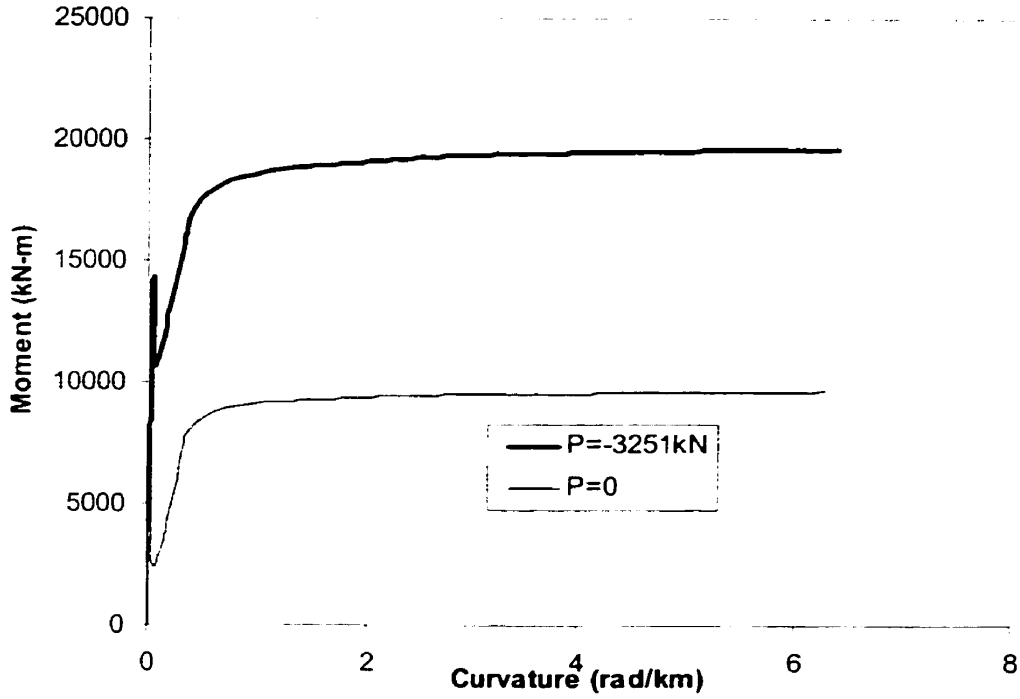

Figure 3-11 Moment-curvature response of the wall (storey 6).

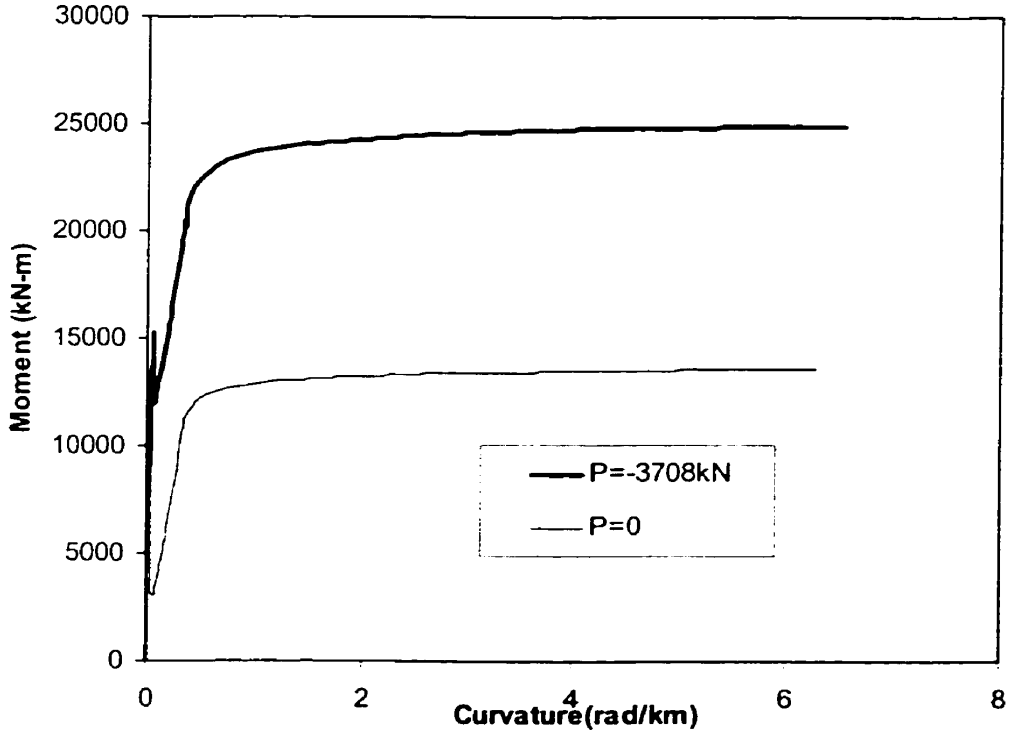

Figure 3-12 Moment-curvature response of the wall (storey 5).

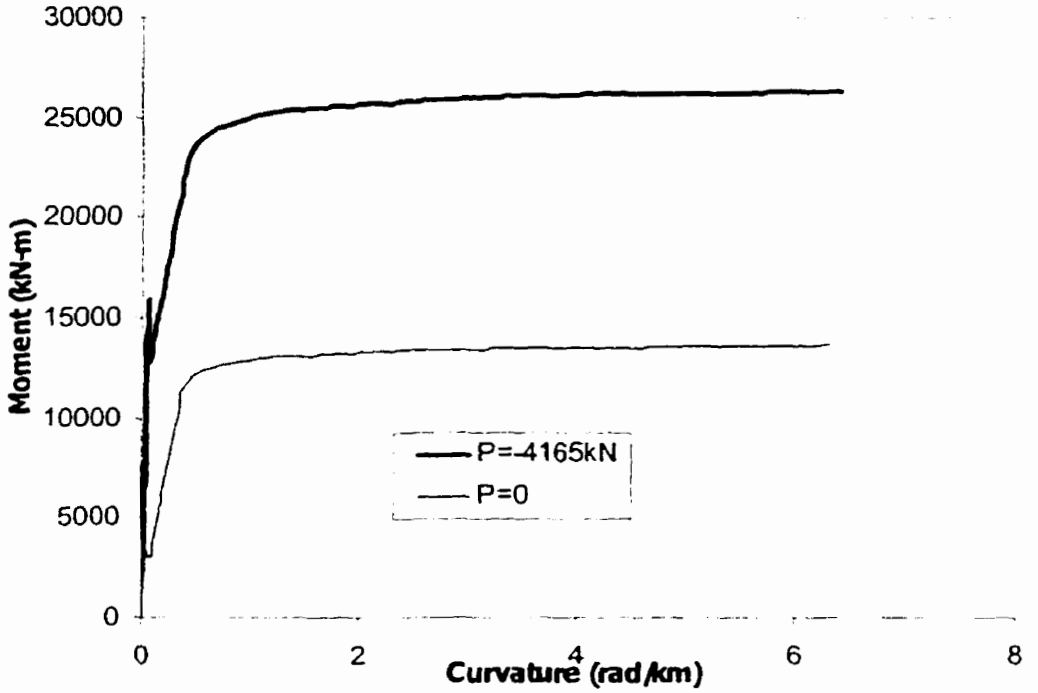

Figure 3-13 Moment-curvature response of the wall (storey 4).

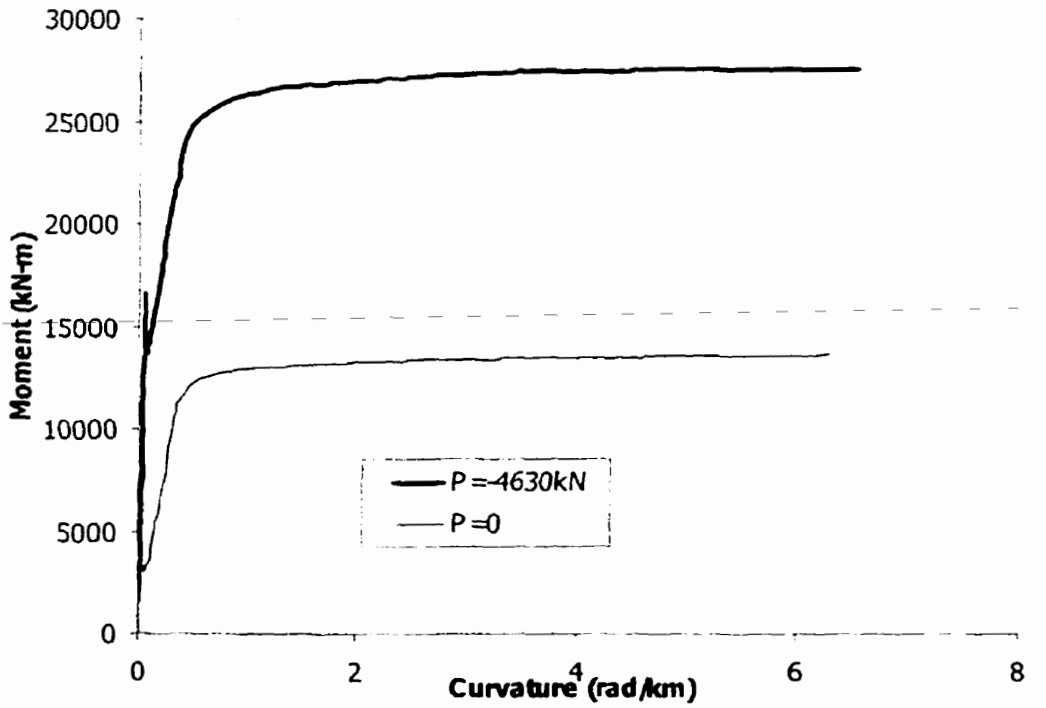

Figure 3-14 Moment-curvature response of the wall (storey 3).

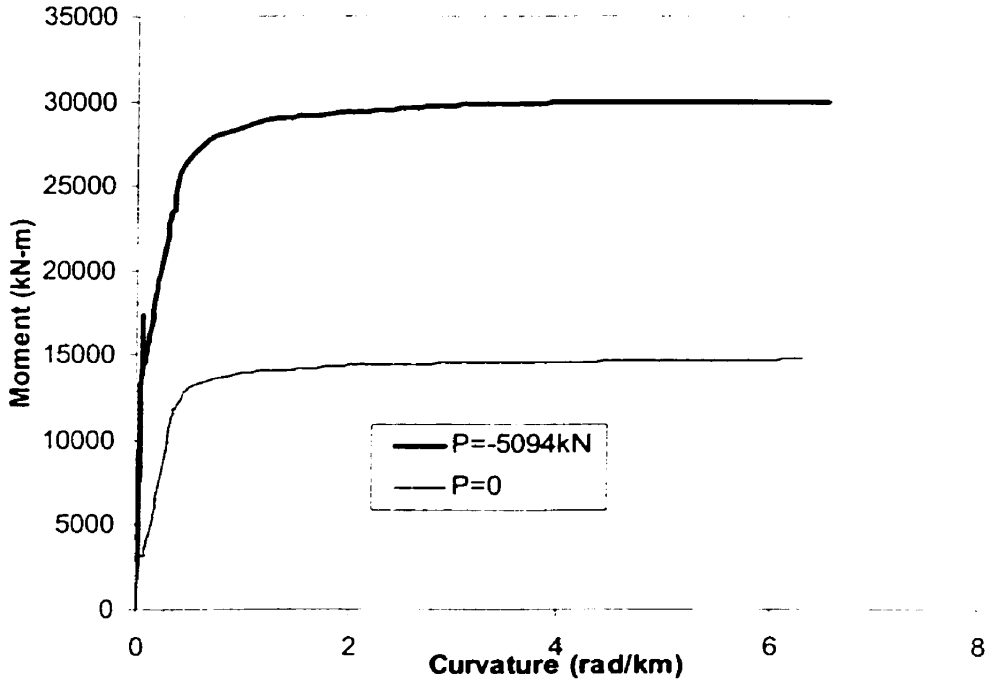

Figure 3-15 Moment-curvature response of the wall (storey 2).

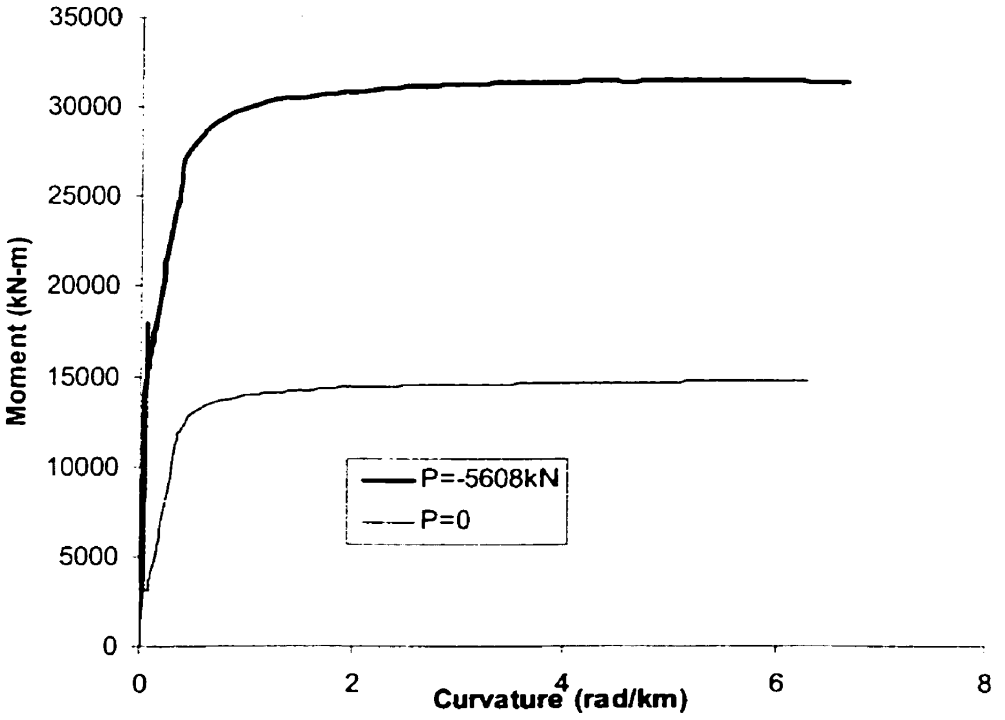

Figure 3-16 Moment-curvature response of the wall (storey 1).

Figure 3-17 shows the yield moment at each storey in the shear-wall structure.

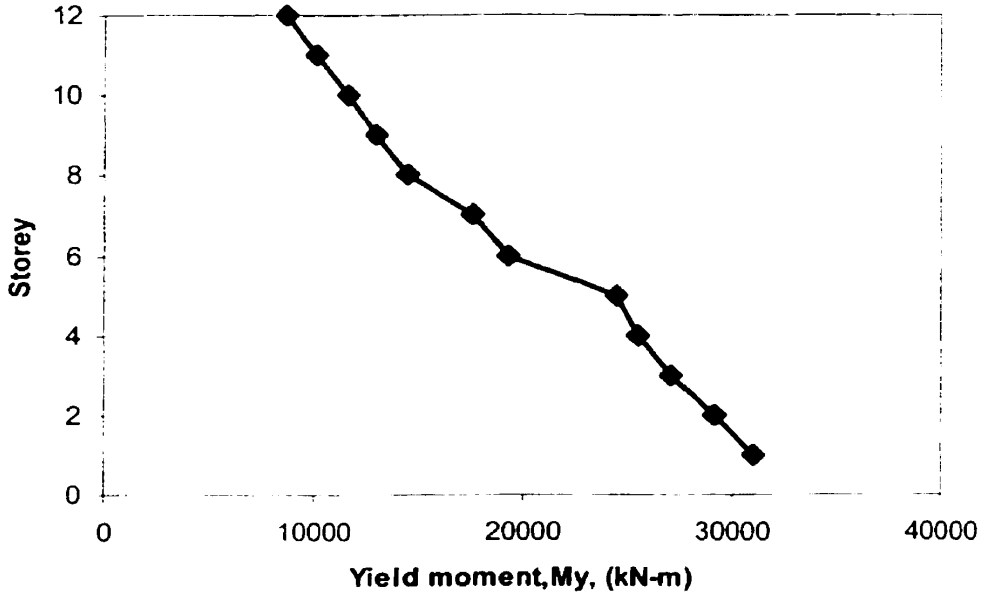

Figure 3-17 Yield moment at each storey in the shear wall building.

3.5 Analyses for earthquake loads

The 12-storey wall frame structure in CPCA 1985 Example 11.5 was originally designed according to the CSA Standard A23.3 – M84 Design of Concrete Structure for Buildings (CSA,1984) and the 1985 National Building Code of Canada (NRCC,1985). In the 1985 NBCC, the earthquake forces were determined using the ductility coefficient, K = 0.7, in the base shear formula, V = vSKIFW. The shear force and the bending moment at the base caused by the factored earthquake loads were V = 1202 kN and M = 23700 kN-m. The axial force at the base as given in the CPCA 1985 Handbook were: P_D = 5417 kN and N_L = 968 kN.

The shear wall is then verified according to the CSA Standard A23.3-M94 Design of Concrete Structures and NBCC 1995 assuming it is a ductile shear wall with a R factor

of 3.5 and the axial loads given in Table 3-2. The design base shear resistance and bending moment at the base are calculated as follows:

The design base shear V to meet NBCC 1995 seismic demand requirement is

$$V = (\frac{V_e}{R})U \tag{3.1}$$

$$V_e = \nu S I F W \tag{3.2}$$

with:

Seismic zones for Montreal: $Z_a = 4$; $Z_v = 2$

Fundamental period of the structure: $T = (0.09h_n)/(D_s)^{1/2} = 0.09*45/6.6^{1/2} = 1.576$ s. The value of F_t is obtained from equation (2.5): $F_t = 0.07\ T\ V = 0.07*1.576*V = 0.11V \leq 0.25\ V$. The seismic load distribution is obtained using equation (2.4) and is summarised in Table 3-6. In this table, the seismic weight at each level of the whole structure includes the dead load plus 25% of the design snow load.

Seismic response factor: $Z_a / Z_v = 2 > 1$; $S = 1.5/T^{1/2} = 1.5/1.576^{1/2} = 1.195$

Peak ground horizontal velocity for Montreal $\nu = 0.10$ m/s

Foundation factor: $F = 1.0$ (rock)

Seismic weight for one wall: W = the total dead load +25% of the snow load

= 46765.5 kN

The elastic base shear V_e is as follows:

$V_e = (0.1)(1.195)(1.0)(1.0)(46765.5) = 5588.5$ kN

Force modification factor: R =3.5 (ductile flexural wall)

The design base shear required by NBCC 1995 V = (5588.5/3.5) 0.6 = 958 kN

The bending moment caused by the earthquake is as follows:

$$M_f = \sum F_x h_x = (31.8174\ m)V$$

The code suggests that a reduction factor J for the overturning moment at the base of the structure be applied: J = 0.8 for T >1.5 S.

So, the moment $M_f = 0.8*(31.8174\ m)V = (25.4539\ m)V = 24385$ kN-m.

With the RESPONSE program, the factored resisting moment, M_r, at the base of the wall with $P_D + 0.5\ P_L = 5608$ kN is 26615 kN-m. The moment M_r is obtained with resistance factors $\phi_c = 0.6$ for the concrete and $\phi_s = 0.85$ for the reinforced steel. Therefore, the factored bending moment resistance at the base exceeds the required factored moment $M_f = 24385$ kN-m. The shear wall was also verified to satisfy detailing requirements according to the CSA Standard A23.3-M94 Design of Concrete Structures and NBCC 1995.

In NBCC 1995, a stability factor θ_x is required to consider P-Δ effects. The formula of the stability factor at any level x is given in equation (2.6). In the above calculation of seismic loads (Table 3-6), P-Δ effects have not been considered because inelastic dynamic analyses including P-Δ effects will be used in this thesis as an alternative to the application of the simplified stability factor approach. The stability factor at each storey is given in Table 3-7 where Δ_{max} is the elastic displacements without P-Δ effects and R is the force modification factor. The value of $R*\Delta_{max}$ is used to estimate the inelastic displacements.

Table 3-6 Seismic loads acting on one shear wall.

Storey	W_x(kN)	h_x (m)	W_x*h_x (kN-m)	$\frac{W_x*h_x}{\Sigma W_x*h_x}$	F_x/V
12	3871	45	174195	0.15065	0.2440
11	3843	41.35	158893	0.13742	0.1223
10	3843	37.7	144868	0.12529	0.1115
9	3843	34.05	130842	0.11316	0.1007
8	3843	30.4	116816	0.10103	0.08989
7	3843	26.75	102791	0.0889	0.07909
6	3873	23.1	89463	0.07737	0.06884
5	3873	19.45	75327	0.06515	0.05796
4	3873	15.8	61191	0.05292	0.04708
3	3963	12.15	48152	0.04164	0.03704
2	3963	8.5	33687	0.02913	0.02591
1	4134	4.85	20049	0.01734	0.01543

Table 3-7 Stability factor at each storey.

Storey	ΣP_i(kN)	$R^*\Delta_{max}$ (mm)	h_s (m)	F_i (kN)	ΣF_i (kN)	θ_x
12	4285	46.73	3.65	233.75	233.75	0.23
11	8386	46.66	3.65	117.16	350.91	0.31
10	12509	46.10	3.65	106.82	457.73	0.35
9	16626	45.12	3.65	96.47	554.20	0.37
8	20739	43.44	3.65	86.11	640.32	0.39
7	24850	41.13	3.65	75.77	716.08	0.39
6	28990	37.98	3.65	65.95	782.03	0.39
5	33127	34.06	3.65	55.53	837.56	0.37
4	37263	29.16	3.65	45.10	882.66	0.34
3	41489	23.24	3.65	35.48	918.15	0.29
2	45714	16.42	3.65	24.82	942.97	0.22
1	50109	9.45	4.85	14.78	957.75	0.10

3.6 Analytical model of the shear wall

The nonlinear time step dynamic analyses of the shear wall under earthquake ground motions were performed using the RUAUMOKO computer program. Two different hysteresis models were used to represent the nonlinear flexural response of the walls. These are described in section 3.7. The computer program SAP90 was also used to compute the elastic response of the wall (static load and modal analyses). For both programs, the 12-storey reinforced concrete structural wall was modelled by 12 beam-column elements with 3 degrees-of-freedom per node corresponding to the horizontal, vertical, and rotational displacements, respectively. The number of nodes along the wall is a function of the mass distribution. One node is assigned to each floor. The gravity loads acting on the wall at a given floor are lumped at the corresponding node.

Figure 3-18 shows the analytical model of the 12-storey shear-wall building. The wall is fixed at its base and wall segments are considered rigidly connected at the wall joints. The damping model used is of the Rayleigh type with the damping matrix proportional

to the mass and the initial stiffness matrices. Rayleigh type viscous damping equal to 5% of critical damping is assumed in the first two modes of vibration.

As mentioned earlier, the analytical model of the 12-storey shear wall also included a gravity column. It is modelled by 12 elements with 2 degrees-of-freedom per node corresponding to the horizontal and vertical displacements, respectively. The gravity column elements are pin-connected at their base and at each floor. The gravity column carries the gravity loads supported by the actual columns stabilised by one wall.

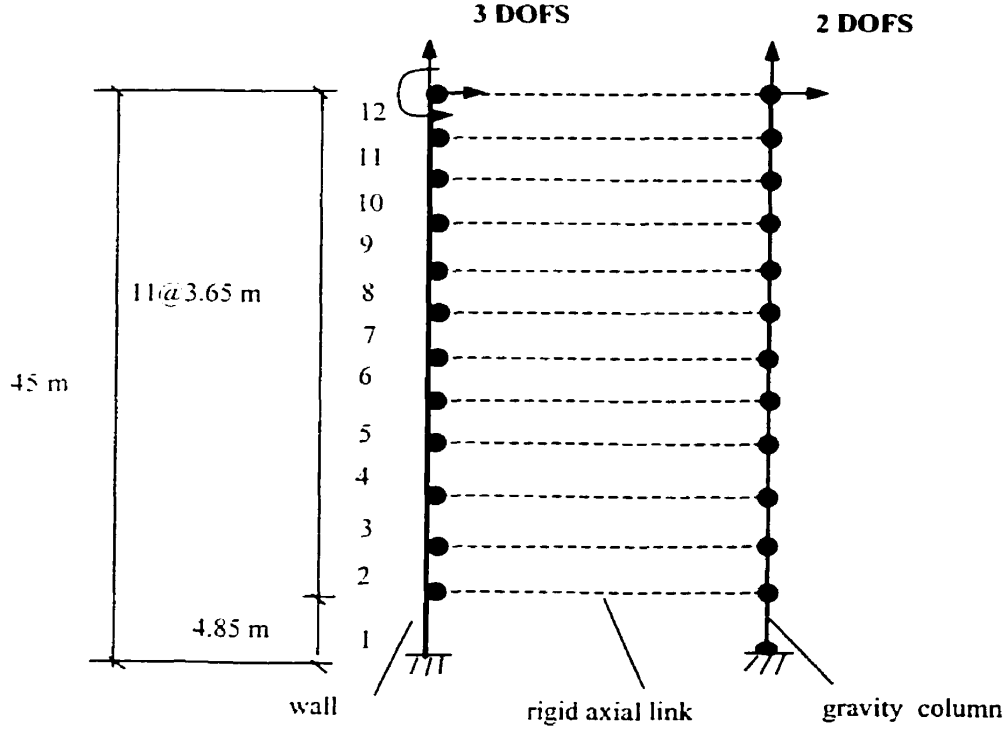

Figure 3-18 Analytical model of the 12-storey shear wall.

The computer program RUAUMOKO has been used to carry out nonlinear analyses. It is designed to produce a piece-wise time-history response of a nonlinear general two-dimensional framed structure to ground accelerations or time varying force excitations. The program allows the user the option to consider P-Δ effects in the analyses. Many

different hysteresis rules are incorporated in the program to represent the inelastic behaviour of frame and spring members. They range from the simple elastic-plastic rules to very complex models, which need over thirty parameters to represent the cyclic load-displacement response. The post-processing unit, DYNAPLOT, gives the user the ability to graphically visualise the displacements and the formation of plastic hinges during the dynamic analyses. The RUAUMOKO program also allows the user to perform pseudo-static (pushover) analyses.

To compute the structural periods of vibration, different values of the moment of inertia were considered for the wall element. The values and definitions for these moments of inertia are as follows:

I_{uncr} : uncracked moment of inertia, which is obtained from RESPONSE program.

I_{cr}: cracked moment of inertia, which is obtained from RESPONSE program.

I_g: moment of inertia of gross concrete section about centroidal axis, neglecting reinforcement: $I_g = 9.126\ m^4$.

I_p: the equivalent moment of inertia of cross section, as defined by Paulay and Priestley (1992):

$$I_p = (100/f_y + P_U/f'_c A_g)\ I_g \qquad (3.3)$$

Where P_U: the axial load considered acting on the wall taken positive when causing compression. It is calculated according to NBCC 1995($P_U = N_D + 0.5\ N_L$) and it also varies along the height of the wall.

A_g,I_g: the area and moment of inertia of the gross cross section, respectively ($A_g = 1.8\ m^4$).

f'_c: the specified compressive strength of concrete ($f'_c = 30$ MPa).

f_y: the specified yield strength of reinforcement ($f_y = 400$ MPa).

$0.7I_g$: the effective moment of inertia recommended in the CPCA Concrete Design Handbook (1995).

Figure 3-19 illustrates EI_{uncr}, EI_{cr} and 0.7 EI_g at the first storey of the wall studied. The yield moment at each storey M_y is obtained from the intersection of the flexural stiffness 0.7 EI_g and yielding branches. The yield curvature Φ_y is then obtained according to the yield moment. The bilinear factor r is determined from the slope between the maximum moment and the yield moment.

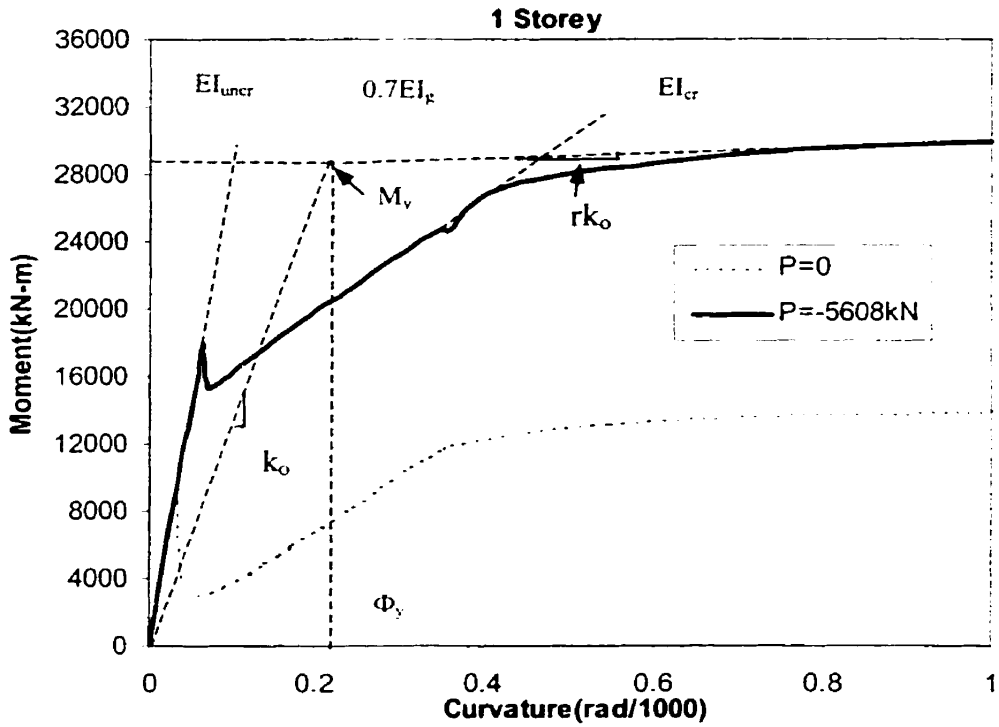

Figure 3-19 Moment-curvature response of the wall.

According to the recommendation of the 1995 CPCA Concrete Design Handbook, the wall effective flexural stiffness equal to 0.7EI_g can also be used in the elastic and inelastic analysis.

A summary of the results using different moments of inertia is given in Table 3-8. The values of the uncracked moment of inertia (I_{uncr}) obtained from the RESPONSE program are a little different from the moment of intertia of the gross concrete section (I_g). The

reason of the small variations among these results is that the uncracked moments of inertia (I_{uncr}) are approximate values obtained from numerical evaluation of the elastic slopes of the moment-curvature relationships computed from RESPONSE. The values with uncracked moments of inertia (I_{uncr}) should theoretically be the same as those corresponding to the moment of inertia of the gross concrete section (I_g).

Table 3-8 Moments of inertia of the wall cross section.

	I_{uncr}	I_{cr}	I_{uncr}	I_{cr}	I_g	I_p	$0.7I_g$
Storey	P≠0	P≠0	P=0	P=0			
	(m^4)	(m^4)	(m^4)	(m^4)	(m^4)	(m^4)	(m^4)
12	9.22	0.610	9.26	0.610	9.126	2.361	6.388
11	9.19	0.600	9.26	0.600	9.126	2.442	6.388
10	9.17	0.600	9.26	0.600	9.126	2.520	6.388
9	9.12	0.600	9.26	0.600	9.126	2.598	6.388
8	9.11	0.620	9.26	0.600	9.126	2.676	6.388
7	9.19	0.830	9.36	0.830	9.126	2.753	6.388
6	9.13	0.840	9.36	0.830	9.126	2.831	6.388
5	9.30	1.250	9.55	1.240	9.126	2.908	6.388
4	9.26	1.280	9.55	1.240	9.126	2.985	6.388
3	9.23	1.310	9.55	1.240	9.126	3.064	6.388
2	9.19	1.380	9.56	1.300	9.126	3.142	6.388
1	9.14	1.420	9.56	1.300	9.126	3.229	6.388

3.7 Hysteresis rules

The results of the **RESPONSE** program (Collins and Mitchell, 1987) are used to define the basic properties of the hysteresis rules used in the inelastic model. A bilinear inelastic model was used for the rotational hysteretic hinging at the wall element ends. It is the simplest rule, which captures the basic features of an inelastic reinforced concrete element under cyclic flexural deformations. With this rule, cracking of the concrete is neglected and the initial elastic stiffness is representative of the cracked section until yielding occurs. Cracking of the concrete was considered in Chapter 4 .

The bilinear model is illustrated in Figure 3-20. The initial flexural stiffness (K_o is obtained from the moment to curvature ratio at first yield. The strain hardening (bi-linear) ratio is obtained from the second branches of the moment-curvature relationship. The yield moment for each storey is determined from the intersection of the elastic and yielding branches. The relationships between the moment resistance and axial loads are given in Table 3-9. The parameters K_o and r are used to describe the hysteresis rule as explained in this section.

Table 3-9 The moment resistances for different axial loads.

Storey	$K_o=0.7EI_g$ (10^6 N.m^2)	r (P=0) (10^{-3})	r (P≠0) (10^{-3})	M_y(P=0) (kN-m)	M_y(P≠0) (kN-m)	Axial load P(kN)
12	6.388	0.222	0.640	7400	8740	-470
11	6.388	0.222	0.484	7400	10154	-948
10	6.388	0.222	0.324	7400	11700	-1411
9	6.388	0.222	0.351	7400	13100	-1873
8	6.388	0.222	0.368	7400	14500	-2333
7	6.388	0.261	0.622	9385	17600	-2792
6	6.388	0.261	0.327	9385	19286	-3251
5	6.388	0.397	0.350	13263	24546	-3708
4	6.388	0.397	0.592	13263	25636	-4165
3	6.388	0.397	0.434	13263	27158	-4630
2	6.388	0.340	0.762	14421	29263	-5094
1	6.388	0.340	0.480	14421	31059	-5608

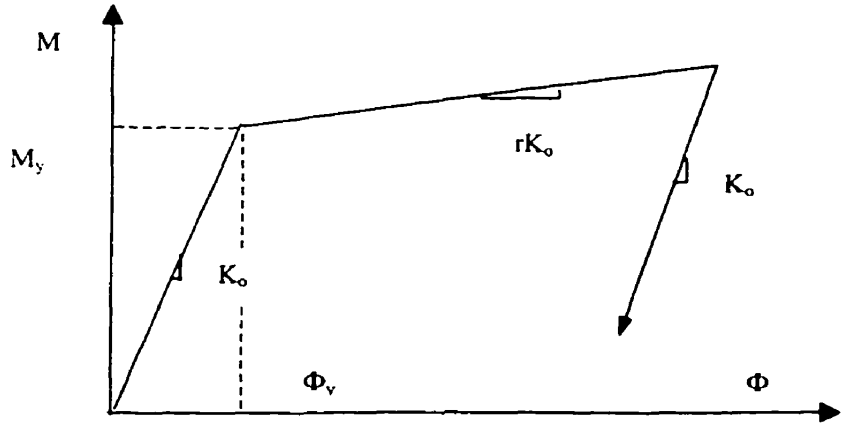

Figure 3-20 Bilinear inelastic moment-curvature model.

Figure 3-21 shows the modified Takeda bilinear hysteresis rule (Otani 1974) which is used to model the moment-curvature response of the shear wall. The initial slope (k_0) corresponds to the stiffness ($0.7EI_g$) of the section before the steel yields. The second slope corresponds to the post-yield condition of the structure. This post-yield slope is related to the initial slope by a factor r. The model then unloads with a slope k_u. Once the moment changes sign, the slope changes again according if opposite yielding has occurred. The envelopes of the first cycle (coordinate of the yielding moments and their corresponding stiffness) were obtained from results of moment-curvature analyses using of the RESPONSE program.

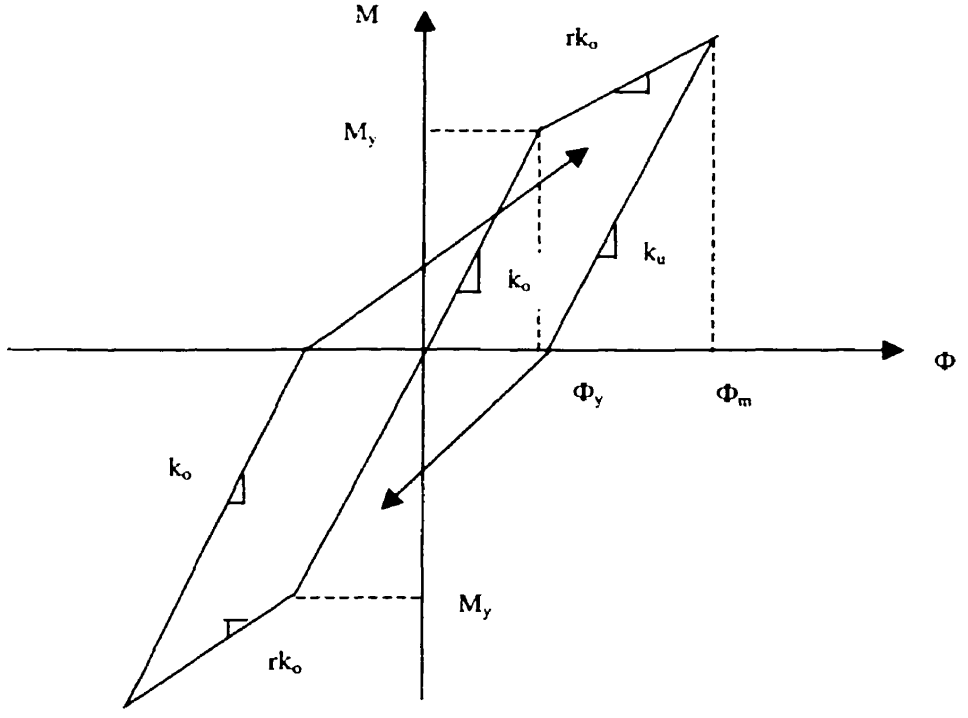

Figure 3-21 Modified Takeda bilinear hysteresis.

CHAPTER 4

EARTHQUAKE RESPONSE ANALYSES OF THE 12-STOREY BUILDING

4.1 Introduction

This chapter presents the results of nonlinear dynamic response analyses performed on the designed 12-storey shear walls to evaluate the importance P-Δ effects under design base ground motions. Several response parameters and damage indices, such as horizontal displacements at the top of the wall, shear forces and bending moments at the base of the wall, ductility demand, and the dissipated hysteretic energy, are used as indicators to assess the seismic response of buildings. Three earthquake accelerograms are selected as input ground motions considering their different characteristics: El Centro 1940 (SOOE), Taft 1959 (S69E), and Parkfield 1966 (N65E). Each record is scaled to match the NBCC 1995 peak ground acceleration of 0.18g for Montreal.

Response analyses under static loading and preliminary response spectrum analysis are performed using the SAP90 computer program (Wilson and Habibullah,1992). Nonlinear static pushover analyses under incremental lateral loading are performed to examine the behaviour and assess the importance of P-Δ effects using the RUAUMOKO computer program. The RUAUMOKO program is then used to perform inelastic dynamic analyses with and without P-Δ effects. Finally, conclusions are made assessing the significance of P-Δ effects for the wall analysed.

4.2 Response parameters and damage indices

4.2.1 Roof displacements

The maximum horizontal roof displacement is an important parameter when assessing P-Δ effects during an earthquake. Most engineering calculations use relative displacements of the structure with respect to its foundation. Excessive displacements may cause loss of stability or excessive damage to structural components. The maximum horizontal roof displacement is also to be controlled to minimize the human perception of motion and to avoid the pounding of adjacent structures.

4.2.2 Ductility

The ductility is defined as the maximum deformation divided by the yield deformation. It is the structural property that will need to be relied on in most buildings if satisfactory behaviour under damage control and survival limit states are to be achieved. There are deformation parameters that may be used to calculate ductility including roof displacements, storey drifts, plastic hinge rotations, deflections, etc. Particular measures of deformations have been established as most appropriate to understand the behaviour of a complete structure. The ductility based on roof displacements, μ_Δ, is computed as the ratio of the peak horizontal roof displacement to the roof displacement that corresponds to the formation of the first plastic hinge in the structure. The latter is obtained from a pushover analysis of the wall when considering NBCC horizontal seismic load pattern. The most common and desirable source of inelastic structural deformations is rotation in potential plastic hinges. For a cantilevered shear wall, the maximum curvature ductility demand, μ_Φ, is a good indicator to characterize the severity of damage of a wall member since the major energy dissipating mechanism is the formation of a rotational plastic hinge at the bottom end of the wall. This ductility indicator was then also retained in this study.

4.2.3 Energy

Energy is also important in the estimation of damage in a structure during an earthquake. The energy balance equation is:

$$E_i = E_k + E_s + E_d + E_h \tag{4.1}$$

where: E_i= the input energy,

E_k= the kinetic energy,

E_s= the recoverable strain energy,

E_d= the damping energy,

E_h= the irrecoverable hysteretic energy.

Assuming that only the hysteretic energy, E_h, contributes to the irrecoverable damage, the ratio of hysteretic energy to input energy E_h/E_i can be considered an good indicator of structural damage.

4.2.4 Damage indices

Structural damage under earthquake loading includes the global structure damage, global substructure storey damage, and local member damage. Several indicators referred to as damage indices can be computed in a nonlinear dynamic analysis to quantify the level of anticipated structural seismic damage. The computation of some of these damage indices requires the evaluation of the ultimate ductility demand for the members. To compute damage indices the following parameters are considered:

μ_m= the maximum ductility,

μ_u = the ultimate ductility,

F_m = the maximum force,

F_y = the yield force,

E_h = the dissipated hysteretic energy,

E_u = the work done at ultimate ductility,

E_m = the work done at maximum ductility.

The parameter μ_m is defined as the maximum computed displacement divided by the yield displacement. Figure 4-1 shows the definition of the maximum ductility, μ_m. The parameter μ_u is the ductility at which the member is assumed to fail under monotonic loading. It is the ratio of the ultimate displacement to the yield displacement, (Figure 4-2).

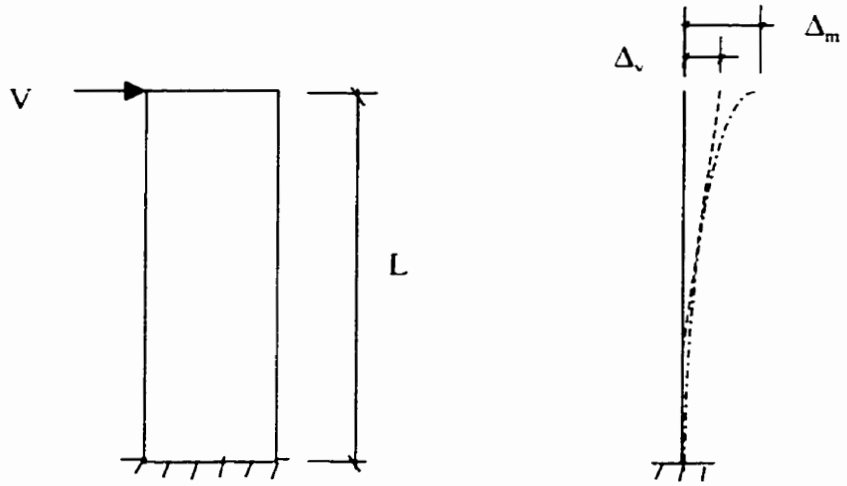

Figure 4-1 Definition of the maximum ductility ($\mu_m = \Delta_m/\Delta_y$).

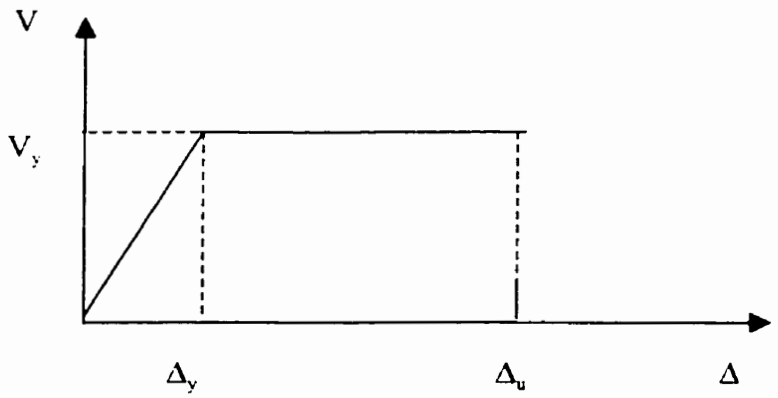

Figure 4-2 Definition of the ultimate ductility ($\mu_u = \Delta_u/\Delta_y$).

The structure, or structural element under consideration is assumed to have failed when the computed damage index, D, reaches or exceeds 1.0. On the contrary, no damage has occurred when D is equal to zero. The damage indices used in the study are as follows:

1. Maximum deformation:

$$D\mu_{\Delta} = \mu_m / \mu_u = \Delta_m / \Delta_u \tag{4.2}$$

$$D\mu_{\Phi} = \mu_m / \mu_u = \Phi_m / \Phi_u \tag{4.3}$$

where $\mu_m = \Delta_m/\Delta_y$, Φ_m/Φ_y

$\mu_u = \Delta_u/\Delta_y$, Φ_u/Φ_y

Δ_m = the maximum computed displacement;

Δ_y = the yield displacement;

Δ_u = the ultimate displacement;

Φ_m = the maximum curvature;

Φ_y = the yield curvature;

Φ_u = the ultimate curvature;

2. Park and Ang (1985) damage indicator:

$$D_{PA} = \mu_m/\mu_u + \beta E_h / F_y \mu_u \tag{4.4}$$

where β = the combination factor.

The damage index D_{PA} is defined as a linear combination of the ratio of the maximum displacement to the ultimate displacement and the irrecoverable hysteretic energy divided by the yield force. The parameter β can be obtained from a regression curve using about 260 experimental results, $-0.3 \leq \beta \leq 1.2$. Williams,Villemure and Sexsmith (1994) proposed that β may be chosen 0.1 for well-reinforced concrete structural elements. If $\beta = 0$, failure due to excessive displacement occurs, while for a value of β ranging between 0.6 and 0.8, failure is governed by accumulation of damage.

4.3 Elastic responses

4.3.1 Modeling assumptions

The free-vibration properties are very important to characterize the dynamic response of a structure. Free-vibration is the result of initial conditions (displacement or velocity), and intrinsic masses and stiffness properties without external dynamic excitation. The natural frequencies indicate the frequencies to which dynamic amplification may be most significant according to the frequency content of the earthquake. The modes of vibration indicate the spatial distribution of the earthquake forces along the height of the building.

The free-vibration response of the 12-storey wall-frame building is studied. As described in Chapter 3, the structural model is composed of the wall and a gravity column. Each node has horizontal, vertical, and rotational displacement degrees-of-freedom, except the node at the base of the wall. The wall is fixed at the base, while the gravity column is pin-connected at the base and at all stories. The concentrated nodal masses are lumped at the joints corresponding to horizontal, and vertical DOF.

4.3.2 Response under static loading

To compute the drift on the 12 storey shear wall building and compare with code limits (NBCC 1995), the static analyses with and without P-Δ effects under code loading is performed using the SAP90 computer program in this section. The values of seismic loads on the shear wall have been given in Table 3-5 in Chapter 3. The total elastic displacements at each storey obtained from the program are summarised in Table 4-1. The shear wall has a base shear of 957.7 kN when not including P-Δ effect. When including P-Δ effect, the shear wall has a base shear of 976 kN. The bending moments at the base of the wall, without any reduction factor J, are 31350 kN-m and 33340 kN-m if

not including and including P-Δ effects, respectively. From these results, the following conclusions can be stated: P-Δ effects may be neglected for the displacement at each storey and base shear under static loading; P-Δ effects can increase the bending moment at the base of the wall.

Table 4-1 Elastic displacements from static loading on the shear wall.

Storey	Total displacement (mm)		Interstorey displacement (mm)	
	(without P-Δ)	(with P-Δ)	(without P-Δ)	(with P-Δ)
12	119.84	128.51	13.35	14.32
11	106.49	114.19	13.33	14.29
10	93.16	99.90	13.17	14.14
9	79.99	85.76	12.89	14.37
8	67.10	71.93	12.41	13.33
7	54.69	58.60	11.75	12.61
6	42.94	45.99	10.85	11.66
5	32.09	34.33	9.73	10.43
4	22.36	23.90	8.33	8.93
3	14.03	14.97	6.64	7.11
2	7.39	7.86	4.69	5.00
1	2.70	2.86	2.70	2.86

The elastic interstorey displacements at each storey without considering P-Δ effects should be multiplied by the force modification factor (R = 3.5) to obtain the inelastic displacements. According to NBCC 1995, the so-computed inelastic interstorey displacements at each storey should not be more than the displacement limit $\Delta = 0.02\ h_s$ where h_s is the storey height. The maximum values are 0.02*4.85*1000 = 97 mm for the first storey and 0.02*3.65*1000 = 73 mm for other storey. Therefore, the results of the calculation show that the inelastic interstorey displacements at each storey can be satisfied the requirement of code limit.

4.3.3 Free-vibration analyses

The free-vibration analyses were carried out with the structural analysis program SAP90

(Wilson and Habibullah, 1992). The first three periods of vibration are given in Table 4-2 for each model values of bending stiffness defined in Chapter 3. The corresponding modes of vibration are shown in Figure 4-3 to Figure 4-5. The following conclusions can be formulated: P-Δ effects can increase the structural periods of vibration; the values with the uncracked moment of inertia (I_{uncr}) obtained from the RESPONSE program are the same as those with moment of inertia of gross concrete sections (I_g), so structural models using I_{uncr} or I_g have the same vibration periods; the periods of vibration are longer after the cross section is cracked due to the decrease in stiffness; if the equivalent moment of inertia of the cross section (I_p) suggested by Paulay and Priestly (1992) is used, the vibration periods are much longer; the first three periods of vibration are 3.389 s, 0.555 s, 0.217 s (with P-Δ) and 3.225 s, 0.551s , 0.216 s (without P-Δ), if the effective moment of inertia 0.7 I_g is used in the calculation of vibration periods.

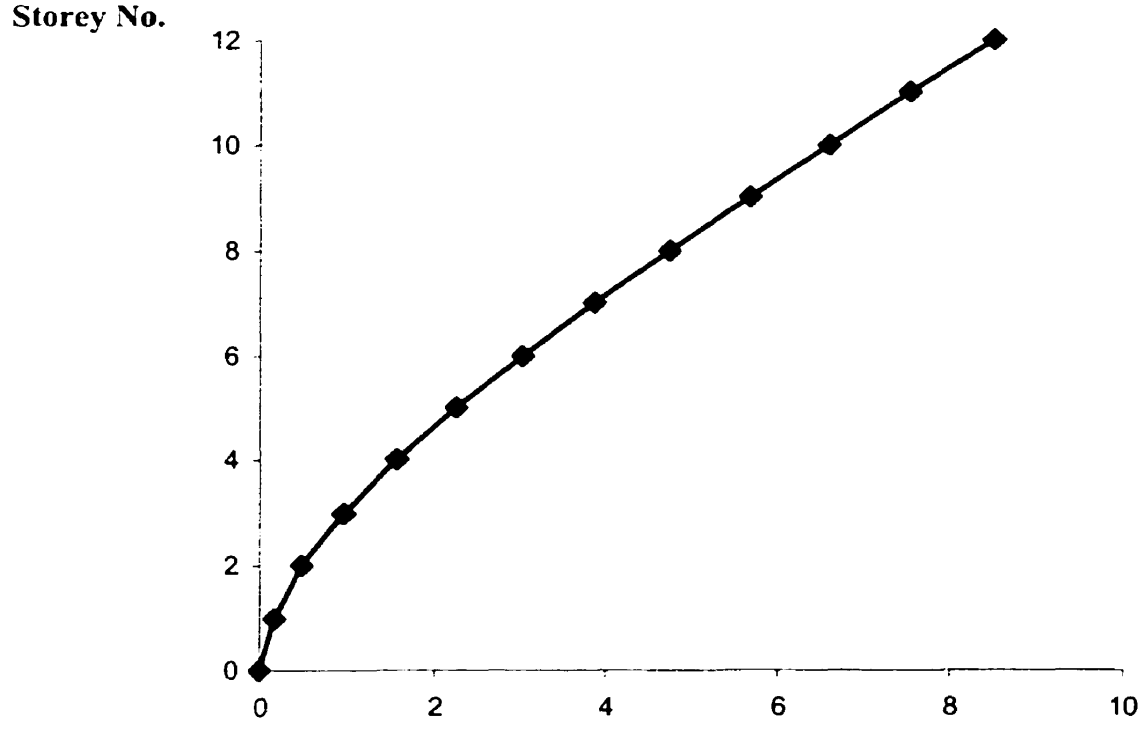

Figure 4-3 First mode shape (I = 0.7 I_g , with P-Δ).

The effective horizontal modal masses are in percentage of the total mass, and the cumulative value for the first three modes are given in Table 4-3.

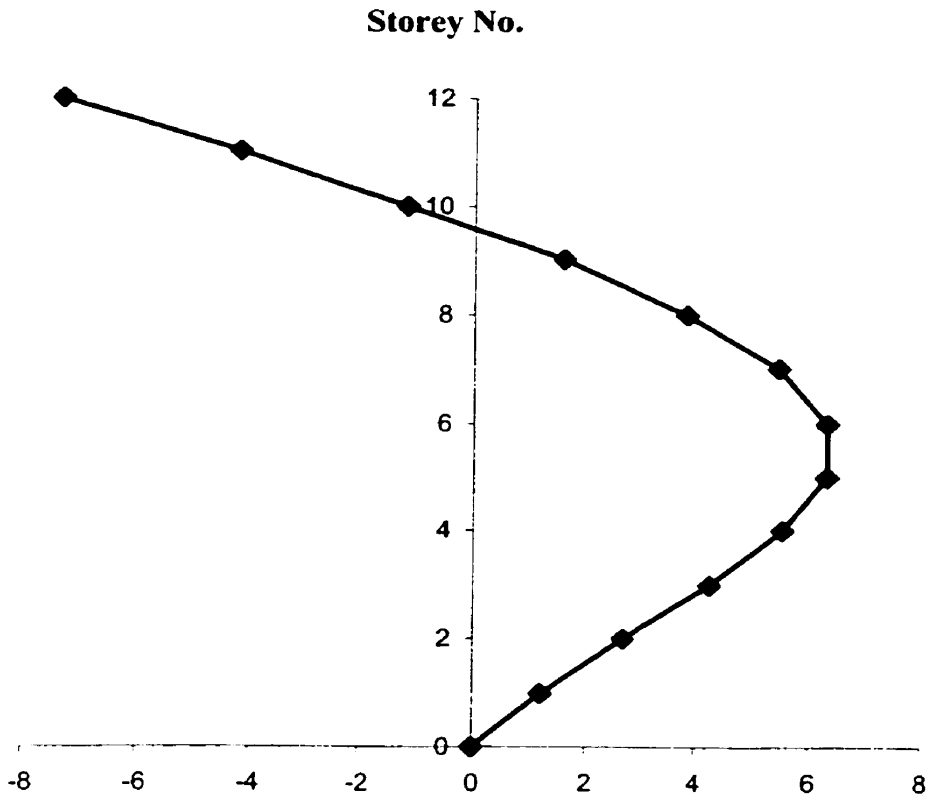

Figure 4-4 Second mode shape ($I = 0.7\ I_g$, with P-Δ).

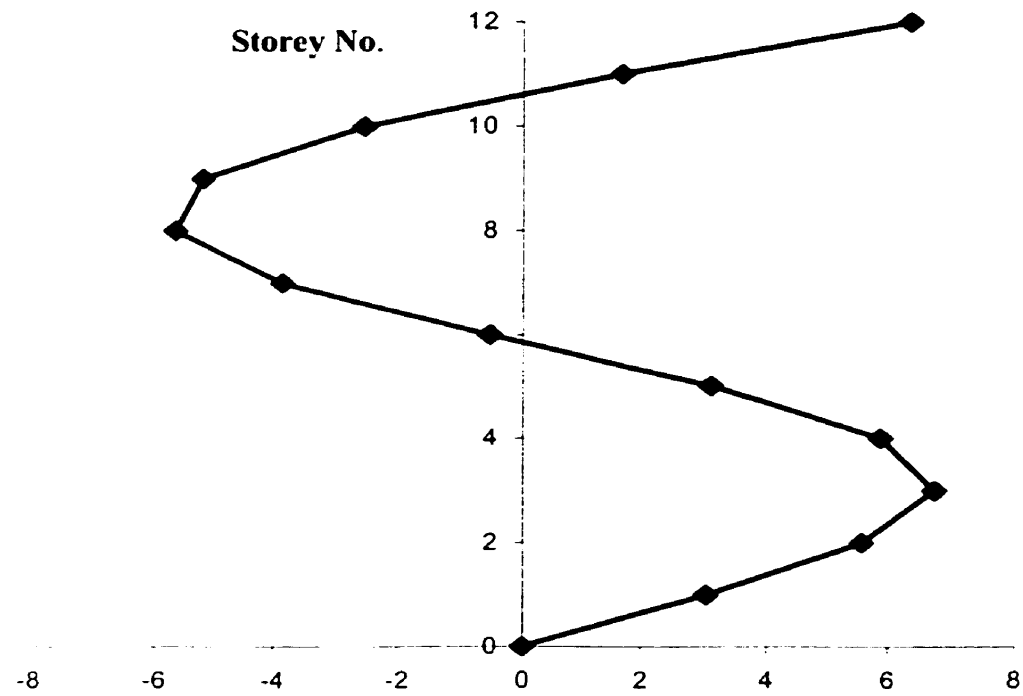

Figure 4-5 Third mode shape ($I = 0.7\ I_g$, with P-Δ).

Table 4-2 First three vibration periods.

		Periods(s)		
Model	**Inertia**	**Mode 1**	**Mode 2**	**Mode 3**
NBCC,1995		1.576		
Response (with P- Δ)	I_{uncr}	2.807	0.477	0.192
(P ≠ 0)	I_{cr}	9.496	1.378	0.49
Response (without P- Δ)	I_{uncr}	2.711	0.475	0.191
(P ≠ 0)	I_{cr}	6.998	1.317	0.483
Response(without P- Δ)	I_{uncr}	2.655	0.469	0.19
(P = 0)	I_{cr}	7.179	1.337	0.488
Gross (with P- Δ)	I_g	2.807	0.477	0.192
Gross (without P- Δ)	I_g	2.711	0.475	0.191
Paulay (with P- Δ)	I_p	5.095	0.794	0.298
Paulay (without P- Δ)	I_p	4.578	0.782	0.296
CPCA,1995 (with P- Δ)	$0.7I_g$	3.389	0.555	0.217
CPCA,1995 (without P- Δ)	$0.7I_g$	3.225	0.551	0.216

Table 4-3 Effective horizontal modal mass in percent of total mass.

		The effective modal mass percentages			
Model	Itertia	Mode 1	Mode 2	Mode 3	Sum
Response (with P- Δ)	I_{uncr}	65.70	21.45	7.18	94.33
(P≠0)	I_{cr}	62.62	20.50	7.95	91.07
Response (without P - Δ)	I_{uncr}	65.80	21.41	7.17	94.38
(P≠0)	I_{cr}	63.54	19.90	7.87	91.31
Response	I_{uncr}	65.73	21.46	7.20	94.39
(P=0)	I_{cr}	63.54	19.90	7.87	91.31
Gross (with P- Δ)	I_g	65.70	21.51	7.16	94.37
Gross (without P- Δ)	I_g	65.76	21.45	7.16	94.37
Paulay (with P- Δ)	I_p	64.53	20.84	7.38	92.75
Paulay (without P- Δ)	I_p	64.70	20.69	7.37	92.76
CPCA,1995 (with P- Δ)	$0.7I_g$	65.44	21.22	7.21	93.87
CPCA,1995 (without P- Δ)	$0.7I_g$	65.53	21.15	7.21	93.89

4.4 Pseudo-static response using push-over analysis

In this section, push-over analysis is performed to assess the P-Δ effects on the inelastic lateral load-displacement response of the wall. The static equivalent loading pattern as given by equation (2.4) was adopted except that the force at the top of the structure, F_t, was neglected. It is illustrated in Figure 4-6.

The detailed calculations of the pushover analyses for the building model with and without P-Δ effects are presented in APPENDIX B. The results of the pushover analyses with and without P-Δ effects are shown in Figure 4-7 and Figure 4-8, respectively. The response of the building model shows that the shear wall carries a base shear of 0.98 times the NBCC 1995 base shear, V, when including the P-Δ, with a relative roof displacement of 0.261 % of the building height. The response without the P-Δ effects

considered for the building model indicates that the shear wall carries a base shear of 1.04V, with a top lateral displacement of 0.253 % of the building height. Therefore, the top lateral displacement is slightly increased due to P-Δ effects when the base shear reaches the maximum value. Pushover analyses involves applying a constantly increasing lateral load to the structure to find its resistance. It is found that the plastic hinges of the shear wall developed only at the base of the wall in the pushover analyses.

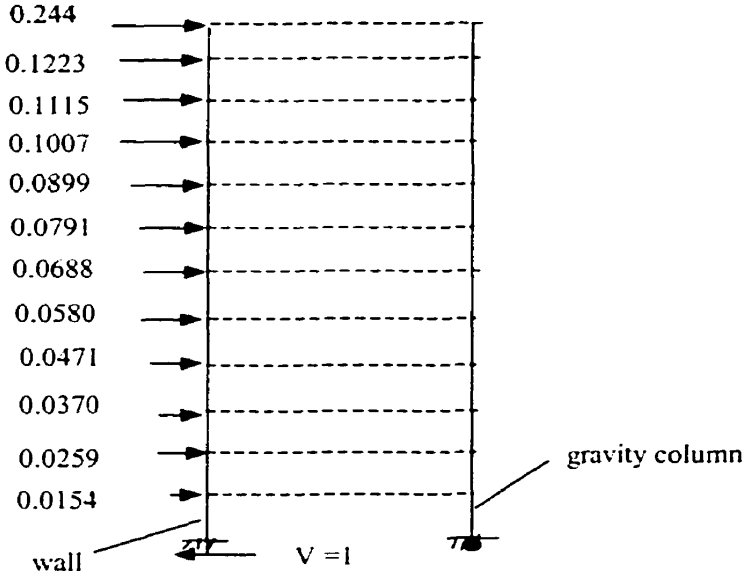

Figure 4-6 Distribution of the lateral load for the push-over analyses.

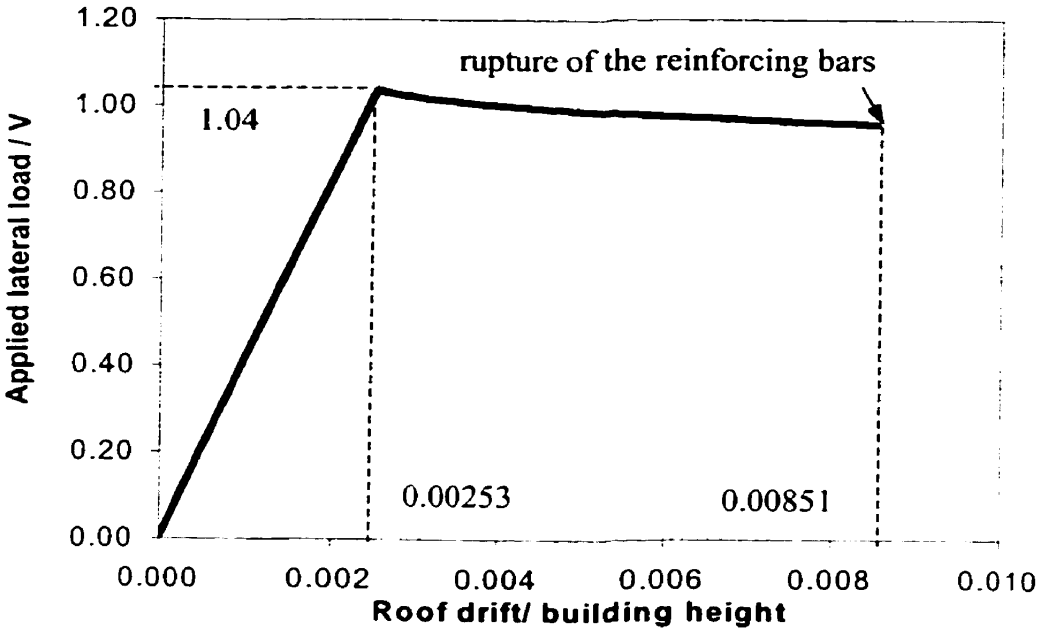

Figure 4-7 Push-over analysis (without P-Δ).

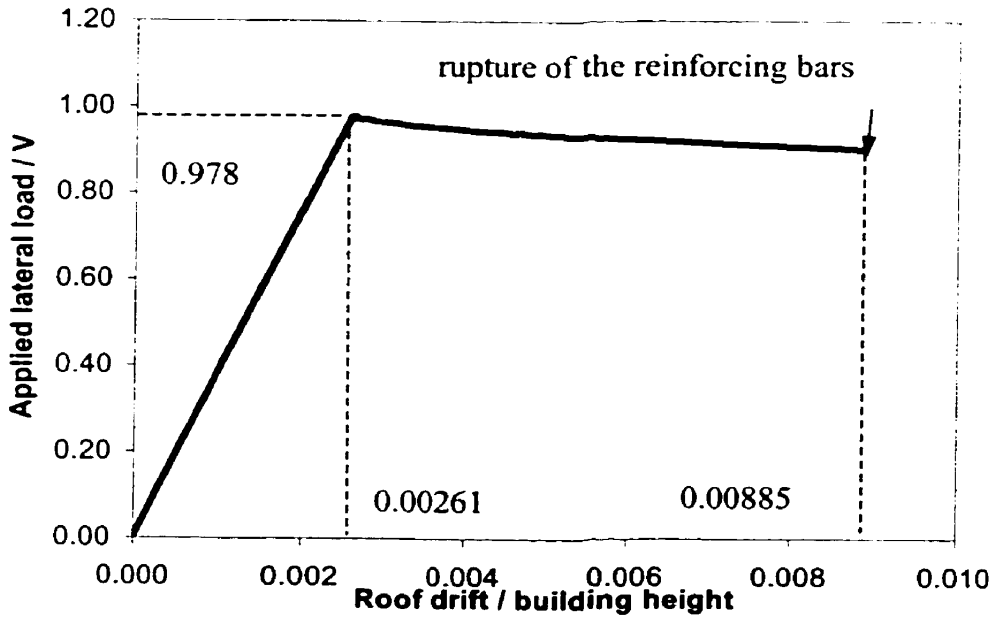

Figure 4-8 Push-over analysis (with P-Δ).

The results of push-over analysis for the yield displacements, the yield curvatures and the ultimate displacements at the base and along the height of the wall are given in Table 4-4.

Table 4-4 The results of push-over analysis.

Storey	Yield curvatures (rad/km)		Yield displacements (mm)		Ultimate displacements (mm)	
	without P-Δ	with P-Δ	without P-Δ	with P-Δ	without P-Δ	with P-Δ
12	0.045	0.045	113	120	383	392
11	0.063	0.063	101	107	--	--
10	0.070	0.070	88	94	--	--
9	0.079	0.079	76	81	--	--
8	0.104	0.104	64	68	--	--
7	0.118	0.118	52	56	--	--
6	0.129	0.129	41	44	--	--
5	0.159	0.159	31	33	--	--
4	0.154	0.154	21	23	--	--
3	0.186	0.186	13	15	--	--
2	0.171	0.171	7	8	--	--
1	0.207	0.207	3	3	--	--

4.5 Response spectrum analysis (NBCC, 1995)

Earthquake response spectra are most useful in earthquake resistant design. In general, the response of a structure to a given earthquake accelerogram is a function of its damping and its natural frequency. For a given SDOF system, spectral displacements, spectral velocities, and spectral accelerations can be plotted on a graph when the SDOF system is subjected to a given earthquake accelerogram. In practice, response spectra are often represented by a graph with multiple logarithmic scales (Figure 4-9).

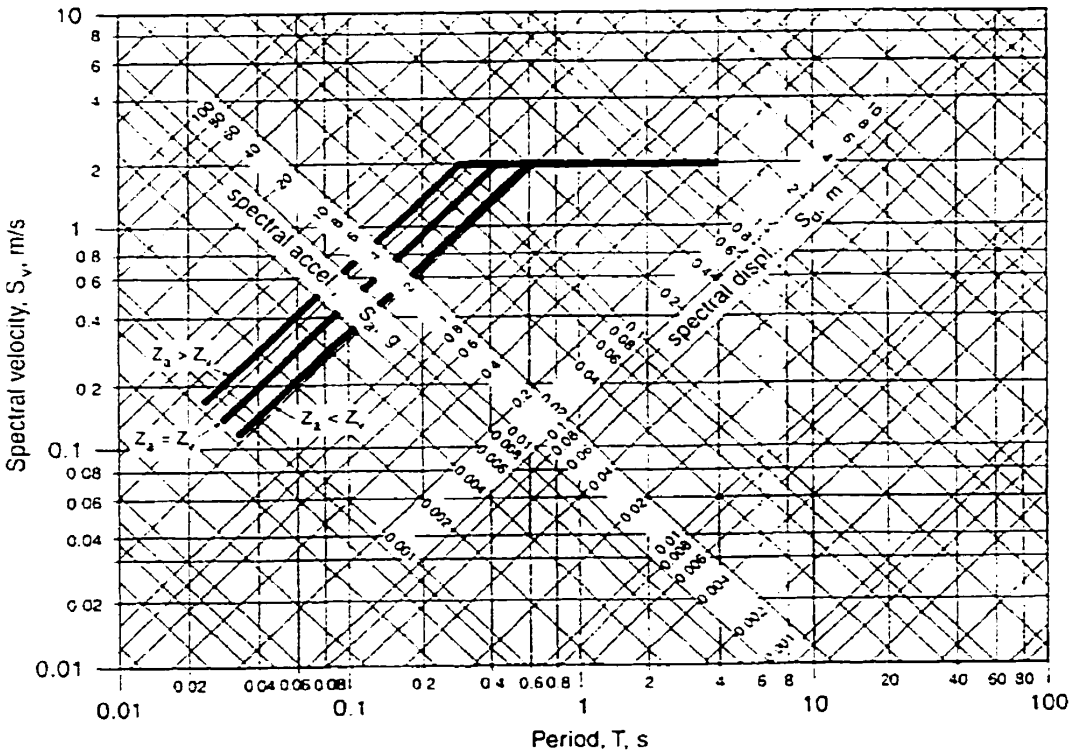

Figure 4-9 Normalized design spectra (NBCC 1996) for peak horizontal ground velocity v = 1 m/s.

Figure 4-9 shows the normalized elastic design spectra in the User's Guide of the NBCC 1995. It is based on 5 percent critical damping and maximum ground horizontal velocity of 1 m/s. For a given site, the design spectrum must be scaled to the peak horizontal

design velocity for the site. For Montreal, the peak ground horizontal velocity v = 0.1 m/s and the peak ground acceleration is equal 0.18 g (1.764 m/s^2).

The response spectra analysis is based on the function of spectral acceleration, Sa, versus the period. The normalised Sa for Montreal, as obtained from the NBCC design spectrum, is given in Figure 4-10. For Montreal, the maximum value of Sa in the short period range, T < 0.305 s, is equal to 0.42 g. If the period T > 0.305 s, the spectral acceleration decreases with the natural periods and the following formula is to be used for the determination of the spectral acceleration: Sa = 0.0408π / T. The SAP90 program is used to carry out the response spectra analysis.

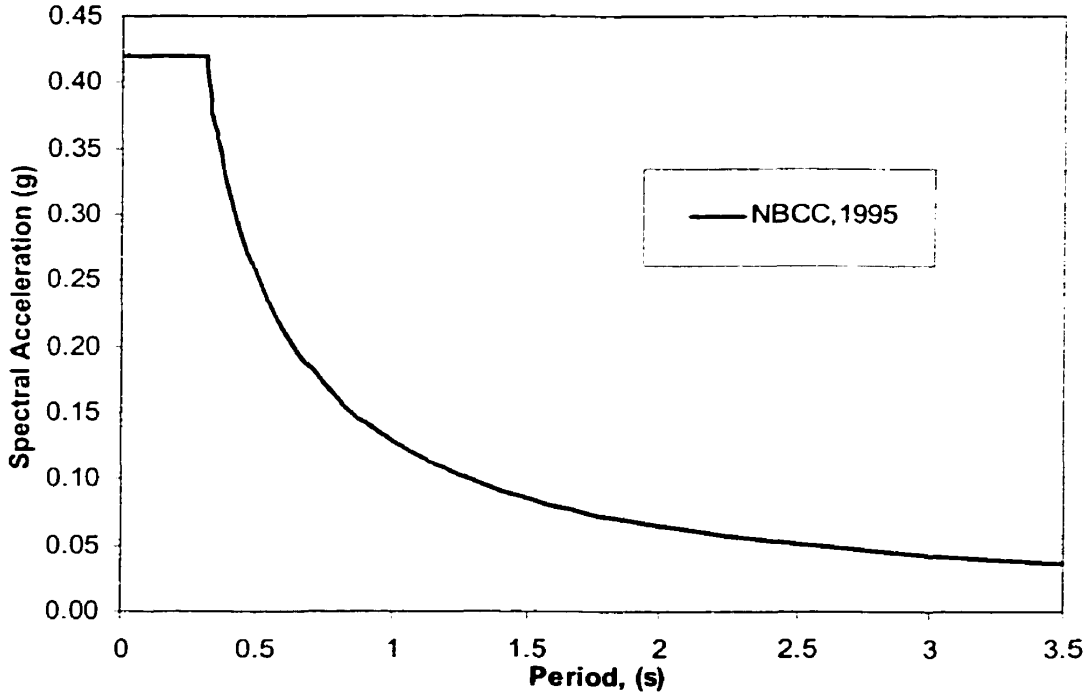

Figure 4-10 Design response spectra for Montreal (NBCC,1995).

The pseudo-dynamic analysis by the response - spectrum approach requires the determination of the natural periods, the free-vibration mode shapes, and the modal participation factors to apply the mode-superposition method. The modal base shears and other modal response quantities can also be obtained from the analysis. Table 4-5

shows that some parameters of first the three modes obtained from the SAP90 program. To get the maximum displacement and member forces (or stresses), the modal responses associated with a particular mode are first calculated and then combined using the Complete Quadratic Combination technique (CQC). The shear wall has a pseudo-dynamic base shear of 3559.8 kN when P-Δ effects are considered and the relative top lateral displacement is 162.8 mm. When not including P-Δ effects, the shear wall has a base shear of 3584.7 kN with a top displacement of 155.3 mm. To obtain the design response quantities, the pseudo-dynamic response should be multiplied by the V/V_{dyn}, where V (V = 958 kN) is the design base shear obtained from the pseudo-static procedure of NBCC 1995. Therefore, the relative top lateral pseudo-dynamic displacement (elastic displacement) is 45.4 mm for P-Δ is considered, and 43.0 mm when not including P-Δ effects. So, the lateral roof displacement will not be increased significantly if the P-Δ effects are considered when the shear wall is analyzed by linear elastic response spectra procedure.

Table 4-5 The results of response spectra analysis (unscaled by V/V_{dyn}).

Parameters	Mode (without P-Δ)			Mode (with P-Δ)		
	Mode 1	Mode 2	Mode 3	Mode 1	Mode 2	Mode 3
Periods of vibration (s)	3.225	0.551	0.216	3.389	0.555	0.217
Mass percentages	65.53	21.15	7.21	65.44	21.22	7.21
Base shear (kN)	1217.7	2942.3	1407.2	1155	2936.9	1408.9
Spectral displacement (mm)	103	23	5	108	23	5

4.6 Selection of ground motions

Three earthquake accelerograms are selected to represent different types of seismic loading. The El Centro 1940 (SOOE) is an historical Western North America type of event which contains a broad range of frequency. The Taft 1959 (S69E) record was considered because it has strong shaking of long duration and higher frequency content. At last, the Parkfield (N65E) record was chosen because it is representative of a pulse type motion. The three earthquake records are shown in Figure 4-11. The first 20 seconds of all records were considered in this study.

(a) El Centro

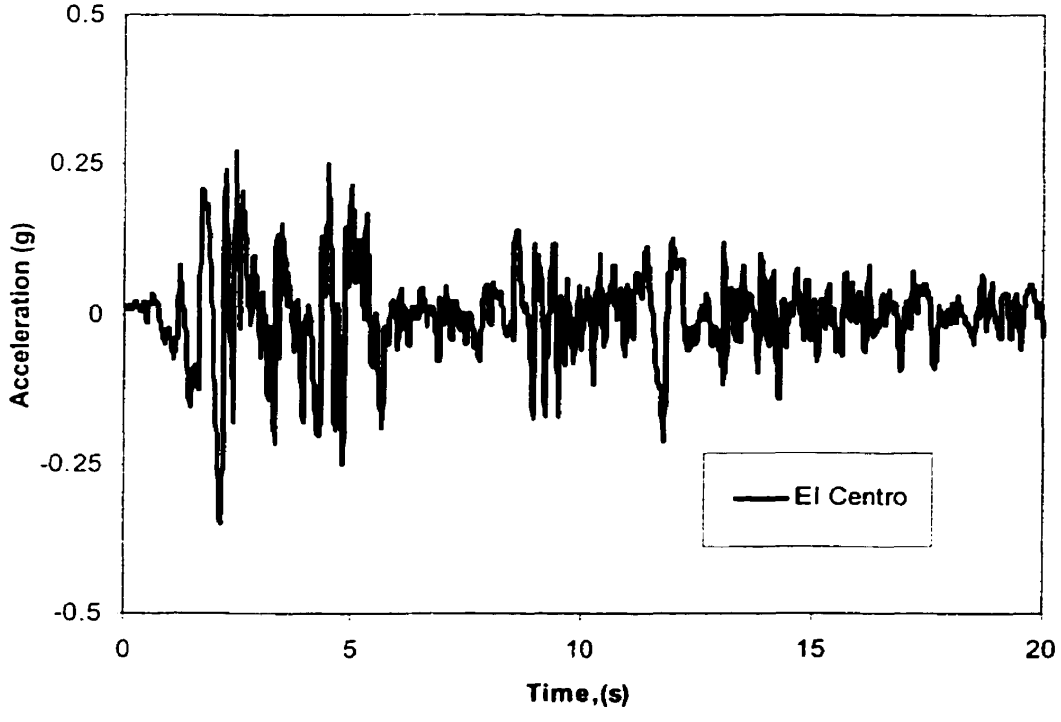

(b) Taft

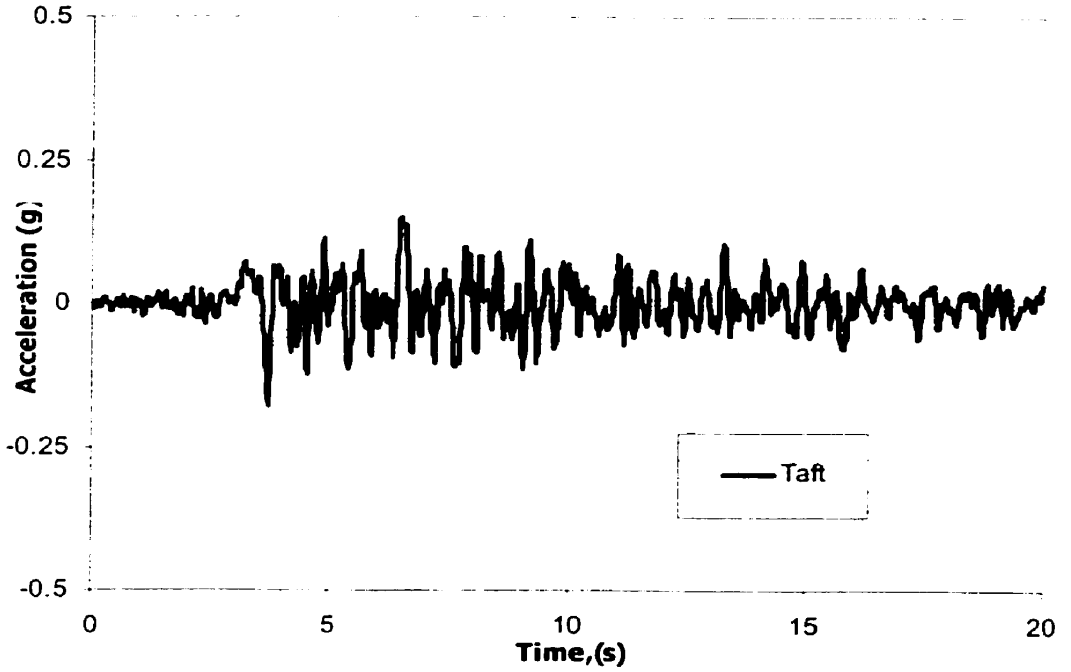

(c) Parkfield

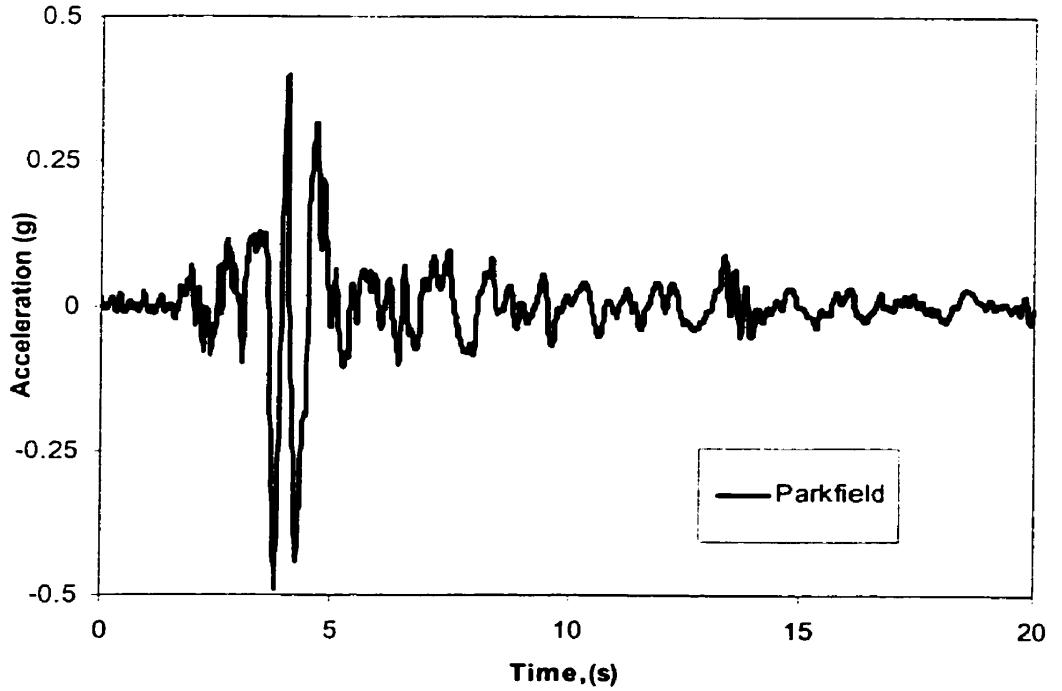

Figure 4-11 Selected earthquake records.

Because the wall is designed according to NBCC 1995, the three earthquake records were scaled to fit the elastic response spectra of NBCC 1995 for Montreal. For each of the ground motions, the records were scaled so that their peak acceleration is normalized to a value of 0.18 g, which corresponds to the peak ground acceleration of NBCC, 1995 for Montreal. Table 4-6 gives the characteristics of the ground motions as scaled.

Table 4-6 Characteristic of earthquake records

Earthquake record	Comp.	PGA (g)	Duration considered	Scaling factor	Scaled PGA (g)
EL Centro	S00E	0.348	20 s	0.517	0.18
Taft	S69E	0.179	20 s	1.006	0.18
Parkfield	N65E	0.489	20 s	0.368	0.18

The related response spectra are calculated from the scaled accelerations time histories using the RESAS computer program for damping value of 5%. Figure 4-12 shows the spectra for the three scaled accelerograms when compared with the design spectra.

(a) El Centro

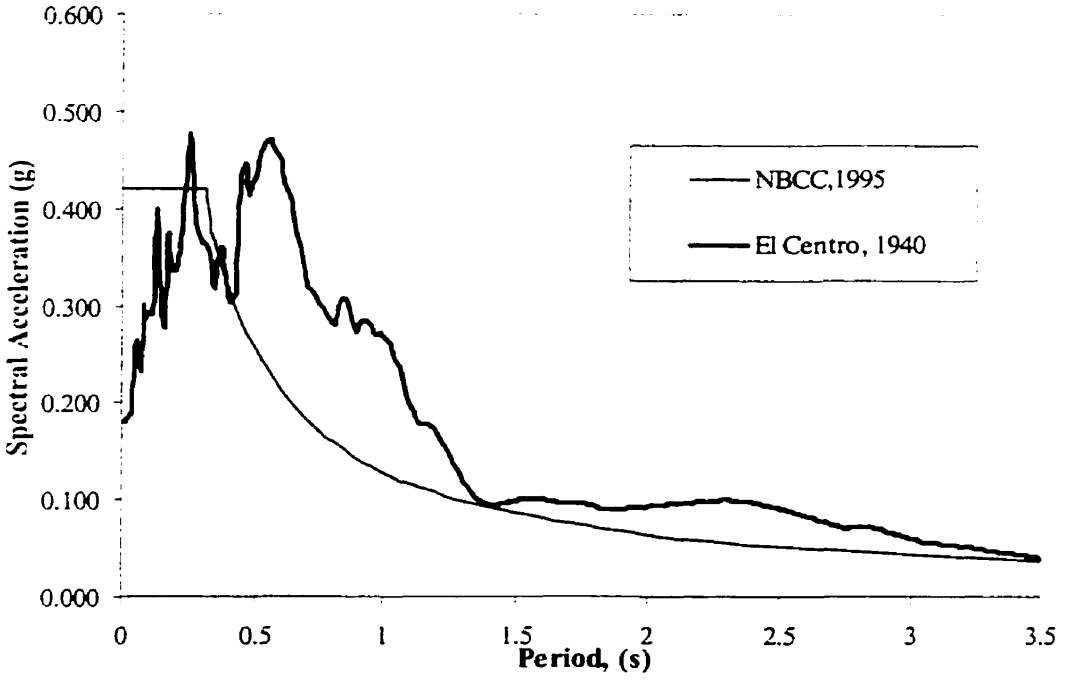

(b) Taft

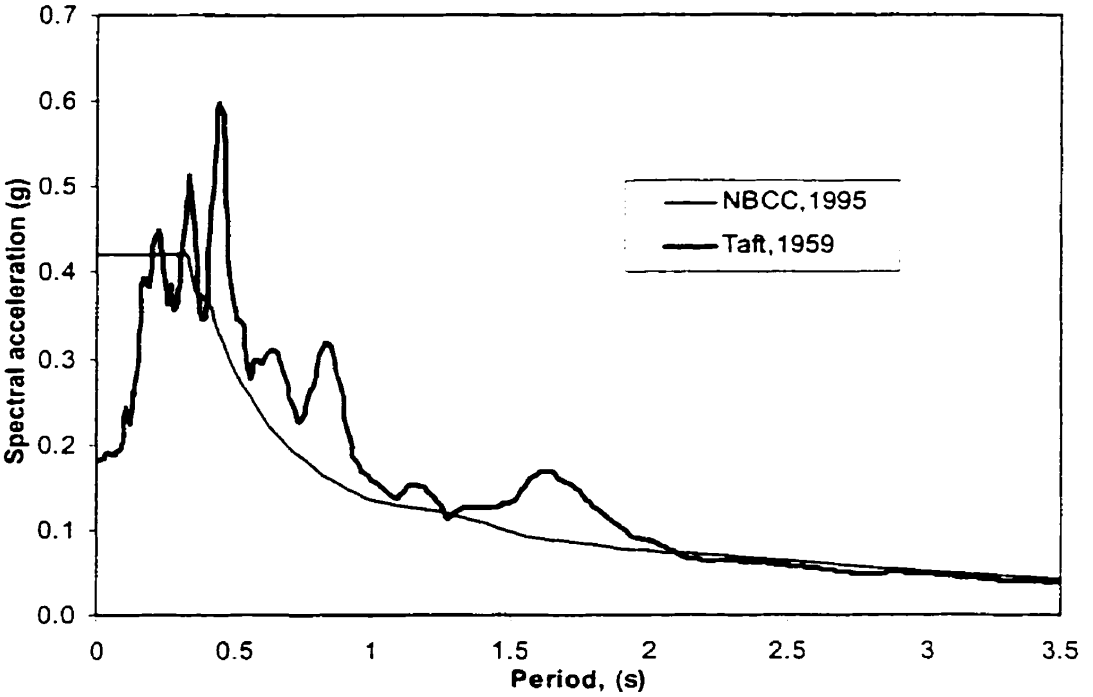

(c) Parkfield

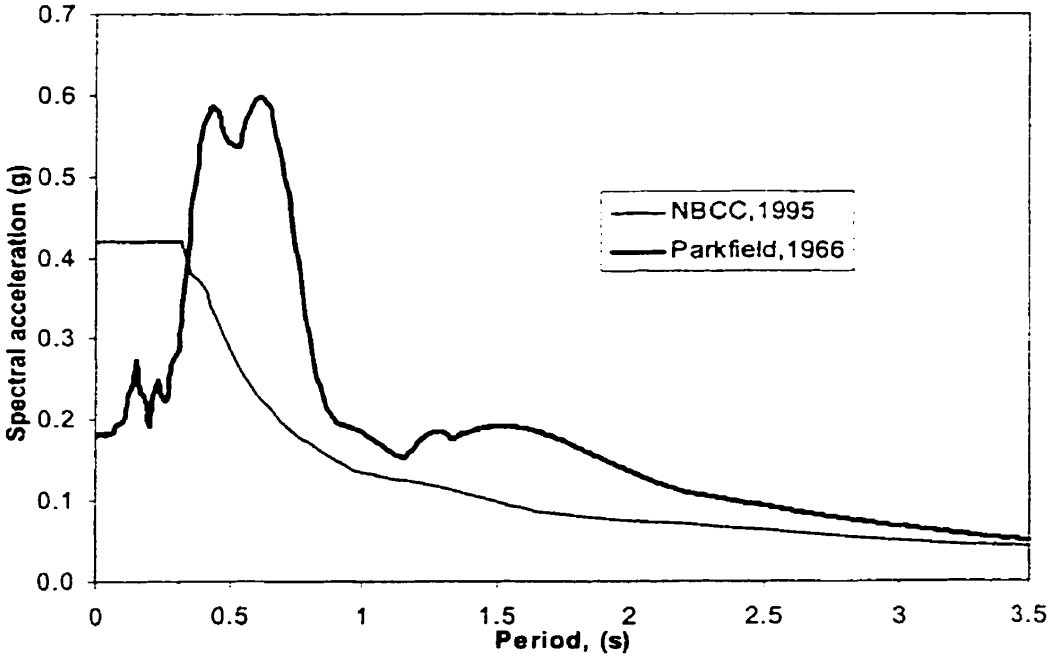

Figure 4-12 Scaled earthquake spectra.

4.7 Transient response

In this section, transient analyses are performed with the RUAUMOKO computer program to produce time-histories of various response quantities from a nonlinear two-dimensional model of the prototype. The wall flexural stiffness is specified as 0.7 EI_g, or 70% of the gross values to allow for cracking. The inelastic behaviour of the wall follows the concept of the Giberson one-component model, which has a possible plastic hinge at one or both ends of the elastic central length of the member (Figure 2-2). Three earthquake records are used to examine the wall response under different types of earthquake loading (Fig.4-12). The time step used is 0.005 s. The duration of ground motion and structural response considered is 20 s. The P-Δ effects are investigated while considering material nonlinearities.

The responses of the structure subjected to three ground motions are described in Figures 4-16 to 4-33 which show: (1) the top lateral displacement time histories, (2) the base shear time histories, (3) the moment-curvature response histories at the base of the wall, (4) the lateral displacement envelopes over the height of the structure, (5) the displacement ductility demands in the walls, and (6) the curvature ductility demands in the wall. Table 4-7 summarizes the peak roof displacements, and maximum base shears obtained from inelastic dynamic analyses.

Table 4-7 Nonlinear response parameters of the shear wall structure.

Earthquake		Peak roof displacement (mm)	Maximum base shear (kN)	Maximum base shear as a ratio of structural weight
EL Centro	without P-Δ	170	3220	0.0689
	with P-Δ	158	3200	0.0684
Taft	without P-Δ	121	2290	0.0490
	with P-Δ	121	2300	0.0492
Parkfield	without P-Δ	264	2890	0.0618
	with P-Δ	254	2930	0.0627

In Table 4-7, maximum base shears of the shear wall under earthquake loading are found to be 2 to 3 times larger than the design base shear obtained from the pseudo-static procedure of NBCC 1995. Part of this can be explained by the Φ factor and J factor. If these factors are set to 1.0, the base shear producing M_y at the base of the wall under NBCC loading pattern is 958 kN. To explain further these results, maximum base shear under El Centro earthquake are studied when not including P-Δ. According to Figure 4-17, the time of the loading is 2.11 s when the base shear reaches its maximum value. The accelerations of the shear wall and inertia forces acting at each storey can be obtained at that time. The shear forces and bending moments produced by these forces at each storey can then be computed. Table 4-8 summarizes all these results. Inertia forces, shear forces and bending moments at each storey under the El Centro earthquake are described in Figures 4-13 to 4-15. The results show that the base shear reach 3400 kN while the bending moment developed at the base of the shear wall is 30297 kN-m which corresponds to the plastic hinge capacity (see Table 3-9 and Figure3-16).

Table 4-8 The results of analysis without P-Δ effects (El Centro)

Storey	Acceleration (m/s^2)	Mass ($N*s^2/m$)	Inertia force F_i (N)	Inertia force F_i (kN)	Shear force V (kN)	Moment M (kN-m)
12	0.761	363265	-276445	-276	276	0
11	0.506	392143	-198424	-198	474	-1007
10	0.252	392143	-98820	-99	573	-2738
9	-0.102	392143	39999	40	533	-4829
8	-0.303	392143	118819	119	414	-6774
7	-0.524	392143	205483	205	209	-8286
6	-0.799	395204	315768	316	-107	-9048
5	-1.08	395204	426820	427	-534	-8697
4	-1.53	395204	604662	605	-1139	-6736
3	-1.76	404388	711723	712	-1815	-2551
2	-1.89	404286	764101	764	-2615	4210
1	-1.86	421837	784617	785	-3400	13766
0	-1.65	0	0	0	-3400	30297

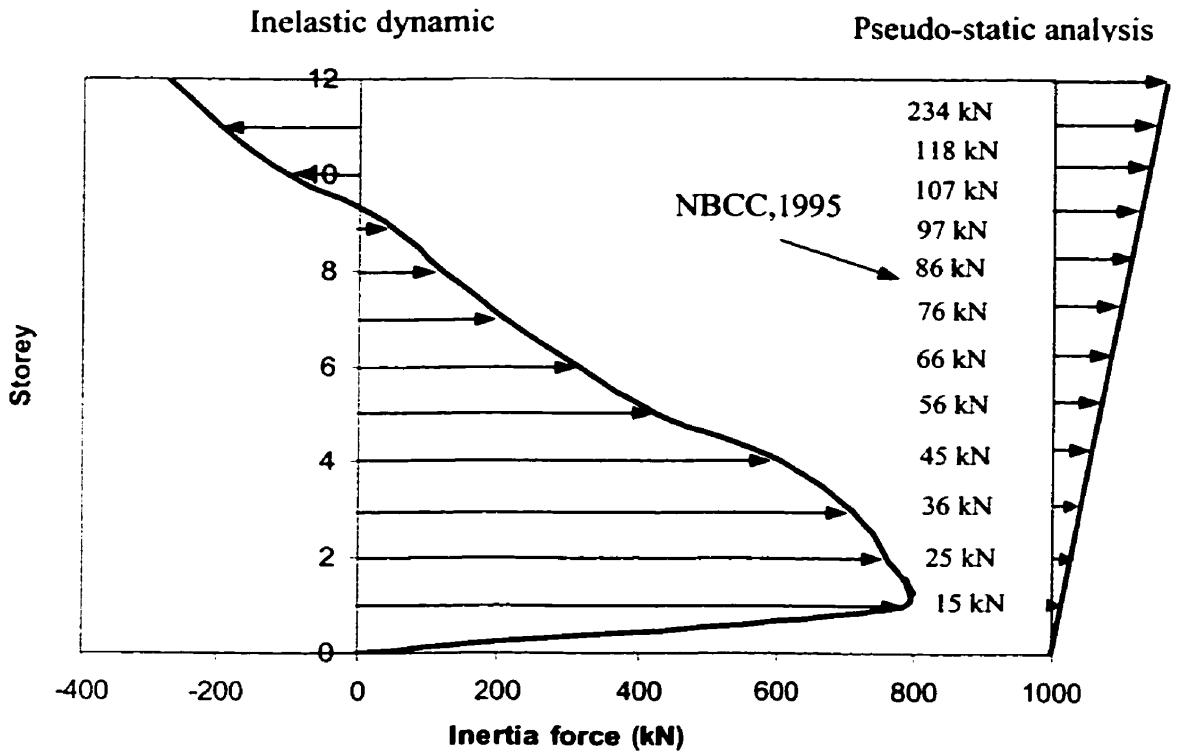

Figure 4-13 Inertia force at each storey - El Centro earthquake (without P-Δ).

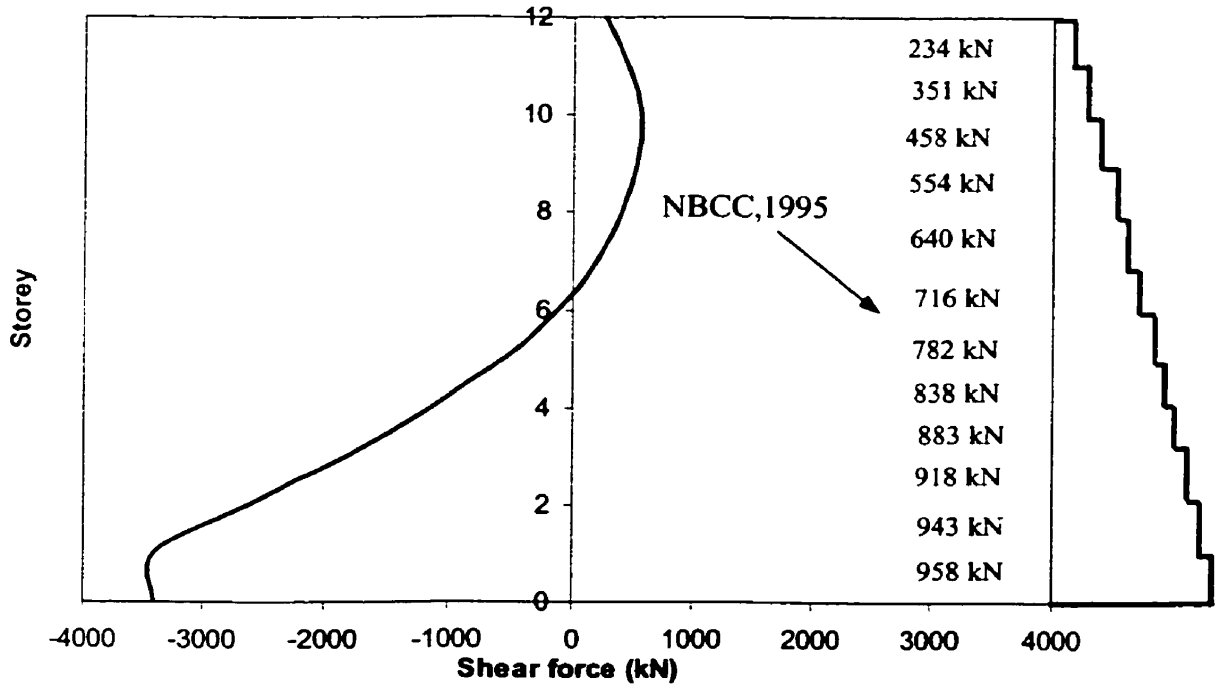

Figure 4-14 Shear force at each storey - El Centro earthquake (without P-Δ).

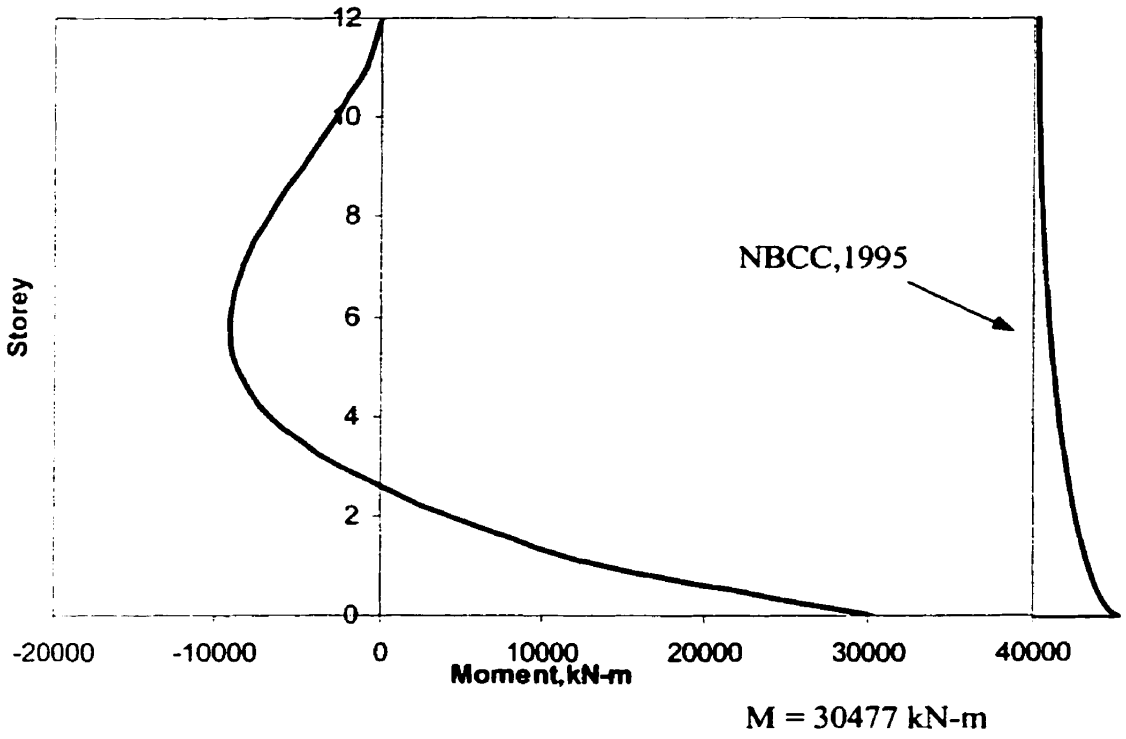

Figure 4-15 Moment at each storey - El Centro earthquake (without P-Δ).

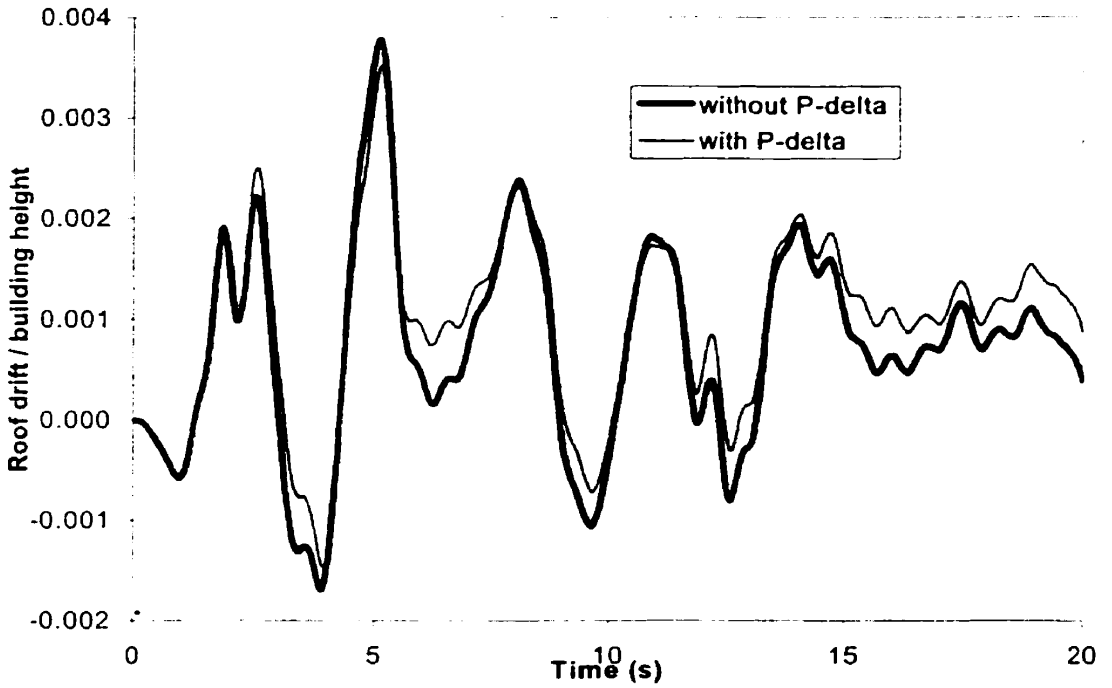

Figure 4-16 Top lateral displacement time history - scaled El Centro earthquake.

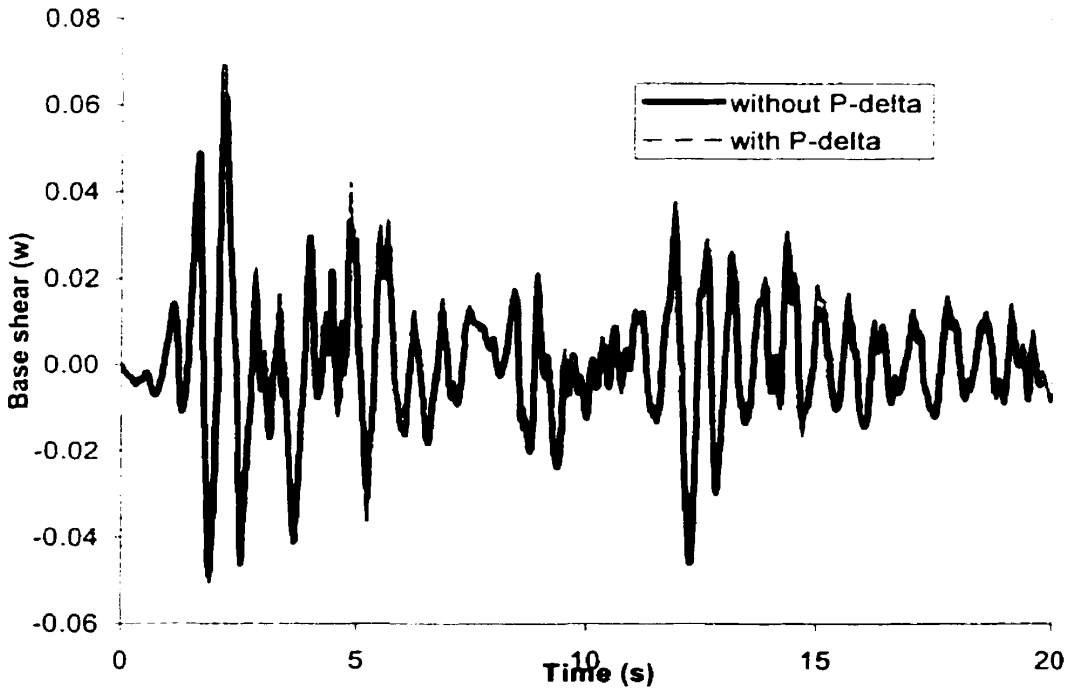

Figure 4-17 Base shear time history - scaled El Centro earthquake.

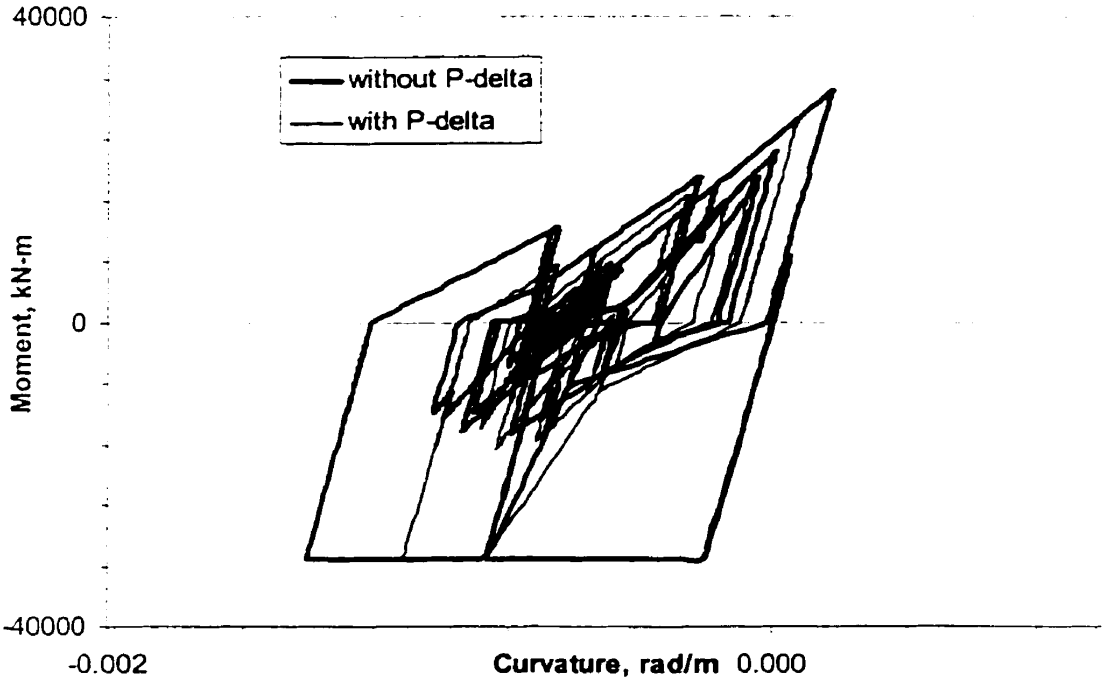

Figure 4-18 Moment – curvature response history at the base of the wall scaled El Centro earthquake.

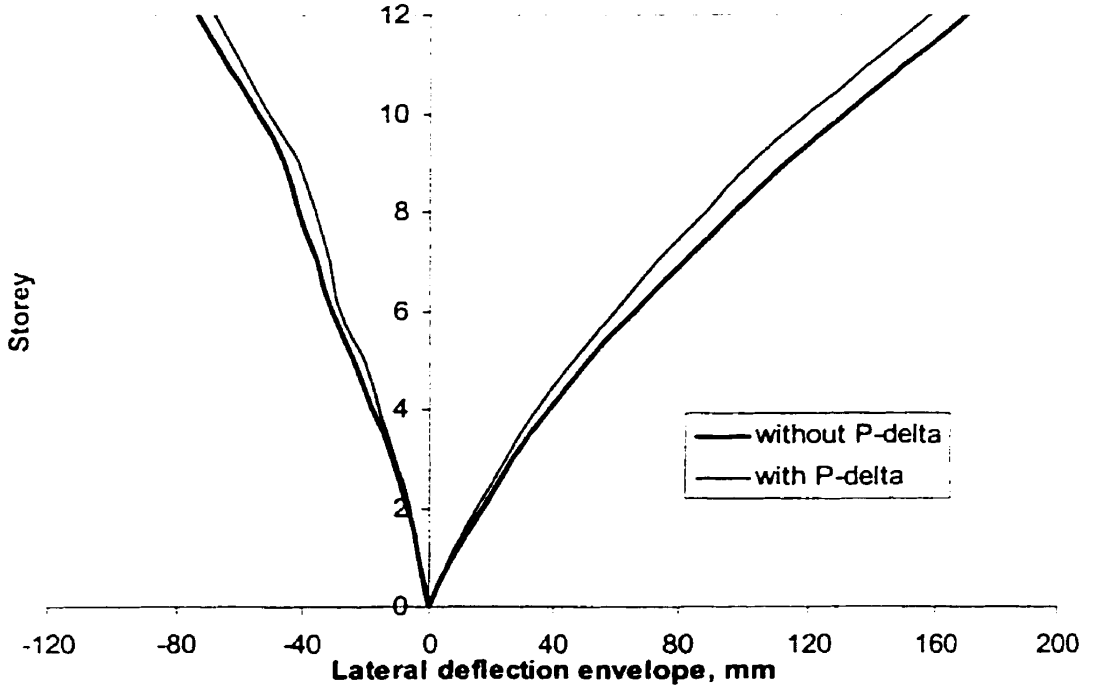

Figure 4-19 Lateral displacement envelope over the height of the structure -scaled El Centro earthquake.

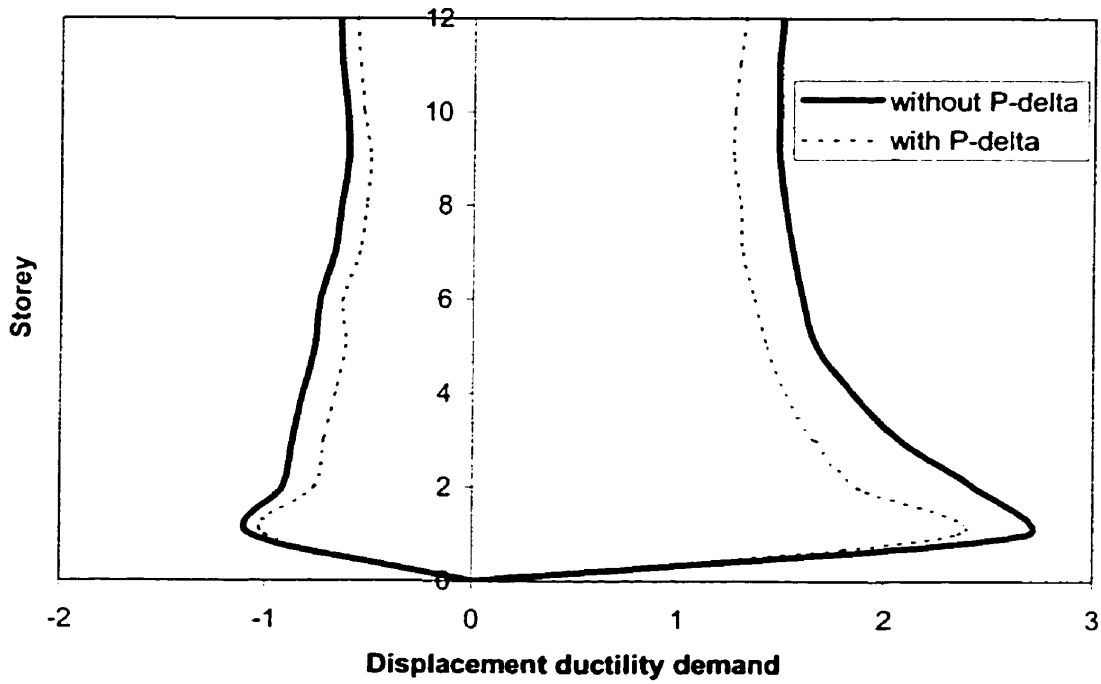

Figure 4-20 Peak displacement ductility demand in the wall - scaled El Centro earthquake.

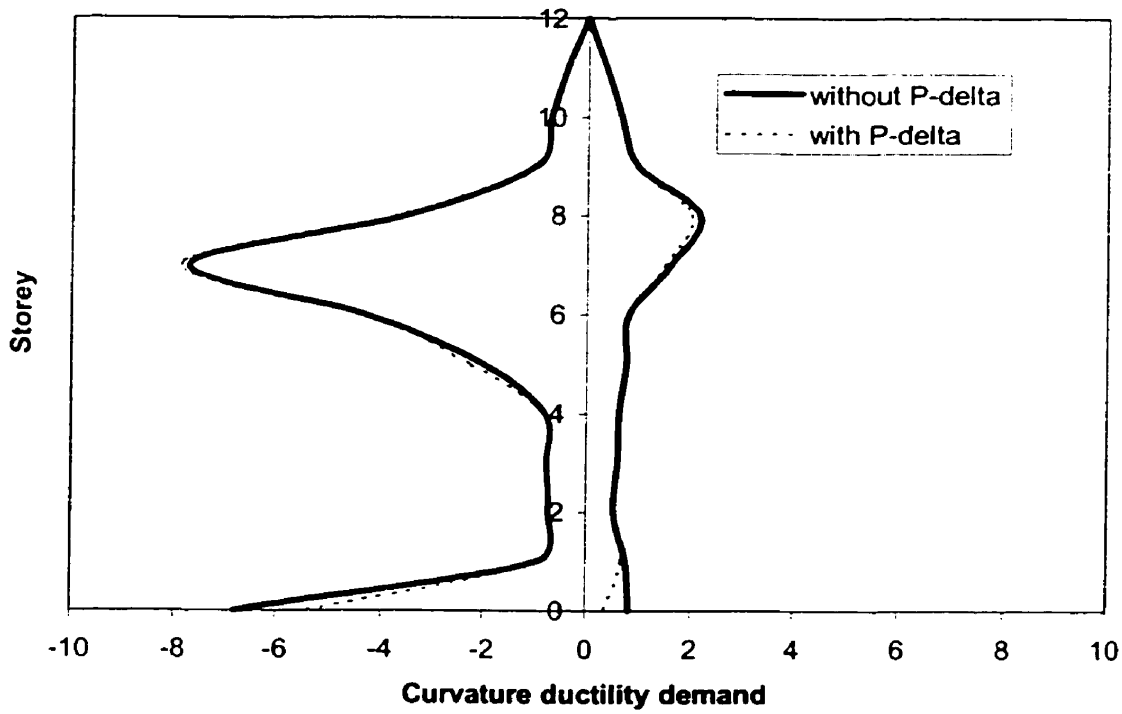

Figure 4-21 Curvature ductility demand in the wall – scaled El Centro earthquake.

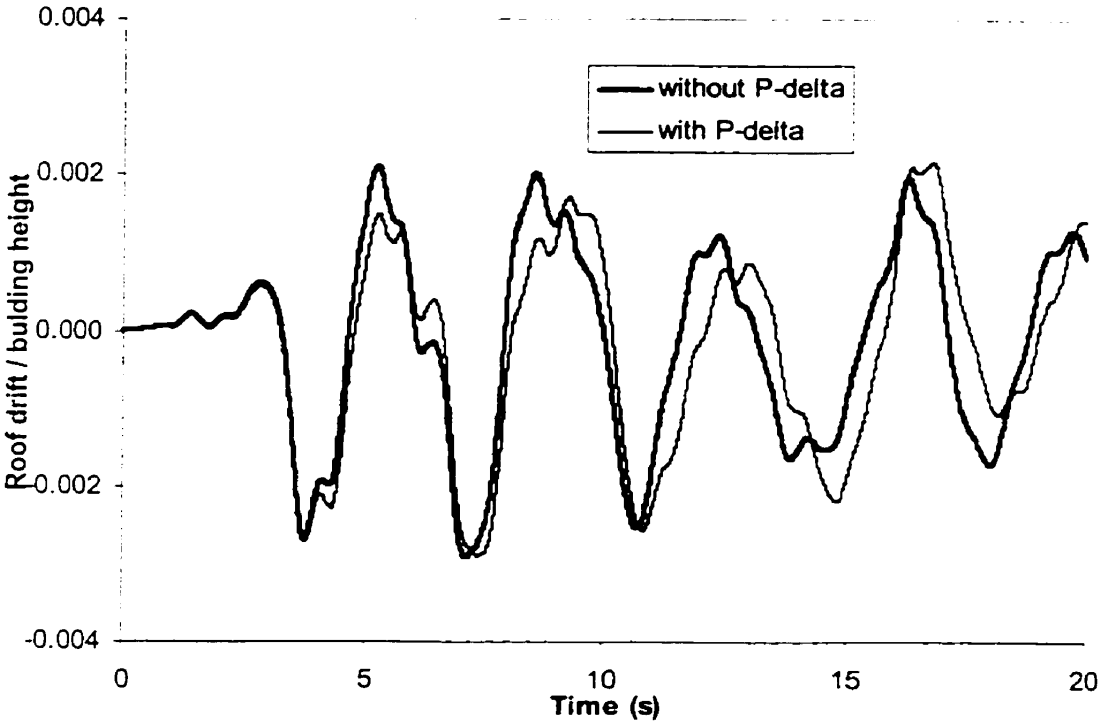

Figure 4-22 **Top lateral displacement time history - scaled Taft earthquake.**

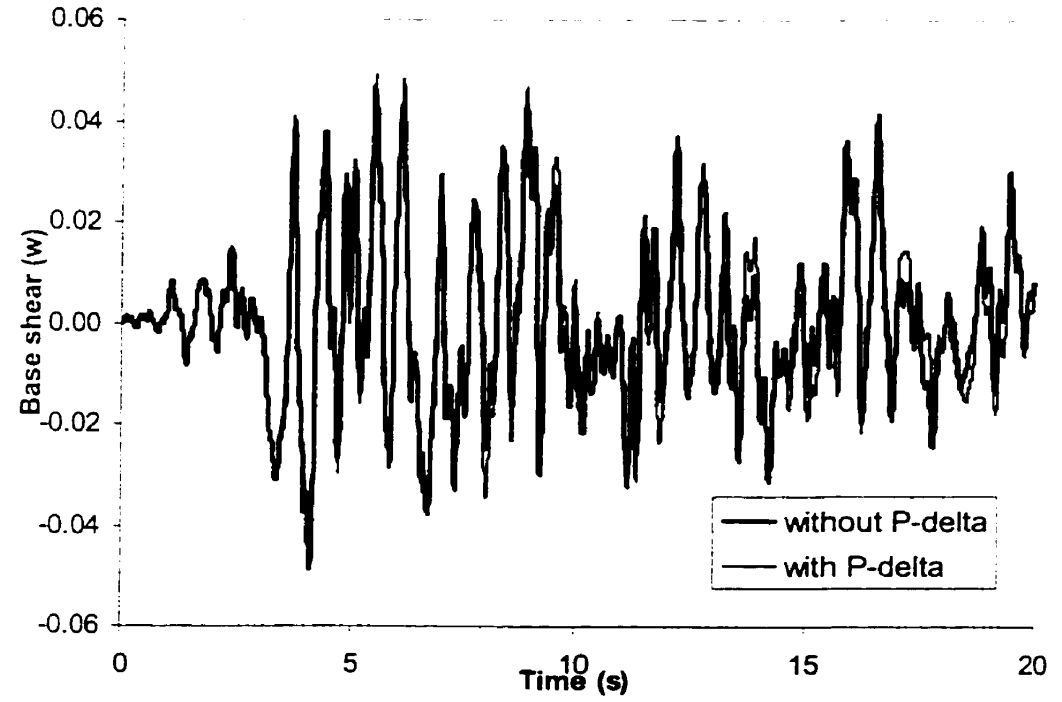

Figure 4-23 **Base shear time history – scaled Taft earthquake.**

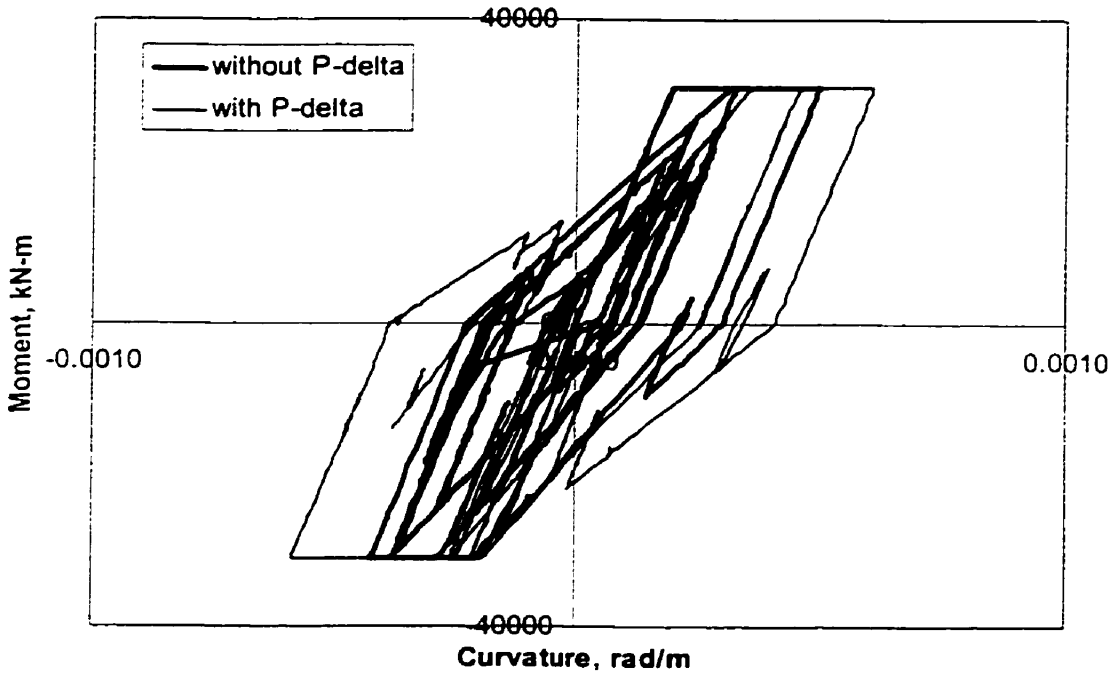

Figure 4-24 Moment-curvature response history for the base of the wall -scaled Taft earthquake.

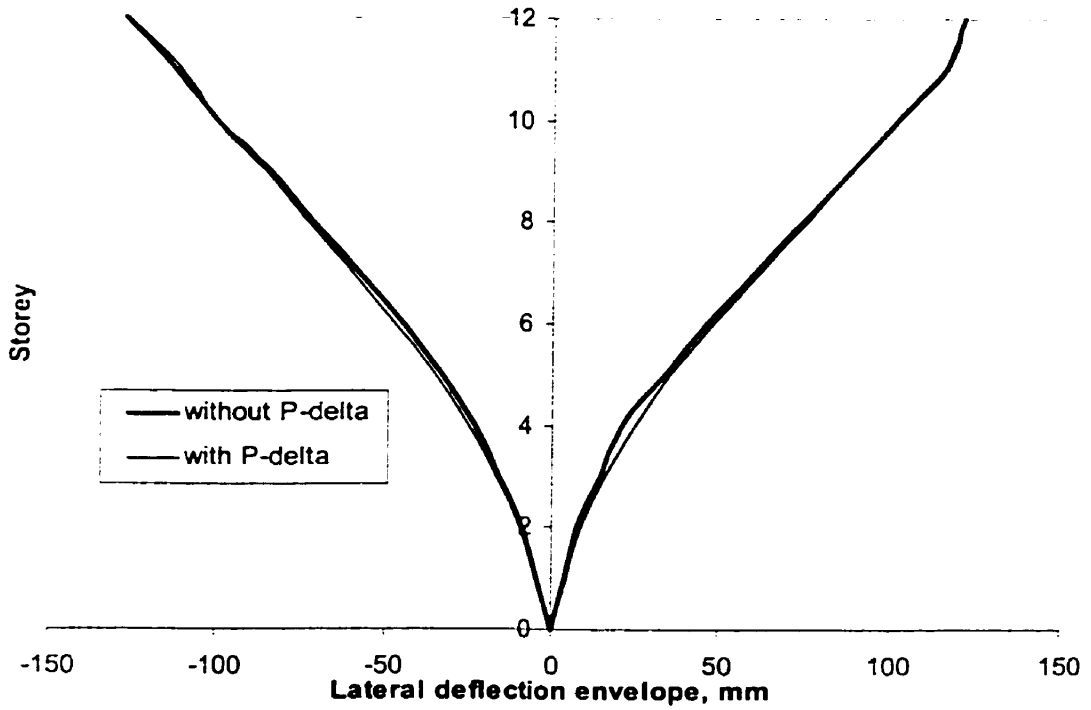

Figure 4-25 Lateral displacement envelope over the height of the structure - scaled Taft earthquake.

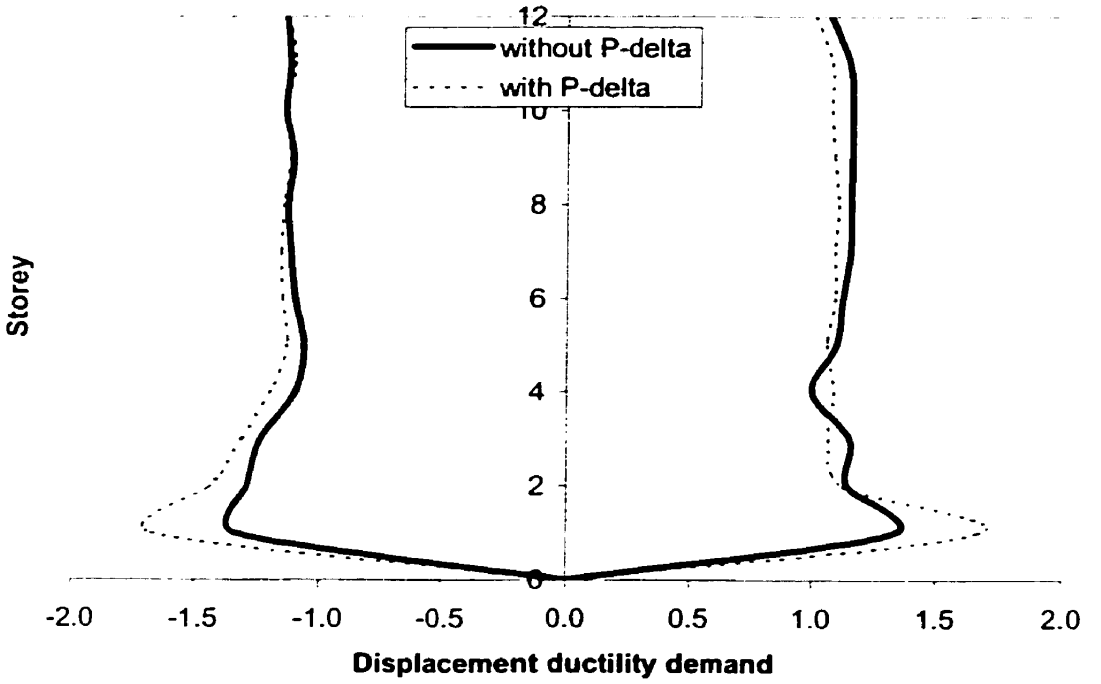

Figure 4-26 Displacement ductility demand in the wall - scaled Taft earthquake.

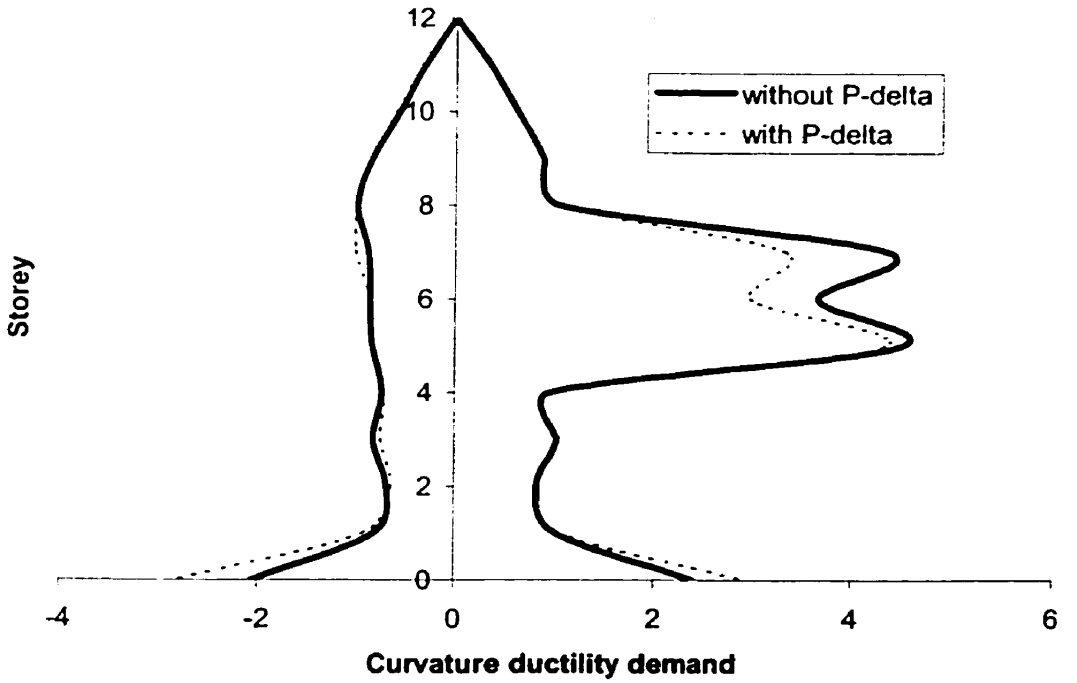

Figure 4-27 Curvature ductility demand in the wall - scaled Taft earthquake.

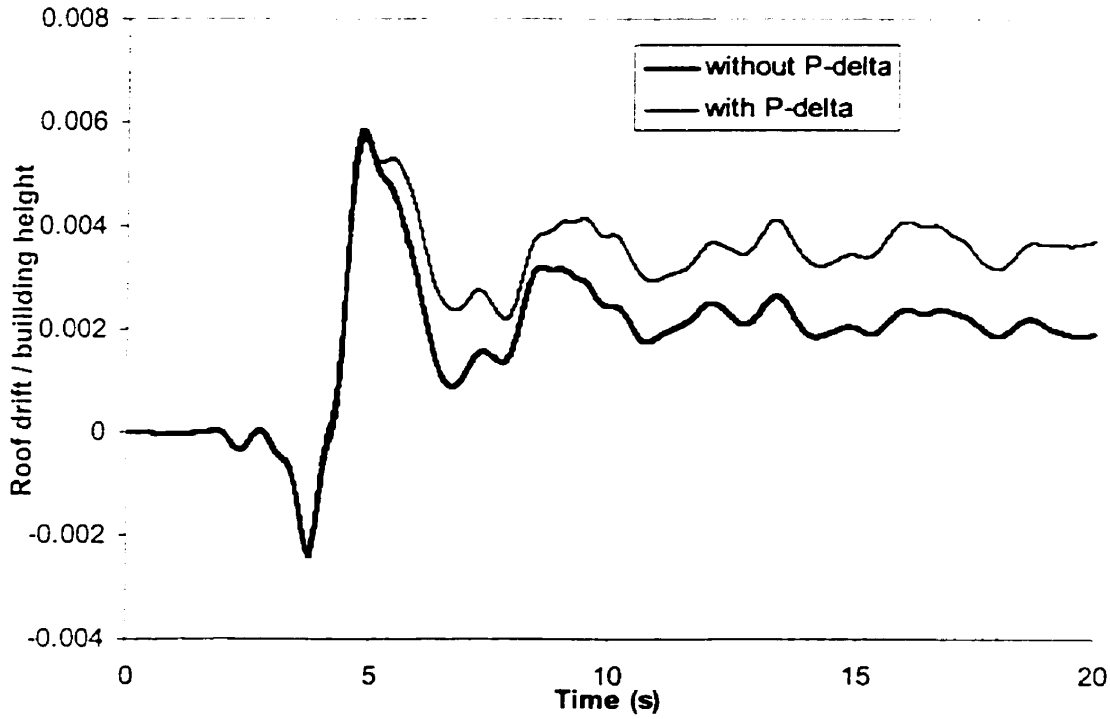

Figure 4-28 Top lateral displacement time history - scaled Parkfield earthquake.

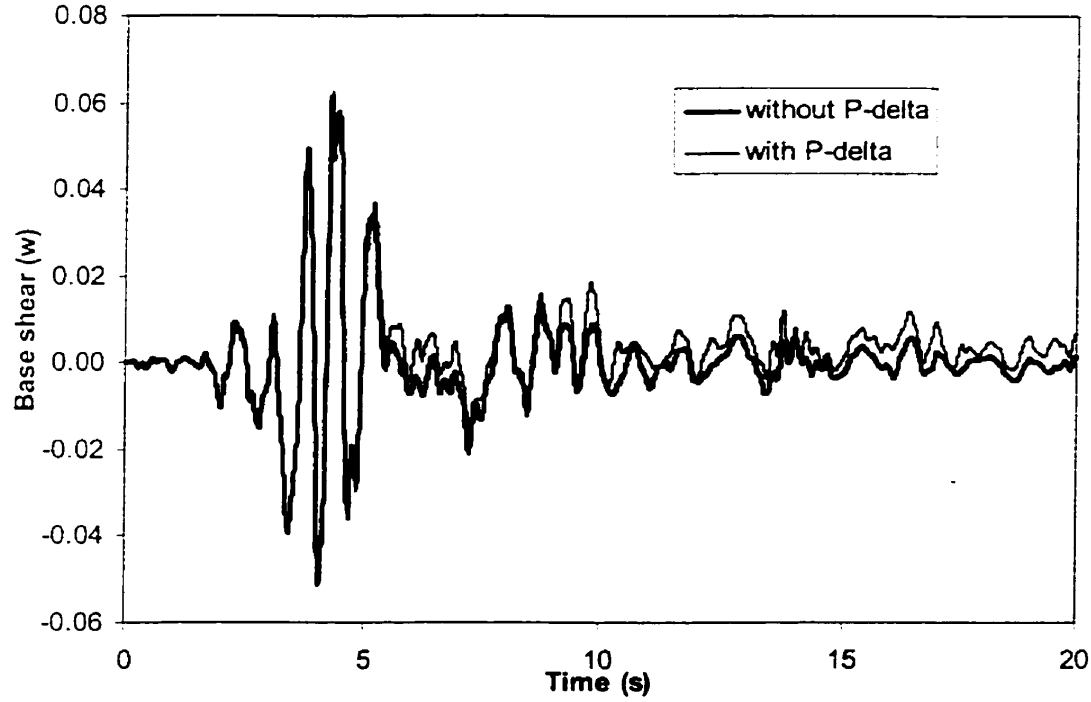

Figure 4-29 Base shear time history - scaled Parkfield earthquake.

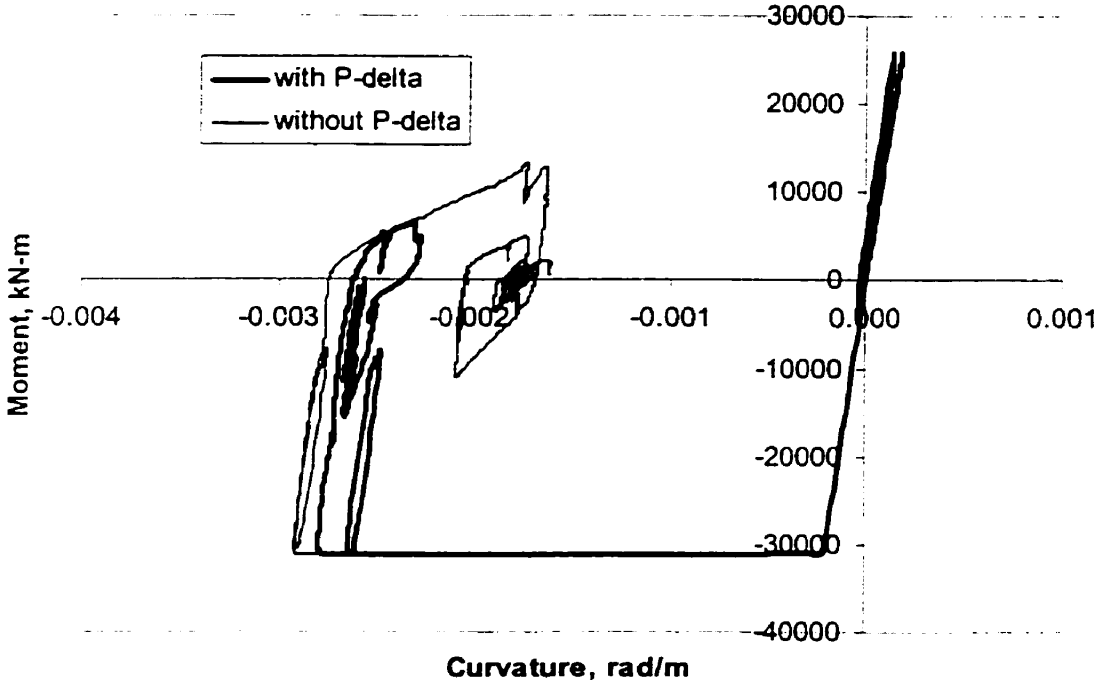

Figure 4-30 **Moment-curvature response history for the base of the wall - scaled Parkfield earthquake.**

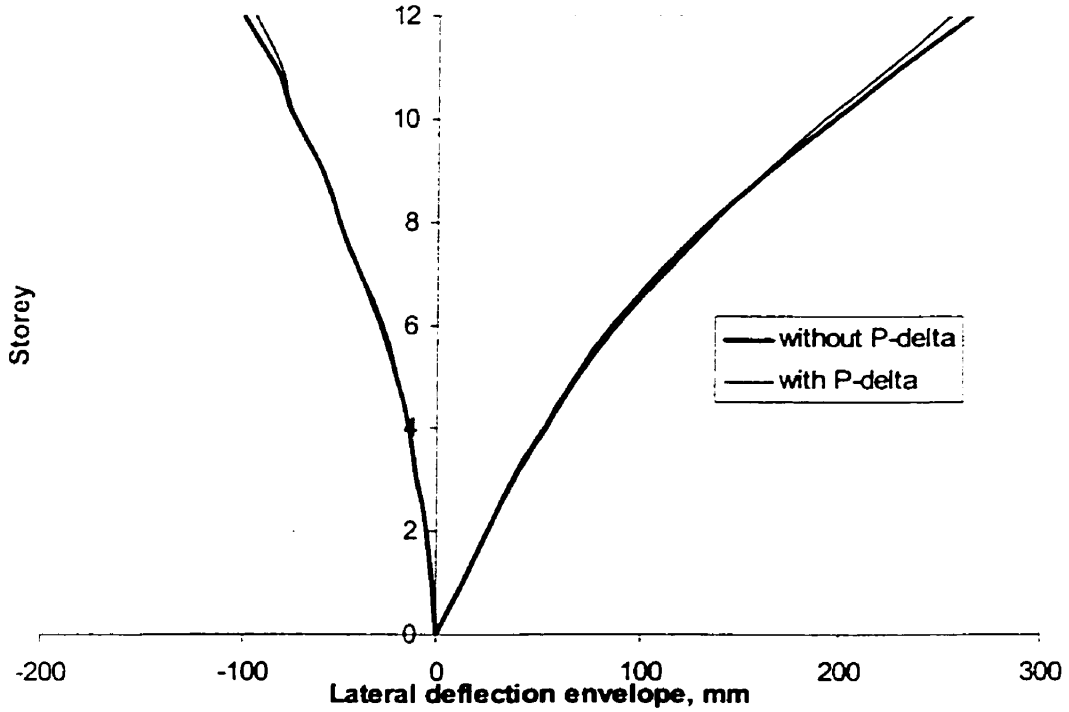

Figure 4-31 **Lateral displacement envelope over the height of the wall - scaled Parkfield earthquake**

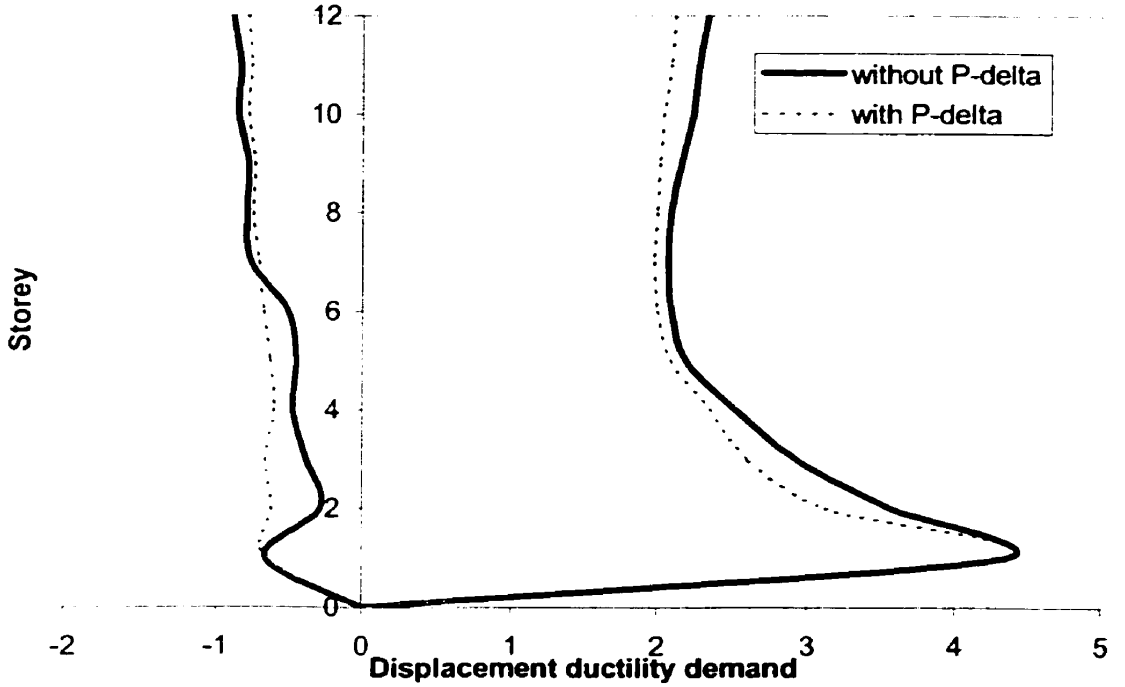

Figure 4-32 Displacement ductility demand in the wall - scaled Parkfield earthquake.

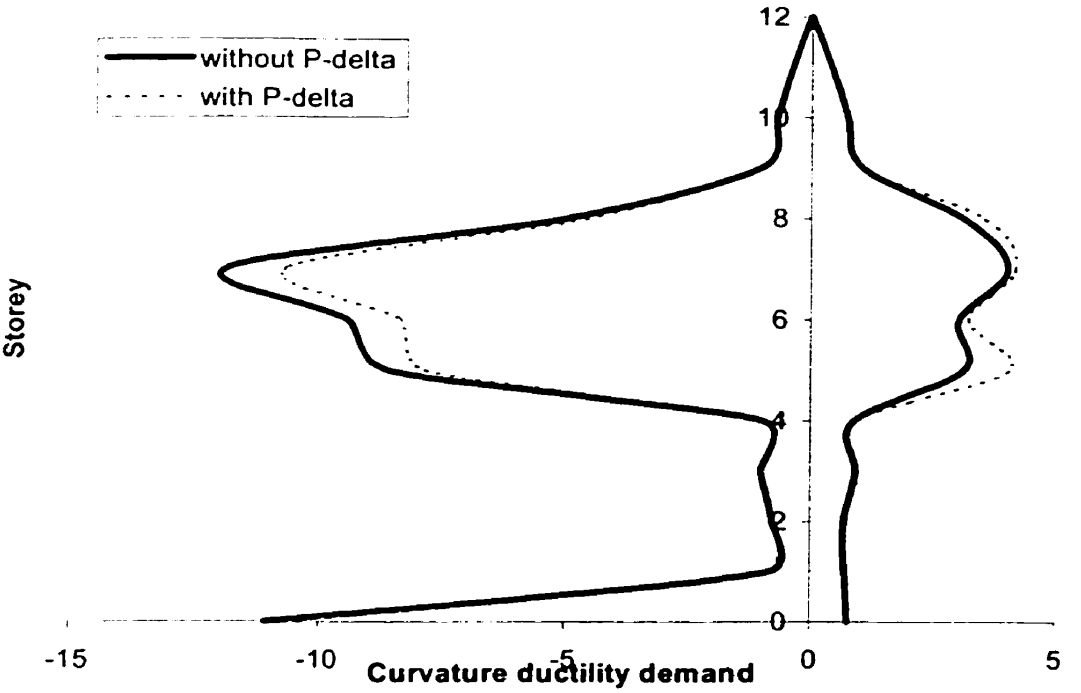

Figure 4-33 Curvature ductility demand in the wall - scaled Parkfield earthquake.

To assess the response of the shear wall, the ductility demands are summarized. The values for the displacement ductility demands and curvature ductility demands at the base and over the height of the wall are given from Table 4-9 to Table 4-14.

Table 4-9 Displacement ductility demand of the shear wall (El Centro).

Storey	The maximum lateral deflection (mm)		The yield displacement (mm)		Displacement ductility demand	
	without P- Δ	with P- Δ	without P- Δ	with P- Δ	without P- Δ	with P- Δ
12	170 (-74)*	158 (-69)	113	120	1.50 (-0.65)	1.32 (-0.57)
11	150 (-65)	138 (-60)	101	107	1.49 (-0.64)	1.29 (-0.56)
10	131 (-54)	119 (-50)	88	94	1.49 (-0.61)	1.27 (-0.54)
9	113 (-46)	102 (-41)	76	81	1.49 (-0.61)	1.26 (-0.50)
8	97 (-41)	88 (-36)	64	68	1.52 (-0.64)	1.29 (-0.53)
7	81 (-35)	73 (-31)	52	56	1.56 (-0.67)	1.30 (-0.55)
6	66 (-30)	60 (-28)	41	44	1.61 (-0.74)	1.36 (-0.63)
5	52 (-24)	47 (-20)	31	33	1.68 (-0.76)	1.42 (-0.62)
4	39 (-17)	35 (-15)	21	23	1.86 (-0.82)	1.52 (-0.67)
3	27 (-11)	25 (-11)	13	15	2.08 (-0.87)	1.67 (-0.72)
2	17 (-6)	15 (-6)	7	8	2.43 (-0.91)	1.88 (-0.76)
1	8 (-3)	7 (-3)	3	3	2.67 (-1.07)	2.33 (-1.00)

* Negative values in brackets correspond to the maximum value reached in the opposite direction.

Table 4-10 Displacement ductility demand of the shear wall (Taft).

Storey	The maximum lateral Deflection (mm)		The yield displacement (mm)		Displacement ductility demand	
	without P- Δ	with P-Δ	without P- Δ	with P-Δ	without P- Δ	with P-Δ
12	121 (-128)*	121 (-127)	113	120	1.07 (-1.13)	1.01 (-1.12)
11	116 (-113)	115 (-111)	101	107	1.15 (-1.12)	1.07 (1.10)
10	102 (-100)	101 (-100)	88	94	1.16 (-1.14)	1.07 (-1.14)
9	88 (-84)	88 (-85)	76	81	1.16 (-1.11)	1.09 (-1.12)
8	74 (-72)	75 (-77)	64	68	1.16 (-1.13)	1.10 (-1.14)
7	60 (-58)	61 (-60)	52	56	1.15 (-1.12)	1.09 (-1.15)
6	46 (-45)	48 (-47)	41	44	1.12 (-1.10)	1.09 (-1.15)
5	34 (-33)	35 (-35)	31	33	1.10 (-1.06)	1.06 (-1.13)
4	21 (-23)	25 (-25)	21	23	1.00 (-1.10)	1.09 (-1.19)
3	15 (-16)	16 (-11)	13	15	1.15 (-1.23)	1.07 (-1.31)
2	8 (-9)	9 (-10)	7	8	1.14 (-1.29)	1.13 (1.43)
1	4 (-4)	5 (-5)	3	3	1.33 (-1.33)	1.67 (-1.67)

* Negative values in brackets correspond to the maximum value reached in the opposite direction.

Table 4-11 Displacement ductility demand of the shear wall (Parkfield).

Storey	The maximum lateral deflection(mm)		The yield displacement (mm)		Displacement ductility demand	
	without P- Δ	with P- Δ	without P- Δ	with P- Δ	without P- Δ	with P- Δ
12	264 (-101)*	254 (-95)	113	120	2.34 (-0.89)	2.12 (-0.79)
11	230 (-85)	224 (-82)	101	107	2.28 (-0.84)	2.09 (-0.77)
10	197 (-75)	192 (-74)	88	94	2.24 (-0.85)	2.04 (-0.79)
9	164 (-60)	163 (-60)	76	81	2.16 (0.79)	2.01 (-0.74)
8	134 (-51)	136 (51)	64	68	2.09 (-0.80)	2.00 (-0.75)
7	108 (-40)	111(-40)	52	56	2.08 (-0.77)	1.98 (-0.71)
6	86 (-21)	88 (-30)	41	44	2.10 (-0.51)	2.00 (-0.68)
5	68 (-14)	69 (-21)	31	33	2.19 (0.45)	2.09 (-0.64)
4	53 (-10)	54 (-14)	21	23	2.52 (-0.48)	2.35 (-0.61)
3	38 (-5)	39 (-10)	13	15	2.92 (-0.38)	2.60 (-0.67)
2	25 (-2)	25 (-5)	7	8	3.57 (0.290	3.13 (-0.63)
1	3 (-2)	13 (-2)	3	3	4.33 (0.67)	4.33 (-0.67)

* Negative values in brackets correspond to the maximum value reached in the opposite direction.

Table 4-12 Curvature ductility demand of the shear wall (El Centro).

Storey	The maximum curvature (rad/km)		The yield curvature (rad/km)		Curvature ductility demand	
	without P- Δ	with P- Δ	without P- Δ	with P- Δ	without P- Δ	with P- Δ
12	0.017 (-0.018)*	0.017 (-0.017)	0.045	0.045	0.38 (-0.40)	0.38 (-0.38)
11	0.042 (-0.044)	0.042 (-0.043)	0.063	0.063	0.67 (-0.70)	0.67 (-0.68)
10	0.069 (-0.071)	0.061 (-0.079)	0.070	0.070	0.99 (-1.01)	0.99 (-1.00)
9	0.171 (-0.276)	0.158 (-0.292)	0.079	0.079	2.16 (-3.49)	2.00 (-3.70)
8	0.168 (-0.801)	0.158 (-0.818)	0.104	0.104	1.62 (-7.70)	1.52 (-7.87)
7	0.097 (-0.514)	0.097 (-0.511)	0.118	0.118	0.82 (-4.36)	0.82 (-4.33)
6	0.101 (-0.258)	0.101 (-0.290)	0.129	0.129	0.78 (-2.00)	0.78 (-2.25)
5	0.104 (-0.125)	0.104 (-0.126)	0.159	0.159	0.65 (-0.79)	0.65 (-0.79)
4	0.098 (-0.117)	0.099 (-0.117)	0.154	0.154	0.64 (-0.76)	0.64 (-0.76)
3	0.103 (-0.135)	0.096 (-0.135)	0.186	0.186	0.55 (-0.73)	0.52 (-0.73)
2	0.134 (-0.160)	0.122 (-0.157)	0.171	0.171	0.78 (-0.94)	0.71 (0.92)
1	0.176 (-1.406)	0.076 (-1.111)	0.207	0.207	0.85 (-6.79)	0.37 (-5.37)

* Negative values in brackets correspond to the maximum value reached in the opposite direction.

Table 4-13 Curvature ductility demand of the shear wall (Taft).

Storey	The maximum curvature (rad/km)		The yield curvature (rad/km)		Curvature ductility demand	
	without P- Δ	with P- Δ	without P- Δ	with P- Δ	without P- Δ	with P- Δ
12	0.015 (-0.014)*	0.015 (-0.015)	0.045	0.045	0.33 (-0.31)	0.33 (-0.33)
11	0.038 (-0.036)	0.038 (-0.038)	0.063	0.063	0.60 (-0.57)	0.60 (-0.60)
10	0.061 (-0.060)	0.062 (-0.061)	0.070	0.070	0.87 (-0.86)	0.89 (-0.87)
9	0.081 (-0.080)	0.082 (-0.080)	0.079	0.079	1.03 (-1.01)	1.04 (-1.01
8	0.454 (-0.093)	0.347 (-0.107)	0.104	0.104	4.37 (-0.89)	3.34 (-1.03)
7	0.432 (-0.104)	0.352 (-0.104)	0.118	0.118	3.66 (-0.88)	2.98 (-0.88)
6	0.580 (-0.110)	0.560 (-0.112)	0.129	0.129	4.50 (-0.75)	4.34 (0.87)
5	0.151 (-0.119)	0.153 (-0.115)	0.159	0.159	0.95 (-0.75)	0.96 (-0.72)
4	0.157 (-0.152)	0.158 (-0.117)	0.154	0.154	1.02 (-0.84)	1.03 (-0.76)
3	0.152 (-0.130)	0.153 (-0.121)	0.186	0.186	0.82 (-0.70)	0.82 (-0.65)
2	0.172 (-0.141)	0.176 (-0.158)	0.171	0.171	1.01 (-0.82)	1.03 (-0.92)
1	0.498 (-0.425)	0.607 (-0.584)	0.207	0.207	2.41 (-2.05)	2.93 (-2.82)

* Negative values in brackets correspond to the maximum value reached in the opposite direction.

Table 4-14 Curvature ductility demand of the shear wall (Parkfield).

Storey	The maximum curvature (rad/km)		The yield curvature (rad/km)		Curvature ductility demand	
	without P- Δ	with P- Δ	without P- Δ	with P- Δ	without P- Δ	with P- Δ
12	0.019 (-0.018)*	0.018 (-0.017)	0.045	0.045	0.42 (-0.40)	0.40 (-0.38)
11	0.046 (-0.044)	0.045 (-0.043)	0.063	0.063	0.73 (-0.70)	0.71 (-0.68)
10	0.073 (-0.071)	0.073 (-0.071)	0.070	0.070	1.04 (-1.01)	1.04 (-1.01)
9	0.245 (-0.393)	0.279 (-0.355)	0.079	0.079	3.10 (-4.97)	3.63 (-4.49)
8	0.417 (-1.239)	0.434 (-1.112)	0.104	0.104	4.01 (-11.91)	4.17 (-10.69
7	0.355 (-1.109)	0.378 (-0.982)	0.118	0.118	3.01 (-9.40)	3.20 (-8.32)
6	0.402 (-1.105)	0.519 (-1.009)	0.129	0.129	3.12 (-8.57)	4.02 (-7.82)
5	0.141 (-0.154)	0.146 (-0.154)	0.159	0.159	0.92 (-0.97)	0.92 (-0.97)
4	0.141 (-0.156)	0.480 (-0.154)	0.154	0.154	0.92 (-1.01)	0.96 (-1.00)
3	0.130 (-0.146)	0.138 (-0.144)	0.186	0.186	0.70 (-0.78)	0.74 (-0.77)
2	0.122 (-0.144)	0.129 (-0.159)	0.171	0.171	0.71 (-0.84)	0.75 (-0.93)
1	0.158 (-2.300)	0.163 (-2.209)	0.207	0.207	0.76 (-11.11)	0.79 (-10.67)

* Negative values in brackets correspond to the maximum value reached in the opposite direction.

Based on the results of response of the shear wall when subjected to three different earthquake ground motions, the following conclusions can be drawn:

(1) The increase of the maximum lateral displacement for each wall storey due to the inclusion of P-Δ effects is minimal under seismic loading, so P-Δ effects may be neglected.

(2) Figure 4-25 shows that the increase in permanent residual displacement due to the inclusion of P-Δ is very large after 5 seconds under the Parkfield earthquake, This is because the Parkfield motion is similar to a pulse loading which affect the lateral displacement. The permanent plastic displacement is produced after a pulse loading is applied.

(3) P-Δ effects are negligible for the base shear under the El Centro and Taft earthquakes. For the Parkfield earthquake, however, the base shear is slightly increased due to the P-Δ effects after 5 seconds.

(4) In most cases, the wall does not exhibit displacement ductility demands greater than 2.0 under the El Centro and Taft earthquakes. However, the displacement ductility demands exceed 2.0 for each storey under the Parkfield earthquake.

(5) P-Δ effects do not cause an increase for the displacement ductility demands and curvature ductility demands at the base and over the height of the wall when subjected to strong ground motions.

4.8 Damage induced by earthquakes

In earthquake-resistant design of reinforced concrete structures, it is generally necessary to permit some degree of damage; otherwise the design would be too costly. To compute

structural damages under earthquake loading, damage indices permit to quantify damage and relate it to economic losses and other consequences such as potential risk of collapse after an earthquake. The deformation and Park and Ang (1985) damage indicators are computed in the study. The damage indices for the deformation are $D\mu_\Delta$ and $D\mu_\Phi$. The parameter $D\mu_\Delta$ is ratio of the maximum computed displacement to the ultimate displacement. The values of the maximum computed displacement for each story can be obtained from the results of computer program RUAUMOKO. The ultimate displacements are determined from the results of the pushover analyses. The damage indices $D\mu_\Delta$ for each story with and without P-Δ effects included in the analyses are given in Table 4-15 under different ground motions. The damage parameter, $D\mu_\Phi$, is defined as the maximum curvature divided by the ultimate curvature. The maximum curvatures are obtained from the output results of RUAUMOKO, while the ultimate curvatures are obtained from the results of the RESPONSE computer program. A summary of the damage indices $D\mu_\Phi$ of the shear wall structure is given from Table 4-16 to Table 4-18. The Park and Ang (1985) damage indicator, which can be considered as the most widely used in the technical literature, is defined as a linear combination of the maximum displacement to ultimate displacement and the irrecoverable hysteretic energy divided by the yield force. The damage indicators D_{PA} are given in Table 4-19.

From the results of inelastic dynamic analyses of the shear wall, several conclusions can be drawn:

(1) The P-Δ effects have little influence on the damage indices $D\mu_\Phi$ under the three-earthquake ground motions at every storey.

(2) Table 4-15 shows that the damage parameter $D\mu_\Delta$, including P-Δ effects, is not much different under three earthquakes compared to the same indices without P-Δ effect.

(3) The P-Δ effects may be neglected for the damage index D_{PA} under seismic excitation.

(4) Structural damages are not increased if P-Δ effects are considered in earthquake-resistant design of shear wall.

Table 4-15 Damage indices $D\mu_\Delta$ of the shear wall (top floor).

Earthquake	The maximum lateral deflection (mm)		The ultimate displacement (mm)		Damage indices $D\mu_\Delta$	
	without P-Δ	with P-Δ	without P-Δ	with P-Δ	without P-Δ	with P-Δ
El Centro	170 (-74)*	158 (-69)	383	392	0.444 (-0.193)	0.403 (-0.176)
Taft	121 (-128)	121 (-127)	383	392	0.316 (-0.334)	0.309 (-0.324)
Parkfield	264 (-101)	254 (-95)	383	392	0.689 (-0.264)	0.648 (-0.242)

* Negative values in brackets correspond to the maximum value reached in the opposite direction.

Table 4-16 Damage indices $D\mu_\Phi$ of the shear wall (El Centro).

Storey	The maximum curvature (rad/km)		The ultimate curvature (rad/km)		Damage indices $D\mu_\Phi$	
	without P-Δ	with P-Δ	without P-Δ	with P-Δ	without P-Δ	with P-Δ
12	0.017 (-0.018)*	0.017 (-0.017)	6.3	6.3	0.003 (-0.003)	0.003 (-0.003)
11	0.042 (-0.044)	0.042 (-0.043)	6.3	6.3	0.007 (-0.007)	0.007 (-0.007)
10	0.069 (-0.071)	0.061 (-0.079)	6.3	6.3	0.011 (-0.011)	0.010 (-0.011)
9	0.171 (-0.276)	0.158 (-0.292)	6.42	6.42	0.027 (-0.043)	0.025 (-0.045)
8	0.168 (-0.801)	0.158 (-0.818)	6.42	6.42	0.026 (-0.125)	0.025 (-0.127)
7	0.097 (-0.514)	0.097 (-0.511)	6.42	6.42	0.015 (-0.080)	0.015 (-0.080)
6	0.101 (-0.258)	0.101 (-0.290)	6.42	6.42	0.016 (-0.040)	0.016 (-0.045)
5	0.104 (-0.125)	0.104 (-0.126)	6.55	6.55	0.016 (-0.019)	0.016 (-0.019)
4	0.098 (-0.117)	0.099 (-0.117)	6.42	6.42	0.015 (-0.018)	0.015 (-0.018)
3	0.103 (-0.135)	0.096 (-0.135)	6.55	6.55	0.016 (-0.021)	0.015 (-0.021)
2	0.134 (-0.160)	0.122 (-0.157)	6.55	6.55	0.020 (-0.024)	0.019 (-0.023)
1	0.176 (-1.406)	0.076 (-1.111)	6.67	6.67	0.026 (-0.211)	0.011 (-0.167)

* Negative values in brackets correspond to the maximum value reached in the opposite direction.

Table 4-17 Damage indices $D_{\mu\Phi}$ of the shear wall (Taft).

Storey	The maximum curvature (rad/km)		The ultimate curvature (rad/km)		Damage indices $D_{\mu\Phi}$	
	without P-Δ	with P-Δ	without P-Δ	with P-Δ	without P-Δ	with P-Δ
12	0.015 (-0.014)*	0.015 (-0.015)	6.3	6.3	0.002 (-0.002)	0.002 (-0.002)
11	0.038 (-0.036)	0.038 (-0.038)	6.3	6.3	0.006 (-0.006)	0.006 (-0.006)
10	0.061 (-0.060)	0.062 (-0.061)	6.3	6.3	0.010 (-0.010)	0.010 (-0.010)
9	0.081 (-0.080)	0.082 (-0.080)	6.42	6.42	0.013 (-0.012)	0.013 (-0.012)
8	0.454 (-0.093)	0.347 (-0.107)	6.42	6.42	0.071 (-0.014)	0.054 (-0.017)
7	0.432 (-0.104)	0.352 (-0.104)	6.42	6.42	0.067 (-0.016)	0.055 (-0.016)
6	0.580 (-0.110)	0.560 (-0.112)	6.42	6.42	0.090 (-0.017)	0.087 (-0.017)
5	0.151 (-0.119)	0.153 (-0.115)	6.55	6.55	0.023 (-0.018)	0.023 (-0.018)
4	0.157 (-0.152)	0.158 (-0.117)	6.42	6.42	0.024 (-0.024)	0.024 (-0.018)
3	0.152 (-0.130)	0.153 (-0.121)	6.55	6.55	0.023 (-0.020)	0.023 (-0.018)
2	0.172 (-0.141)	0.176 (-0.158)	6.55	6.55	0.026 (-0.022)	0.027 (-0.024)
1	0.498 (-0.425)	0.607 (-0.584)	6.67	6.67	0.075 (-0.064)	0.091 (-0.088)

* Negative values in brackets correspond to the maximum value reached in the opposite direction.

Table 4-18 Damage indices $D_{\mu\Phi}$ of the shear wall (Parkfield).

Storey	The maximum curvature (rad/km)		The ultimate curvature (rad/km)		Damage indices $D_{\mu\Phi}$	
	without P-Δ	with P-Δ	without P-Δ	with P-Δ	without P-Δ	with P-Δ
12	0.019 (-0.018)*	0.018 (-0.017)	6.3	6.3	0.003 (-0.003)	0.003 (-0.003)
11	0.046 (-0.044)	0.045 (-0.043)	6.3	6.3	0.007 (-0.007)	0.007 (-0.007)
10	0.073 (-0.071)	0.073 (-0.071)	6.3	6.3	0.012 (-0.012)	0.012 (-0.012)
9	0.245 (-0.393)	0.279 (-0.355)	6.42	6.42	0.038 (-0.061)	0.043 (-0.055)
8	0.417 (-1.239)	0.434 (-1.112)	6.42	6.42	0.065 (-0.193)	0.068 (-0.173)
7	0.355 (-1.109)	0.378 (-0.982)	6.42	6.42	0.055 (-0.173)	0.059 (-0.153)
6	0.402 (-1.105)	0.519 (-1.009)	6.42	6.42	0.063 (-0.172)	0.081 (-0.157)
5	0.141 (-0.154)	0.146 (-0.154)	6.55	6.55	0.022 (-0.024)	0.022 (-0.024)
4	0.141 (-0.156)	0.480 (-0.154)	6.42	6.42	0.022 (-0.024)	0.023 (-0.024)
3	0.130 (-0.146)	0.138 (-0.144)	6.55	6.55	0.020 (-0.022)	0.021 (-0.022)
2	0.122 (-0.144)	0.129 (-0.159)	6.55	6.55	0.019 (-0.019)	0.020 (-0.024)
1	0.158 (-2.300)	0.163 (-2.209)	6.67	6.67	0.024 (-0.345)	0.024 (-0.331)

* Negative values in brackets correspond to the maximum value reached in the opposite direction.

Table 4-19 Damage indices D_{PA} of the shear wall (first floor).

Earthquake	Damages indices $D\mu_{\Delta}$		$M_y \Phi\mu\, l_p$		βE_h	βE_h	Damages indices D_{PA}	Damages indices D_{PA}
	without P-Δ	with P-Δ	without P-Δ	with P-Δ	without P-Δ	with P-Δ	without P-Δ	with P-Δ
El Centro	0.444	0.403	104880	104880	7680	6190	0.517	0.462
Taft	0.316	0.309	104880	104880	4810	5440	0.362	0.361
Parkfield	0.689	0.648	104880	104880	7450	6660	0.760	0.712

4.9 Conclusions

The following conclusions can be drawn for the results of the earthquake response analyses of the 12-storey building considered in this study:

(1) Including P-Δ effects in the analysis of the shear wall buildings undergoing earthquake loading has little effect on the maximum lateral displacement, base shear, and damage indices $D\mu_{\Phi}$.

(2) The numerical results obtained in this study show that P-Δ effects on the displacement ductility and curvature ductility demand of the shear wall are negligible under seismic ground motions.

(3) For ground motions containing large acceleration pulses, P-Δ effects may increase significantly the residual (inelastic) displacement as compared to the situation where P-Δ effects are neglected. The magnitude of residual displacements has a direct incidence on the post-earthquake structural strength that can be mobilized before collapse.

(4) The analyses show that P-Δ effects do not increase the structural damage parameter $D\mu_\Delta$ as compared to the values computed without P-Δ effects. Thus P-Δ effects are not detrimental to the seismic response of the wall.

(5) The structural ductility demand and damage parameter vary with the storey under consideration.

(6) Based on the study presented herein, P-Δ effects may be neglected for the 12-storey shear wall building considered.

CHAPTER 5

EFFECTS OF VARIATIONS IN THE MODELING PARAMETERS OF THE BUILDING ANALYZED

5.1 Introduction

The effects of varying the modelling parameters for the 12-storey shear-wall building analyzed are discussed in this chapter. First, the objectives of this parametric study are presented. Then, modelling parameters of the wall analyzed, such as the amount of axial force in the gravity column, different categories of earthquake records, hysteresis rules, and viscous damping ratios, are selected to examine their influence on the seismic response of the wall. The RUAUMOKO computer program is used to perform inelastic dynamic analyses with and without P-Δ effects. Different indices, such as the maximum roof displacement, are used to evaluate the effects of the selected modelling parameters on the significance of P-Δ effects for the building analyzed.

5.2 Objectives

In this chapter, modelling parameters are varied to assess the sensitivity of the seismic response of the shear wall to these parameters. In Chapter 4, the results of inelastic dynamic analyses of the shear wall, with and without P-Δ effects, under different earthquake records have been studied. Different response quantities have been examined, including the top lateral displacement, the shear forces and bending moments at the base of the wall, and the ductility demand. However, the influence on the seismic response due to variations in the wall modelling parameters needs to be studied further. The specific objectives of the parametric study presented in this chapter are to assess:

(1) The influence of the amount of gravity loading on the behaviour of the wall.

(2) The influence of the frequency content and duration of the applied ground motions on the nonlinear seismic response for a typical shear wall building.

(3) The influence of the following modelling parameters on the seismic response of the wall: (i) using tri-linear degrading stiffness hysteresis rule, (ii) varying strain hardening ratio of the reinforcing steel, and (iii) varying the amount of the viscous damping.

To achieve these objectives, nonlinear earthquake response analyses are performed on the typical 12-storey shear wall building. The P-Δ effects are examined when varying the above modelling parameters.

5.3 Selected parameters

The main parameters considered in the study are:

- The axial force in the gravity column, corresponding either to the actual design value P computed in chapter 3, or larger values arbitrarily set equal to 2P and 5P. The axial loading in the wall will be remained in the calculation. The lateral resistance of the structure is not increased. Therefore, increasing P corresponds to evaluate buildings located in lower seismic regions or buildings which carry significant gravity live load not included in the seismic weight.

- Eastern and Western North America types of earthquake ground motions. For the Eastern earthquake, the Saguenay 1988 record is chosen because it has a high predominant frequency near 10 Hz. The El Centro 1940 record is selected as representative of Western North America type of earthquake. It has a low predominant frequency near 2 Hz.

- The hysteresis rules for the flexural response of the wall: bilinear hysteresis rule versus trilinear degrading stiffness hysteresis rule and amount strain hardening of steel. The bilinear inelastic model is shown in Figure 3-20. The trilinear inelastic model considered for the inelastic analysis is introduced in this chapter and it is illustrated in Figure 5-15. The steel stress-strain model considering the strain hardening of steel is shown in Figure 5-17.

- The viscous damping ratio (ξ). For the inelastic dynamic analyses with the bilinear hysteresis rule, Rayleigh type damping is assumed based on 2% and then 7% damping in the first mode and second mode of vibration instead of 5% damping as assumed in Chapter 4.

To carry out the comparisons of earthquake response analyses, the organization of the parametric analysis is shown in Figure 5-1.

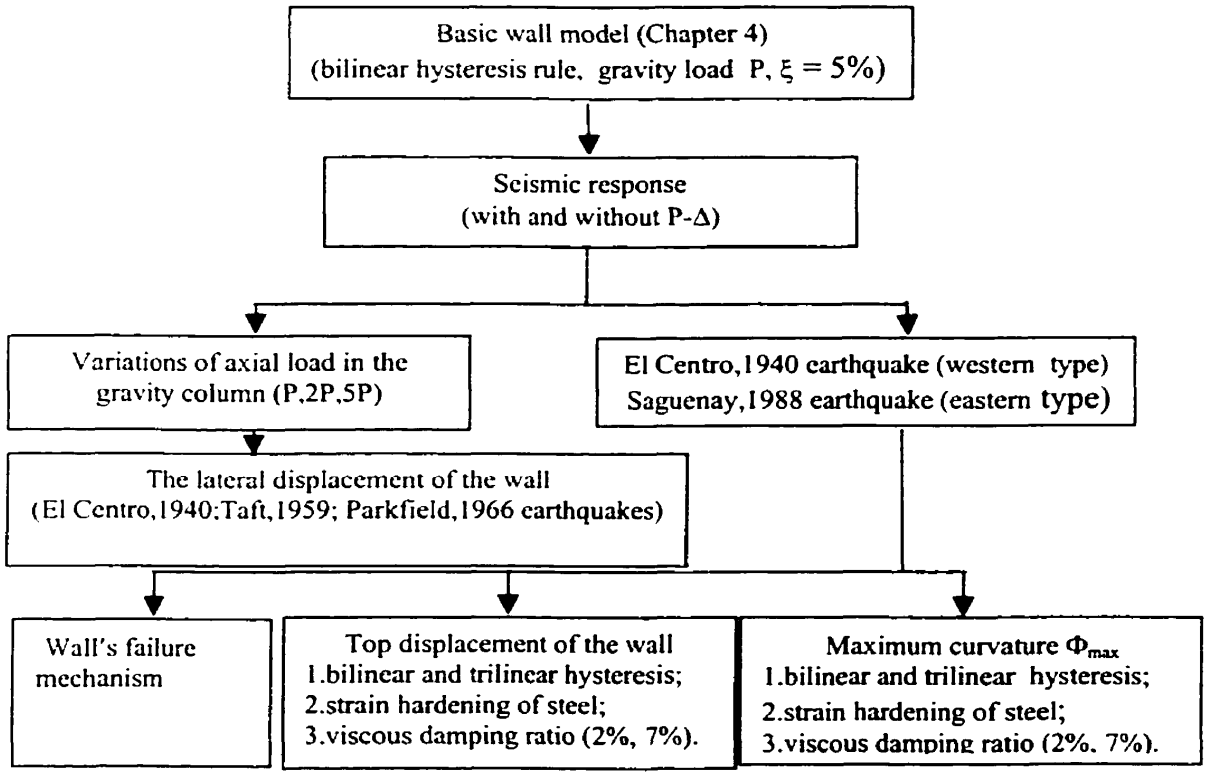

Figure 5-1 Organization of the parametric analysis.

5.4 Earthquake response analyses

5.4.1 Axial load in the gravity column

The variation of the axial load in the gravity column is considered to verify its influence on the wall horizontal displacements. The axial load in the gravity column is increased from P to 2P, and 5P (where P is the actual design axial force acting in the gravity column computed in Chapter 3). The top lateral displacement time histories under each earthquake ground motion are shown in Figure 5-2 to 5-4. For El Centro earthquake, the top lateral displacements almost reach their maximum values at the same time when the axial load is increased from P to 2P, and 5P. The roof horizontal displacements have not significant increased if the axial load is increased from P to 2P. When the axial load reaches 5P, the shear wall building collapsed at 6.5 s. The time when maximum top displacement of the wall occurs changes under Taft and Parkfield ground acceleration when the axial load is increased from P to 2P, and 5P.

The displacement shape of the wall is explained at various time steps. Under the El Centro 1940 ground acceleration, scaled to a PGA = 0.18g for Montreal, when including P-Δ effects, the deflected shapes at 3.94 s, 4.1 s, 4.5 s, and 5.13 s are respectively shown in Figure 5-5. These particular times are selected from the top lateral displacement time history shown in Figure 4-16. The roof horizontal displacements reach their maximum values when the times are 3.94 s and 5.13 s. In Figure 5-5, the horizontal axis is the lateral displacement of the wall. The vertical axis is the number of storey. Figure 5-5 shows the effects of variations of the axial force at various time steps. The axial load in the gravity column has a little effect on the wall horizontal displacement at 4.5 s and 5.13 s if the axial load is increased from P to 2P. However, the horizontal displacement at the top of the wall is significantly increased when the axial load is increased from 2P to 5P.

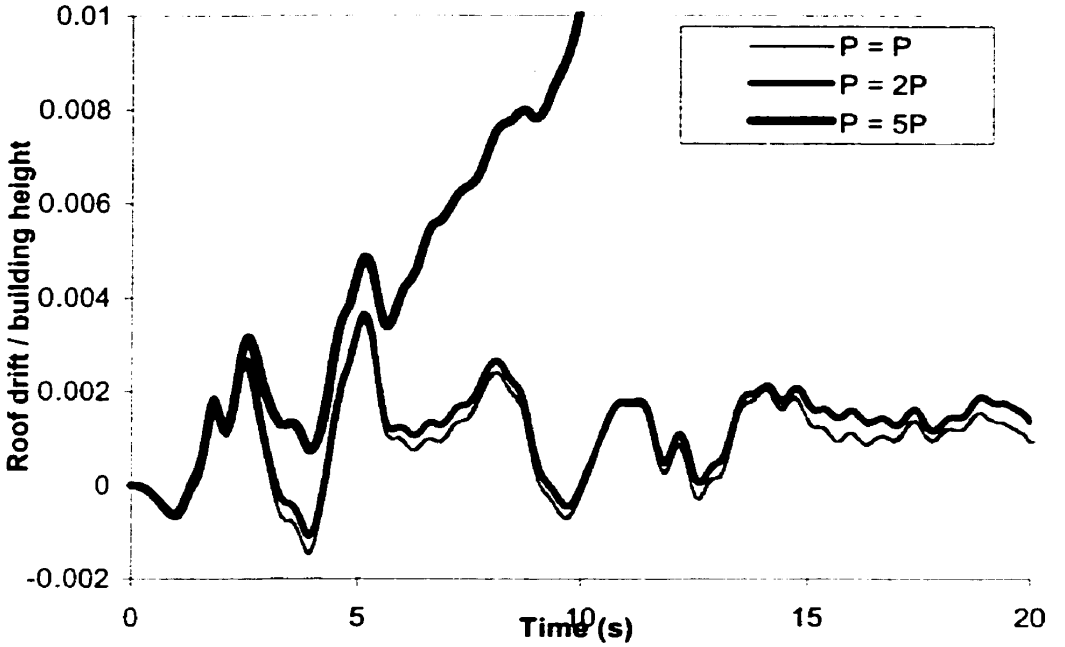

Figure 5-2 Top lateral displacement time history - scaled El Centro earthquake (with P-Δ).

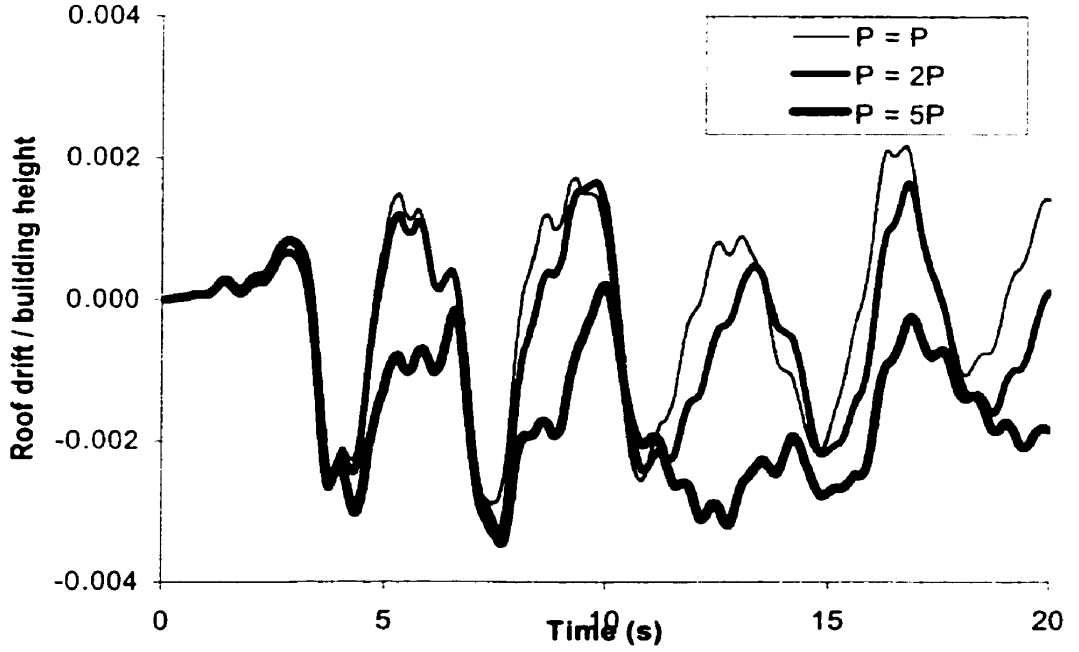

Figure 5-3 Top lateral displacement time history - scaled Taft earthquake (with P-Δ).

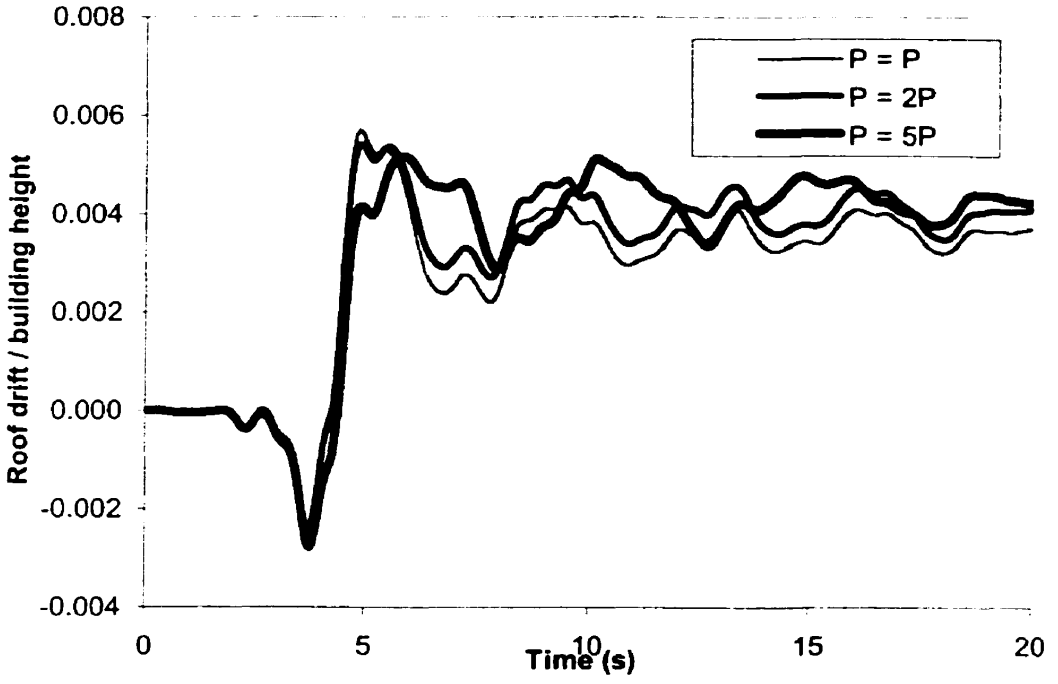

Figure 5-4 Top lateral displacement time history - scaled Parkfield earthquake (with P-Δ).

The first three periods of vibration are given in Table 5-1 for different axial loads. If the axial force in the gravity column is increased from P to 2P, the first periods of vibration of the shear wall are lengthened from $T_1 = 3.380$ s to $T_1 = 3.556$ s. When the axial force is 5P, the first period of vibration of the shear wall is $T_1 = 4.278$ s.

Table 5-1 First three vibration periods.

Axial force in the gravity columns	Periods (s)		
	Mode 1	Mode 2	Mode 3
P (without P-Δ)	3.217	0.547	0.213
P (with P-Δ)	3.380	0.551	0.214
2P (with P-Δ)	3.556	0.558	0.217
5P (with P-Δ)	4.278	0.570	0.219

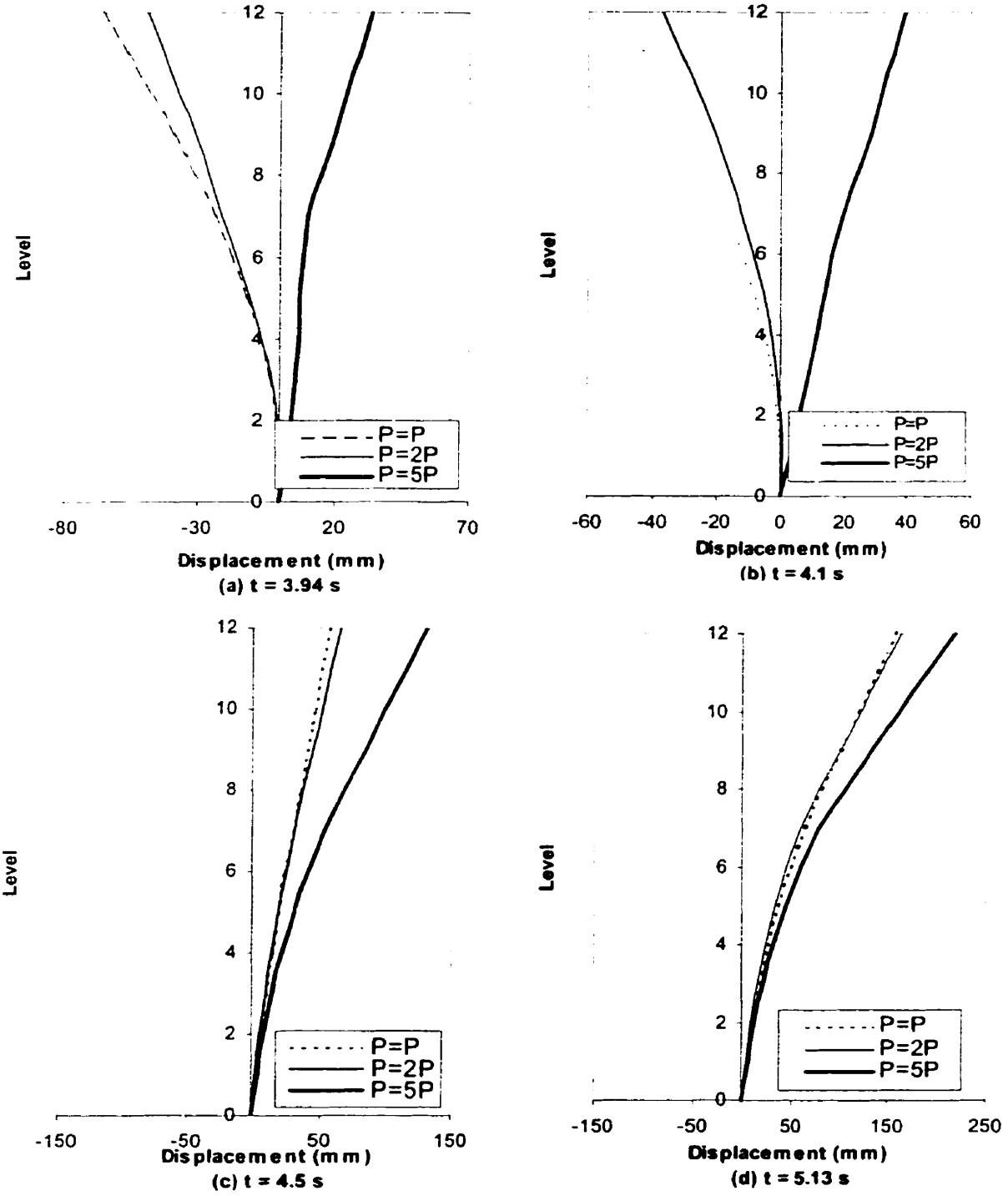

Figure 5-5 Response of the shear wall - scaled El Centro earthquake (with P-Δ).

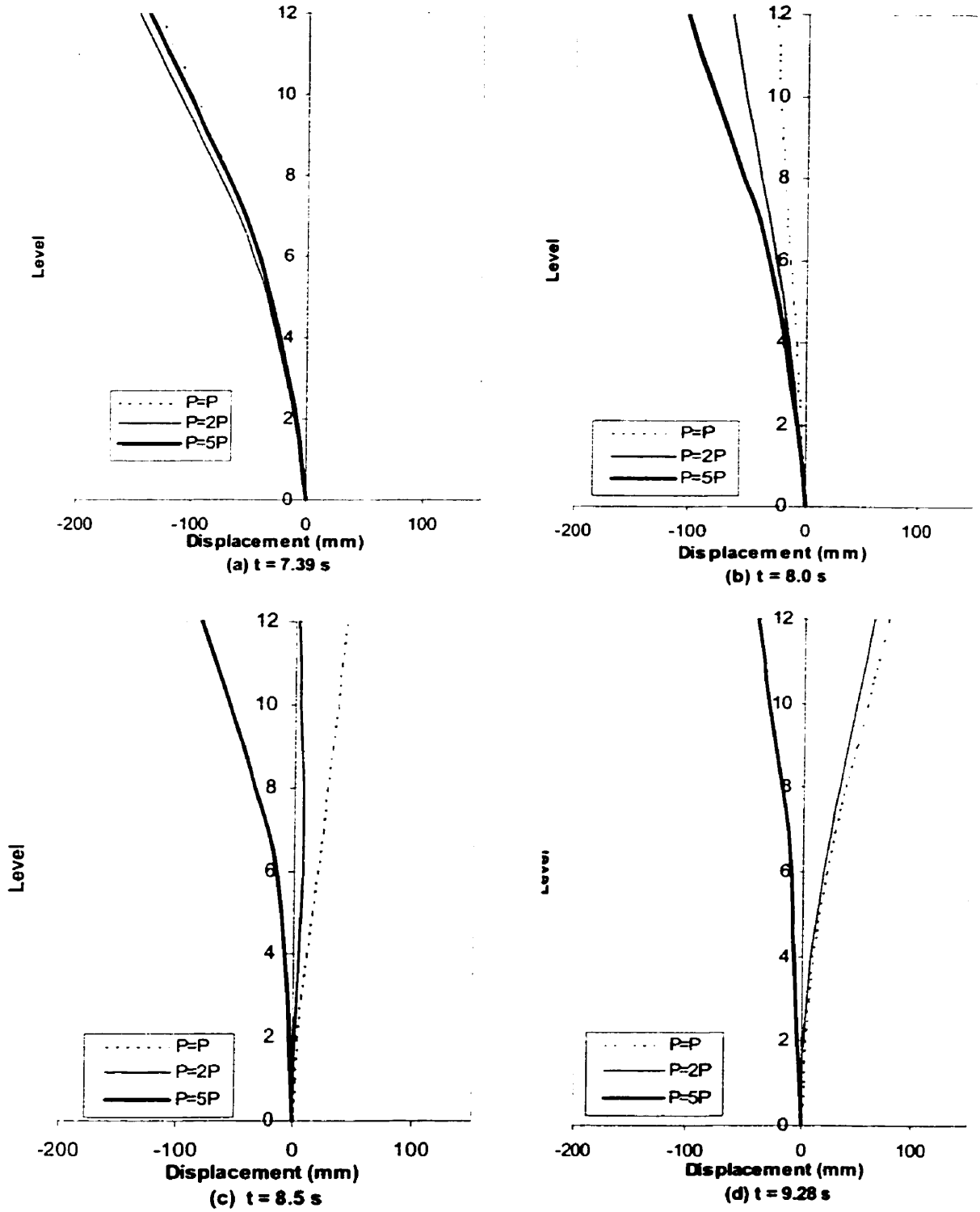

Figure 5-6 Response of the shear wall - scaled Taft earthquake (with P-Δ).

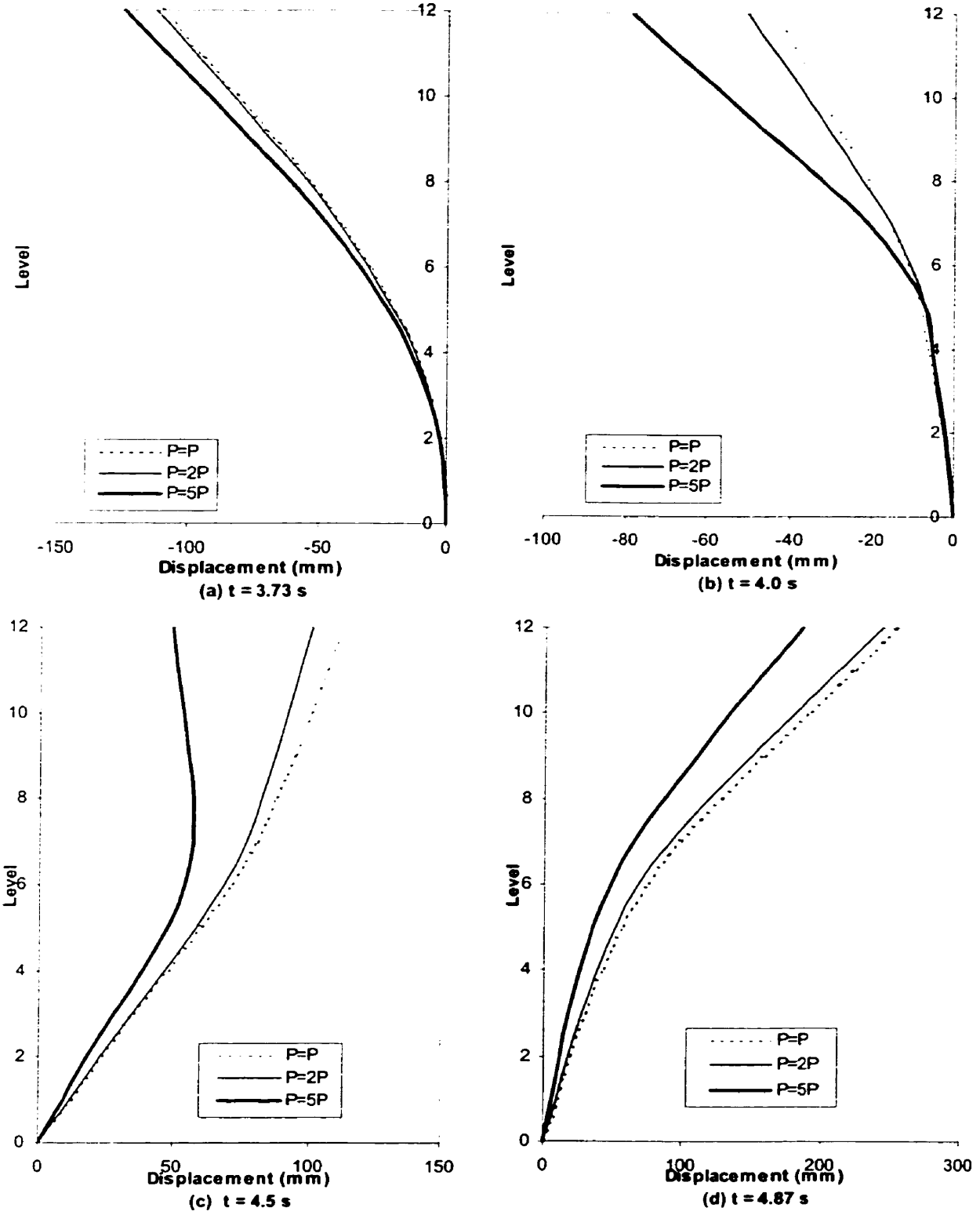

Figure 5-7 Response of the shear wall - scaled Parkfield earthquake (with P-Δ).

The displaced shapes of the wall at 7.39 s, 8.0 s, 8.5 s, 9.28 s under scaled Taft ground accelerations and at 3.73 s, 4.0 s, 4.5 s, 4.87 s under scaled Parkfield ground accelerations are also given in Figure 5-6, and Figure 5-7, respectively. These particular times are selected from the top lateral displacement time history to scaled Taft and Parkfield ground accelerations in Figure 4-22 and Figure 4-28. Under Taft earthquake motion, the axial load has a little influence on the wall horizontal displacements at 7.39 s. The influence of the axial load on the wall horizontal displacements is increased largely when the deflected shapes at 8.0 s, 8.5 s and 9.28 s are considered. For the Parkfield earthquake, the roof horizontal displacements reach their maximum values when the times are 3.73 s and 4.87 s. When the axial load is increased from 2P to 5P, the wall horizontal displacements is also increased largely.

To assess the response of the shear wall, the curvature ductility demands are summarised. The value of curvature ductility demands under the actual axial load P have been given in Chapter 4. The curvature ductility demands under the axial load 2P and 5P are given from Table 5-2 to 5-4. When the axial load is increased to 5P, the shear wall collapsed, so the curvature ductility demand under the axial load 5P can not be obtained in Table 5-4. The curvature ductility demands in the wall under El Centro, Taft and Parkfield earthquakes are given in Figure 5-8 to Figure 5-10. The results show that the curvature ductility demands are increased at mid-height of the wall if the axial load is increased from P to 2P, and 5P. The plastic hinge is developed at mid-height of the wall. The reason is that the longitudinal reinforcing steels were changed from 8-No.25 to 8-No.20 at level 6.

Table 5-2 Curvature ductility demand of the shear wall---with P-Δ (El Centro).

Storey	The maximum curvature (rad/km)		The yield curvature (rad/km)		Curvature ductility demand	
	2P	5P	2P	5P	2P	5P
12	0.016 (-0.017)*	--	0.045	0.045	0.36 (-0.38)	--
11	0.042 (-0.043)	--	0.063	0.063	0.67 (-0.68)	--
10	0.068 (-0.069)	--	0.070	0.070	0.97 (-0.99)	--
9	0.134 (-0.287)	--	0.079	0.079	1.70 (-3.63)	--
8	0.096 (-1.242)	--	0.104	0.104	0.92 (-11.94)	--
7	0.090 (-0.638)	--	0.118	0.118	0.76 (-5.41)	--
6	0.091 (-0.278)	--	0.129	0.129	0.71 (-2.16)	--
5	0.094 (-0.125)	--	0.159	0.159	0.59 (-0.79)	--
4	0.090 (-0.120)	--	0.154	0.154	0.58 (-0.78)	--
3	0.090 (-0.139)	--	0.186	0.186	0.48 (-0.75)	--
2	0.112 (-0.158)	--	0.171	0.171	0.65 (-0.92)	--
1	0.059 (-0.965)	--	0.207	0.207	0.29 (-4.66)	--

* Negative values in brackets correspond to the maximum value reached in the opposite direction.

Table 5-3 Curvature ductility demand of the shear wall---with P-Δ (Taft).

Storey	The maximum curvature (rad/km)		The yield curvature (rad/km)		Curvature ductility demand	
	2P	5P	2P	5P	2P	5P
12	0.015 (-0.015)*	0.015 (-0.011)	0.045	0.045	0.33 (-0.33)	0.33 (-0.24)
11	0.039 (-0.037)	0.038 (-0.028)	0.063	0.063	0.62 (-0.59)	0.60 (-0.44)
10	0.063 (-0.060)	0.063 (-0.047)	0.070	0.070	0.90 (-0.86)	0.90 (-0.69)
9	0.085 (-0.079)	0.081 (-0.064)	0.079	0.079	1.08 (-1.00)	1.03 (-0.81)
8	0.608 (-0.092)	1.107 (-0.074)	0.104	0.104	5.85 (-0.88)	10.64 (-0.71)
7	0.406 (-0.097)	0.601 (-0.076)	0.118	0.118	3.44 (-0.82)	5.09 (-0.64)
6	0.637 (-0.096)	0.714 (-0.066)	0.129	0.129	4.94 (-0.74)	5.53 (-0.51)
5	0.152 (-0.104)	0.151 (-0.058)	0.159	0.159	0.96 (-0.65)	0.95 (-0.36)
4	0.157 (-0.110)	0.153 (-0.064)	0.154	0.154	1.02 (-0.71)	0.99 (-0.42)
3	0.150 (-0.118)	0.140 (-0.069)	0.186	0.186	0.81 (-0.63)	0.75 (-0.37)
2	0.168 (-0.148)	0.161 (-0.071)	0.171	0.171	0.98 (-0.87)	0.94 (0.42)
1	0.536 (-0.190)	0.570 (-0.065)	0.207	0.207	2.59 (-0.92)	2.75 (-0.31)

* Negative values in brackets correspond to the maximum value reached in the opposite direction.

Table 5-4 Curvature ductility demand of the shear wall—with P-Δ (Parkfield).

Storey	The maximum curvature (rad/km)		The yield curvature (rad/km)		Curvature ductility demand	
	2P	5P	2P	5P	2P	5P
12	0.017 (-0.017)*	0.016 (-0.017)	0.045	0.045	0.38 (-0.38)	0.36 (-0.38)
11	0.044 (-0.043)	0.042 (-0.042)	0.063	0.063	0.70 (-0.68)	0.67 (-0.67)
10	0.071 (-0.071)	0.069 (-0.071)	0.070	0.070	1.01 (-1.01)	0.99 (-1.01)
9	0.235 (-0.330)	0.263 (-0.365)	0.079	0.079	2.97 (-4.18)	3.33 (-4.62)
8	0.611 (-1.260)	0.870 (-1.181)	0.104	0.104	5.88 (-12.12)	8.37 (-11.36)
7	0.450 (-1.077)	0.651 (-0.867)	0.118	0.118	3.81 (-9.13)	5.52 (-7.35)
6	0.632 (-0.951)	1.010 (-0.504)	0.129	0.129	4.90 (-7.37)	7.83 (-3.91)
5	0.147 (-0.150)	0.155 (-0.138)	0.159	0.159	0.92 (-0.94)	0.97 (-0.87)
4	0.149 (-0.149)	0.161 (-0.137)	0.154	0.154	0.97 (-0.97)	1.05 (-0.89)
3	0.139 (-0.140)	0.154 (-0.154)	0.186	0.186	0.75 (-0.75)	0.83 (-0.83)
2	0.130 (-0.146)	0.144 (-0.175)	0.171	0.171	0.76 (-0.85)	0.84 (-1.02)
1	0.165 (-1.986)	0.178 (-1.503)	0.207	0.207	0.80 (-9.59)	0.86 (-7.26)

* Negative values in brackets correspond to the maximum value reached in the opposite direction.

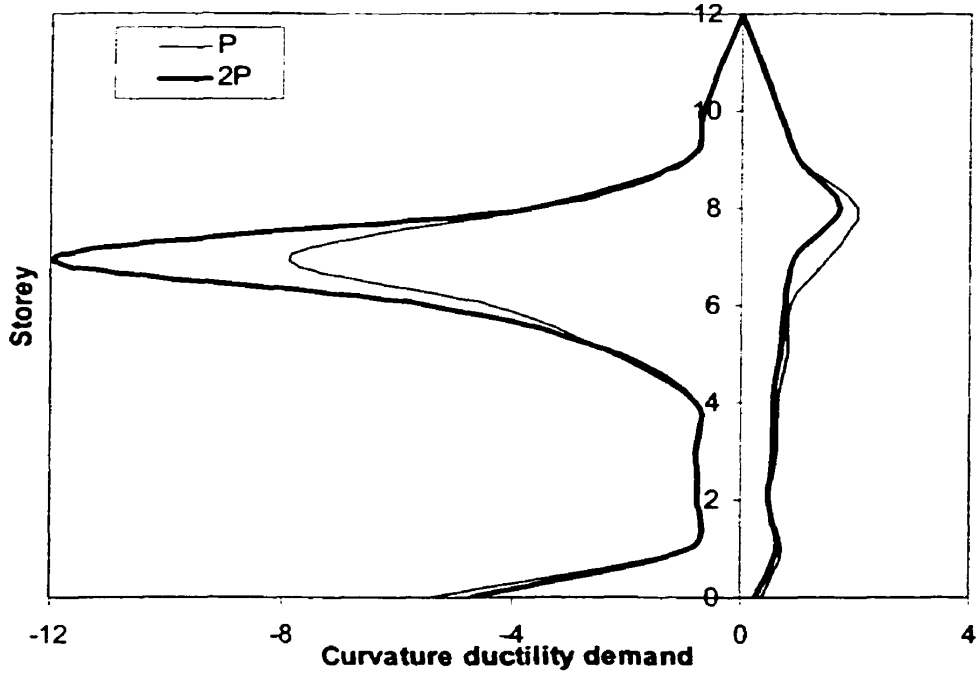

Figure 5-8 Curvature ductility demand in the wall - scaled El Centro earthquake (P = P, 2P).

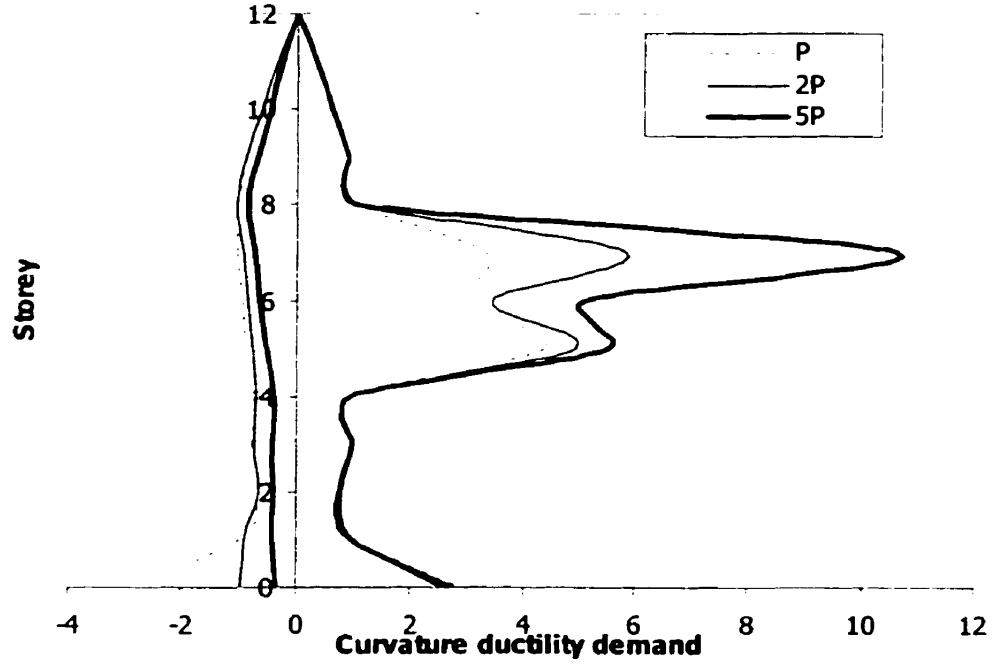

Figure 5-9 Curvature ductility demand in the wall - scaled Taft earthquake (P = P, 2P, 5P).

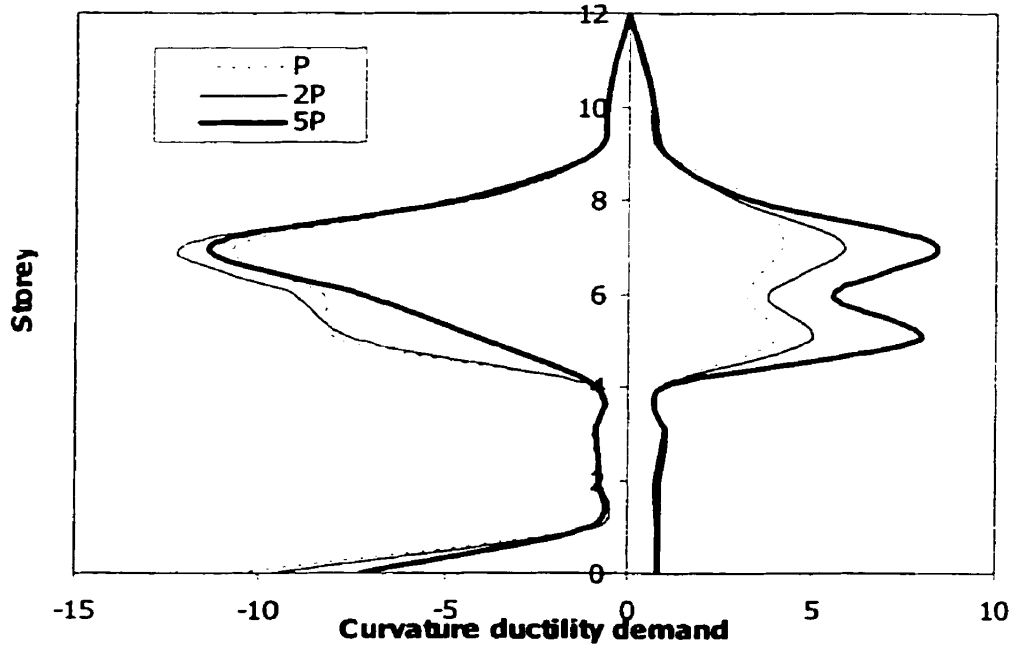

Figure 5-10 Curvature ductility demand in the wall - scaled Parkfield earthquake (P = P, 2P, 5P).

Based on the response results of the shear wall when the axial force in the gravity column is increased from P to 2P and 5P, the following conclusions can be obtained:

(1) The first period of vibration of the shear wall is lengthened if the axial load in the gravity columns is increased from P to 2P and 5P.

(2) The axial load in the gravity columns when including P-Δ effects has a significant effect on the wall horizontal displacement if the axial load is increased from 2P to 5P. The horizontal displacement is mainly increased on one side of the wall.

(3) Longer period may decrease the lateral displacement of the shear wall. For example, the horizontal displacement of the wall is decreased at 4.1s and at 4.5s under El Centro earthquake as well as at 8.5s and at 9.28s under Taft earthquake, when the axial force in the gravity column is increased from P to 2P.

(4) Reduced effective stiffness for a given load should increase the lateral displacement. Under El Centro earthquake, the horizontal displacement of the wall is increased when the axial force is 5P.

(5) In general, the deformed shape of the wall exhibits more local curvature when the axial force in the gravity column is increased. It happens at 6^{th} floor due to the decrease of the longitudinal reinforced steel at this storey.

5.4.2 Application of Eastern and Western North America types of earthquakes

To study the effect of the frequency content of the ground motions on the seismic response of the 12-storey wall, Eastern and Western North America type earthquakes have been considered.

The El Centro, 1940 (SOOE) record is chosen as the ground motion to represent Western North America. It is considered because it has a low predominant frequency around 2 Hz. The earthquake record is shown in Figure 4-11. The characteristics of the ground motions are given in Table 4-6.

For the Eastern earthquake, a record from the Saguenay (N124E), 1988 event is selected because it is the largest recorded seismic event in Eastern Canada.

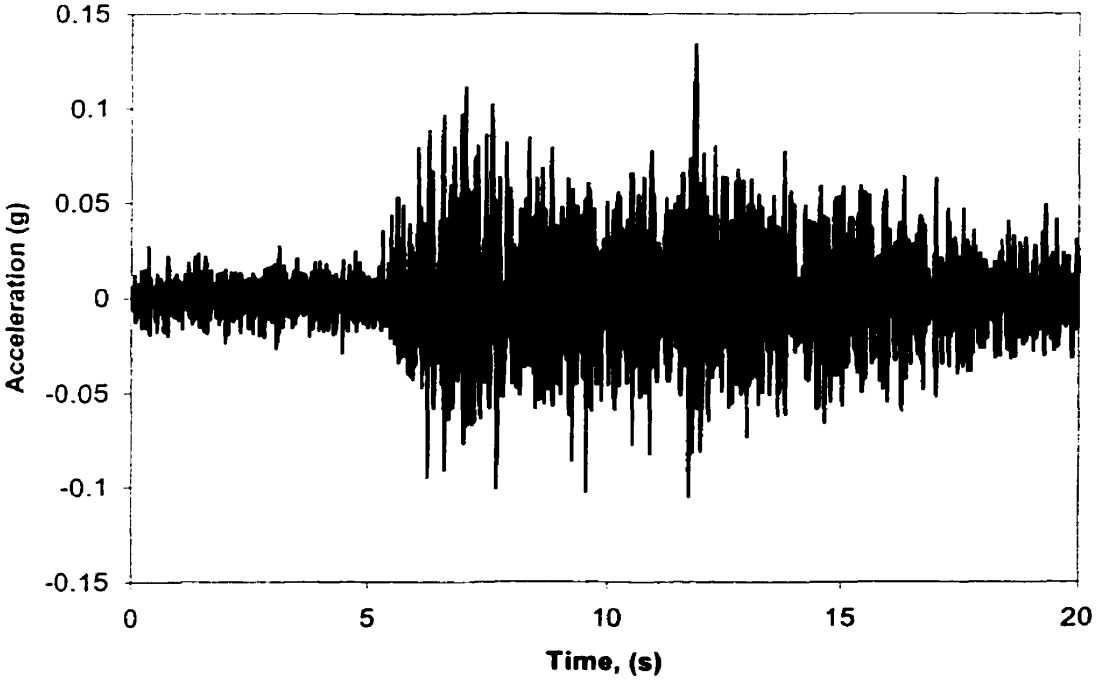

Figure 5-11 Saguenay earthquake record.

The 1998 Saguenay record selected has a high predominant frequency near 10 H_Z with a peak ground acceleration of 0.131g. The earthquake record is shown in Figure 5-11. The first 20 seconds of the record are considered. The scaling factor for the accelerogram is 1.374 to attain a peak ground acceleration of 0.18g. Figure 5-12 shows the spectra for the scaled accelerogram when compared with the NBCC 1995 spectra for 5% damping. The spectral acceleration Sa reaches 0.038 g at the first period (T_1 = 3.389).

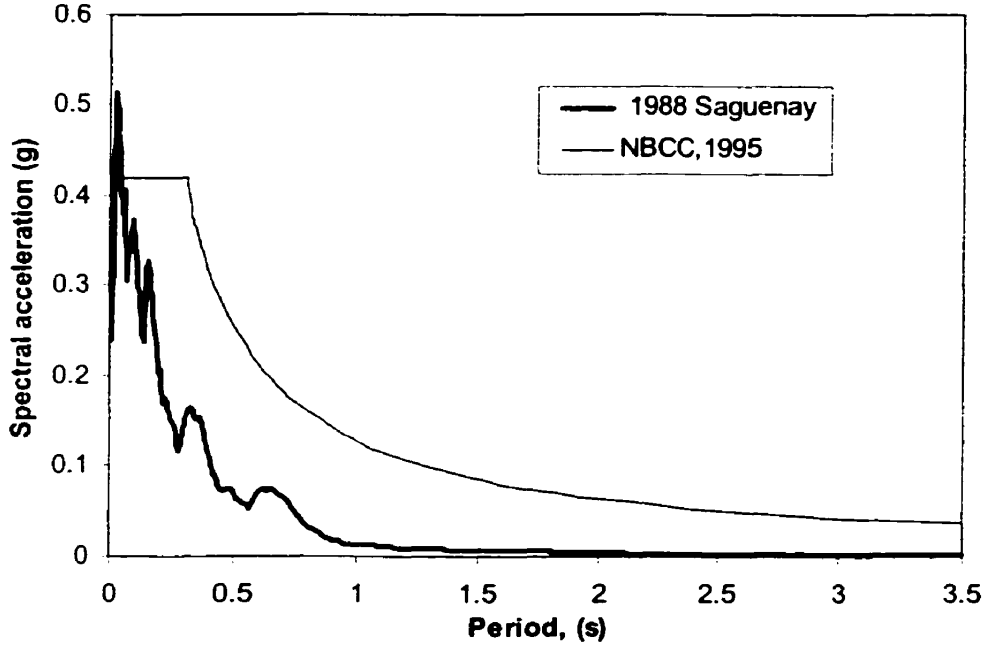

Figure 5-12 Scaled earthquake spectra.

The response of the structure subjected to 1988 Saguenay ground motions was obtained from the RUAUMOKO computer program. The results of inelastic dynamic analyses of the shear wall, with and without P-Δ, under the El Centro earthquake records have been studied in Chapter 4. Table 5-5 summarises the results of response parameters under El Centro and Saguenay earthquake ground motions. Comparing the results of response parameters of the shear wall, the following conclusions can be obtained: the values of all response parameters under El Centro earthquake are larger than those under Saguenay ground motions. This is because the El Centro record has a low frequency content (2 H_z)

as compared to that of the Saguenay record (10 H_z); P-Δ effects have little influence on the response parameters except for the maximum base shear under Saguenay earthquake which is reduced while including P-Δ effects. Structural damages may be neglected under the Saguenay record, P-Δ effects are not detrimental to the response of the shear wall. Figure 5-13 shows the curvature ductility demand in the wall to scaled Saguenay earthquake ground acceleration. The curvature ductility demands at each storey in the wall are less than 1.0 under the Saguenay earthquake. Therefore, the structural damage can be neglected.

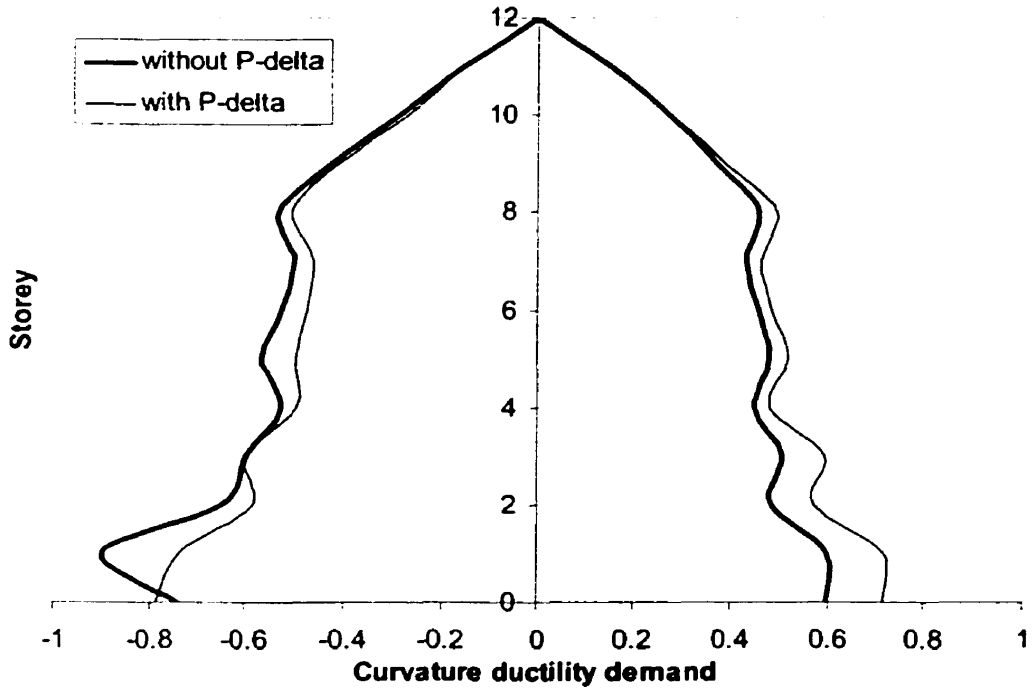

Figure 5-13 Curvature ductility demand in the wall - scaled Saguenay earthquake.

Analyses are performed with the RUAUMOKO computer program to study the failure mechanism of the 12-storey shear wall under earthquake ground motions. The intensity of ground motions is increased progressively by carrying out a series of analyses with larger and larger scaling factors to examine the wall's failure. Figure 5-14(a) and Figure 5-14(b) show the variations of peak roof displacement under El Centro and Saguenay earthquakes if including P-Δ effects. For El Centro earthquake, the wall collapsed due to plastic hinge formation at the base of the wall when the intensity of ground motions is increased to 0.396 g. The wall failure also took place at the base of the wall under Saguenay earthquake ground accelerations, but this occured when the peak ground acceleration was increased to 1.134 g. If not including the P-Δ effects, wall failure could not develop in this model if the intensity of ground motions is increased progressively.

Table 5-5 Nonlinear response parameters of the shear wall.

Response parameters (maximum values)	Earthquakes (PGA = 0.18g)			
	El Centro		Saguenay	
	P-Δ	No P-Δ	P-Δ	No P-Δ
Roof displacement (mm)	158	170	63	82
Base shear (kN)	3200	3220	995	1310
Peak displacement ductility demand μ_m	1.33	1.44	0.53	0.69
Peak curvature ductility demand μ_Φ	5.37	6.79	0.60	0.74
Damage indice $D\mu_\Delta$	0.403	0.444	0.160	0.213
Damage indice $D\mu_\Phi$	0.167	0.211	0.019	0.023

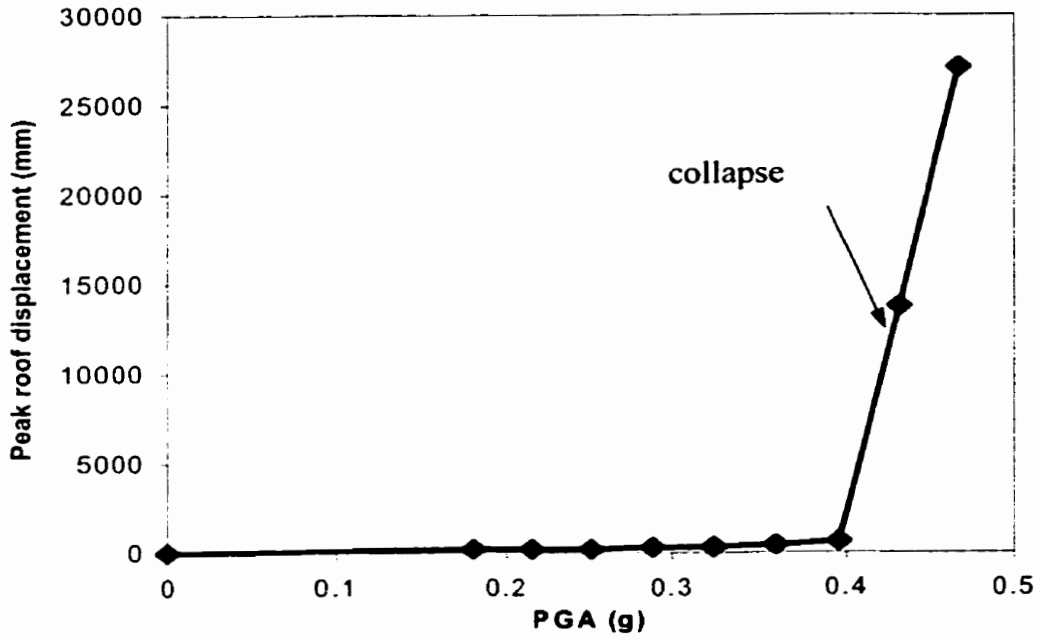

Figure 5-14(b) Variation of peak roof displacement - scaled El Centro earthquake (with P-Δ).

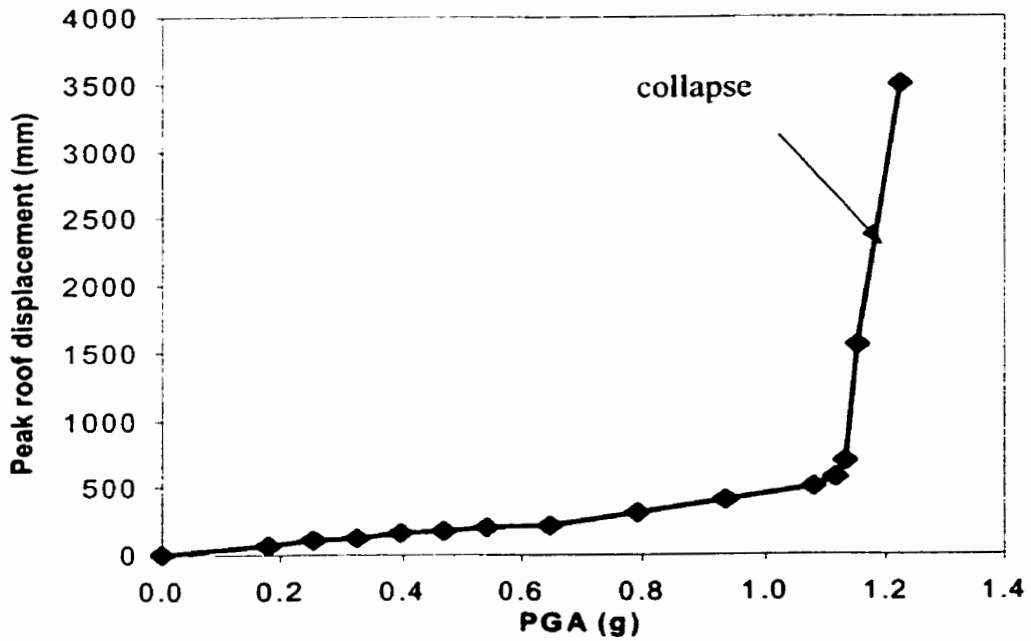

Figure 5-14(a) Variation of peak roof displacement - scaled Saguenay earthquake (with P-Δ).

5.4.3 Trilinear degrading stiffness hysteresis rules and strain hardening of steel

1. Trilinear degrading stiffness hysteresis rules

To assess the variation in representing the inelastic moment-curvature response, all inelastic analyses are conducted for two different degrading hysteresis rules: a bilinear hysteresis rule and a trilinear hysteresis rule. The bilinear hysteresis rule considered for the inelastic analysis has been introduced in chapter 4 and the results of inelastic dynamic analyses of the shear wall have been obtained under different earthquake records. The other hysteresis rule considered for the inelastic analysis is a trilinear degrading hysteresis rule. With this rule, cracking of the concrete is considered before yielding of the tensile reinforcement.

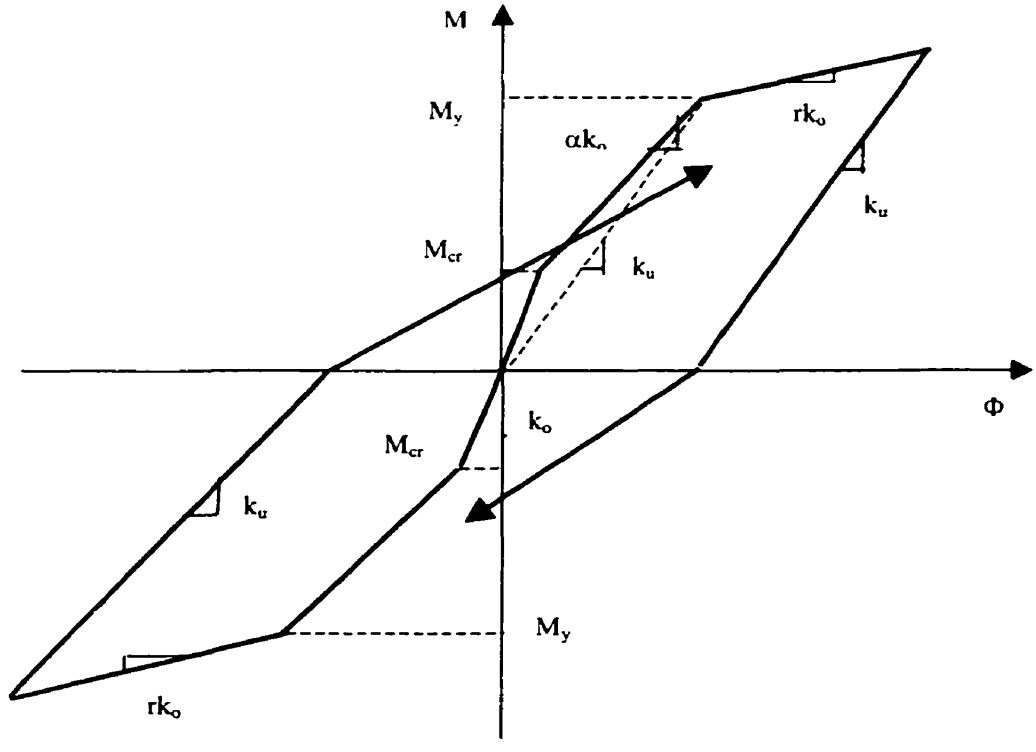

Figure 5-15 Muto degrading trilinear hysteresis.

Figure 5-15 shows the MUTO (Carr,1996) degrading trilinear hysteresis rule, which is used as the moment-curvature model in the analyses of the wall. The initial slope (k_o) corresponds to the gross stiffness (EI_g) of the section before cracking occurs. After cracking of the structure, the slope changes due to the stiffness reduction (EI_{cr}). The post-cracking slope is related to the initial slope by a factor α. The MUTO degrading tri-linear model follows an origin-center philosophy, therefore, after cracking has occurred, the model comes back through the origin with a slope, k_u. The third slope is related to the initial slope by a factor r. During the reverse loading, the model returns again with a slope, k_u. Once the loading crosses the abscissa, the slope changes again if opposite yielding has occurred. This model is suitable for reinforced concrete members because it follows a realistic understanding of the behaviour of loading and unloading with strength degradation. The envelopes of the first cycle (coordinates of the cracking and yield moments and their corresponding stiffness) are obtained from results of moment-

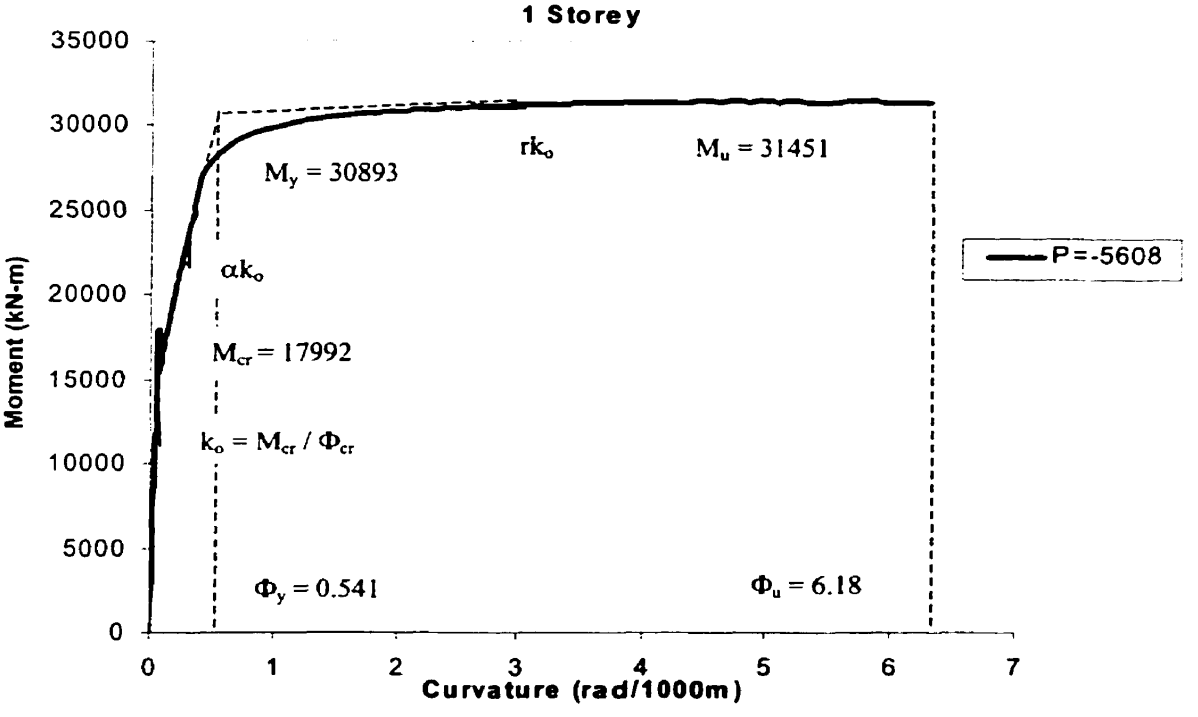

Figure 5-16 Moment – curvature response of the wall (storey 1).

curvature analyses with the RESPONSE computer program.

Figure 5-16 shows the relationship between moment and curvature of the wall for the bottom storey from the RESPONSE program. The cracking moment M_{cr} = 17992 kN-m, yielding moment M_y = 30893 kN-m and the ultimate moment M_u = 31451 kN-m are shown in Figure 5-16. The response also indicates that the shear wall for the bottom storey has a yield curvature Φ_y = 0.541 (rad /km), and Φ_u = 6.18 (rad/km). From the initial slope corresponding to the stiffness (EI_g) of the section before cracking occurs, the uncracked moment of inertia I_g equals 9.126 m^4. The factor α, which relates the initial slope and the post-cracking slope, is 0.157. The factor r, which relates the initial slope and the post-yielding slope, is also obtained from results of moment-curvature analyses and its value is $0.487*10^{-3}$.

2. Strain hardening of steel

The relationship between moment and curvature of the wall for each storey has been obtained from the RESPONSE computer program. The results are given in Chapter 3. The steel type is described by a bilinear stress-strain relationship in the program. The steel stress-strain model is presented in Figure 3-4 (b). To assess the influence of the strain hardening of steel on the wall response, the trilinear stress-strain relationship of steel is considered in the RESPONSE computer program to obtain the moment-curvature responses. The steel stress-strain model is given in Figure 5-17. Due to the consideration of strain hardening of the steel, different values for f_y and f_u are given in Figure 5-17. The strain of steel ε_{rupt} equals 0.20 when f_s reaches f_u = 500 MPa.

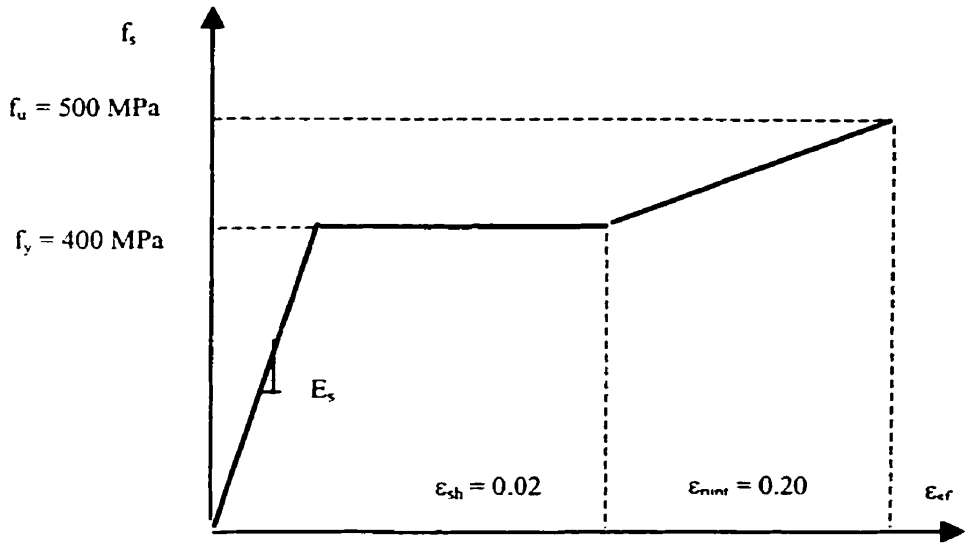

Figure 5-17 Stress- strain relationship of reinforcing bar (trilinear).

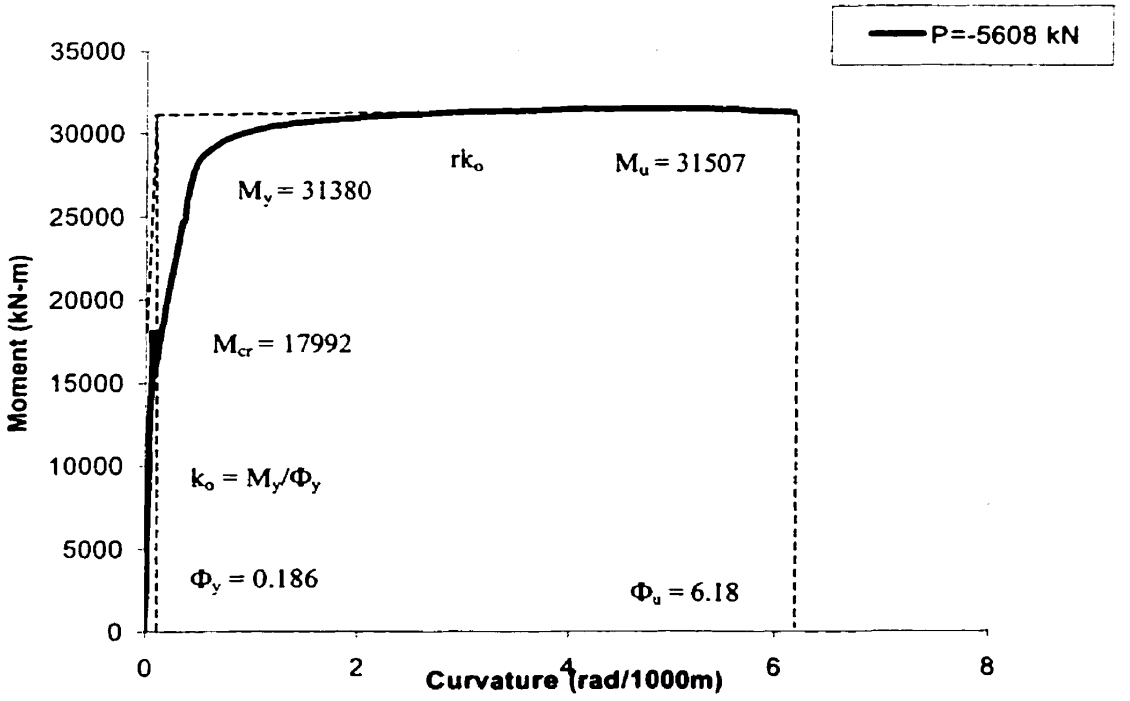

Figure 5-18 Moment-curvature response of the wall including steel strain hardening (storey 1).

Figure 5-18 shows the nonlinear moment-curvature response of the wall for the bottom storey including strain hardening of the steel. The bilinear hysteresis rule analysis is considered for the inelastic analyses in Figure 5-18. The yielding moment M_y equals 31380 kN-m and its corresponding curvature is 0.186 rad/km. The curvature reaches its maximum value (Φ_u = 6.18 rad/km) when the steel is broken. The bilinear factor, r, is obtained from the second branch of the moment-curvature relationship and its value is $0.169*10^{-3}$.

3. Results of analyses

(1) The top lateral displacement of the wall

To assess the effects of the hysteresis rules and the strain hardening of steel on the wall's response, the RUAUMOKO program is used to perform inelastic analyses with and without P-Δ effects under El Centro and Saguenay earthquakes. The top lateral displacement time histories with and without P-Δ effects are given in Figure 5-19 to Figure 5-22 under the El Centro and the Saguenay earthquakes.

From the results of the top lateral displacement time histories of the shear wall, the following conclusions are drawn:

(1) Under El Centro earthquake, the influence of the strain hardening of steel on the top lateral displacement of the shear wall with and without P-Δ effects may be neglected. If the trilinear degrading hysteresis rule is considered for the inelastic analysis, the top displacements of the wall are slightly smaller than those of the bilinear and hardening hysteresis models.

(2) For Saguenay ground accelerations, the strain hardening of the steel does not have any effect on the top lateral displacement of the wall when not including P-Δ effects. However, the peak top lateral displacement of the wall is increased by 32 % when including P-Δ effects if we compare the results from the bilinear hysteresis rule without the strain hardening of the steel with the results that include the strain hardening of the steel.

(3) For analyses with and without P-Δ effects, the lateral displacement tend to be slightly smaller when the trilinear hysteresis rule is used instead of the bilinear rule.

(4) When including P-Δ effects, the maximum top displacement of the wall indicates a slight natural period elongation under Saguenay ground acceleration if the trilinear degrading hysteresis rule is considered for the inelastic analysis as compared to the bilinear rule.

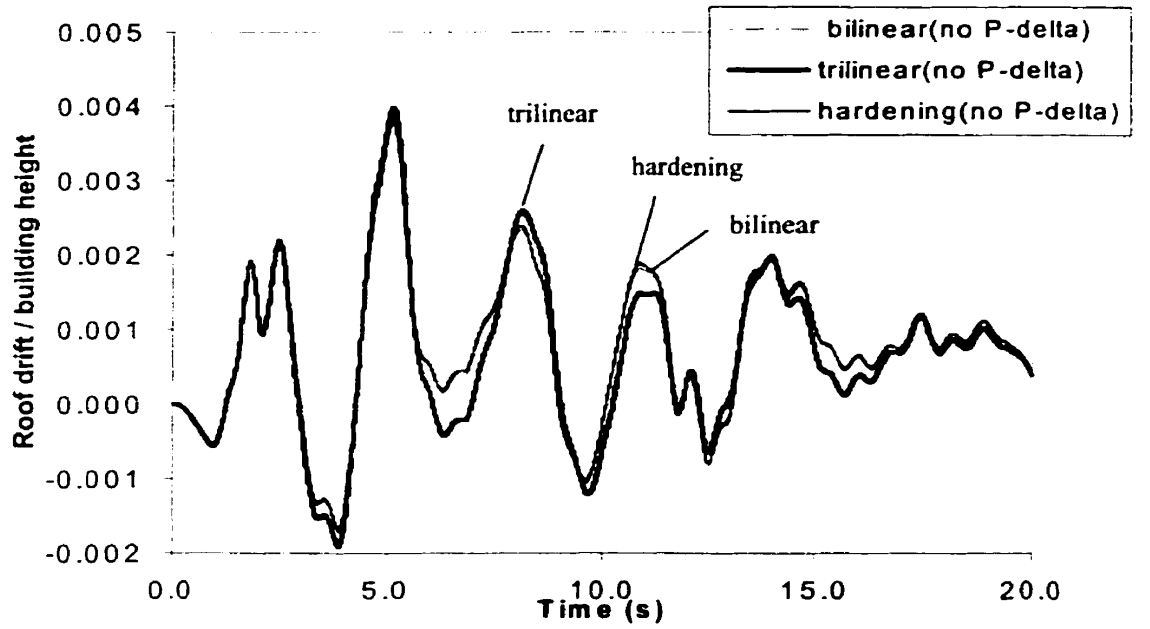

Figure 5-19 Top lateral displacement time history - scaled El Centro earthquake (without P-Δ).

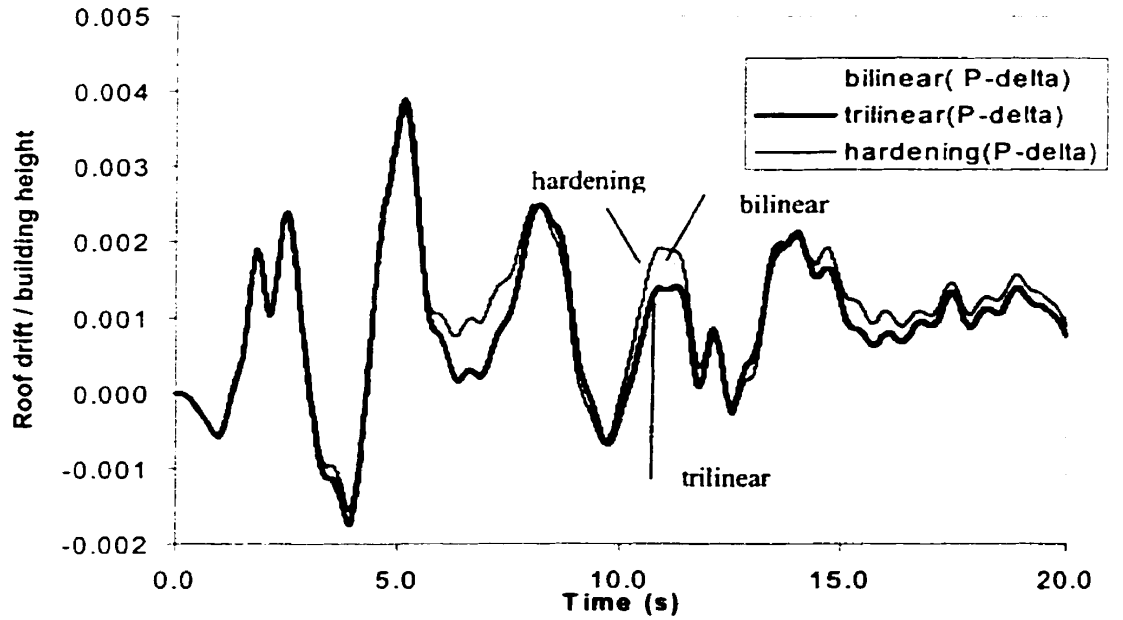

Figure 5-20 Top lateral displacement time history - scaled El Centro earthquake (with P-Δ).

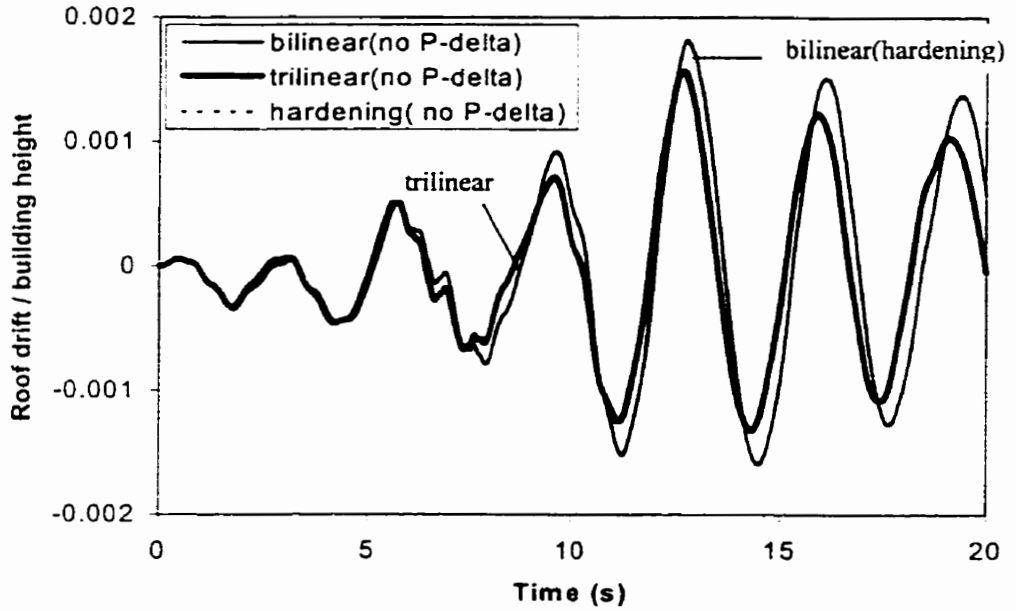

Figure 5-21 Top lateral displacement time history - scaled Saguenay earthquake (without P-Δ).

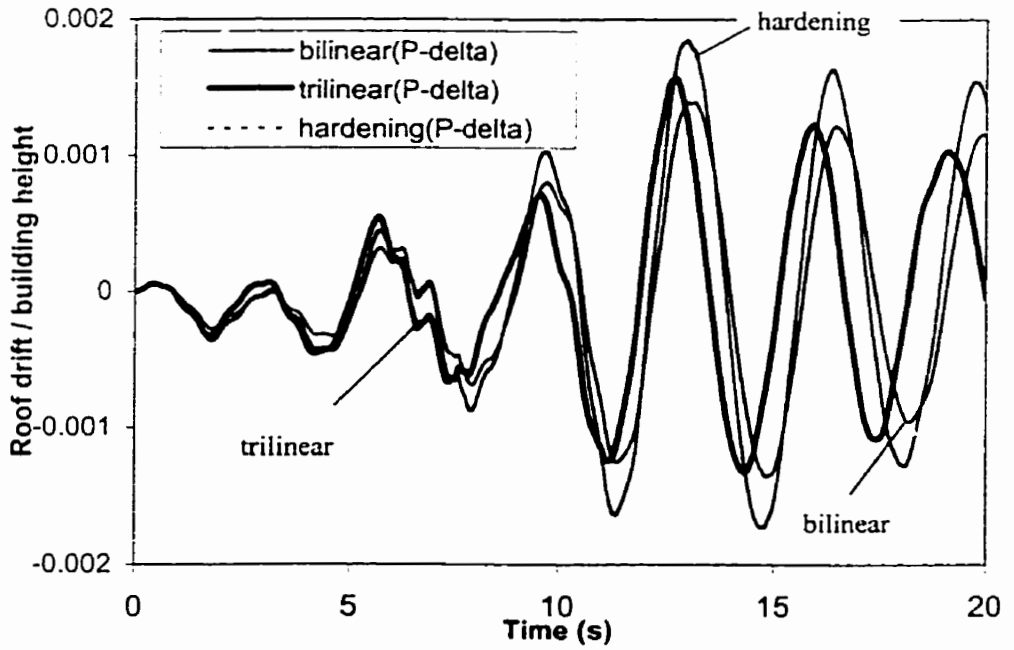

Figure 5-22 Top lateral displacement time history - scaled Saguenay earthquake (with P-Δ).

(2) Maximum curvature of the wall

The results of curvature time histories for the base of the wall with P-Δ and without P-Δ are illustrated in Figure 5-23 to Figure 5-26. The following results can be drawn from the analyses:

(1) The trilinear hysteresis rule has an important effect on the maximum curvature under the El Centro earthquake, the maximum curvature is decreased by as much as 70%. However, including the effects of strain hardening of the steel has no influence on the maximum curvature.

(2) For the Saguenay earthquake, the influence of the trilinear hysteresis rule and the effect of strain hardening of the steel on the maximum curvature are small if they are considered in the analysis.

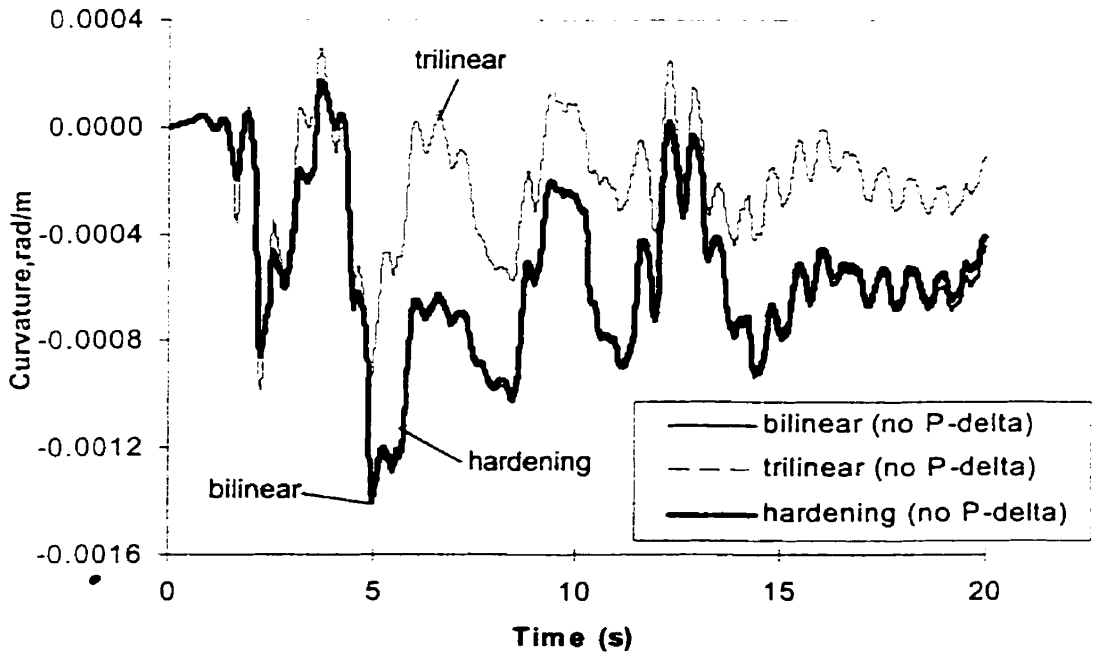

Figure 5-23 **Curvature time history for the base of the wall - scaled El Centro earthquake (without P-Δ).**

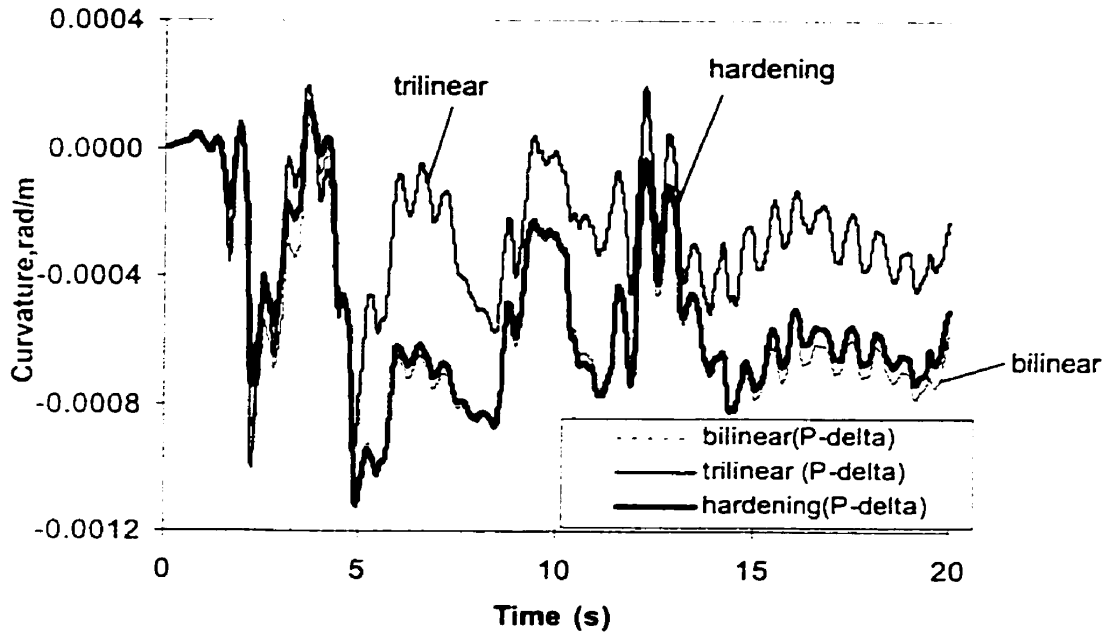

Figure 5-24 Curvature time history for the base of the wall - scaled El Centro earthquake (with P-Δ).

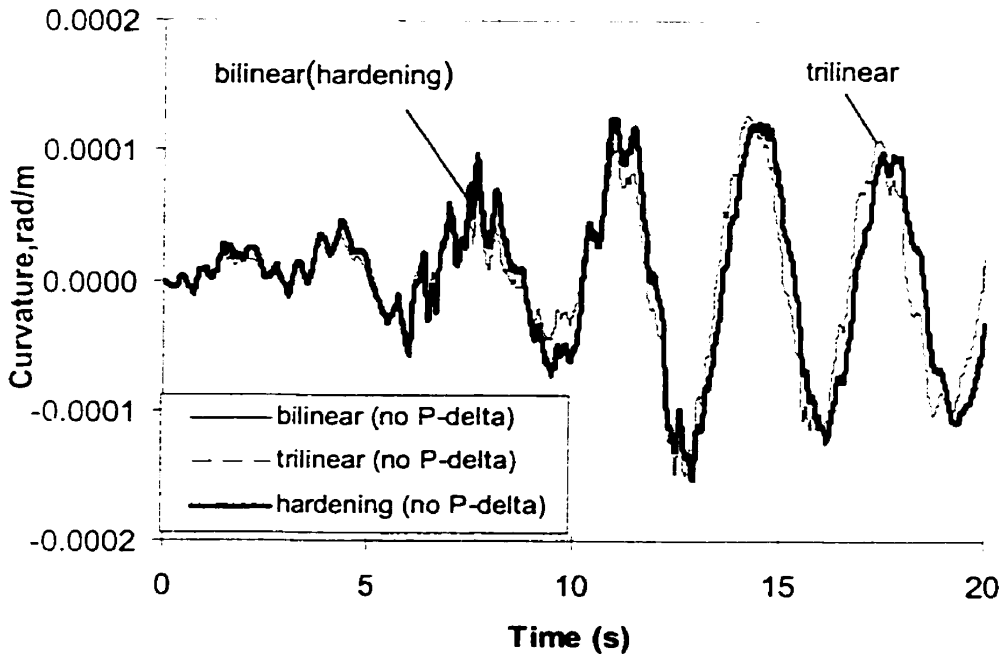

Figure 5-25 Curvature time history for the base of the wall - scaled Saguenay earthquake (without P-Δ).

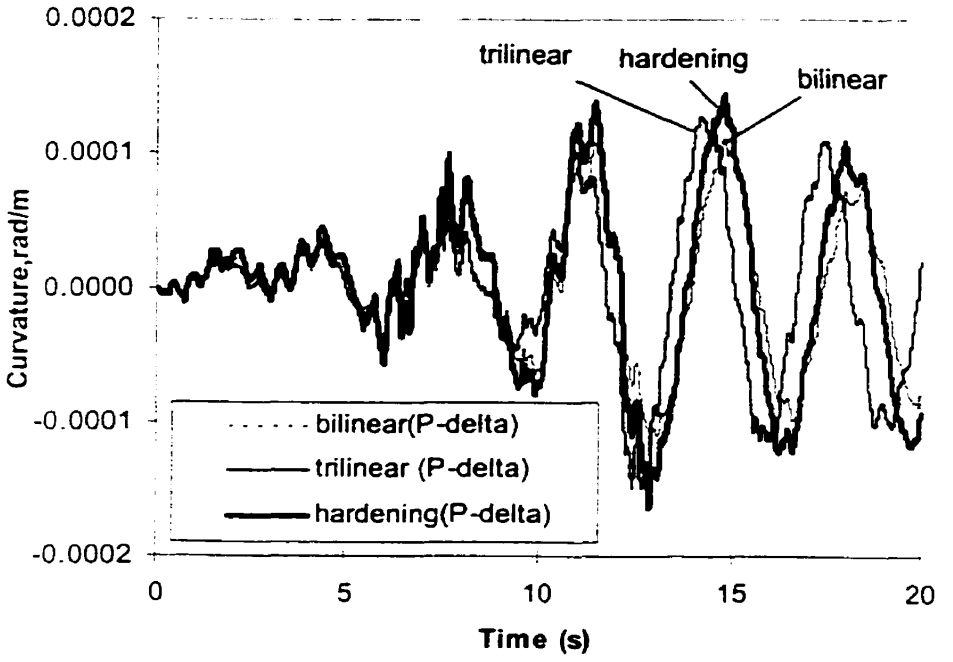

Figure 5-26 Curvature time history at the base of the wall - scaled Saguenay earthquake (with P-Δ).

(3) Moment-curvature response histories

The moment-curvature hysteresis at the base of the wall with and without P-Δ effects are given in Figure 5-27 to Figure 5-31 under the El Centro and the Saguenay earthquakes. The following conclusions are drawn:

(1) Under El Centro earthquake, P-Δ effects on the moment-curvature responses at the base of the wall may be neglected if trilinear degrading hysteresis rule and the steel strain hardening are considered in the analysis.

(2) For Saguenay earthquake, the moment is proportional to the curvature at the base of the wall if bilinear degrading hysteresis rule and the steel strain hardening are

considered. This is because the shear wall remains in the elastic regime at the base of the wall.

(3) The influence of P-Δ effects on the moment-curvature response at the base of the wall may be neglected under Saguenay earthquake.

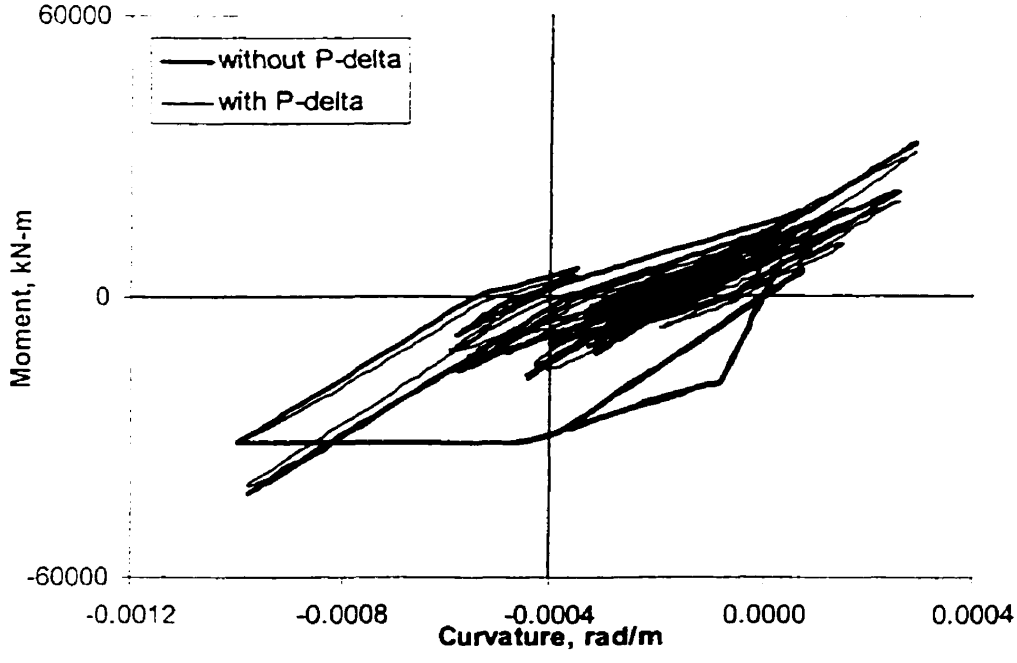

Figure 5-27 **Moment –curvature response history at the base of the wall - scaled El Centro earthquake (trilinear hysteresis rule).**

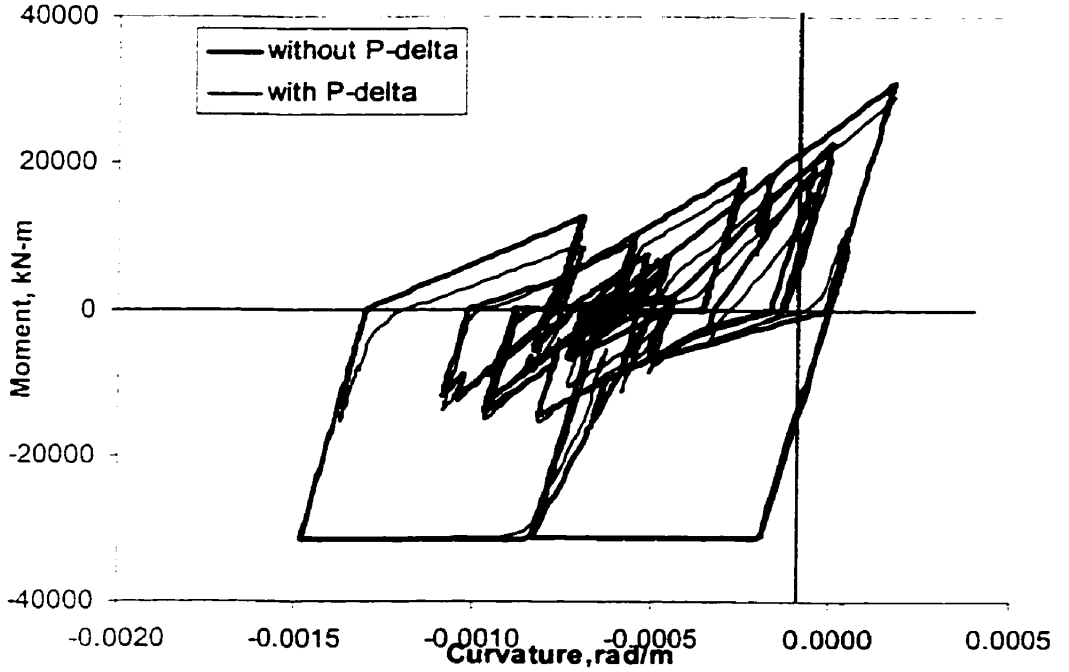

Figure 5-28 **Moment-curvature response history at the base of the wall - scaled El Centro earthquake (bilinear including the steel strain hardening).**

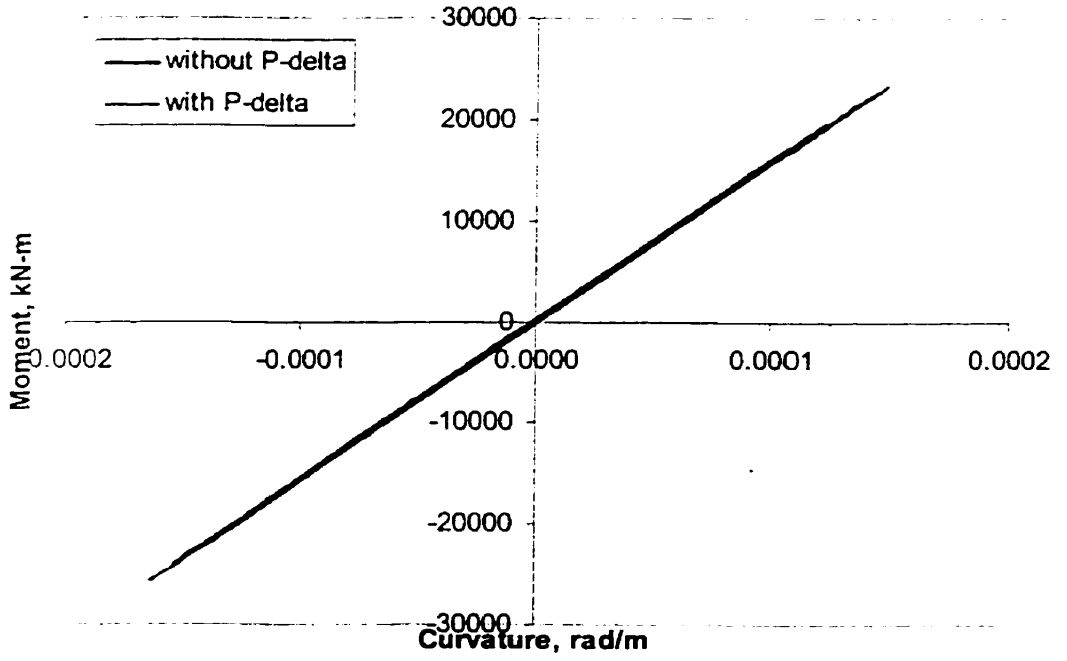

Figure 5-29 **Moment-curvature response history at the base of the wall - scaled Saguenay earthquake (bilinear hysteresis rules).**

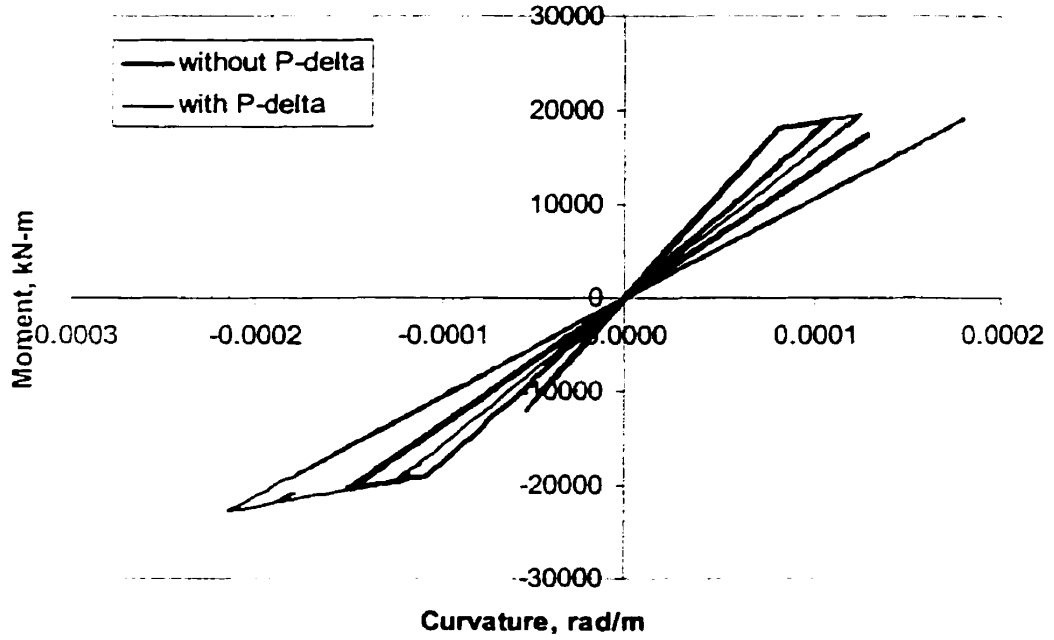

Figure 5-30 **Moment-curvature response history at the base of the wall - scaled Saguenay earthquake (trilinear hysteresis rule).**

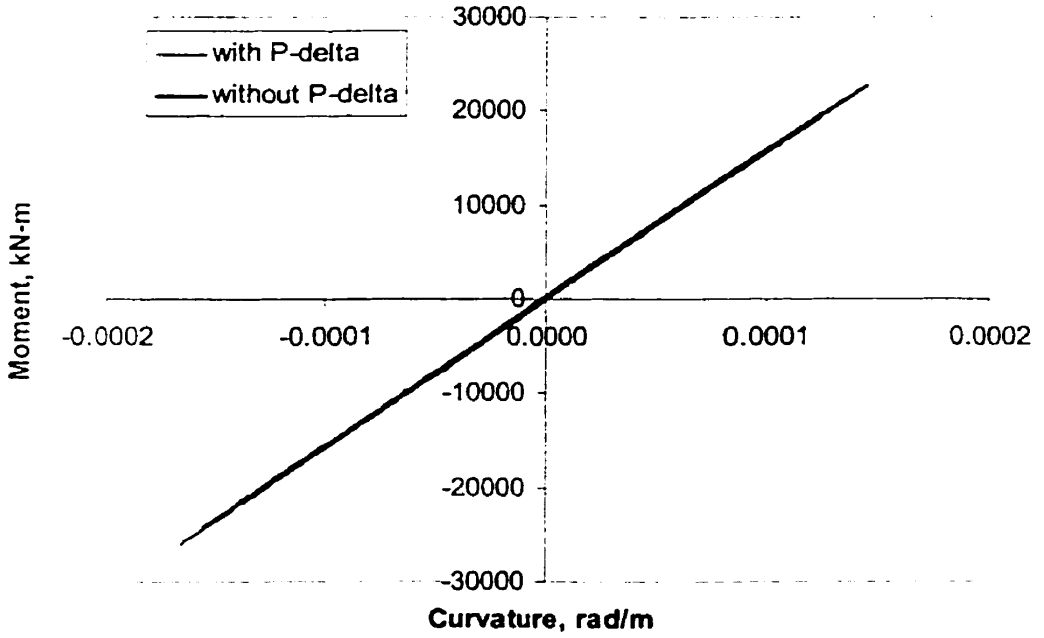

Figure 5-31 **Moment-curvature response history at the base of the wall - scaled Saguenay earthquake (bilinear including the steel strain hardening).**

5.4.4 Viscous damping ratio

1. Damping model

For the inelastic dynamic analyses with the bilinear hysteresis rule, Rayleigh type damping is assumed based successively on 2%, 5% (recommended by NBCC 1995 for elastic analysis) and 7% damping in the first third modes of vibration corresponding to a cumulative modal mass equal to 94% of the total mass of the wall in the horizontal direction. To examine the influence of the selected damping ratio on the seismic response of the wall, the RUAUMOKO computer program is used to perform inelastic dynamic analyses with and without P-Δ effects under El Centro and Saguenay earthquakes.

2. Results of analyses

(1) The top lateral displacement of the wall

The RUAUMOKO computer program is used to derive the top lateral displacement of the wall with and without P- Δ effects under El Centro and Saguenay earthquakes. The results are given in Figure 5-32 to Figure 5-35.

The following conclusions are drawn from the results:

(1) The influence of viscous damping ratio on the top lateral displacement of the shear wall under El Centro earthquake is not very significant if a 7% damping ratio is considered instead of 5% damping ratio. However, the top lateral displacement with P-Δ effects is increased after 13 seconds if the viscous damping ratio is assumed as 2%.

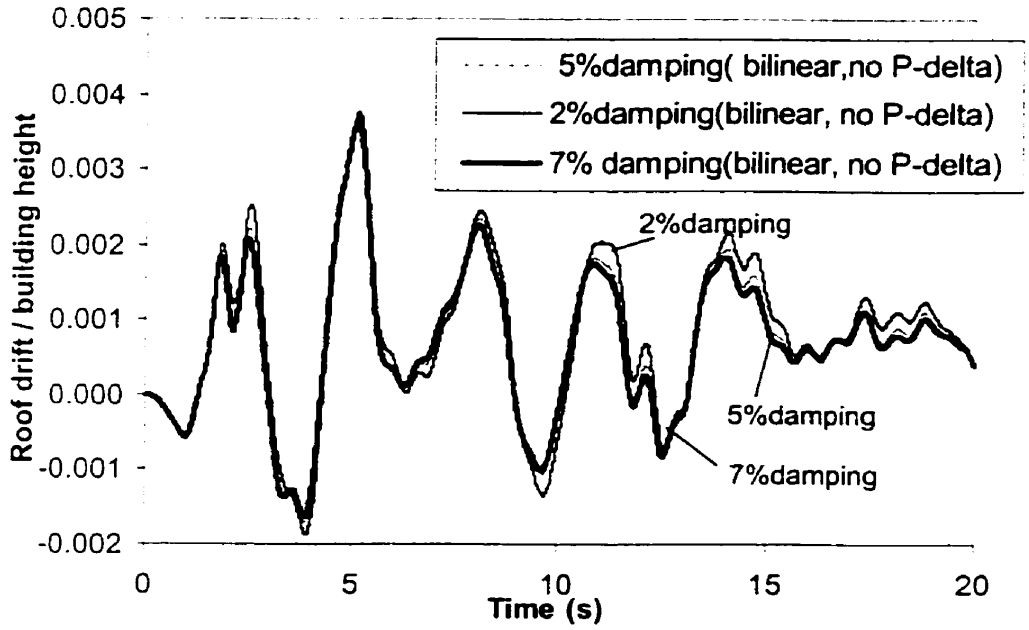

Figure 5-32 Top lateral displacement time history - scaled El Centro earthquake (without P-Δ).

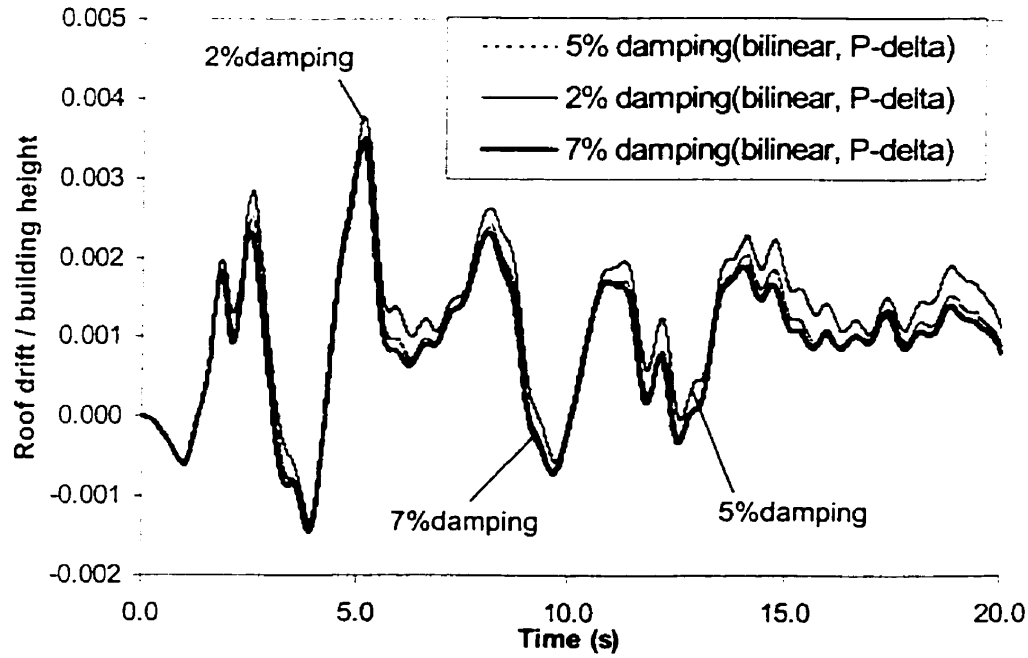

Figure 5-33 Top lateral displacement time history - scaled El Centro earthquake (with P-Δ).

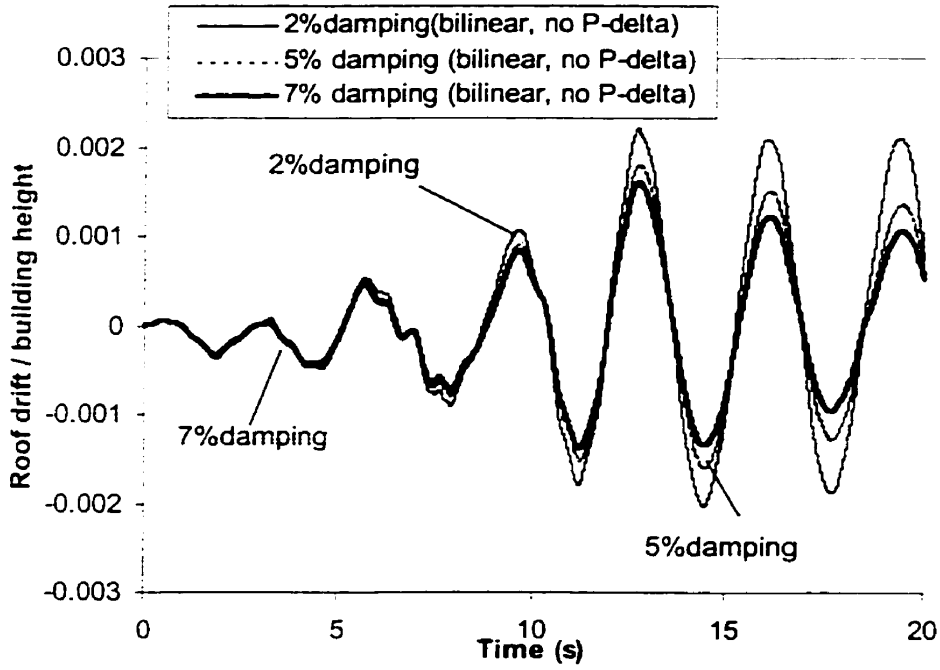

Figure 5-34 Top lateral displacement time history - scaled Saguenay earthquake (without P-Δ).

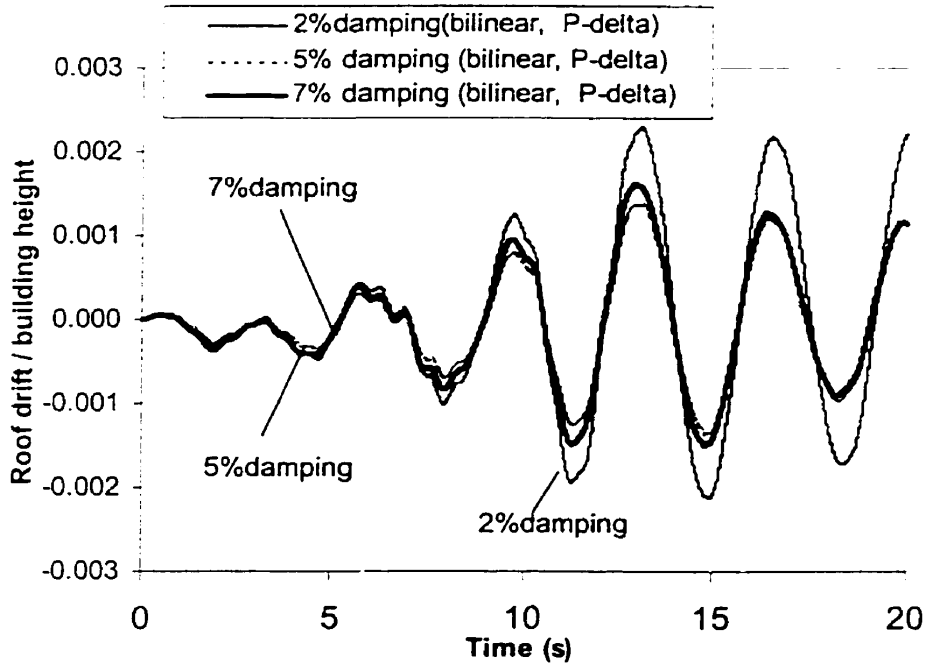

Figure 5-35 Top lateral displacement time history - scaled Saguenay earthquake (with P-Δ).

(2) Under Saguenay earthquake, the top lateral displacement is increased by 22% (without P-Δ) and 65% (with P-Δ) if a 2% viscous damping ratio is considered instead of 5%. However, the effect of viscous damping ratio on the top lateral displacement may be neglected when 7% damping ratio is assumed.

(3) Most shear wall structures experiencing significant cracking during an earthquake will have viscous damping ratio in excess of 5%. Therefore, the influence of viscous damping ratio on roof displacement may be neglected.

(2) Maximum curvature of the wall

Maximum curvatures of the wall can also be obtained from the RUAUMOKO computer program if Rayleigh type damping is assumed based on 2%, 5%, and 7% damping. The results are shown in Figure 5-36 to Figure 5-39.

From the results of these analyses of the shear wall, several conclusions can be drawn:

(1) The influence of viscous damping ratio on maximum curvature of the shear wall under El Centro and Saguenay earthquakes is not very significant if a 7% damping ratio is considered instead of 5% damping ratio.

(2) Figure 5-36 shows that maximum curvature of the wall without P-Δ effects will be decreased by 17% if 2% damping ratio is considered as compared to the value computed with 5% damping.

(3) For Saguenay ground motion, using a 2% damping ratio has a significant influence on the maximum curvature of the wall, the maximum curvature of the wall is increased by 147% (with P-Δ) and 45% (without P-Δ) when compared to 5% damping.

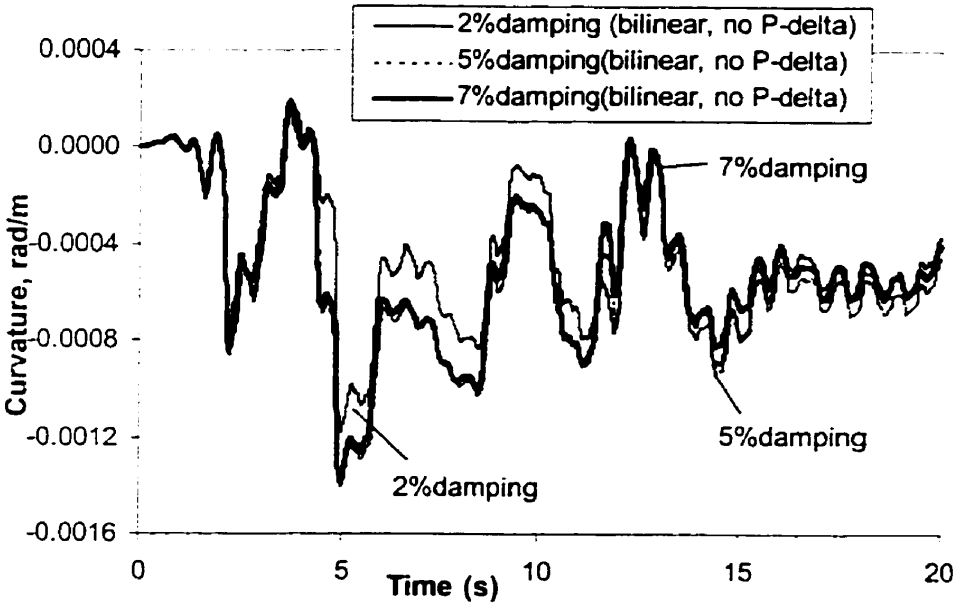

Figure 5-36 Curvature time history for the base of the wall - scaled El Centro earthquake (without P-Δ).

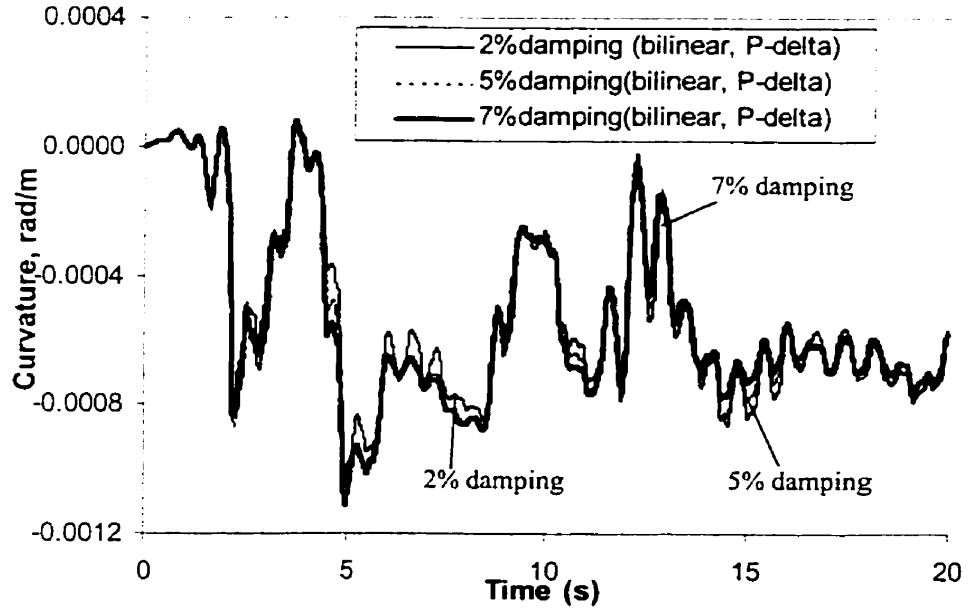

Figure 5-37 Curvature time history for the base of the wall - scaled El Centro earthquake (with P-Δ).

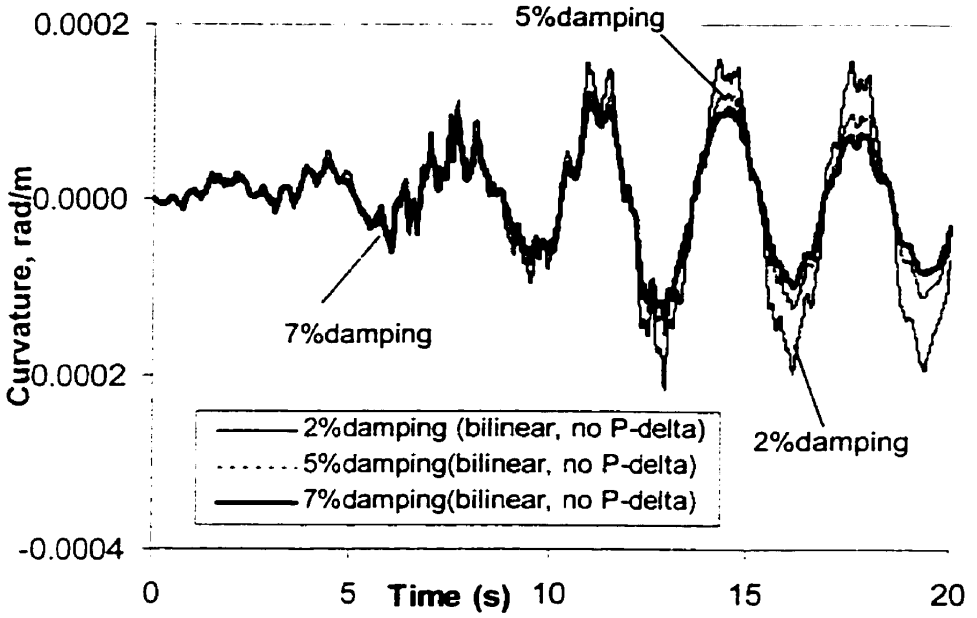

Figure 5-38 Curvature time history for the base of the wall - scaled Saguenay earthquake (without P-Δ).

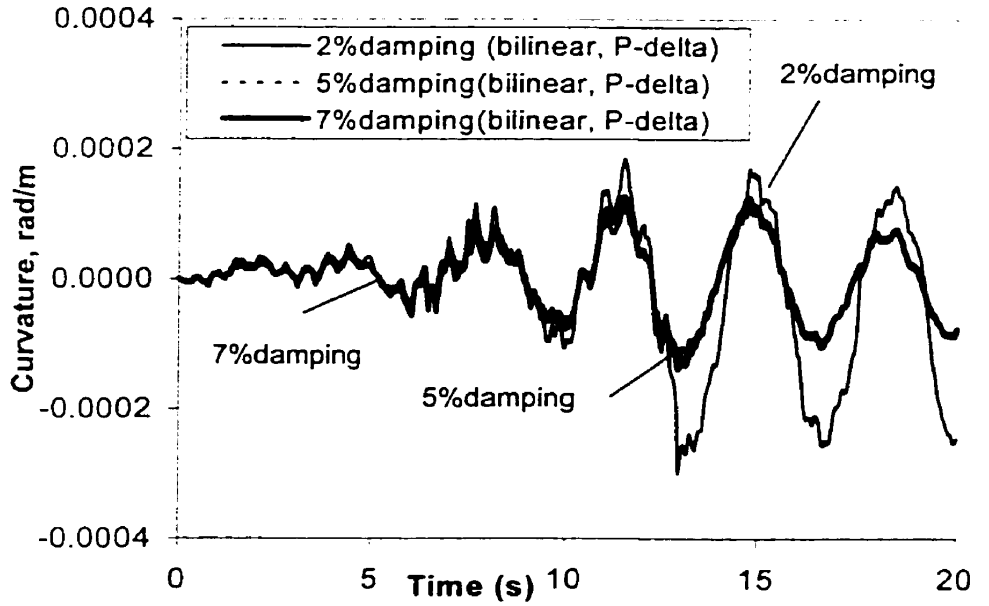

Figure 5-39 Curvature time history for the base of the wall - scaled Saguenay earthquake (with P-Δ).

5.5 Discussion

1. The influence of the axial force on the wall's horizontal displacement

The first modelling parameter considered for the inelastic analysis is the axial force in the gravity column. The effects of variations of the axial force on the wall horizontal displacement at various time steps are presented in Figure 5-5 to Figure 5-7. The deflected shapes are determined at some particular times. These particular times are obtained from peak amplitudes of the top lateral displacement time history to scaled El Centro, Taft and Parkfield earthquakes in Chapter 4. The axial force in the gravity column is increased from P to 2P, and 5P.

When the axial force is increased from P to 2P, the first periods of vibration of the shear wall is lengthened from 3.380s to 3.556s. The lateral displacement of the wall may be decreased due to larger period. For example, under El Centro earthquake, the maximum top horizontal displacement of the wall at 4.1s is 50.3mm when the axial force is P. However, the maximum top horizontal displacement of the wall is decreased to 37.3mm when the axial force is increased to 2P. The axial load in the gravity columns has a significant effect on the wall horizontal displacement if the axial load is increased from 2P to 5P, the maximum top horizontal displacement of the wall is increased from 65 mm to 131mm at 4.5 s.

The deformed shape of the wall exhibits more curvature when the axial force in the gravity columns is increased. Finally, the wall collapsed due to plastic hinge formation at the base of the wall if the axial load is significantly increased. The curvature at 6^{th} floor is increased largely due to change in the longitudinal reinforcing steel.

2. The influence of the hysteresis rules and the strain hardening of steel

The 1940 El Centro and 1988 Saguenay records are chosen as ground motions to represent Western and Eastern North America, respectively. The top lateral displacement time histories and maximum curvatures of the wall with and without P-Δ are given in Figure 5-19 to Figure 5-26. Based on the results of the analyses, the trilinear degrading rule has significant effects on the top lateral displacement time histories and maximum curvature of the wall. Under El Centro earthquake, the top lateral displacement with P-Δ at 11.3 s is 77.4mm when the bilinear degrading rule is considered for the inelastic analysis and 63.72mm when the trilinear degrading rule is considered. For the Saguenay earthquake, the maximum curvature without P-Δ at 14.2 s is 1.28E-4 rad/m due to the consideration of the trilinear degrading rule and it is 1.1E-4 rad/m if the bilinear hysteresis rule is considered in the analysis.

To assess which form of hysteresis rule, bilinear or trilinear, is more appropriate to model the earthquake response of shear walls, it is most appropriate to compare the results from numerical simulations with those from historical evidences or experimental evidences from shake table experiment. As an example, the CAMUS (1998) International Benchmark (Queval et al. 1998) was carried out to compare different modelling procedures to predict the seismic shake table response of a 7.06 m * 1.02 m reinforced concrete shear wall model. The results indicated that the bilinear hysteresis model was more appropriate to predict the response of the wall including P-Δ effects compared to the response obtained from the trilinear hysteresis model. The trilinear hysteresis model tended to dissipate too much energy through the inelastic cracking mechanism. It is thus recommended to use the bilinear hysteresis model at this stage. However, further studies are required to generalise this recommendation.

The influence of the strain hardening of steel on the top lateral displacement and maximum curvature of the wall is minimal under El Centro earthquake. The strain

hardening effects may be neglected. However, the top lateral displacement of the wall under the Saguenay earthquake are increased as compared to results without the strain hardening of the steel if including P-Δ effects. Figure 5-22 shows that the top lateral displacement of the wall at 13 s is 83.25 mm (strain hardening of steel) and 62.19mm (bilinear). However, the results show that the damage indices $D\mu_{\Delta}$ is 0.212 (with the strain hardening of steel) and 0.158 (without the strain hardening of steel). The variation of the damage indices is not significant and the building is still very far from collapse. Therefore, P-Δ effects may be neglected under the Saguenay earthquake if including the influence of the strain hardening of steel on the top lateral displacement.

3. The influence of the viscous damping ratio

To examine the effects of variation of the viscous damping ratio on the top lateral displacement and maximum curvature of the wall, damping ratios 2%, 5% 7% are assumed in the analyses. The results are given in Figure 5-32 to Figure 5-39. Figure 5-32 and Figure 5-37 show that the influence of viscous damping ratio on the top lateral displacement if not including P-Δ effect and maximum curvature of the wall if including P-Δ effects may be neglected under El Centro earthquake.

If viscous damping ratio is considered as 2%, the top lateral displacement and maximum curvature of the wall will be increased under Saguenay earthquake. For example, the top displacement of the wall at 12.7s is 99.5mm (2% damping) and 82.35mm (5% damping) if not including P-Δ effects. Figure 5-27 also shows that curvature of the wall at 13s is –3E-4 rad/m (2% damping) and –1.23E-4 rad/m (5% damping) if including P-Δ effects. If viscous damping ratio is considered as 7%, the maximum curvatures of the wall under Saguenay earthquake are very close to those attained considering 5% damping.

5.6 Conclusions

In this chapter, an evaluation of the influence of some modelling parameters on the earthquake response of the shear wall has been presented. Some conclusions can be drawn:

1. Axial load in the gravity column can have a significant influence on the wall's horizontal displacement. Under El Centro earthquake, the maximum top horizontal displacement of the wall is increased from 65 mm to 131mm at 4.5 s when the axial force is increased from 2P to 5P.

2. The numerical results obtained in this chapter show that the top displacements of the wall are slightly smaller than those of the bilinear hysteresis models if the trilinear degrading rule is considered under El Centro earthquake. Previous studies indicates that bilinear rules are preferable to trilinear rule to predict the seismic response of shear wall structures (Queval et al.1998).

3. Including the strain hardening of steel have not influenced the top displacement and maximum curvature of the wall when including P-Δ effects.

4. The analyses show that the influence of the damping ratio 2% on the top lateral displacement and maximum curvature of the wall is more important under Saguenay earthquake. If viscous damping ratio is considered as 7%, the effects of damping ratio on the maximum curvature of the wall under Saguenay earthquake becomes insignificant as compared to the values attained while using 5% damping ratio.

5. When the intensity of earthquake ground motion is increased, the wall collapsed due to plastic hinge formation at the base of the wall under El Centro and Saguenay earthquakes if including P-Δ effects. However, when P-Δ effects are not included in

the analysis, the wall can not reach a failure state with the constitutive model adopted even though the intensity of earthquake ground motion is increased largely.

CHAPTER 6

CONCLUSIONS

6.1 Summary

This thesis has presented a study of P-Δ effects on the inelastic seismic response of a typical reinforced concrete shear wall building. It consists of four sections. The first section described the current state of research work done on the P-Δ effects in building structures and reviews previously published work. The second section presented the model of a typical 12-storey shear wall building to perform elastic and inelastic earthquake response analyses. The structural wall designed according to NBCC 1995 was modelled by 12 beam-column elements with 3 degrees-of-freedom per node. The RESPONSE computer program (Collins and Mitchell,1987) was used to derive the relationship between moment and curvature of the wall for each storey.

The third section presented inelastic dynamic analyses with and without P-Δ effects under El Centro 1940, Taft 1959, and Parkfield 1996 earthquakes. The results of response analyses were compared to assess the importance of P-Δ effects. The response parameters, such as the top lateral displacements, base shear, moment-curvature responses, lateral displacement envelopes, displacement ductility, curvature ductility demands, and damage indices, were used to examine the structural response.

The last section presented the results of a parametric study to assess the effects of varying key modelling parameters of the shear wall building. The main parameters in this study were:

- Axial force in the gravity columns (P, 2P, 5P).

- The frequency content of the ground motions (El Centro, 1940, and Saguenay, 1988).
- The hysteresis rules (bilinear hysteresis rules and trilinear hysteresis rules).
- Strain hardening of steel.
- Viscous damping ratio (bilinear hysteresis rules, ξ= 2%, 5%, and 7%).

6.2 Conclusions

From the results of the research work performed in this thesis, several conclusions can be drawn:

(1) The stability factor approach introduced in NBCC 1995 to consider P-Δ effects in the design and analysis of shear wall structures appears to be overly conservative. A maximum stability factor, θ , reaching 0.39 would be necessary to counteract P-Δ effects (see Table 3-7). The strength of several storeys would need to be increased by approximately 39% by the simplified stability factor approach. However, the results of detailed inelastic dynamic analyses without any strength increase to counteract P-Δ effects indicate that this increase in strength is not necessary since P-Δ effects were found insignificant in all analyses performed. However, residual inelastic displacements might be increased by P-Δ effects in the case where seismic ground accelerations contain long acceleration pulses. This might influence the post-seismic load carrying capability of the building and deserve further considerations in the future.

(2) P-Δ effects can lengthen the structure periods of vibration. For the building studied, the first period of vibration is 3.389s with P-Δ, and 3.225s without P-Δ effect. After

the cross section is cracked, the periods of vibration are lengthened due to the decrease in elastic stiffness.

(3) Including P-Δ effects in the analysis of a typical shear wall building undergoing earthquake loading has little effect on the maximum lateral displacement, base shear, displacement ductility demand, curvature ductility demand, and damage indices $D_{\mu\Phi}$ defined as the maximum curvature divided by the ultimate curvature.

(4) Inelastic dynamic analysis has shown that maximum base shears of the shear wall could be 2 to 3 times larger than the design base shear obtained from the pseudo-static procedure of NBCC 1995. Part of this can be explained by Φ the material resistance factor, and J the overturning reduction factor. However, the main reason is coming from the spatial distribution of the accelerations and related inertia forces along the height of the wall. Inelastic analyses have shown large accelerations in the bottom part of the wall, while the code assumes large accelerations in the upper part of the wall. Since the bending moment at the base of the wall computed from the inelastic dynamic analyses could be nearly identical to the code value, corresponding to the yield moment for a bilinear system, larger inertia forces, and corresponding base shear, must be developed in the dynamic analyses to maintain the moment equilibrium.

(5) Inelastic dynamic analyses has shown that plastic hinges may be developed in the middle of the wall instead of the base of the wall. This could be explained by the variations in the longitudinal steel reinforcement along the height of the wall. It may cause the critical section for plastic energy dissipation to be located above the base of the wall, thus modifying the anticipated failure mechanism.

(6) The variation of the structural damage parameter $D\mu_{\Delta}$, which is ratio of the maximum computed displacement to the ultimate displacement when including P-Δ effects, is small compared with the values computed without P-Δ effects.

(7) For the El Centro 1940 earthquake, the influence of axial force in the gravity column on the wall's horizontal displacement is not significant when the axial force is increased from P to 2P. However, the wall's horizontal displacement is significantly increased, from 65 mm to 131 mm at comparable times, if the axial force is increased from 2P to 5P. Under Taft earthquake, the order of increase in the wall horizontal displacement at critical times is from 2.6 mm to 80 mm if the axial force is increased from 2P to 5P. When the axial force is increased from P to 2P, the axial force has a little effect on the wall's horizontal displacement under Parkfield and Taft earthquakes. This indicates that reasonable uncertainties in the axial load acting on the structure at the time of the earthquake (P to 2P) will not significantly increase P-Δ effects for shear wall structures.

(8) If the trilinear degrading hysteresis rule is considered for the inelastic analysis, the maximum curvature under El Centro 1940 earthquake is decreased by 70% as compared to the results obtained for the bilinear hysteresis rule. For the Saguenay earthquake, the maximum curvature without P-Δ at 14.2 s is 1.28E-4 rad/m due to the consideration of the tri-linear degrading rule and it is 1.1E-4 rad/m if the bilinear hysteresis rule is considered in the analysis. Previous studies indicates that the bilinear rule is preferable to model the inelastic response of shear wall structures (CAMUS 1998).

(9) The effects of the strain hardening of steel on the top lateral displacement and the maximum curvature under low frequency Western and high frequency Eastern North America type of earthquake ground motions is not significant when comparing the

results with and without P-Δ effects. However, the results considering P-Δ effects indicate that if significant steel strain hardening is considered for Eastern North America type of earthquake, the peak lateral displacements could be increased by as much as 32% as compare with the case without the strain hardening of the steel. However, the buildings was still very far from collapse as indicated by the damage indices. The results show that the damage indices $D\mu_{\Delta}$ is 0.212 with the strain hardening of the steel, and 0.158, without the strain hardening of the steel. A value of $D\mu_{\Delta}$ equals to 1 indicates a potential failure of the wall. This demonstrates that the seismic results are sensitive to the characteristics of the hysteresis rule adopted (with or without the strain hardening of the steel).

(10) The study shows that the wall top lateral displacement under the 1988 Saguenay earthquake ground motions is increased by 65 % (with P-Δ) if 2% damping ratio is considered as compared to the results with 5% damping. However, the effects of the 7% damping ratio may be neglected as compared to the results using 5% damping ratio. Most shear wall structures experiencing significant cracking during an earthquake will have viscous damping ratio in excess of 5%. The viscous damping coefficient does not appear to be a critical parameter affecting P-Δ effects.

6.3 Recommendations for future work

Due to its limited scope, this thesis has left several areas for further study of P-Δ effects on the inelastic seismic response of R/C shear wall buildings. It is suggested that the following areas be considered:

- To assessment of the effects of inelastic response due to variations in the amount of reinforcing steel in shear wall buildings.

- To study of P-Δ effects in a typical reinforced concrete coupled wall structures.

- To further study the influence of P-Δ effects on the inelastic seismic response of more shear walls buildings of different sizes and configurations.

- Some experimental work is required to validate the results of P-Δ numerical analyses on a reinforced concrete wall building model. In particular, cracking and damping should be examined.

- To develop simplified seismic design guidelines in NBCC that will recognise the fact that shear wall structures are not sensitive to P-Δ effects as compared to moment resisting frame structures.

REFERENCES

CAMUS, 1998. "CAMUS" International Benchmark, Experimental results, Synthesis of the participants reports. Seismic Mechanic Study Laboratory of CEA, CEN SACLAY, and the AFPS Benchmark Workgroup, France.

CARR, A. -J. 1996. Ruaumoko - Inelastic Dynamic Analysis Program. Department of Civil Engineering, University of Canterbury, New Zealand.

COLLINS, M. P. and MITCHELL, D. 1987. Prestressed concrete basics. Canadian Prestressed Concrete Institute, Ottawa, Ontario, Canada.

CÔTÉ, B. 1997. Amplification de la résistance séismique pour contrer les effets P-delta dans les bâtiments multi-étagés. Master Thesis, Department of Civil Engineering, École Polytechnique de Montréal, Montréal, Canada.

CPCA. 1995. Concrete design handbook. Canadian Portland Cement Association, Ottawa, Ontario, Canada.

CPCA. 1985. Concrete design handbook. Canadian Portland Cement Association, Ottawa, Ontario, Canada.

CSA. 1994. A23.3-M94. Design of Concrete Structures. Canadian Standards Association, Rexdale, Ontario, Canada.

CSA. 1984. A23.3-M84. Design of Concrete Structures. Canadian Standards Association, Rexdale, Ontario, Canada.

EC8, 1998. Design Provisions for Earthquake Resistance of Structures. European Pronorm ENV 1998, Brussels.

FENWICK, R. C., DAVIDSON, B. J., and CHUNG, B. T. 1992. P-Δ actions in seismic resistant structures. Bulletin of the New Zealand National Society for Earthquake Engineering, Vol.25, No. 1, 1992, pp.56-69.

LINDE, P. and MOEHLE, J.P. 1998. Evaluation of R/C structural walls designed according to EC8. Proceedings of 11th European Conference on Earthquake Engineering, Paris, France,1998, pp.1-11.

MONTGOMERY, C.J. 1980. Influence of P-Δ effects on seismic design. Canadian Journal of Civil Engineering, Vol.8, 1981, pp.31- 43.

NBCC 1985. National Building Code of Canada. National Research Council of Canada, Ottawa, Ontario, Canada.

NRCC. 1990. National Building Code of Canada. National Research Council of Canada, 10th edition, Ottawa, Ontario, Canada.

NRCC. 1995. National Building Code of Canada. National Research Council of Canada, 11th edition, Ottawa, Ontario, Canada.

NRCC. 1996. User's Guide. National Building Code of Canada. National Research Council of Canada, Ottawa, Ontario, Canada.

NEUSS, C.F., and MAISON, B.F. 1983. Analysis for P-Δ effects in seismic response of buildings. Computers and Structures, Vol.19, No.3, 1984, pp 369-380.

OTANI, S. 1974. A computer Program for Inelastic Response of R/C Frames to Earthquakes. Report UILU-Eng-74-2029, Civil Engineering Studies, University of Illinois at Urbana-Champaign, Nov.1974.

PARK, Y-J and ANG, A.H-S. 1985. Mechanistic Seismic Damage Model for Reinforced Concrete. J.Struct. Div. ASCE, Vol 111, No.4, April 1985. pp722-757.

PAULAY, T. and PRIESTLEY. 1992. Seismic design of reinforced concrete and masonry buildings. John Wiley and Sons, New York, USA.

QUEVAL, J. C., COMBESCURE, D., SOLLOGOUB, P., COIN, A., and MAZARS, J. 1998. "CAMUS" experimental program in-plane seismic tests of 1/3rd scaled R/C bearing walls. Proceedings of the 11th European Conference on Earthquake Engineering, Paris, France,1998, pp1-11.

SHARPE, R. D. 1974. The Seismic Response of Inelastic Structure. Ph.D Thesis, Department of Civil Engineering, University of Canterbury, New Zealand, Novermber,1974.

THOMSON, E. D., CARR, A. J., and MOSS, P. J. 1991. P-Delta effects in the seismic response of ductile reinforced concrete frame. Proceedings Pacific Conference on Earthquake Engineering, Department of Civil Engineering, University of Canterbury, New Zealand, 1991, pp.49-60.

WILLIAMS, M. S., VILLEMURE, I. and SEXSMITH, R. G. 1997. Evaluation of Seismic Damage Indices for Concrete Elements Loaded in Combined Shear and Flexure. ACI Structural Journal, V.94, No.3, May-June 1997, pp.315-322.

WILSON, E. L. and HABIBULLAH, A. 1992. SAP90 - Structural Analysis Program. Computers and Structures, Inc., Berkeley, California, USA.

APPENDIX A

CALCULATION OF AXIAL LOADS ON THE WALLS ACCORDING TO NBCC 1995

Storey 12:

Dead loads:

Slab (110mm thick): 0.11(m)*24(kN/m^3)*15(m)*3(m) = 118.8 kN

Roof insulation: 0.5 (kN/m^2)*15(m)*3(m) = 22.5 kN

Secondary beams (300*240): 0.3(m)*0.24(m)* 24(kN/m^3)* 3(m)*4
= 20.74 kN

Beams of frame (400*440): 0.4(m)*0.44(m)* 24(kN/m^3)* 3(m)*2
= 25.34 kN

0.4(m)*0.44(m)* 24(kN/m^3)*4.5(m)*2
= 38.02 kN

Wall (200mm thick): 0.2(m)*5.4(m)*3.65(m) * 24(kN/m^3) = 94.61 kN

Columns: 0.6(m)*0.6(m)*3.65(m)*24 (kN/m^3)*2 = 63.07 kN

Mechanical services loading: 0.5 (kN/m^2)* 15(m)*3(m) = 22.50 kN

P_D = 405.58 kN

Live loads:

Snow load: 2.2(kN/m^2)*15(m)*3(m) = 99 kN

Mechanical services loading: 1.6(kN/m^2)*6(m) * 3(m) = 28.8 kN

P_L = 127.8 kN

Storey 11:

Dead loads:

Slab (110mm thick): 118.8 kN

Secondary beams (300*240): 20.74 kN

Beams of Frame (400*440): 25.34+38.02 = 63.36 kN

Wall (200mm thick): 94.61 kN

Columns: 63.07 kN

Partition loading: 1.0(kN/m^2)* 15(m)*3(m) = 45 kN

Mechanical services loading: 0.5(kN/m^2)* 15(m)*3(m) = 22.5 kN

Storey 12: 405.58 kN

P_D = 833.66 kN

Live loads:

Cumulative floor area reductive factor: $0.3+\sqrt{9.8/B} = 0.3+\sqrt{9.8/63} = 0.694$

0.694 [18*1.6(kN/m^2)+27*2.4(kN/m^2)+18*4.8(kN/m^2)] = 124.92 kN

Storey 12: 99 kN

P_L = 127.8 + 99 = 226.8 kN

Storey 10:

Dead Load:

P_D = 833.66 + 118.8 + 20.74 + 63.36 + 94.61 + 63.07 + 45 + 22.5

= 1261.74 kN

Live Load:

Cumulative floor area reductive factor: $0.3+\sqrt{\frac{9.8}{108}} = 0.601$

0.601 [18*1.6(kN/m^2)+27*2.4(kN/m^2)*2+18*4.8(kN/m^2)*2] = 199.05 kN

Storey 12: 99 kN

P_L = 298.05 kN

Storey 9:

Dead Load:

P_D = 1261.74 kN + 428.08 kN = 1689.82 kN

Live Load:

Cumulative floor area reductive factor $0.3+\sqrt{9.8/153}=0.553$

$0.553\ [18*1.6(kN/m^2)+27*2.4(kN/m^2)*3+18*4.8(kN/m^2)*3] = 266.77\ kN$

Storey 12: 99 kN

P_L = 365.77 kN

Storey 8:

Dead Load:

P_D = 1689.82 kN + 428.08 kN = 2117.9 kN

Live Load:

Cumulative floor area reductive factor $0.3+\sqrt{9.8/198}=0.522$

$0.522\ [18*1.6(kN/m^2)+27*2.4(\ kN/m^2)*4+18*4.8(\ kN/m^2)*4] = 330.74\ kN$

Storey 12: 99 kN

P_L = 429.74 kN

Storey 7:

Dead load:

P_D = 2117.9 kN + 428.08 kN = 2545.98 kN

Live Load:

Cumulative floor area reductive factor $0.3+\sqrt{9.8/243}=0.501$

$0.501[18*1.6(kN/m^2)+27*2.4(kN/m^2)*5+18*4.8(\ kN/m^2)*5] = 393.18$ kN

Storey 12: 99 kN

P_L = 492.18 kN

Storey 6:

Dead load:

P_D = 2545.98 kN + 428.08 kN = 2974.06 kN

Live Load:

Cumulative floor area reductive factor $0.3+\sqrt{9.8/288}=0.485$

$0.485[18*1.6(kN/m^2)+27*2.4(kN/m^2)*6+18*4.8(kN/m^2)*6] = 453.96$ kN

Storey 12: 99 kN

P_L = 552.96 kN

Storey 5:

Dead load:

P_D = 2974.06 kN + 428.08 kN = 3402.14 kN

Live Load:

Cumulative floor area reductive factor:

$$0.3+\sqrt{9.8/333}=0.472$$

$0.472[18*1.6(kN/m^2)+27*2.4(kN/m^2)*7+18*4.8(kN/m^2)*7] = 513.16$ kN

Storey 12: 99 kN

P_L = 612.16 kN

Storey 4:

Dead load:

P_D = 3402.14 kN + 428.08 kN = 3830.22 kN

Live Load:

Cumulative floor area reductive factor:

$$0.3+\sqrt{\frac{9.8}{378}}=0.461$$

$0.461[18*1.6(kN/m^2)+27*2.4(kN/m^2)*8+18*4.8(kN/m^2)*8] = 570.90$ kN

Storey 12: 99 kN

P_L = 669.9 kN

Storey 3:

Dead load:

Slab: 118.8 kN

Secondary beams: 20.74 kN

Beams of Frame (400*490): 0.4*0.49*24*3*2 = 28.22 kN

0.4*0.49*24*4.5*2 = 42.34 kN

Wall: 94.61 kN

Columns: 63.07 kN

Partition loading: 45 kN

Mechanical services loading: 22.5 kN

Storey (4-12): 3830.22 kN

P_D = 4265.5 kN

Live Load:

Cumulative floor area reductive factor: $0.3+\sqrt{\frac{9.8}{423}}=0.452$

$0.452[18*1.6(kN/m^2)+27*2.4(kN/m^2)*9+18*4.8(kN/m^2)*9] = 628.1$ kN

Storey 12: 99 kN

P_L = 727.1 kN

Storey 2:

Dead load:

P_D = 4265.5 kN + 435.28 kN = 4700.78 kN

Live Load:

Cumulative floor area reductive factor: $0.3+\sqrt{9.8/468}=0.445$

$0.445[18*1.6(kN/m^2)+27*2.4(kN/m^2)*10+18*4.8(kN/m^2)*10] = 685.66$ kN

Storey 2: 99 kN

P_L = 784.7 kN

Storey 1:

Dead load:

Slab: 118.8 kN

Secondary beams: 20.74 kN

Beams of Frame: 70.56 kN

Wall: 0.2m*5.4m*4.85m*24 kN/m^3 = 125.71 kN

Columns: 0.6m*0.6m*4.85m*24 kN/m^3*2 = 83.8 kN

Partition loading: 45 kN

Mechanical services loading: 22.5 kN

P_D = 4700.78 kN + 487.11 kN = 5187.89 kN

Live Load:

Cumulative floor area reductive factor: $0.3 + \sqrt{9.8/513} = 0.438$

0.438[18*1.6(kN/m^2)+27*2.4(kN/m^2)*11+18*4.8(kN/m^2)*11] = 741.1 kN

Storey 12: 99 kN

P_L = 840.1 kN

APPENDIX B

PUSH-OVER ANALYSIS OF THE 12 STOREY WALL USING THE RUAUMOKO COMPUTER PROGRAM

To estimate the ultimate strength of the wall, and to assess the P-Δ effects on the lateral load-displacement response, the RUAUMOKO program is used to perform pushover analyses. Pushover analyses used a monotonically increasing lateral load, which is representative of the equivalent static forces resulting from the first mode of vibration of the structure. To perform a pushover analysis using RUAUMOKO, the lateral loads are applied using the dynamic solution algorithm. A ramp with a very long rise time in relation to the fundamental period is used to increase very slowly the magnitude of the loads to avoid any dynamic effects. It is illustrated in Figure B-1.

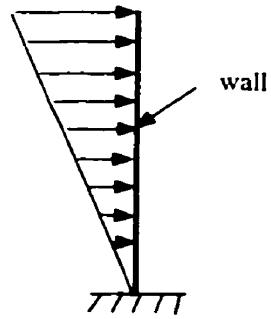

(a) Spatial distribution of load {f(s)}.

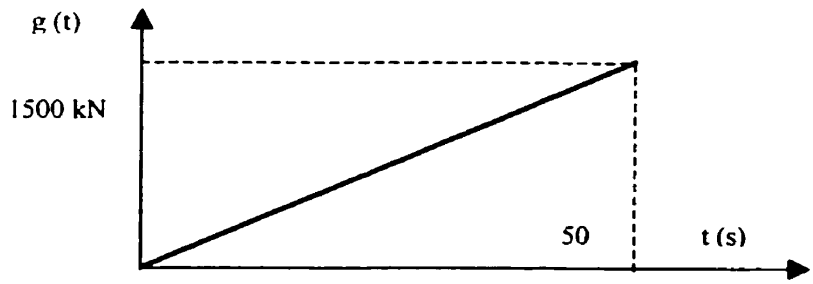

(b) Time function

Figure B-1 Modeling procedure for pushover analyses; applied load = {f (s, t)} = {f(s)} g(t).

The results of the pushover analyses for the building model without P-Δ effects are given in Figures B-2 to B-4, describing: (1) the curvature time history for the base of the wall, (2) the top lateral displacement time history, (3) the moment-curvature response history for the base of the wall, (4) the acceleration and the velocity time history at mid-height and at the top of the wall.

The ultimate curvature $\Phi_u = 6.67$ rad/km at the bottom of the wall is given in Table 4-4 and corresponds to rupture of the reinforcing bars in tension. According to Figure B-2, the time of the loading is 44.2 s when the curvature reaches the ultimate value. Figure B-3 shows that the top lateral displacement at that time is then 398 mm. Finally, the result of the pushover analyses without P-Δ effects is shown in Figure B-7. In Figure B-7, the vertical axis is the total applied lateral load normalized with respect to the NBCC lateral seismic force, V ($V = V_e^* U/R$). The horizontal axis is the ratio of the roof lateral displacement to the wall height. The response of the building model shows that the shear wall carries a base shear of 1.04 times the code base shear V at 33.2 s when P-Δ effects are not included, with a relative roof displacement of 0.253 % of the building height.

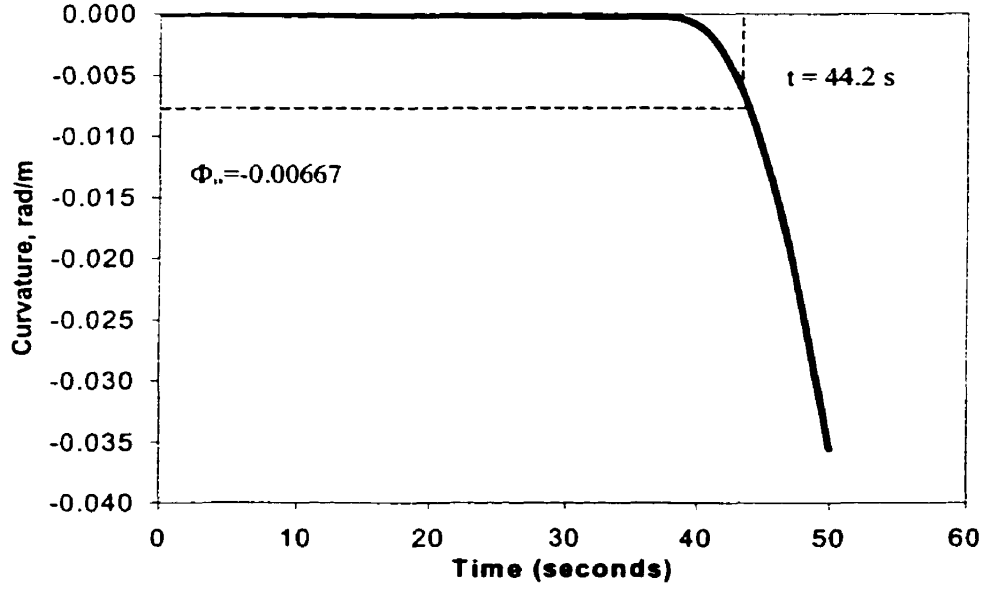

Figure B-2 Curvature time history at the base of the wall (without P-Δ).

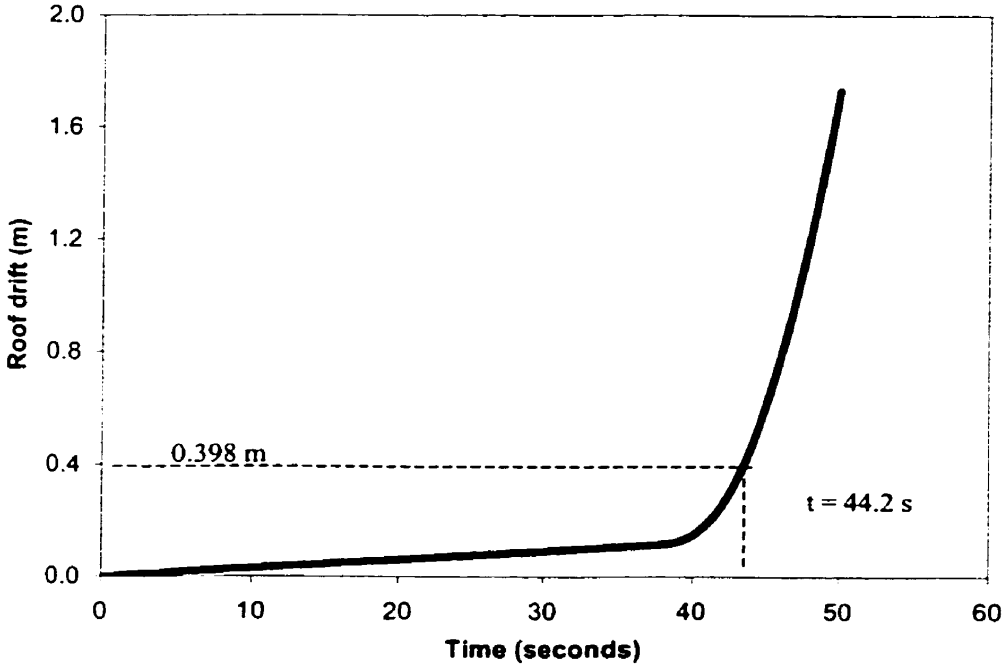

Figure B-3 Top lateral displacement time history (without P-Δ).

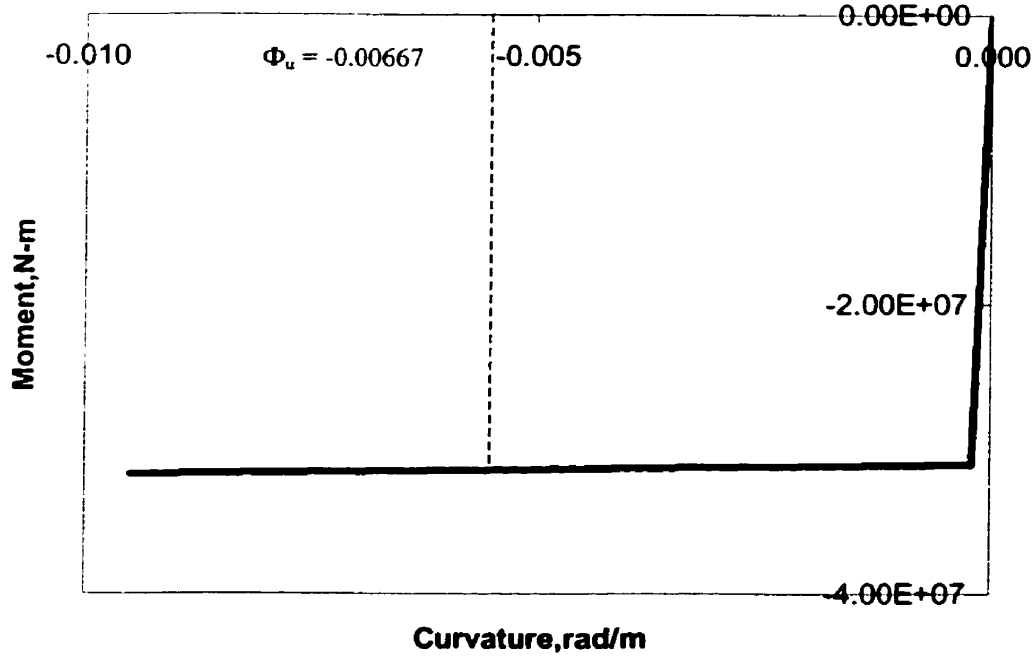

Figure B-4 Moment-curvature response for the base of the wall (without P-Δ).

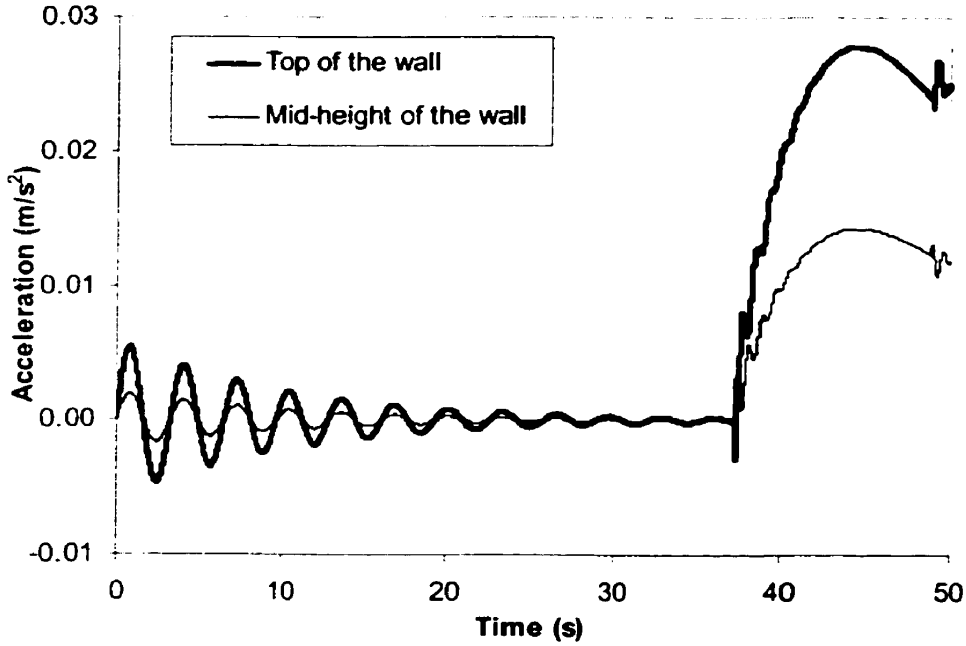

Figure B-5 Acceleration time history at mid-height and at the top of the wall.

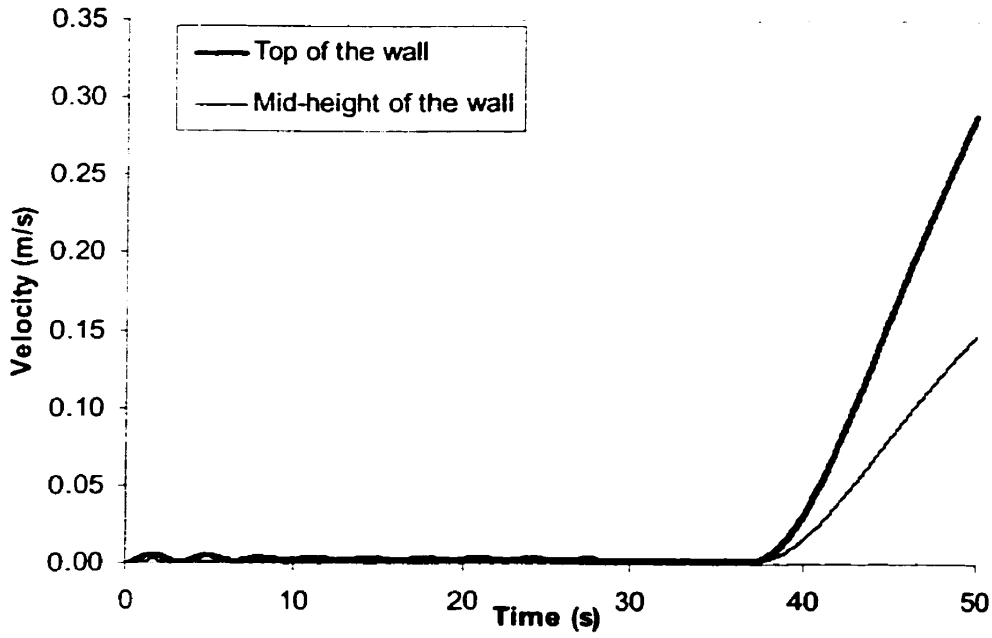

Figure B-6 Velocity time history at mid-height and at the top of the wall.

The acceleration and velocity of the top of the wall are increased largely at that time. Because of the effects of inertia forces and damping forces activated by the collapse mechanism, the applied force-displacement relationship exhibits a negative slope after the applied lateral load reaches the maximum value.

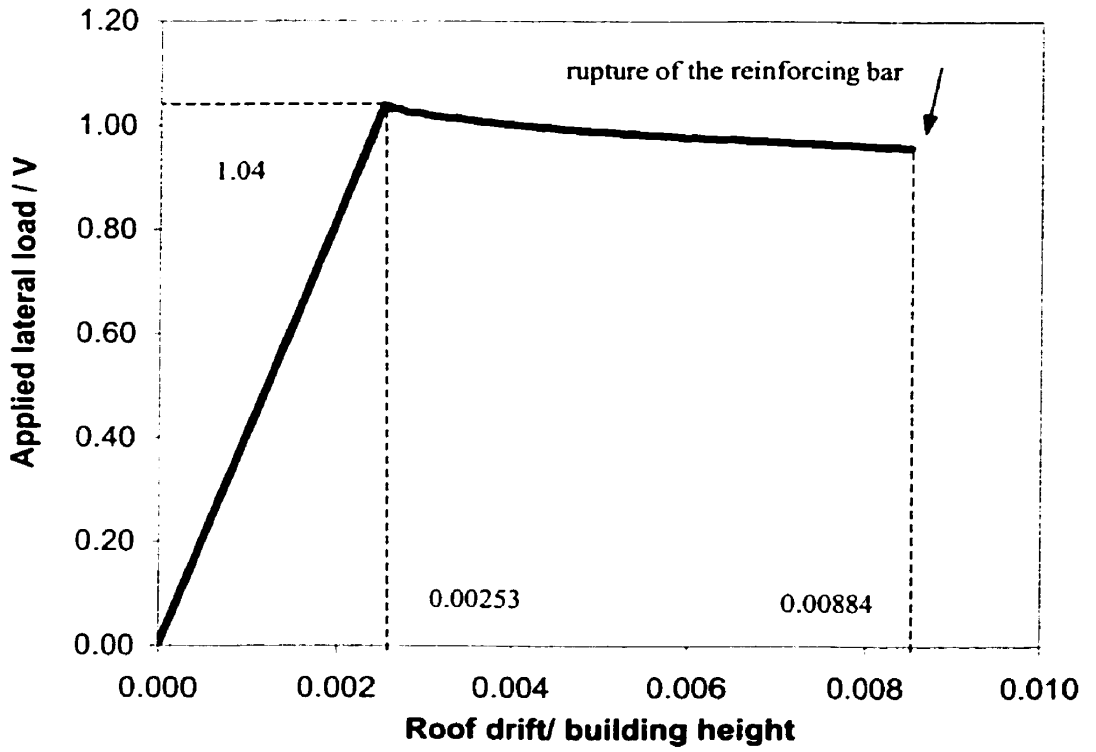

Figure B-7 Push-over analysis (without P-Δ).

The results of the pushover analyses for the building model with P-Δ effects included are also shown in Figures B-8 to B-10. In Figure B-8, the time of the loading is 39.8 s when the curvature equals the maximal value Φ_u = 6.67 rad/km and the top lateral displacement is 401 mm. Figure B-11 shows the relationship between the applied lateral load and the roof drift. The response with P-Δ effects considered for the building model indicates that the shear wall carries a base shear of 0.978 V, with a top lateral displacement of 0.261% of the building height.

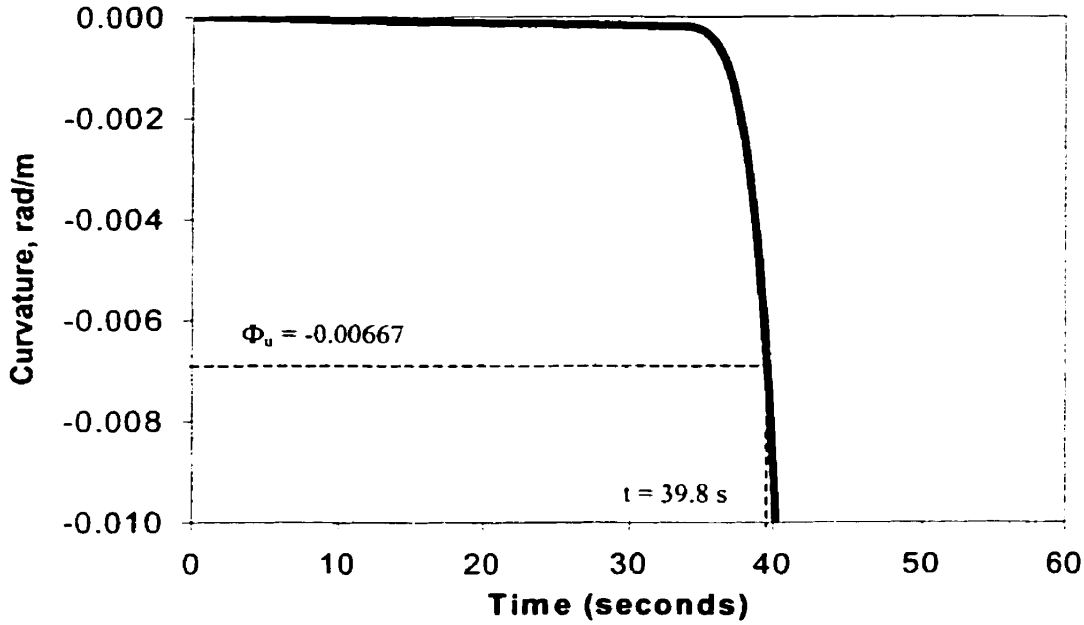

Figure B-8 Curvature time history for the base of the wall (with P-Δ).

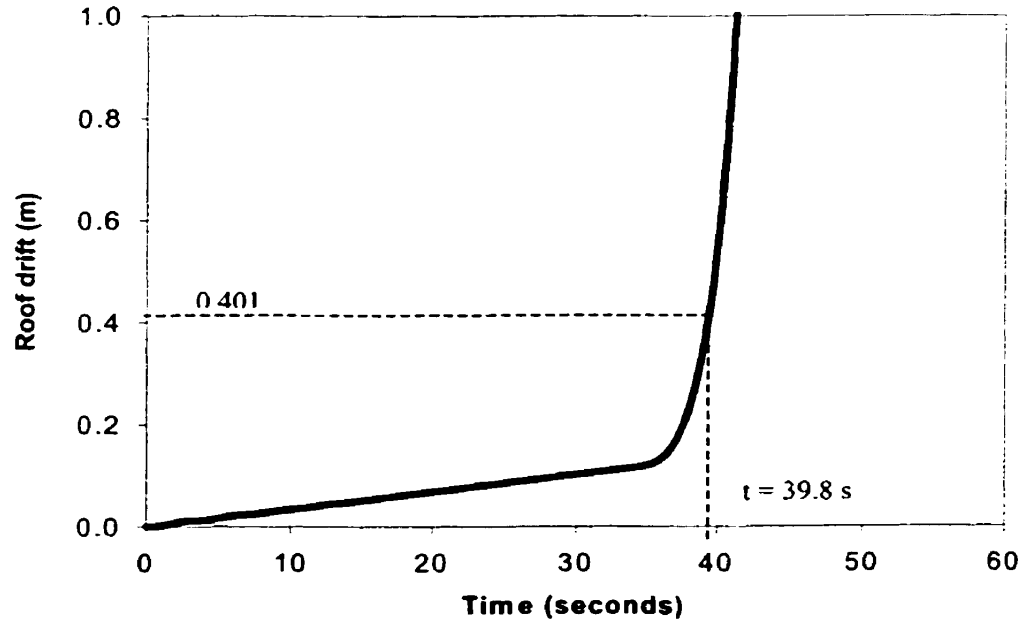

Figure B-9 Top lateral displacement time history (with P-Δ).

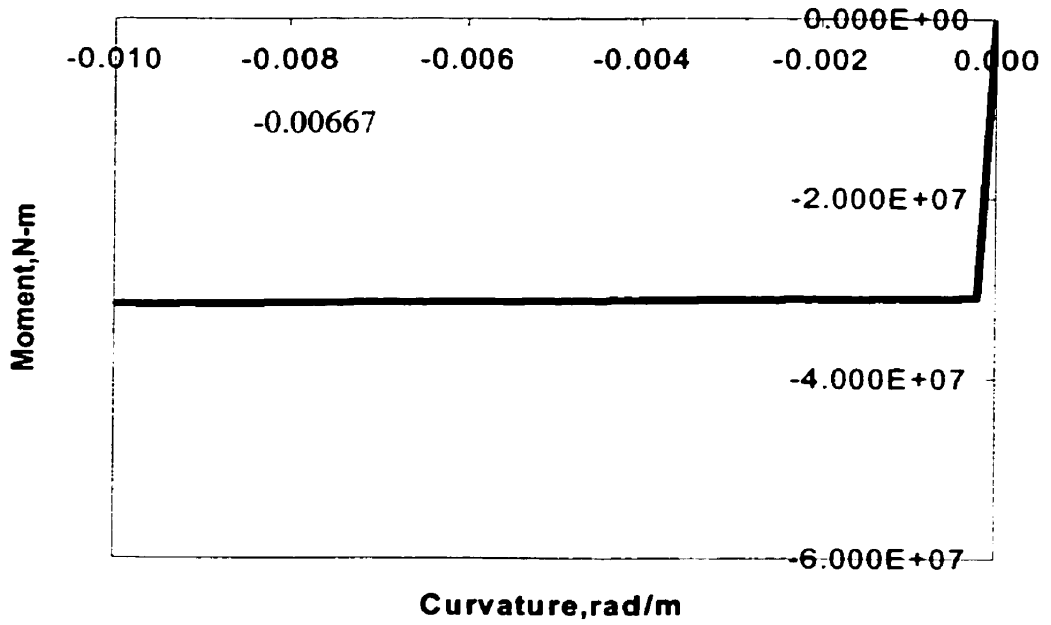

Figure B-10 Moment-curvature response for the base of the wall (with P-Δ).

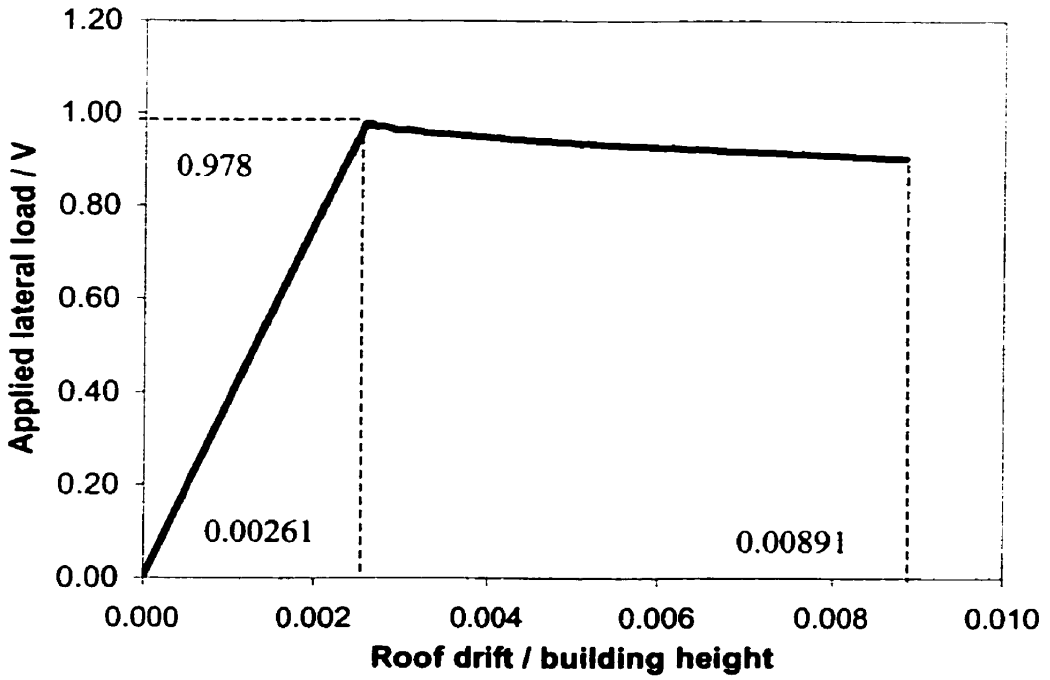

Figure B-11 Push-over analysis (with P-Δ).

APPENDIX C

INPUT FILE FOR THE PUSHOVER ANALYSES USING RUAUMOKO COMPUTER PROGRAM

```
12 storey shear wall(push-over)---without P-delta
2 0 1 0 0 -1 0 2 0
26 24 13 3 1 2 9.806 5.0 5.0 0.01 50.0 1.0
0 1 5 0 1.0 10.0 0.0 0.0
0 0 0 0 0

NODES
1    0.0   0.0    1 1 1    0 0 0
2   21.0   0.0    1 1 0    0 0 0
3    0.0   4.85   0 0 0    0 0 0
4   21.0   4.85   0 0 0    3 0 0
5    0.0   8.5    0 0 0    0 0 0
6   21.0   8.5    0 0 0    5 0 0
7    0.0  12.15   0 0 0    0 0 0
8   21.0  12.15   0 0 0    7 0 0
9    0.0  15.8    0 0 0    0 0 0
10  21.0  15.8    0 0 0    9 0 0
11   0.0  19.45   0 0 0    0 0 0
12  21.0  19.45   0 0 0   11 0 0
13   0.0  23.1    0 0 0    0 0 0
14  21.0  23.1    0 0 0   13 0 0
15   0.0  26.75   0 0 0    0 0 0
16  21.0  26.75   0 0 0   15 0 0
17   0.0  30.4    0 0 0    0 0 0
18  21.0  30.4    0 0 0   17 0 0
19   0.0  34.05   0 0 0    0 0 0
20  21.0  34.05   0 0 0   19 0 0
21   0.0  37.7    0 0 0    0 0 0
22  21.0  37.7    0 0 0   21 0 0
23   0.0  41.35   0 0 0    0 0 0
24  21.0  41.35   0 0 0   23 0 0
25   0.0  45.0    0 0 0    0 0 0
26  21.0  45.0    0 0 0   25 0 0
```

```
ELEMENTS
1   1   1   3
2   2   3   5
3   3   5   7
4   4   7   9
5   5   9   11
6   6   11  13
7   7   13  15
8   8   15  17
9   9   17  19
10  10  19  21
11  11  21  23
12  12  23  25
13  13  2   4
14  13  4   6
15  13  6   8
16  13  8   10
17  13  10  12
18  13  12  14
19  13  14  16
20  13  16  18
21  13  18  20
22  13  20  22
23  13  22  24
24  13  24  26

PROPS
1 FRAME
  1 0 0 4 0 1
  24.648E9 10.27E9 1.8  1.5 6.388 0.0 0.0 0.0
  0 0.000480 0 0
  0.0 0.0 31.06E6 -31.06E6 31.06E6 -31.06E6
  0.0 0.6 1 2
  0.0 0.0 32.22 32.22 32.22 32.22 0.0 0.0 0.0 0.0 0.0 0.1
2 FRAME
  1 0 0 4 0 1
  24.648E9 10.27E9 1.8 1.5 6.388 0.0 0.0 0.0
  0 0.000762 0 0
  0.0 0.0 29.27E6 -29.27E6 29.27E6 -29.27E6
  0.0 0.6 1 2
  0.0 0.0 38.3 38.3 38.3 38.3 0.0 0.0 0.0 0.0 0.0 0.1
3 FRAME
  1 0 0 4 0 1
  24.648E9 10.27E9 1.8 1.5 6.388 0.0 0.0 0.0
```

```
   0 0.000434 0 0
   0.0 0.0 27.16E6 -27.16E6 27.16E6 -27.16E6
   0.0 0.6 1 2
   0.0 0.0 34.52 34.52 34.52 34.52 0.0 0.0 0.0 0.0 0.0 0.1
 4 FRAME
   1 0 0 4 0 1
   24.648E9 10.27E9 1.8 1.5 6.388 0.0 0.0 0.0
   0 0.000592 0 0
   0.0 0.0 25.64E6 -25.64E6 25.64E6 -25.64E6
   0.0 0.6 1 2
   0.0 0.0 42.53 42.53 42.53 42.53 0.0 0.0 0.0 0.0 0.0 0.1
 5 FRAME
   1 0 0 4 0 1
   24.648E9 10.27E9 1.8 1.5 6.388 0.0 0.0 0.0
   0 0.000350 0 0
   0.0 0.0 24.55E6 -24.55E6 24.55E6 -24.55E6
   0.0 0.6 1 2
   0.0 0.0 41.19 41.19 41.19 41.19 0.0 0.0 0.0 0.0 0.0 0.1
 6 FRAME
   1 0 0 4 0 1
   24.648E9 10.27E9 1.8 1.5 6.388 0.0 0.0 0.0
   0 0.000327 0 0
   0.0 0.0 19.29E6 -19.29E6 19.29E6 -19.29E6
   0.0 0.6 1 2
   0.0 0.0 49.77 49.77 49.77 49.77 0.0 0.0 0.0 0.0 0.0 0.1
 7 FRAME
   1 0 0 4 0 1
   24.648E9 10.27E9 1.8 1.5 6.388 0.0 0.0 0.0
   0 0.000622 0 0
   0.0 0.0 17.60E6 -17.60E6 17.60E6 -17.60E6
   0.0 0.6 1 2
   0.0 0.0 54.41 54.41 54.41 54.41 0.0 0.0 0.0 0.0 0.0 0.1
 8 FRAME
   1 0 0 4 0 1
   24.648E9 10.27E9 1.8 1.5 6.388 0.0 0.0 0.0
   0 0.000368 0 0
   0.0 0.0 14.50E6 -14.50E6 14.50E6 -14.50E6
   0.0 0.6 1 2
   0.0 0.0 61.73 61.73 61.73 61.73 0.0 0.0 0.0 0.0 0.0 0.1
 9 FRAME
   1 0 0 4 0 1
   24.648E9 10.27E9 1.8 1.5 6.388 0.0 0.0 0.0
   0 0.000351 0 0
   0.0 0.0 13.10E6 -13.10E6 13.10E6 -13.10E6
```

```
  0.0 0.6 1 2
  0.0 0.0 81.27 81.27 81.27 81.27 0.0 0.0 0.0 0.0 0.0 0.1
10 FRAME
  1 0 0 4 0 1
  24.648E9 10.27E9 1.8 1.5 6.388 0.0 0.0 0.0
  0 0.000324 0 0
  0.0 0.0 11.70E6 -11.70E6 11.70E6 -11.70E6
  0.0 0.6 1 2
  0.0 0.0 90 90 90 90 0.0 0.0 0.0 0.0 0.0 0.1
11 FRAME
  1 0 0 4 0 1
  24.648E9 10.27E9 1.8 1.5 6.388 0.0 0.0 0.0
  0 0.000484 0 0
  0.0 0.0 10.15E6 -10.15E6 10.15E6 -10.15E6
  0.0 0.6 1 2
  0.0 0.0 100 100 100 100 0.0 0.0 0.0 0.0 0.0 0.1
12 FRAME
  1 0 0 4 0 1
  24.648E9 10.27E9 1.8 1.5 6.388 0.0 0.0 0.0
  0 0.000640 0 0
  0.0 0.0 8.74E6 -8.74E6 8.74E6 -8.74E6
  0.0 0.6 1 2
  0.0 0.0 140 140 140 140 0.0 0.0 0.0 0.0 0.0 0.1
13 FRAME
  1 0 0 4 0 0
  24.648E9 10.27E9 3.815 3.18 0.0874 0.0 0.0 0.0
  0 0 0 0
  22.4E6 -1.736E8 0.0 0.0 0.0 0.0
  0.0 0.6 1 2

WEIGHTS
3   4138221.0  0.0
5   3966046.0  0.0
7   3967046.0  0.0
9   3876951.0  0.0
11  3876951.0  0.0
13  3876951.0  0.0
15  3846923.0  0.0
17  3846923.0  0.0
19  3846923.0  0.0
21  3846923.0  0.0
23  3846923.0  0.0
25  3563630.0  0.0
```

```
LOADS
1    0   0
2    0   0
3    0 -514000
4    0 -3881000
5    0 -464000
6    0 -3761000
7    0 -465000
8    0 -3761000
9    0 -457000
10   0 -3679000
11   0 -457000
12   0 -3680000
13   0 -459000
14   0 -3681000
15   0 -459000
16   0 -3652000
17   0 -460000
18   0 -3653000
19   0 -462000
20   0 -3655000
21   0 -463000
22   0 -3660000
23   0 -478000
24   0 -3692000
25   0 -470000
26   0 -3746000

SHAPE
3   0.01543
5   0.02591
7   0.03704
9   0.04708
11 0.05796
13 0.06884
15 0.07909
17 0.08989
19 0.1007
21 0.1115
23 0.1223
25 0.134
26 0.0
```

```
EQUAKE
3 1 0.01 1.0

START
1    0.0   0.0
2    50.0 1500000.0
```